Injectable hydrogels for the improved delivery of treatments in spinal cord injury

by

Timothy Mark O'Shea

B.Eng. (Medical) First Class Honours

M.S. (Engineering Management)

Queensland University of Technology, 2009

SUBMITTED TO THE HARVARD-MIT PROGRAM IN HEALTH SCIENCES AND TECHNOLOGY IN PARTIAL FULFILLMENT OF THE REQUIREMENTS FOR THE DEGREE OF

DOCTOR OF PHILOSOPHY IN MEDICAL ENGINEERING

AT THE

MASSACHUSETTS INSTITUTE OF TECHNOLOGY

June 2015

Signature redacted

Signature of Author: _____

Timothy Mark O'Shea

Harvard-MIT Program in Health Sciences and Technology

May 18, 2015

Signature redacted

Certified by: _____

Robert S. Langer, ScD

David H. Koch Institute Professor, Massachusetts Institute of Technology

Thesis Supervisor

Signature redacted

Accepted by: _____

Emery N. Brown, MD, PhD

Director, Harvard-MIT Program in Health Sciences and Technology

Professor of Computational Neuroscience and Health Sciences and Technology

Injectable hydrogels for the improved delivery of treatments in spinal cord injury

by

Timothy Mark O'Shea

Submitted to the Harvard-MIT Program in Health Sciences and Technology on May 18, 2015 in partial fulfillment of the requirements for the Degree of Doctor of Philosophy in Medical Engineering

ABSTRACT

Spinal cord injury (SCI) results in sudden life-altering paralysis with chronic medical consequences. Although no clinical therapy is currently available to reverse paralysis, a number of biomacromolecule drug candidates in the form of proteins, enzymes and monoclonal antibodies have demonstrated restoration of function in studies with SCI animal models. However, the inability to address drug formulation stability issues and overcome delivery barriers has limited the clinical translation of these promising drugs. To address this inadequacy, we designed a versatile injectable hydrogel platform and investigated its utility for local delivery of biomacromolecules to SCI contusion lesions.

To develop this hydrogel platform we synthesized a library of different tri-thiol-functionalized ethoxylated polyol esters (TEPE) and combined these entities with PEG diacrylates (PEGDA) of various molecular weights to form crosslinked materials with diverse physiochemical properties using Michael addition thiol-ene chemistry. This hydrogel platform afforded unprecedented temporal control over both material degradation and the triphasic release of model biomacromolecule drugs over a 5 to 35 day period. Favorably, these materials display fast and controllable gelation kinetics under physiological conditions as well as non-swelling hydrolytic degradation profiles making them amendable for use in volume constrained anatomical sites within the spinal cord. Many of the biomacromolecule drugs of interest for SCI are complex and fragile making them susceptible to aggregation, denaturation and loss of activity during biomaterial encapsulation and controlled release. We devised a strategy to improve the long-term functional stability of biomacromolecules within hydrogels by covalently incorporating trehalose, a non-reducing disaccharide, into hydrogel networks by reacting trehalose diacrylate monomers with TEPEs and PEGDA. The covalent incorporation of trehalose within hydrogels afforded prolonged stabilization and controlled release of model enzymes *in vitro* and *in vivo* via a proposed mechanism of strong and ordered hydrogen bonding interactions. There is currently limited information pertaining to the performance of hydrogel therapies in non-penetrating contusive SCI, which represents the dominant injury mode observed clinically. Therefore, in the final part of this thesis we evaluated biomacromolecule drug delivery outcomes following intrathecal and intraparenchymal injection of

hydrogel within rat thoracic SCI contusion lesions. Intraparenchymal hydrogel injection but not intrathecal administration afforded prolonged release of biomacromolecules locally within spinal cord parenchymal tissue over a two week period. Using a fluorescently labeled model drug, FITC-Dextran, we observed localized diffusion of drug within the neuropil as well as evenly distributed punctated deposits within the extracellular space that appeared to drain into local perivascular spaces. Overall, this work validates novel strategies for improved localization, temporal delivery and long term functional stability of promising biomacromolecule drug candidates in SCI.

Thesis Supervisor:

Robert Langer, Sc.D

Title: David H. Koch Institute Professor, MIT

Thesis Committee Chair:

Jeffrey M. Karp, Ph.D.

Title: Associate Professor of Medicine, HMS

Thesis Readers:

Larry Benowitz, Ph.D.

Title: Professor of Surgery and Ophthalmology, HMS

Bradley Olsen, PhD

Title: Paul M. Cook Career Development Assistant Professor of Chemical Engineering, MIT

ACKNOWLEDGMENTS

Completing the MEMP PhD program has been one of the greatest accomplishments of my life to date. This academic milestone was only possible because of the support of many great people who have all made a significant contribution to my life in both a professional and personal context. As such I would like to individually acknowledge their contributions:

My thesis advisor, Professor Robert Langer, whose support and guidance allowed me to work on research that I am particularly passionate about and produce impactful and pragmatic scientific solutions that might one day help people. Thank you Bob for your mentorship.

My thesis committee members, Jeff Karp, Larry Benowitz and Brad Olsen who generously donated their time on a regular basis to actively involve themselves in my research and provide practical solutions to the difficult problems I faced throughout the thesis. Thank you gentlemen for this valuable support.

The many colleagues within the Langer lab who, from the very first day I started in the lab in October 2009, have been so giving of their time and always willing to teach me a new skill, train me on an instrument or help me with an experiment, no matter how menial the task. I would like to acknowledge in particular Chris Pritchard, Daniel Siegwart, Chris Levins, Chris Alabi, Avi Schroeder, Paulina Hill, Pamela Podell, David Han, Omar Khan, Volkan Yesilyurt, Matthew Webber, Eunha, Mark Tibbitt and Eric Appel for their research contributions and mentorship. I would also like to thank the team at InVivo Therapeutics Corporation for valuable discussions and research support.

My close friends from back home in Australia and the many other friends who I have met here in the US over the course of my time in HST. Thank you for your support throughout the PhD journey. I want to particularly thank Ben Harvey for inspiring me, keeping me honest and making sure I stay connected with home. Also, James Dahlman for being a great scientific colleague, room-mate and friend over the past 5 years. And of course, Rachel Ellman, for your unconditional love and uncompromising support. Meeting you Rachel was the greatest thing that happened to me during the PhD.

Finally, my family, especially mum, dad and Adrian who have been an unwavering source of support throughout this PhD process and for putting up with me for all these years.

I would like to also acknowledge the primary financial supporter of this research work, InVivo Therapeutics Corporation, as well as personal fellowship support from the General Sir John Monash Foundation and the Harvard-MIT Division of Health Science & Technology.

TABLE OF CONTENTS

LIST OF FIGURES

LIST OF SUPPLEMENTARY FIGURES

LIST OF TABLES

1 THESIS INTRODUCTION

Spinal cord injury (SCI), caused by traumatic destruction of the central nervous system (CNS) structure that transmits information between the brain and the body, results in life-altering paralysis. Although improvements in acute surgical intervention and critical care medicine have contributed to reducing early mortality rates, those affected by SCI face chronic medical issues affecting cardiovascular, musculoskeletal, respiratory, bladder, bowel and sexual function that require lifelong management. There is currently no therapy that can reverse paralysis due to SCI. This medical inadequacy has motivated scientific investigations over the past several decades to uncover the specific biological mechanisms underlining CNS injury and repair. As a direct result of these studies, several promising drug candidates that demonstrate restoration of function when administered following SCI in animals have been identified. These drugs, which derive from many diverse categories of therapeutic classes ranging from small molecules to complex biomacromolecules, target specific mechanisms of SCI pathophysiology and are effective across a range of time periods post injury.

The exciting preclinical data that has been generated coupled with the obvious clinical need for new effective paralysis treatments has prompted the independent re-evaluation of many of these drugs to test the robustness of their effect on recovery. Specifically, as part of the National Institute of Neurological Disorders and Stroke (NINDS) sponsored "Facilities of Research Excellence—Spinal Cord Injury" (FORE-SCI) replication studies initiative, several leading SCI research labs in the US were provided with resources to reassess the most promising drug treatments as identified by a consortium of experts within the SCI field[1]. For the most part, these preclinical replication studies failed to recapitulate the functional recovery improvements previously attributed to the specific therapeutics. Separately, but around the same time, a number of other promising drug candidates that had already been successfully validated across independent preclinical studies progressed to human clinical trials. Unfortunately, the results from these SCI clinical trials have also been mostly disappointing with only a minimal effect size, if any, observed in treatment groups. As a consequence, once highly anticipated clinical SCI drug programs have been delayed, shelved or even terminated. The underlying causes of these independent failures are difficult to diagnose and are likely multi-factorial in nature. However, a common theme that has emerged time and again throughout many study reports assessing clinical translation of promising therapies is the unsatisfactory delivery of drugs locally to the injured spinal cord, the site of action for

most potential SCI therapeutics. The most common drug delivery limitations and problems frequently cited within the SCI literature include:

i. Insufficient drug doses reaching or accumulating at the site of injury within the spinal cord using traditional non-invasive oral or parenteral delivery methods because of the relatively impermeable tissue barriers of the CNS, namely the blood spinal cord barrier (BSCB) and the meninges;
ii. Undesirable off-target effects associated with the high systemic drug doses that are needed for achieving any effect at the SCI lesion site because of the limited drug penetration across the BSCB; and
iii. Formulation issues associated with individual drugs themselves due to a combination of unfavorable properties such as low purity, high endotoxin level, variable aqueous solubility, limited solution and thermal stability and insufficient pharmacokinetics/pharmacodynamics among others that necessitates repeat, often invasive, dosing.

In order to compensate for these drug delivery limitations preclinical researchers often utilize methods that are deemed by many clinicians and regulatory experts to be not scalable, or even readily amenable, for human use. Furthermore, such methods predispose the preclinical animal studies to significant drug delivery variability that may confound outcomes. These unsatisfactory drug delivery approaches include:

i. Parenteral administration of very high drug concentrations that are barely tolerated by the animal;
ii. Use of toxic concentrations of organic solvents such as dimethyl sulfoxide (DMSO) and ethanol to solubilize hydrophobic small molecule drugs for parenteral administration that are again barely tolerated by the animal;
iii. Application of repeat invasive injections directly into SCI lesions that requires multiple frequent invasive surgeries; and
iv. Use of long-term indwelling catheters/minipumps that often lead to unreliable drug dosing and are prone to fibrosis, occlusion and unfavorable immunogenicity. Unintended dislodgment or incorrect placement of indwelling catheters can also cause additional irreversible injury to the spinal cord.

Ultimately, unsatisfactory delivery methods as well as a limited understanding of the bio-distribution and pharmacokinetics of promising drug candidates has compromised their repeat pre-clinical efficacy and potential clinical translation. The failure to consider clinical delivery challenges in the initial preclinical investigation of a potential SCI drug will continue to result in reproducibility and product development problems. With this in mind, the **overall goal** of this thesis is to develop a clinically viable solution to the drug delivery insufficiencies in SCI by designing a versatile hydrogel platform that can be applied locally through a single injection to the SCI lesion at the time of surgical decompression and that possesses appropriate functionality that addresses the delivery challenges relevant to numerous SCI drug candidates.

1.1 SIGNIFICANCE OF THIS THESIS

Unsatisfactory drug delivery is a fundamental and readily identifiable problem limiting the clinical translation of discoveries made by the SCI research community. However, a viable solution that provides for effective and tunable delivery of diverse classes of therapeutics such that optimal parameters can be established has yet to emerge. This thesis focuses on the development of an innovative solution to these drug delivery inadequacies through the rational design of an injectable hydrogel platform. By making subtle chemistry modifications to the oligomers that comprise this platform, a range of materials with diverse structural properties can be fabricated and used to deliver numerous classes of drugs with temporal control. This thesis will demonstrate how this readily translatable injectable system can achieve: (a) tunable drug delivery over days to weeks through innovative chemical engineering; (b) long-term stabilization of fragile therapeutics such that functionally active drug can be delivered throughout the entire period of controlled release; and (c) effective localization of treatments to the spinal cord contusion lesion via a surgical procedure that is clinically feasible. The successful development of this platform technology as well as preliminary validation of its successful use in rat contusion injuries as part of the work described in this thesis makes a significant contribution to the field of SCI research. In particular, the main outcome of this thesis is the provision of an engineering tool that can be readily adopted by neurobiologists working in the SCI field to robustly test new SCI drugs. Since such a versatile drug delivery platform is not currently available to the SCI research community, despite being widely sought after, this work fills an important void. This hydrogel platform may be used in the future to better deliver previously identified drugs of promise as well as assist in the screening of new drug candidates that may have an important spatiotemporal component

to their effect for SCI treatment. Furthermore, it is worth considering that the drug delivery challenges identified for SCI are not unique ones and many other diseases and disorders, affecting organs such as the brain, heart and spine among many others, may benefit from the new insight provided by this thesis research.

1.2 Specific Aims

The **overall objective** of this thesis is to develop and test novel biomaterial technologies that may be used to augment the localization, temporal delivery and long term functional stability of promising drug candidates for SCI. The core focus of the work involves the application of novel polymer chemistry and materials science techniques to design biomaterial systems that have specific applicability for use in clinical SCI and overcome delivery limitations identified for a number of different drug classes.

The **specific aims** of this thesis involve the development and optimization of an injectable biomaterial platform, assessing its chemical and structural properties as well as undertaking preliminary evaluation of its appropriateness for use in SCI drug delivery applications.

The specific aims of this thesis are the following:

i. Synthesize a library of biodegradable hydrogel materials based on a common biorthogonal gelation chemistry, characterize the structure-function correlates within this library and identify specific non-swelling candidates that may be amenable to delivering drugs to a spinal cord contusion injury.
ii. Investigate the covalent incorporation of pharmaceutical excipients into the hydrogel platform to addresses the stability challenges facing many fragile biomacromolecule SCI drug candidates.
iii. Characterize spatiotemporal drug delivery outcomes achieved with the hydrogel platform in a rat contusion model of SCI using various surgical application approaches.

1.3 THESIS OUTLINE

This thesis is separated into seven chapters. Chapter 1 introduces the rationale for this thesis work as well as the specific aims of the research. Chapter 2 compromises important background information that provides for a detailed rationale as to why the development of viable drug delivery solutions is an important area of investigation. This detailed literature review highlights how enhanced understanding of SCI pathophysiology accumulated over the past several decades has led to the development of drug candidates that target specific biological mechanisms of SCI. This second chapter further explores the favorable functional recovery outcomes attributed to these drug candidates in SCI animal models while also outlining the delivery limitations that have contributed to their poor repeatability and ultimately impaired their translational potential. An analysis of how biomaterials have been used to improve the performance of several of these drugs, as well as an investigation into the limitations associated with current biomaterial technology and areas for potential improvement will also be addressed. This literature review has been submitted for peer review and publication at the time of thesis submission.

The third chapter of the thesis outlines the fabrication and characterization of a hydrogel platform developed by synthesizing eight different tri-thiol ethoxylated polyol esters (TEPEs) and reacting them with varied molecular weight PEGDAs to form a library of hydrogel materials. The contents of this chapter were published in the journal *Advanced Materials* as: O'Shea, T. M., et al. (2015). Synthesis and Characterization of a Library of In-Situ Curing, Nonswelling Ethoxylated Polyol Thiol-ene Hydrogels for Tailorable Macromolecule Delivery. *Advanced Materials* (27): 65-72.

Chapter 4 focuses on building upon the platform described in the previous chapter and introduces a new functional monomer, trehalose diacrylate, to form novel hydrogels that leverage the protein stabilizing potential of this non-reducing disaccharide. By covalently incorporating the trehalose into the ethoxylated polyol hydrogel template the stabilization of particularly fragile biomacromolecules during long-term controlled release is explored. Furthermore, the trehalose hydrogel's ability to mitigate protein damage during potential manufacturing stressors is investigated. This chapter has been submitted for publication and was under peer review at the time of thesis submission.

Within Chapter 5 the important elements pertaining to surgical administration of the hydrogel platform to a contusive SCI are addressed. Using a rat contusion injury model, which replicates the dominant mode of clinical injury, the hydrogel biocompatibility and drug delivery performance are assessed. The work comprising this chapter will be submitted for publication in the near future.

Chapter 6 outlines broader applications outside of SCI where the current hydrogel has found utility, due to the material's favorable physiochemical, drug delivery and biocompatibility properties. Applications discussed within this chapter include: the development of sustained treatments for various peripheral nerve radiculopathies; comparative analysis of hydrogels for vitreous humor replacement in the eye as well as basic biological investigations where hydrogels are used to delivery biomacromolecules to study peripheral nerve demyelination and glioblastoma stem cell recruitment. These studies have been performed in conjunction with external collaborators and have led to a number of published or submitted papers. Summaries of the results from these studies as well as their implications for future use of the hydrogel platform will be discussed.

In the final chapter of this thesis the conclusions that can be drawn from the current research, the work's contributions and implications for the field, as well as recommendations for future areas of investigation will be discussed.

2 BACKGROUND

2.1 INTRODUCTION

A spinal cord injury (SCI) causes dramatic and sudden changes to a person's health and wellbeing that persist with permanent life-long consequences. The worldwide incidence of SCI is estimated at 10.4 to 83 per million of the population and predominately affects the younger male demographic, crippling them at the prime of their lives[2,3]. For this young male population, aged 15-30 years, the incidence of SCI has been documented to be as high as 132 per million in some developed countries[4] **(Figure 2.1)**.

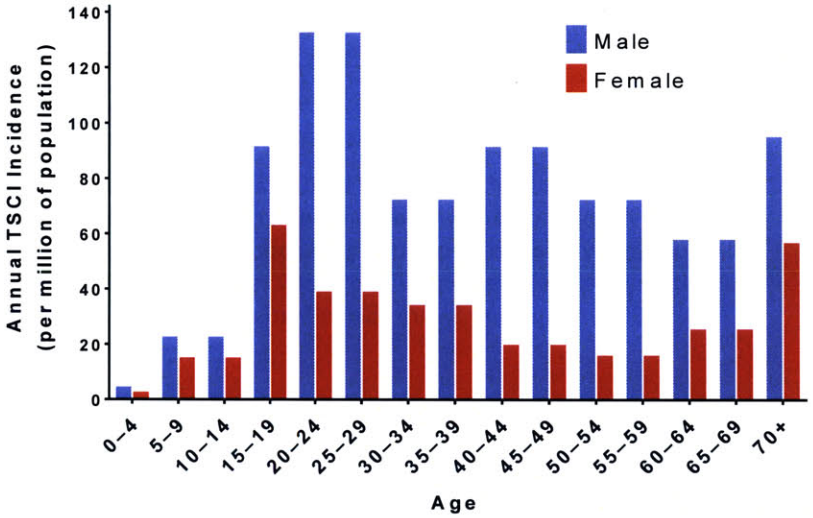

Figure 2.1 The annual incidence of SCI in Canada, segregated by age and gender, shows that the young male population is the dominant demographic affected by SCI. (Adapted from: WHO. 2013. International Perspectives on SCI)

Although improved trauma response and acute surgical intervention have contributed to reducing early mortality rates, those affected by SCI continue to require lifelong disability management for recurrent problems affecting multiple organ systems [5-7]. Specifically, chronic issues affecting cardiovascular[8], musculoskeletal[9], respiratory[10], bladder, bowel and sexual function as well as complications from urinary, skin and many other infections persist throughout a patient's lifetime[11]. The cost associated with the chronic SCI population, owing to the need for lifelong disability management, has been conservatively estimated at $9.7 billion annually in the US[12]. The high cost of SCI care can place a significant financial burden on the families of those affected, with estimated yearly costs in one developed country, Australia, shown to accumulate to an amount that is greater than the average yearly

salary **(Figure 2.2).** While these figures are alarming, in reality however, they fail to encompass the many intangible costs of SCI, with burden of disease on families and the community, lost work productivity, and many other associated unquantifiable parameters contributing to the overall societal impact.

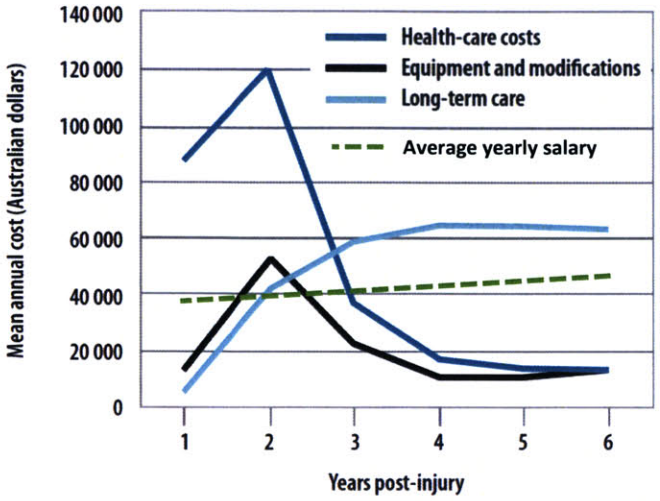

Figure 2.2 The mean annual cost of care for SCI in Australia demonstrates the high cost of both initial hospital care as well as long term care, which exceeds the average individual yearly salary of the country. (Adapted from: WHO. 2014. International Perspectives on SCI and Australian Bureau of Statistics. 2011. 5673.0.55.003 - Wage and Salary Earner Statistics).

The clinical community currently has no effective therapy that can reverse paralysis. This situation however is not from lack of trying. To date, several therapeutic candidates that demonstrate encouraging functional recovery have emerged within the preclinical rodent research literature[13-15]. Excitingly, many of these candidates have begun to be explored in the human population through the initiation of clinical trials[16,17]. However, for many of these treatment paradigms successful clinical conversion has proven difficult. The underlying causes of these independent failures are difficult to isolate and are likely polymorphous in nature. However, a common theme throughout many study reports assessing clinical translation of promising therapies is the problem of delivery. The specific underlying delivery challenges involve the inability to achieve localization of treatments to the desired tissue region within the spinal cord at appropriate local therapeutic concentrations without inducing off target complications. These delivery limitations usually stem from unfavorable physiochemical properties of the drug such as solubility, lipophilicity, charge and molecule size as well as the constraints created by the relatively impermeable tissue barriers of the CNS, namely the blood spinal cord barrier (BSCB) and the meninges.

For many promising SCI therapies, local long-term sustained treatment is required to maximize the prospect of efficacious outcomes. However, localized or systemic administration approaches that would accomplish this for SCI are seldom attempted clinically. By contrast, in the original SCI preclinical animal studies that provide the initial efficacy data for candidate drugs *in vivo*, researchers often use local delivery techniques and administration regimes that are difficult to translate or replicate in clinical human use. Such delivery techniques include: (1) intravenous administration of very high, potentially unsafe, drug concentrations[18,19]; (2) the use of potentially toxic concentrations of organic solvents such as dimethyl sulfoxide (DMSO) or ethanol to solubilize hydrophobic small molecule drugs[20,21]; (3) repeat invasive injections into the SCI lesion[22]; and (4) indwelling catheters positioned at the site of injury that pose a significant infection, immunogenicity and gliosis/fibrosis risk[23,24]. It is important to acknowledge that the goal of these original preclinical studies is not to create a ready to go treatment "product" but rather to examine the underlying biological effect of drugs delivered in a controlled "best case" scenario. However, in order to successfully translate these discoveries into treatments ready for clinical trials, robust pre-clinical results under simulated clinical conditions will be required. The incorporation of a proven, clinically safe delivery platform that can be used to evaluate many different treatments would therefore be useful in such an endeavor.

Delivery inefficiencies and unsatisfactory understanding of biodistribution and pharmacokinetics have also clouded the repeated pre-clinical efficacy of promising candidate treatments. Specifically, in recently reported National Institute of Neurological Disorders and Stroke (NINDS) sponsored "Facilities of Research Excellence—Spinal Cord Injury" (FORE-SCI) replication studies[1] on promising treatments for SCI a commonly cited cause of the often disappointing and inconsistent outcomes were delivery issues such as uncertain biodistribution, patency of catheter pumps and solubility of the drug solution [20,25,26]. In light of these inconsistent and unfavorable results, the development and validation of clinically appropriate methods for delivering these promising treatments is a critical research and development endeavor for the SCI field. Within this chapter we will summarize the elements of SCI pathophysiology that have been identified as potential targets for intervention as well as highlight several of the emerging candidate treatments that have leveraged this biological understanding to achieve improved functional outcomes in preclinical SCI models. Furthermore, we will describe the limitations associated with the current methods of delivery of these therapeutics and outline how innovative biomaterials engineering is starting to be used to overcome delivery challenges and augment therapeutic efficacy. Overall, this background and literature review chapter is intended to provide a comprehensive analysis

of the status of drug therapies for SCI as well as direction for how improvements can be made in their delivery through the use of biomaterials.

2.2 Pathological Mechanisms of SCI

Comprehensive understanding of the pathological elements of traumatic SCI is needed for the development of clinically appropriate therapies. While there are still many unknown elements associated with SCI pathology, the past two decades have produced important new knowledge describing the intricate details of the cellular level events activated at the local injury site[27] **(Figure 2.3)**. In traumatic SCI the initial injury to the cord is induced by a misdirected bony segment of vertebrae or other external stimulus penetrating through, or applying increased pressure on, the spinal cord tissue and depending on this stimulus the injury can manifest as a laceration, compression, distortion, or contusion lesion. The dominant injury type in clinical SCI is a non-penetrating compression/contusion lesion, which is estimated to account for approximately 69% of cases[27]. While it is the abrasive loading on the cord that ultimately instigates injury, a multitude of secondary host responses provoke an exacerbation of the primary injury zone and augment the observed functional loss[27,28]. Initial elements of this "secondary injury" are brought on by a compromised blood-spinal cord barrier (BSCB) and disruption of associated microvasculature that gives rise to excessive bleeding, hemorrhage and necrosis as well as the local activation and systemic migration of inflammatory cells. The cells involved in this inflammatory response may well partake in both beneficial and destructive activities but in the acute phase of SCI without intervention they are understood to primarily induce further cord damage[29]. Additional injury is facilitated via multiple inflammation associated mechanisms such as: pro-inflammatory cytokine induced cellular apoptosis; excessive glutamate release and associated over activation of NMDA and AMPA receptors causing excitotoxicity; as well as iron induced up regulation of nitric oxide and superoxide anions leading to the formation of peroxynitrite and other peroxide species that results in free radical generation, oxidative stress, lipid peroxidation and accumulation of many intra- and extracellular derived damage-associated molecular pattern molecules (DAMPs) [29-33]. As a result of the widespread hemorrhage and oxidative stress, activated alkene and reactive aldehyde species such as malondialdehyde, acrolein and 4-hydroxynonenal are generated from the breakdown of susceptible phospholipids and these powerful electrophiles readily react with, and denature, fragile biomolecules located both intracellularly and within the extracellular matrix (ECM) [34,35]. This ongoing ECM destruction peaks at 24 hours post injury and persists throughout at least the first week post injury,

conferring damage of tissue within a broader injury zone than what is apparent immediately after the initial mechanical trauma [36,37]. Other localized tissue remodeling induced by inflammation processes includes significant axonal demyelination which leads to the accumulation of myelin associated glycoprotein, oligodendrocyte myelin glycoproteins, semaphorins and ephrins locally as well as the degradation of the dominant extracellular matrix macromolecule, hyaluronan, into fragments of damaging low molecular weight species that can exacerbate the inflammatory response [27,38-40]. Recent analysis of the inflammation timeline in SCI suggests prolonged late stage inflammation, which peaks 60 days post injury and may persist for in excess of 180 days[41]. This insight suggests that neuroinflammation and tissue destructive mechanisms associated with the response may persist at significantly elevated levels well into sub-acute and early chronic phases of SCI.

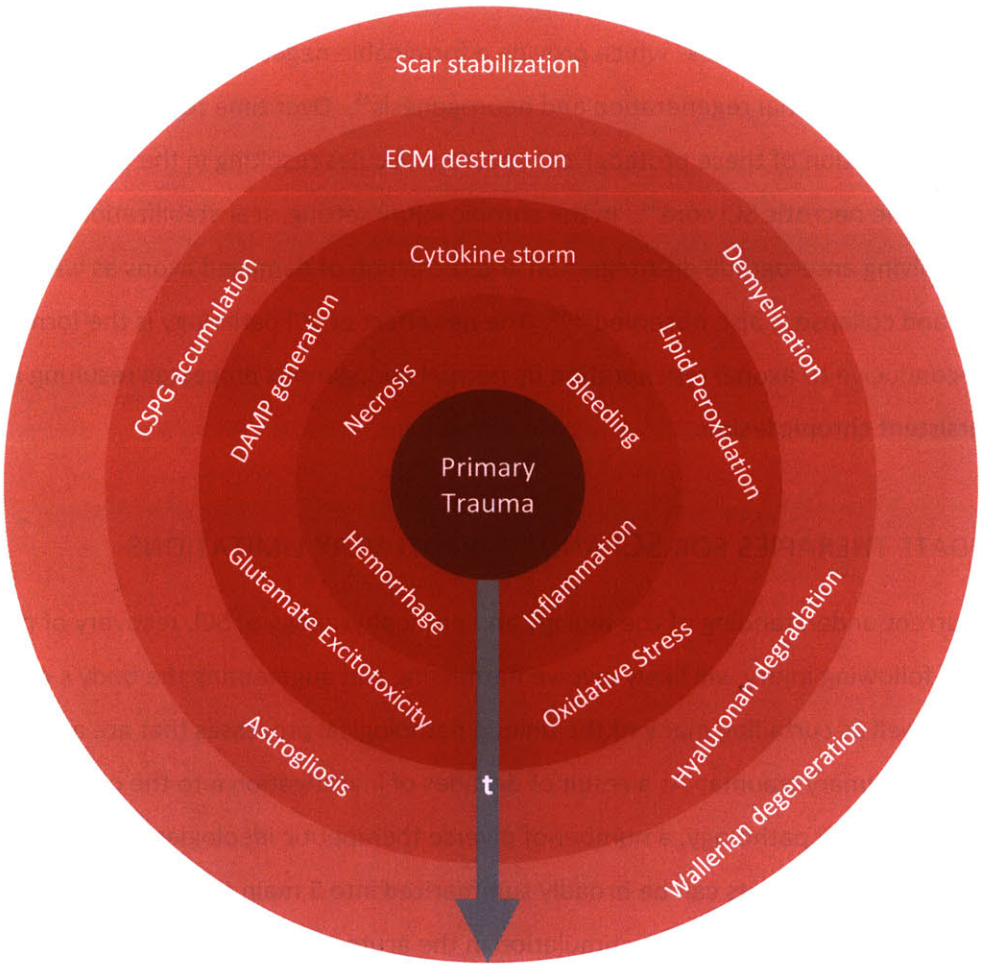

Figure 2.3 The progression of cellular events in SCI demonstrates a complex and multi-element pathophysiology that has a significant temporal component.

Inflammatory processes and associated mechanisms such as DAMP generation and demyelination act to also stimulate astrogliosis which involves the formation of a reactive phenotype in the local astrocyte population[42]. Evidence from *in vivo* studies suggests that astrogliosis is an initially favorable wound healing and injury isolation response involving the consolidation of healthy viable neurons, axons and oligodendrocytes as well as partitioning of the necrotic core of the SCI lesion through the release of growth factors and cytokines, repair of the BSCB and the synthesis and organization of a new repair ECM[43]. However, this injury containment comes at a cost, with the accumulation of axon regeneration inhibiting proteoglycans such as phosphocan, neurocan, aggrecan, brevican and versican dominating the extracellular environment of the spinal cord surrounding the lesion[38,44]. These dominant glycoproteins that demonstrate up-regulated synthesis as part of the injury response contain a high percentage of chondroitin sulfate glycosaminoglycans (GAG) that emanate as side chains from a multi-domain core protein and it is these sugar "brushes" which provide a formidable negatively charged barrier that inhibits any endogenous axonal regeneration and neurogenesis[45]. Over time reactive astrocytes coordinate the organization of these proteoglycan macromolecules resulting in the formation of a dense gliotic scar around the necrotic SCI core[44]. In the chronic injury setting, scar stabilization, Wallerian degeneration involving anterograde disintegration and retraction of damaged axons as well as growth cone dystrophy and collapse is also observed[30,44]. The net effect of SCI pathology is the formation of an injury site non-conducive to axonal regeneration by normal endogenous processes resulting in an unresolved persistent chronic lesion.

2.3 CANDIDATE THERAPIES FOR SCI AND THEIR DELIVERY LIMITATIONS

Based on our current understanding of the biology and pathophysiology of SCI, recovery of motor and sensory function following injury will likely involve harnessing and augmenting the body's endogenous repair capacity as well as curtailing many of the unique pathological processes that are activated following the initial primary trauma. As a result of decades of investigation into the cellular level mechanisms specific to SCI pathology, a number of diverse therapeutic ideologies have been developed. Currently, the focus of treatments can be broadly summarized into 5 main categories: (1) Reducing inflammation and innate immune system stimulation in the acute stages of injury[46,47]; (2) Protecting undamaged penumbra tissue by re-establishing vascular perfusion, preventing cellular apoptosis, providing trophic support or mitigating oxidative stress and lipid peroxidation processes[48]; (3) Removing or neutralizing extracellular matrix molecules that are inhibitory to axon repair/plasticity[38]; (4)

Stimulation of endogenous regeneration and plasticity in damaged and preserved axons[49]; and (5) Reconstructing damaged tissue with cell replacements[50]. Therapeutic approaches using small molecule drugs, biomolecules (e.g. small peptides/proteins, growth factors, enzymes and antibodies), gene therapy and cell transplants have been investigated addressing these goals[51]. A number of combination type approaches that attempt to leverage multiple concepts have also been explored[52-56]. Within this chapter we have chosen to focus our attention on pharmaceutical therapeutic candidates that have generated promising preclinical SCI functional recovery data but that are also characterized by delivery limitations that currently preclude their successful translation to clinical SCI **(Table 2.1, 2.2 and 2.3)**. Therapies from this list fall into the first three therapeutic ideologies described above. We have made an effort to include an examination of relevant drug candidates that have been evaluated across multiple independent studies as well as those that have been re-explored as part of replication initiatives. Drugs that have shown promise in SCI but are readily administered by conventional methods (i.e. intravenous, intraperitoneal or orally) have not been included in this review but are covered in detail elsewhere[15]. Furthermore, while cell transplantation and gene therapy are important areas of investigation in SCI, these treatment approaches are beyond the scope of this review and we direct the interested reader to a number of good reviews and commentaries on this topic[57-59].

Despite having diverse molecular targets and chemical characteristics the promising drug candidates described here all possess common clinical administration requirements and limitations [60]. Specifically, several common delivery challenges continue to hamper the clinical utility of many of these promising candidates. Specifically, these challenges pertain to: (1) lack of specificity in the delivery of treatments to the damaged central nervous system (CNS) or to the desired cell populations/extracellular matrix molecules in the vicinity of the spinal cord lesion; (2) limited control over pharmacokinetics such as drug concentration and duration of treatment action at the desired location; and (3) restricted long term stability of the therapeutic agent being administered. As part of the detailed examination of SCI drug candidates this section of the review will also identify the relevant specific delivery limitations affecting these drugs that must be addressed if progression to clinical use is to be realized.

2.3.1 MITIGATING INFLAMMATION

Unique inflammatory processes are elicited in the spinal cord following traumatic injury, many of which are responsible for exacerbating the injury profile within the contused spinal cord and represent targets for therapeutic intervention[29]. Methylprednisolone sodium succinate (MPSS), a glucocorticoid which acts to minimize lipid peroxidation, reduce the migration of leukocytes and diminish vascular

permeability during inflammation has demonstrated beneficial outcomes for patients with SCI when administered in the early acute stages of SCI[46]. Following extensive pre-clinical evaluation in the 1970's and 1980's, clinical trials conducted as part of the NASCIS studies showed marginally improved outcomes upon administration of high doses of bolus and then sustained intravenous infusion of MPSS when started within eight hours of injury[61]. However, systemic administration of such high doses of MPSS often lead to significant complications such as local wound infection, GI hemorrhage, sepsis, hyperglycemia, respiratory failure and pneumonia which has led to higher rates of mortality independent of the severity of injury[19]. As a consequence of these off-target effects initial clinical excitement surrounding the drug has been curtailed in recent years and its use in acute SCI is now not recommended at all by the American Association of Neurological Surgeons[19]. MPSS is a small molecule pro-drug of methylprednisolone, which uses a sodium succinate ester to improve the water solubility of the glucocorticoid allowing it to be administered at high concentrations via intravenous injection. MPSS is used extensively to treat acute exacerbations in Multiple Sclerosis (MS) patients with somewhat good success. The action of MPSS is highly non-specific and, because of limited drug penetration across the BSCB, extremely high systemic doses must be administered in order to accumulate sufficient drug at the spinal cord lesion. These high doses induce the substantial off target effects described above and generate an unacceptable risk to benefit profile in acute SCI. Improved delivery methods that can ensure enhanced spinal cord parenchyma infusion of MPSS at these critical acute time points could help enhance therapeutic efficacy and establish more favorable outcomes.

Table 2.1 Candidate drugs for mitigating inflammation in SCI

Drug	Drug Description	Mechanisms of Action	Route of Administration	Preclinical Data	Clinical Data	Delivery Limitations
Methylpredni -solone sodium succinate (MPSS)	synthetic glucocorticoid prodrug	Anti-inflammatory; reduces lipid peroxidation; decreases vascular permeability	IV	A number of studies in 1970's and 1980's on cats, dogs and non-human primates demonstrated functional recovery and histological improvements	24 hr dosage (30 mg/kg i.v. bolus plus 23 h infusion as 5.4 mg/kg) showed neuro logical improvements if administered within 8 hrs post injury	Limited BSCB penetration; Significant off-target effects due to high doses of drug
CD11d mAb	mAb against the CD11d subunit of the CD11d/CD18 integrin on neutrophils/mon o-cytes	Reduces infiltration of neutrophils into the spinal cord lesion. Encourages migration and apoptosis of certain leukocytes already in the spinal cord lesion	IV	Rat studies; Administration starting at or before 6 hrs post injury and for a 48 hr duration showed improved locomotion and inclined plane performance, decreased allodynia, decreased autonomic dysreflexia.	Under development with Eli Lilly	Localization, long term storage stability, formulation challenges, immunogenicity at repeat doses
TNF- α mAb	mAb against TNF-α (e.g. Infliximab and Etanercept)	Neutralizes TNF-Alpha, a major inflammatory cytokine.	SC and IP	Rat studies; Administration at time of injury or several hours post injury showed reduced oxidative stress and histological evidence of a reduction in inflammation	Clinically approved for other indications	

In an effort to prevent the off-target effects seen with anti-inflammatory or immunosuppressive small molecule therapies inflammatory modulating biomacromolecules have also been explored in preclinical SCI animal studies. Various antibodies that neutralize specific elements of the inflammatory response following SCI have been explored extensively. For example, a monoclonal antibody (mAb) against the CD11d subunit of the CD11d/CD18 integrin, a receptor found almost exclusively on leukocytes such as neutrophils and monocytes, has demonstrated enhanced neurological recovery outcomes in rats receiving a thoracic clip compression injury[62,63]. Specifically, intravenous (IV) administration of the CD11d mAb no later than 6 hours post injury and for a duration of 48 hours post injury resulted in improved locomotion and inclined plane performance, decreased allodynia, decreased autonomic dysreflexia in response to balloon distension of the colon as well as reduced neutrophil infiltration and greater white matter sparing[62-64]. A FORE-SCI study was initiated to re-evaluate this promising treatment. The replication study did show a promising trend towards enhanced functional recovery and greater neuroprotection in the form of preserved myelin regions on histology but these outcomes were not statistically significant[65]. While intravenous dose response studies have been conducted for this therapy it is unclear how this translates to the proportion of CD11d mAb neutralized leukocytes systemically versus present within the SCI lesion. Furthermore, no studies have assessed the effect of CD11d mAb administration past 48 hours. Given that significant neutrophil and monocyte concentrations may persist within the SCI lesion up to several weeks post injury, it is hypothesized that a more prolonged duration of CD11d mAb administration may be advantageous[29,66].

TNF-α represents another viable inflammatory target for antibody therapy in SCI as it is one of the first inflammatory cytokines that is released in high concentrations following primary trauma and plays a pivotal role in secondary injury mechanisms and the initiation of the inflammatory response[67,68]. Infliximab and Etanercept, which are clinically approved TNF-α receptor antibodies used in auto-immune diseases such as rheumatoid arthritis, Crohn's disease and psoriasis have been investigated for SCI in clip compression models [68,69] as well as in a spinal cord ischemia model induced by infrarenal aortic cross clamping[70]. In these studies the antibody was applied via subcutaneous (SC) or intraperitoneal (IP) injection at the time of injury or at several hours post injury. Across multiple studies these TNF-α inhibition treatments showed reduction in oxidative stress markers and a less-severe inflammatory response.

The aforementioned antibody therapies target relevant elements of acute inflammation with greater sensitivity and specificity as well as demonstrate longer half-life's than MPSS or any other corresponding small molecule inhibitors[71]. However, antibodies that target elements beyond those present in the systemic circulation face substantial delivery challenges for use as treatments in SCI. Due to their large size and the limited BSCB penetration of these biomolecules they must be administered at very high doses in order to obtain meaningful therapeutic local concentrations[72]. In fact, it has been estimated in other CNS disease research that only 0.05–0.2% of a systemically administered dose of antibody ever passes the blood brain barrier (BBB) and reaches the brain. Developing ways of enhancing the penetration of antibody into the CNS has been the focus of much recent research of which the SCI field may benefit[73,74]. Other than localization, antibodies also pose significant long term storage, stability and formulation challenges as well as the potential for unfavorable immunogenicity when administered systemically at repeat doses all of which must be addressed before clinical translation of individual candidates is possible[72,75].

2.3.2 PRESERVING THE PENUMBRA

Without re-establishment of oxygen, glucose and growth factor transport to the uninjured penumbra (under-perfused tissue) surrounding the primary lesion, this ischemic tissue quickly becomes infarcted causing unfavorable propagation of the SCI. Salvaging this tissue from destruction has been a focus of much preclinical SCI research **(Table 2.2)**. Anti-apoptotic and growth/repair supporting drugs such as, minocycline[76-79], erythropoietin (EPO)[80], taxol[21], and growth factors/neurotrophins [81,82] in particular have demonstrated a capacity to improve the protection of the penumbra as well as promote favorable uninjured cell sprouting leading to enhanced functional outcomes.

Minocycline, a tetracycline antibiotic that has similar anti-inflammatory mechanisms of action as MPSS (reducing proinflammatory cytokine levels and free radical damage as well as decreasing T-lymphocyte migration) while also offering anti-apoptotic neuroprotection, has been shown to promote functional recovery in rat contusion models when administered IP [76-79]. In one study of minocycline the drug out-performed MPSS in relation to behavioral outcomes on the Basso Beattie Bresnahan locomotor rating scale[77]. However, while this drug does demonstrate more effective penetration across the BBB as compared to MPSS, high doses of the drug are required when administered IP or orally in order to

achieve any significant neuroprotection. In fact, the oral or IP concentrations of minocycline that are required for neuroprotection (approximately 22–100 mg/kg multiple times daily) in rodent studies are approximately two orders of magnitude higher than the corresponding doses of the drug currently used clinically to treat infectious diseases (3 mg/kg/day) [83]. Administration of minocycline IV has been advocated as a means of improving the delivery efficiency of minocycline for neuroprotection, however unfavorable results in replication studies using both IP and IV delivery methods suggest that both may be inadequate for achieving rapid and sustained high local concentrations of minocylcine at the spinal cord lesion [83-85]. It is possible too that the stability of minocycline, which is known to readily epimerize and lose activity under mild acid and alkaline conditions, may be a relevant delivery constraint that may be contributing to the mixed results [86,87]. Others have incorporated minocycline into an intrathecal osmotic mini-pump in an attempt to enhance local spinal cord drug concentrations and have shown enhanced success in treating SCI chronic pain by attenuating the microglial activiation[88]. These results suggest local application of minocycline may enhance the therapeutic effect, however additional pre-clinical studies investigating the functional improvements using such an approach are needed. Despite the preclinical discrepancies human clinical trials have been initiated for minocycline and the recent results of a phase II study documented functional improvement trends in the minocycline treatment group but these were not statistically significant[89]. Minocycline still ranks as one of the most promising acute neuroprotective candidates by experts in the SCI field due mainly to its comparatively robust preclinical efficacy and relatively prolonged therapeutic window[90].

Erythropoietin (EPO), a 30.4 kDa cytokine has also been explored extensively as an anti-apoptotic therapy in a variety of CNS injuries such as stroke and SCI [15,80,91-93]. When administered IP or IV a recombinant form of EPO provided for enhanced neuroprotection and reduced lesion cavitation in clip compression and contusion injuries as well as acting to reduce lipid peroxidation and delay the increase of damaging inflammatory cytokines [80,94]. In terms of clinical translation, EPO has also been ranked highly as a priority candidate in focused evaluations of possible therapies by leaders in the SCI community due to the relatively robust results obtained pre-clinically across a number of independent studies and the already clinical application of the drug for other indications[15,90]. However, in the corresponding FORE-SCI replication study as well as some other independent studies the functional improvements following SCI attributed to EPO could not be replicated [95,96]. The source of this non-reproducibility is unclear although it has been hypothesized that limited BBB penetration, protein

stability as well as the systemic toxicity associated with high EPO doses as possible causes of variability[97]. It is known that oxygen free radicals can have a significant effect on the activity of EPO[98]. Given the high local concentration of free radicals within the acutely injured spinal cord it is worth considering the possibility of drug damage/denaturation of the limited amount of drug that is actually able to diffuse into the inhospitable lesion. Such a consideration is not isolated to just EPO and the influence of SCI pathology on drug stability and activity should be at the forefront of any preclinical examination. Finally, high doses of EPO are required for neuroprotection *in vivo* and given its long plasma half-life, IV regimes of the drug may considerably disrupt erythropoiesis leading to undesirable side-effects such as polycythemia and secondary stroke [99,100].

Taxol, a formulation of paclitaxel in Cremophor EL (polyethoxylated castor oil) and dehydrated ethanol (50:50, v/v) originally developed and studied as a chemotherapy agent has also been shown to provide neuroprotection from CNS injury, reduce fibrotic scarring and promote functional recovery in a rat contusion model[21]. A subsequent study showed that Taxol was effective in minimizing astrogliosis as well as reducing the infiltration and activation of macrophages and microglia respectively following contusive SCI[101]. In both of these studies due to its very poor aqueous solubility and low drug bioavailability Taxol was infused into the SCI lesion using an intrathecal catheter and osmotic minipump over the course of 28 days. Despite positive results in these SCI studies as well as considerable *in vitro* cell culture and optic nerve crush *in vivo* data supporting the positive effect of Taxol induced microtubule stabilization on axon preservation and growth[102,103], a recent FORE-SCI study of the drug demonstrated only partial replication with no functional recovery being noted[104]. Within the replication study for taxol it was acknowledged that achieving sustained delivery of taxol at the lesion using the catheter system was not trivial (due to solubility limitations) and required customization of a commercially available osmotic pump. This suggests that improved methods of administration may be required in order for taxol to be a robust treatment option for SCI.

Table 2.2 Candidate drugs for preserving the penumbra in SCI

Drug	Drug Description	Mechanisms of Action	Route of Administration	Preclinical Data	Clinical Data	Delivery Limitations
Minocycline	Tetracyline antibiotic	Reduces pro-inflammatory cytokine levels; Anti-apoptotic neuroprotection	IV; IP and Intrathecal catheter	Numerous Rat studies; 22–100 mg/kg multiple times daily provides acute neuroprotection	Phase II data	Very high systemic doses required; drug stability issues; inability to get sufficient local dosing
Erythropoietin (EPO)	30.4 kDa Cytokine	Neuroprotection; reducing lipid peroxidation	IP, IV	Rat studies; neuroprotection and reduced lesion cavitation; reduced cytokine expression and lipid peroxidation. No FORE-SCI replication.	Used clinically for other indications	Stability concerns; off target effects with high doses
Paclitaxel/Taxol	Taxane drug derived from Pacific yew tree formulated in Cremophor EL and dehydrated ethanol (50:50 v/v)	Stabilizes microtubules	Intrathecal minipump	Rat studies; reduced spinal cord scarring; promoted neuroprotection; No FORE-SCI replication	Cancer chemotherapy	Drug solubility and stability issues ; toxic organic solvents used; poor bioavailability
Neurotrophins (NT-3, BDNF, CNTF, GDNF)	Small protein growth factors	Neuroprotection and axon growth and sprouting	Direct intraparenchymal injection; Intrathecal minipump	Rat studies; Neuroprotection and sprouting of axons locally.	-	Local delivery and long term stability issues; off target effects.
Angiogenic Factors (VEGF/EGF/PDGF)	Small protein growth factors	Promotes angiogenesis; Re-establish BSCB	Direct intraparenchymal injection; Intrathecal minipump	Rat studies; Neuroprotection; Repair of BSCB	-	Local delivery and long term stability issues; cocktail of factors required; uncertain temporal window for effect

A multitude of different growth factors and neurotrophins such as VEGF, EGF, PDGF, b-FGF, BDNF, NGF, NT-3, GDNF and CTNF have been explored across numerous SCI preclinical studies [105-110]. The local application of these factors individually as well as in combination via either direct intraparenchymal injection or slow intrathecal infusion using an osmotic minipump have demonstrated an ability to protect tissue from destruction following SCI and also promote sprouting of intact axons. Furthermore, re-establishment of vascular perfusion and BSCB integrity through augmented angiogenesis by application of individual or cocktails of recombinant vascular growth factors such as FGF-2, VEGF, EGF and PDGF has shown to be an effective means of preserving this penumbra tissue and promoting functional recovery[111-114]. However, it does appear that favorable outcomes with this approach may require a specific cocktail of factors to be administered within a finite time window[111]. This suggests that spatial and temporal control of growth factor delivery is critical for success with this type of therapy.

2.3.3 Overcoming extrinsic inhibition

Extracellular glial derived inhibition of SCI regeneration is brought about by two categories of molecules: (i) myelin derived proteins (Nogo A, MAG etc.) which are expressed by oligodendroglia and are present in the debris of demyelinated axons; and (ii) a prominent gliosis composed of reactive astrocytes synthesizing chondroitin sulphate proteoglycans (CSPGs) induced through an injury specific reactive cellular phenotype[115]. The extracellular inhibitory species interact with receptors on intact and damaged axons and initiate intracellular signaling cascades which provoke destructive remodeling of the actin and microtubule cytoskeleton resulting in dystrophic axonal retraction bulbs[38,116]. Small molecule and biomolecule drugs that act on constituents of extrinsic inhibition have been identified with a number of these having been explored extensively by independent investigators in preclinical models of SCI. These drugs include: an anti–Nogo-A antibody[117,118]; Nogo-66 receptor antagonist peptide, NEP1–40[119]; the rho pathway inhibitor, BA-210 or Cethrin® [120-122]; chondroitinase ABC to degrade CSPGs[22]; as well as a small molecule EGFR inhibitor which helps reduce the potency of these extracellular inhibitors on preserved axons[20]. Using these drugs for specific extracellular biomolecular targeting opens up the potential for later stage chronic SCI intervention providing possible treatment time windows beyond just the initial acute phase of injury as would be the case for the former categories of therapies examined here.

The Nogo-A membrane protein derived from CNS myelin was first identified as an inhibitor of axonal regeneration by Schwab and colleagues[123,124]. In an attempt to neutralize Nogo-A's inhibitory effect on axonal repair and growth a number of monoclonal antibodies and recombinant antibody fragments have been raised against defined regions of Nogo-A and tested in preclinical models of SCI in rats and primates[125,126]. Specific clinically relevant monoclonal antibodies explored include: (1) variant 11C7 which is raised against an 18–amino acid peptide sequence of Nogo-A from Rat; and (2) variant 7B12 from a recombinant Nogo-A fragment that is synthesized in bacteria; and (3) a humanized version, hNogo[118,126]. Local treatment of Nogo-A neutralizing antibodies into the subdural space for two weeks using an intrathecal osmotic minipump infusion system demonstrated enhanced corticospinal tract plasticity and improved motor recovery on ladder walk, locomotion and narrow beam tests in a partial transection (T shaped) lesion model in Lewis rats[118]. Further testing of the 11C7 and hNogo antibody variants in a cervical hemisection model in macaque monkeys confirmed the promotion of functional recovery in the form of enhanced manual dexterity [126,127] as well as axonal sprouting[126,128] with four weeks of treatment. However, in the primate study in order to obtain four weeks of treatment a second surgery was required at two weeks in order to remove the first empty pump and implant another full pump to ensure an additional 2 weeks of antibody infusion. The limitations of this delivery method must be addressed for optimized clinical use of Nogo-A antibodies. The humanized version of Nogo-A antibody (designated ATI355) has undergone Phase 1 clinical trial evaluation by Novartis, whereby eligible patients with ASIA A thoracic and cervical injuries received intrathecal infusion of the antibody in a dose escalation from 24 hours to 4 weeks through an indwelling catheter commencing between 4 and 14 days post injury. However, concerns regarding the risk of meningitis associated with such long-term CNS catheter access led to single bolus only injections of the antibody being explored in later patient cohorts[129]. At the time of thesis submission no results had been communicated on the outcomes of the phase 1 trial, in which 52 patients had received the Nogo-A antibody treatment at the conclusion of enrollment in September 2011. Novartis has however indicated an intent to register the drug with the FDA after 2017[130,131].

Another approach to neutralize the effect of myelin-derived inhibitors has been to interfere with their binding to a common receptor, Nogo 66 Receptor (NgR), which is found on oligodendrocytes. To block NgR, a peptide antagonist derived from Nogo designated NEP 1-40 (sequence: acetyl-RIYKGVIQAIQKSDEGHPFRAYLESEVAISEELVQKYSNS-amide; Molecular weight = 4625 Da), was synthesized

on solid phase by Strittmatter and colleagues. The application of this peptide to a thoracic dorsal hemisection lesion by intrathecal infusion showed enhanced functional locomotor recovery as well as sprouting of corticospinal tract and serotonergic fibers when administered at 75 μg/kg/day for 4 weeks[132]. Additional studies highlighted the robustness of the NEP 1-40 effect on functional recovery with a peptide administration delay of up to one week post injury still producing favorable outcomes when delivered via subcutaneous injection or infusion for two weeks at a much higher dose, 11.6 mg/kg/day[119]. Despite success in other CNS trauma studies[133,134], a FORE-SCI initiated replication study could not replicate the extent of axonal sprouting nor the functional recovery previously observed with the peptide administered sub-cutaneously[135]. Furthermore, in this replication, as in the original study, an unusually high mortality rate was observed for animals receiving sub-cutaneous administration of vehicle and drug (approximately 20% mortality in each study). Since NEP 1-40 is a neutral peptide with a high proportion of hydrophobic amino acids, DMSO (17% of total volume) was required to solubilize the peptide in these studies. The chronic use of DMSO in the vehicle and treatment groups could represent the source of the increased mortality observed. While DMSO is generally considered to be a safe solvent when used in aqueous dilutions it is known to induce severe hemolysis, renal failure and cardiac dysfunction among others complications[136]. A recently reported alternative to the NEP 1-40 peptide for NgR receptor neutralization is a ligand-binding fragment (AA 27-310) of the NgR1 receptor, designated NgR1(310)-Fc protein. This fusion protein can also serve as a decoy/block of myelin inhibitors[137,138]. Humanized versions of this protein have been developed and have shown enhanced functional recovery when delivered via intracerebroventricular infusion[139]. Interestingly, this recent study also demonstrated the feasibility of repeat intrathecal lumbar administration of the drug as a means of more appropriate clinical delivery[139]. Applying the NgR1(310)-Fc protein using the lumbar location every four days for four weeks in rats was sufficient to ensure a sustained level of protein within the CSF and promote behavioral improvements. In this study a two phase decay of the drug was observed: (1) rapid elimination over 12 hours and then (2) a slower decay with a half life of 2 days for rat and 5 days for non-human primates. Given the more prolonged retention time of the protein in higher animal species the authors hypothesized that human dosing could involve fortnightly lumbar intrathecal administration of the protein and still be efficacious. This is the first description of the use of a more clinically applicable administration regime for local therapy to the spinal cord and other therapies outlined in this review may benefit from a similar investigation.

Table 2.3 Candidate Drugs for overcoming extrinsic inhibition in SCI

Drug	Drug Description	Mechanisms of Action	Route of Administration	Preclinical Data	Clinical data	Delivery limitations
Anti-Nogo Antibody	Monoclonal Antibody	Neutralizes Nogo-A, a myelin derived protein	Intraparenchymal injection; intrathecal minipump.	Multiple rat studies over the past two decades have demonstrated functional recovery. Non-human primate studies also conducted	Phase I trial completed but yet to be reported on by Novartis	Antibody localization and long term stability
NEP 1-40 / NgR1(310)-Fc protein	Small peptide	Antagonist of Nogo 66 Receptor	Intraparenchymal injection; intrathecal minipump	Rat studies; locomotor recovery and corticospinal tract sprouting	-	Drug solubility issues requiring organic solvents
BA-210/Cethrin	Recombinant protein derived from a toxin	Toxin made by Clostridium Botulinum. Specific inhibitor of Rho. Contains a transport sequence	Clinically BA-210 + tisseal applied to the dura during spinal decompression	Rat studies; improved functional recovery and lesion size reduction.	Phase IIb study completed and reported.	Drug localization, long term stability
Chondroitnase ABC	Bacterial Lyase Enzyme	Degrades CSPGs	Intraparenchymal injection; Intrathecal minipump	Multiple rat studies over the past decade.	-	Drug localization, thermal stability
PD168393	Synthetic small molecules	EGF receptor (ErbB1) inhibitor. Interferes with the signaling from extrinsic inhibition.	Intrathecal minipump	Rat studies; No FORE-SCI replication	-	Drug solubility and stability; achieving sufficient local drug concentrations

An alternative approach for mitigating the effect of extracellular derived inhibitors on axon regeneration and plasticity is to interfere with the activation of important intracellular machinery that control cell growth downstream of the cell receptor binding event. A specific focus of research in line with this idea has been on the role of the GTPase, RhoA. Acting as an intracellular switch RhoA regulates axonal growth during development but also provokes destructive remodeling of the actin cytoskeleton following its activation by extracellular inhibitors resulting in dystrophic axonal retraction bulbs and cell apoptosis [38,116]. Rho activation to the Rho-GTP state is quickly elevated following SCI (as early as 90 minutes after injury) within neurons and glial, peaking at around three days and persisting for at least seven days, making it a viable target for possible acute intervention[140]. The rho pathway inhibitor, BA-210 (formulation trade name: Cethrin®) was developed by McKerracher and colleagues as a treatment for SCI [120-122]. BA-210 (MW~ 25.7 kDa) is a recombinant cell permeable variant of C3 transferase, which is an ADP-ribosyltransferase toxin produced by *Clostridium botulinum* that functions to catalyze the addition of ADP-ribose to the Asn 41 residue of Rho irreversibly inactivating the intracellular protein [121]. In recent preclinical studies, BA-210 was applied to rat SCI models to assess efficacy. Administration of BA-210 was performed extradurally and was formulated in a fibrin gel to ensure localization. In a rat contusion injury model a dose of 15 µg of BA-210 was required to inactivate RhoA to non-injured sham levels at 24 hours. By using BA-210 pre-dosing followed by application of a hemisection lesion from 2 hrs to 7 days the temporal effect of BA-210 was examined. In this experiment, a 50 µg dose was shown to be sufficient to keep the activation of RhoA at sham levels for 4 days, however by 7 days RhoA activation had returned to non-treated injury levels[121]. Finally, animals treated within a 24 hour window after injury with BA-210 showed moderately improved motor functional recovery and a reduced lesion size at doses of 15 µg. This treatment has progressed to Phase I/IIa clinical trials the details of which have been reported extensively [141,142]. This 48 thoracic and cervical patient trial performed a dose escalation of BA-210 from 0.3 mg to 9 mg co-applied with the commercial fibrin gel TISSEEL (designated Cethrin®) onto either the anterior or posterior dural surface of the spinal cord following decompression and spine stabilization surgery. The mean time of drug application was 52 hours. Some functional recovery improvements were noted in patients within the cervical injury cohort who received the BA-210 treatment. The duration of delivery of BA-210 and the length of RhoA inactivation seems to be a major limitation affecting the optimal performance of this therapy. Drug release data on BA-210 from the fibrin matrix either *in vitro* or *in vivo* has not been published. However, it is known that encapsulation of non-binding equivalent size biomolecules within the TISSEEL gel lead to rapid diffusion *in vitro*, with half of total loaded drug leaking out of the system in the first 24 hours with complete

release observed by 4 days[143]. A similar rate of release for BA-210 is supported by the preclinical SCI data[121]. Furthermore, the pharmacokinetic data from the Cethrin® clinical trial suggests that higher doses of drug did not result in a significantly more prolonged release of drug using the fibrin gel supported by the fact that C_{max} increased with escalating dose but not T_{max} or $T_{1/2}$. There are also other limitations associated with the fibrin gel such as rapid proteolytic degradation and immunogenic risks in certain patient cohorts which support the need for alternatives to be investigated.

Another thoroughly evaluated drug within the extrinsic inhibitory category is Chondroitinase ABC (ChABC), a bacterial enzyme that has been applied to digest the glycosaminoglycan (GAG) chains on the dominant astrogliosis derived extracellular matrix product, CSPGs, that surrounds the SCI lesion in high density[45]. This lyase type enzyme uses a beta-elimination catalytic mechanism to facilitate the specific digestion of Chondroitin-4-sulfate (A), Chondroitin-6-sulfate (C) and dermatan sulfate (B) GAG chains [144]. ChABC has shown extensive efficacy in SCI by numerous independent investigators as a stand-alone treatment or in combination with other therapy modalities [22,145-148]. In these studies ChABC has been shown to augment axon regeneration and plasticity as well as promote functional recovery in a variety of different rodent SCI models including hemisection and contusion injuries [13,22,45]. Advantageously, ChABC has a robust therapeutic efficacy window ranging from acute immediate intervention to chronic use (intervention at 4 weeks post injury in rodent model) [149,150]. In all pre-clinical studies of this treatment local SCI application of the ChABC has been necessary to achieve the favorable functional recovery results. Such local administration has involved either: (1) direct intraparenechymal injection at the injury epicenter; (2) injection at locations slightly rostral/caudal to the lesion where there is a high density of CSPGs; or (3) intrathecal infusion using indwelling catheter technology. Since CSPG concentration seems to peak around 7 days after injury and persistent synthesis of these GAGs has been observed post injury, prolonged activity of ChABC will be necessary for establishing efficacy with this treatment. Supporting this hypothesis are results from a number of single dose ChABC studies in which treatment in more severe, clinically relevant, contusion models failed to show functional improvements[146,151]. It is important to note that in order to achieve persistent local therapeutic dosing of ChABC the above routes of administration require reapplication of freshly prepared enzyme every other day for 10-14 days[149]. While it has been suggested that some enzyme activity can be maintained up to 10 days after a single injection *in vivo*, it is unclear for how long therapeutic concentrations of ChABC are maintained[152]. The half-life of ChABC detection within CNS tissue is approximately 4.66 days

(self-calculated from paper data) and suggests particular susceptibility of the enzyme to denaturation *in vivo*[152]. *In vitro* evidence also confirms that ChABC is particularly susceptible to thermal stresses with an even shorter half-life in solution at 37°C than what was observed *in vivo* [153,154]. Excitingly, a number of pharmaceutical excipients have shown an ability to enhance the long-term stability of ChABC for up to several weeks *in vitro*[155]. Since an administration regime involving multiple local injections is not readily clinically feasible, efforts have been made to address the stability challenge of ChABC through the use of gene therapy and cell technology[156,157]. However, while some of these approaches have led to exciting pre-clinical data, substantial formulation development work is still required to develop a safe vector for the gene therapy of which the ongoing CHASE-IT consortium is actively leading [131]. It is uncertain however how such approaches applied to SCI will be received by regulatory agencies [158].

A final promising therapy for mitigating the inhibitory extracellular effects following injury involves the use of a small molecule EGFR inhibitor, PD168393. This drug was initially developed for cancer applications but was later shown to prevent the inhibition from myelin debris and CSPGs on axon regeneration of cerebellar granule cells *in vitro* as well as promote regeneration of optical nerve fibers after crush injury [159,160]. The specificity of PD 168393 to inhibit the EGF receptor (ErbB1) and consequently allow primary neurons to overcome axonal regeneration inhibition from extrinsic factors was subsequently validated within *in vitro* receptor knockout studies[161]. On the basis of this promising data, Olson and colleagues assessed the drug's efficacy in a rodent contusion study[20]. In this study they showed that intrathecal administration of the drug led to enhanced motor, sensory and bladder recovery. Given the promising results from this study, PD 168393 was re-evaluated in a FORE-SCI replication study. However, this follow-up study failed to replicate the original results and alarmingly instead showed inferior functional outcomes with use of the drug compared to the SCI control group[26]. The authors of the replication study noted several limitations associated with the delivery of the PD 168393 drug including: (1) excessive movement of the cannula attached to the osmotic pump causing additional damage to the spinal cords of numerous animals; (2) drug solution precipitation over time and (3) solubility variability amongst different drug lots. Surprisingly, despite obvious drug property differences between the initial study and the replication no chemical properties characterization was performed as part of this replication. A detailed analysis of the chemistry of PD 168393 shows that it contains an acrylamide moiety, with this functional group required for achieving the irreversible inhibition of the EGF receptor. Specifically, the acrylamide group reacts with a free cysteine at the 773

residue on the EGF receptor irreversibly alkylating it by a Michael addition mechanism[159]. It is possible that without incorporation of a radical inhibitor or with inappropriate long-term storage that the acrylamide functionality on PD 168393 may be compromised leading to molecule homopolymerization that results in decreased DMSO/aqueous buffer solubility, reduced drug activity and consequently the generation of inconsistent *in vivo* results. While it is unclear whether drug instability is the specific cause of the PD 16393 non-replication in this instance, the solubility issues identified serve as a cautionary tale for the importance of ensuring preserved drug integrity during long-term delivery in preclinical testing of any therapeutic for SCI.

2.4 Drug delivery in SCI using biomaterials

The most promising drug candidates for SCI all currently face considerable delivery limitations that represent significant barriers for clinical progression. Some of the universal challenges that are routinely highlighted throughout the literature and were identified in this chapter include: (1) Insufficient drug doses reaching the site of injury within the spinal cord using non-invasive delivery methods such as IV or IP administration because of the relatively impermeable BSCB; (2) Undesirable off-target effects associated with high systemic drug doses; (3) Local spinal cord administration requirements for certain drugs; (4) Unreliable or underperforming catheter and pump technology used for local administration; (5) Formulation issues associated with aqueous solubility and stability of compounds resulting in uncertain local administration; and (6) Short half-life for drugs that reach the desired site of action in the spinal cord necessitating repeat invasive dosing. To address these limitations scientists and engineers have turned to developing and utilizing innovative biomaterial technologies as a means of improving drug formulations to ensure controlled and targeted delivery of these therapeutics. Biomaterial technology encompasses any substance other than the drug itself that interacts with the host biological tissue or fluids. Materials used in drug delivery can be sourced from both natural and synthetic sources and a number of materials have extensive preclinical and clinical safety support behind them. These materials can be fabricated into bulk implants, formulated into particles on the nano- or micro- scale or assembled into combinations of different size scale elements and can be applied either locally at the SCI lesion or systemically. A number of biomaterial approaches have been utilized to improve the delivery of the candidate drugs described in the previous section to the CNS.

2.4.1 MPSS

Biomaterial systems for controlled local and systemic targeted delivery of MPSS have been developed. Bellamkonda and colleagues designed a system whereby MPSS was encapsulated within poly(lactic-co-glycolic acid) (PLGA) nanoparticles prepared using a double emulsion method and then embedded within an agarose gel. This combination system has been applied to the dural surface of a contusion injury and to a dorsal over-hemisection lesion both in rats [162,163]. Using a fluorophore conjugated to MPSS for visualization this group observed that drug penetration into the contused spinal cord parenchyma was only achieved when the dura mater had been compromised during surgery suggesting that topical delivery across intact dura mater is not readily possible[162]. This important finding suggests that intrathecal or intraparenchymal injection approaches are required for contusion type lesions. Within the contusion study, animals receiving the treatment that showed a damaged dural surface demonstrated reduced lesion sizes at 7 days through this topical local delivery. In a subsequent study using the dorsal over-hemisection injury, improved functional performance on grid and beam walking was observed up to four weeks after injury with the local biomaterial treatment[163]. More recently, methylprednisolone-loaded nanoparticles formulated by grafting carboxymethylchitosan (CMCht) to a poly(amidoamine) (PAMAM) dendrimeric core were applied to a lateral hemisection rat model in an effort to improve local intracellular uptake of the drug[164]. Moderately improved locomotor scores were observed in animals treated with MPSS loaded nanoparticles compared to MPSS applied at the hemisection lesion, although the underlying biological mechanisms responsible for this improvement *in vivo* were not confirmed.

In an effort to improve the systemic delivery of methylprednisolone to the CNS and reduce the off target effects seen with the naked drug, the use of PEGylated liposomes have been extensively explored. In a model of multiple sclerosis (experimental autoimmune encephalomyelitis (EAE)), poly(ethylene glycol) (PEG) liposomes facilitated high, prolonged concentrations of the drug prednisolone within spinal cord parenchymal tissue for up to 42 hours whereas naked glucocorticoid was only marginally detectable at 2 hours and not at all there after[165]. The use of the liposomes resulted in reduced T-cell and macrophage infiltration within in spinal cord in this investigation. However, while this study showed prolonged drug circulation and some increased CNS uptake, high serum levels of drug were also observed which may still lead to significant off-target events. More recently, others have addressed this issue by enhancing the BBB penetration of MPSS containing nanoparticles by conjugating glutathione to the surface of the liposome[166]. This formulation modification resulted in an 8.5 fold increase in MPSS concentration within

CNS tissue compared to free MPPS correlating with a significant decrease in disease burden at one week within an EAE model. Particles containing the conjugated glutathione showed a greater effect than liposomes without it. Excitingly, in a follow up study by this group, they showed that these particles were more effective than free methylprednisolone at an order of magnitude lower dose in treating the EAE model and specifically lowering macrophage infiltration by 50% and reducing the extent of demyelination[167]. This technology (tradename: 2B3-201 developed by BBB Therapeutics) has yet to be applied to models of traumatic spinal cord injury but given that the technology is now being tested in pre-clinical ALS[168] and a Phase One trial of relapsing-remitting MS (NCT02048358) it certainly warrants consideration for SCI preclinical investigation. Furthermore, this glutathione liposome particle platform may find utility for the improved CNS delivery of other similar small molecule drugs for SCI.

2.4.2 *Minocycline*

A thermosensitive injectable physical hydrogel composed of a block copolymer of tetronic (tetra-functional block copolymer of ethylene oxide and propylene oxide repeat units) and oligolactide was used to deliver minocycline to a hemisection SCI injury[169]. By delivering minocycline using the tetronic-oligolactide hydrogel a reduction in infiltrating macrophages and synthesis of CSPGs was observed as well as an increase in axonal density within the lesion site. In an effort to enhance the CNS localization of minocycline, prevent the need for multiple daily high doses of the drug as well as ensuring its enhanced stability *in vivo* a number of biomaterial nanoparticle formulations have been developed which may also find utility in SCI. The use of PEG liposomes stabilized with calcium chloride increased the circulation time of minocycline such that a sustained benefit in the MS EAE model was seen when doses were administered at 5 day intervals, compared to a required daily dosing schedule for the drug alone to achieve the same effect[170]. The metal binding properties of minocycline have been leveraged to create Polyion complex (PIC) micelles, another form of nanoparticles amenable to IV administration[86]. These PIC nanoparticles were composed of a block copolymer of carboxymethyldextran-block-poly(ethylene glycol) and have been shown to enhance minocycline stability *in vitro* while not comprising the activity of the drug. Further studies are needed to assess the effect of these encapsulation technologies on the performance of minocycline in SCI.

2.4.3 EPO

Local delivery of EPO using a controlled release biomaterial system has been investigated for SCI. Specifically, Shoichet and colleagues used an injectable physically crosslinked hydrogel derived from a blend of hyaluronan and methylcellulose (HAMC) to improve the performance of EPO locally in SCI[171]. This HAMC hydrogel cures rapidly *in situ* due to the phase transition of the methycellulose at 37°C and the blended material has shown favorable safety and some stand-alone efficacy when administered intrathecally to the spinal cord following a clip compression injury[172]. The *in vitro* studies using this material to encapsulate EPO showed rapid release over a 16 hour period via diffusion mediated release with 80% total activity preservation. Upon administration of the physical hydrogel intrathecally they observed fast initial loss of material (approximately 65% within the first 24 hrs) likely due to sol dissolution prior to the onset of gelation and limited material preservation thereafter with complete degradation and clearance by around 4 days. Despite the limited material preservation *in vivo*, improved performance of EPO delivered by the hydrogel was observed. Specifically, delivering EPO from the hydrogel resulted in a reduced lesion cavity size and a higher preserved neuron count but ultimately functional recovery improvements were not observed. Further studies showed benefit in using the HAMC hydrogel-EPO system in a stroke model whereby epi-cortical administration demonstrated decreased cavity sizes when applied 4 days and 11 days post stroke [97]. The reactive astrocytic response and activated microglia, as measured by GFAP and CD68 staining respectively, was also reduced with this treatment. Although these reports are encouraging, enhanced outcomes may be achieved if engineering issues associated with the rapid release of drug and fast dissolution of the hydrogel material can be addressed. Others have shown that PLGA nanoparticles improve the performance of EPO in a model of stroke leading to enhanced functional recovery, reduced infarcted volumes and the need for 10-fold lower IV doses of EPO to achieve equivalent neuroprotection [173]. With these encouraging results and the existing clinical use of recombinant EPO for other indications further investigation of this drug with other biomaterial platforms is warranted.

2.4.4 TAXOL/PACLITAXEL

Given Paclitaxel's prominent use as a cancer chemotherapeutic agent and its inherent solubility limitations a number of approaches to improve delivery using biomaterial technology have been developed for non-SCI CNS applications[174]. Specially, Paclitaxel has been loaded into a variety of locally applied drug delivery systems using hydrophobic polyesters such as PLGA and Polilactofate as well a

PEG-PLGA block copolymer hydrogel formulation leading to improved survival in animal brain tumor models [175-177]. Furthermore, PLGA particles encapsulating Paclitaxel coated with glutathione have shown to offer improved BBB penetration, similar to that seen with MPSS formulations described before, offering a systemic administration alternative for paclitaxel [178]. Currently in clinically use for several non-CNS applications such as pancreatic and breast cancers is Abraxane®, a Paclitaxel bound albumin nanoparticle[179]. This formulation is organic solvent free and has consequently shown reduced toxicity and increased efficacy. Unfortunately, to date none of these technologies have been investigated for use in SCI. However, given the strong mechanistic understanding for the effectiveness of Paclitaxel as an axon microtubule stabilizer and the inconsistent *in vivo* SCI results, exploration of some of these well characterized biomaterial technologies for enhanced delivery of Paclitaxel to SCI is certainly warranted.

2.4.5 NEUROTROPHINS/GROWTH FACTORS

Local delivery of individual and combinations of growth factors and neurotrophins has been explored extensively using a number of different biomaterial platforms and has been reviewed extensively elsewhere [180,181]. These therapeutic candidates have received the most attention by biomaterials researchers most likely due to their well-characterized mechanism of action, demonstrated preclinical efficacy in SCI, commercial availability and the fact that they are relatively stable proteins amenable to various biomaterial formulation procedures. Unique injectable biomaterial hydrogels made from HAMC, bioinert synthetic PEG, poly(N-isopropylacrylamide)-PEG copolymer (PNIPAAm-g-PEG), agarose, natural fibrin and collagen biomacromolecules have been used by independent investigators to deliver FGF-2[182,183], VEGF[184], EGF/FGF2[185], VEGF/EGF[111]; BDNF[186-188] or NT-3[189-191]. In most of these studies a trend towards increased white matter sparing, reduced lesion sizes and in some instances functional recovery improvements through use of the biomaterial system to deliver these biomolecule drugs has been noted. Pre-fabricated scaffolds/hydrogels have also been used to deliver neurotrophic growth factors to SCI. Specifically, freeze dried porous agarose scaffolds were coated with a collagen hydrogel encapsulating BDNF[192] and a non-biodegradable poly(2-hydroxyethyl-methacrylate) (PHEMA) hydrogel was soaked in BDNF before implantation[193]. The SCI model used in almost all these studies involved a hemisection injury or similar dural penetrating lesion, which allows for the material to be implanted or injected into the free space created by the resulting SCI. However, there are a few notable exceptions to this type of injury model. In one instance, local application of PLGA nanoparticles encapsulating GDNF was applied directly to a thoracic contusion model resulting in improved functional outcomes and

enhanced axonal density at the lesion without enhanced glial activation[194]. Furthermore, just like with their EPO studies, Shoichet and colleagues applied a collagen gel intrathecally to deliver the EGF/FGF2 combination to a clip compression model[185]. Interestingly, to enhance tissue penetration and stability of FGF2 delivered locally by intrathecal administration this group subsequently pegylated FGF-2 and demonstrated persistent enhanced concentrations of drug within the injured spinal cord[183]. Further studies by this group have utilized a combination biomaterial system whereby NT-3 or FGF-2 was first encapsulated within PLGA nanoparticles prepared by double emulsion before being embedded within the readily permeable HAMC hydrogel matrix[182,195]. Controlled release of NT-3 and FGF-2 using this system was extended from 24 hours seen with the hydrogel alone to up to 28 and 18 days *in vitro* respectively. The extended release formulations demonstrated a triphasic release profile characteristic of biomacromolecule diffusion from PLGA. With this now prolonged delivery functional improvements were noted in a clip compression model for NT-3 at 21 days post injury while in the same model sustained FGF-2 treatment resulted in enhanced angiogenesis/vasoprotection at the lesion site. While this approach is promising, the need to fabricate nanoparticles under harsh conditions that include the use of organic solvents as well as sonication and lyophilization processes can cause considerable loss of encapsulated protein activity during formulation and requires the use of carefully selected excipients for optimized preservation of biomolecule integrity[196].

2.4.6 Anti-Nogo-A Antibody

The same combination HAMC hydrogel-PLGA nanoparticle system utilized for sustained NT-3 and FGF-2 delivery has also been investigated *in vitro* for delivery of anti-Nogo A antibody[197]. In this study the use of trehalose and hyaluronan as excipients was required for enhanced stabilization of the antibody during processing and also delivery. However, despite the incorporation of these excipients the observed bioactivity of the drug still followed a sharp exponential decay with less than 10% active antibody detected at 7 days. These data suggest that enhanced systems that can ensure prolonged stability of encapsulated proteins during controlled release is a major priority particularly for these more complex biomacromolecules. In another study, a nogo-66 receptor antibody was conjugated to a hyaluronan-polylysine hydrogel via a reversible hydrazone linkage and demonstrated evidence of gliosis reduction and enhanced axonal growth when implanted as a bulk scaffold into a SCI hemisection lesion[198]. This is one of the first studies within the SCI field to demonstrate the feasibility of drug conjugation to a biomaterial system as a viable approach for extending protein release *in vivo*.

2.4.7 CHONDROITINASE ABC

Several biomaterial systems have been used for local application of ChABC to SCI. Given ChABC's susceptibility to thermal denaturation at 37°C, Bellamkonda and colleagues also utilized trehalose as a stabilizing agent to prolong the release of active drug. Using a high concentration of trehalose (1M), ChABC remained functionally active for 4 weeks and upon lipid microtubule encapsulation achieved extended release and maintained activity for 15 days *in vitro*. For *in vivo* delivery to a dorsal over-hemisection, ChABC encapsulated lipid microtubules were embedded into a 1% agarose gel that was applied topically on the dorsal surface of the dural penetrating lesion. Treated animals demonstrated increased CSPG digestion at 2 weeks that was preserved for 6 weeks and in addition behavioral outcomes and local axonal sprouting was improved[199]. Enhanced behavioral and histological outcomes were noted when both ChABC and NT-3 was loaded into the lipid microtubules and applied to the SCI[199]. In another study a commercially available Fibrin gel, Tisseel, that was further crosslinked with the naturally derived compound Genipin achieved extended release of functionally active ChABC *in vitro* for up to three weeks[200]. The injection of this system into a hemisection model resulted in significantly enhanced concentrations of Chondroitinase ABC and a lower local GAG concentration being observed at three weeks post injury[200]. It is interesting to note that in this study no significant thermal denaturation of ChABC was observed. On the back of the favorable results achieved with the ChABC/Neurotrophin combination, others have incorporated the two biomacromolecules into electrospun fiber scaffolds that were implanted into a transection injury model[201]. Specifically, NGF and ChABC were encapsulated into alginate hydrogel beads that were then loaded into a polydioxinone (PDS) aligned fiber scaffold. Using this biomaterial system active NGF was released for up to 10 days *in vitro* while ChABC was detectable only up to 4 days. Despite the limited release time significant functional recovery was noted at 21 days post injury.

To our knowledge, the remaining drugs identified as promising candidates in the previous section of the review have not yet been evaluated using any biomaterial technology. The exception to this is Cethrin® which has only been studied with a fibrin matrix and the details of this were covered in the previous section. It is not entirely clear why CD11d and TNF-α antibodies, NEP 1-40 peptide or PD 168393 have not yet been evaluated using appropriate drug delivery technology, but given the current limitations associated with each drug, future investigations with such systems would seem to be warranted.

2.5 ADDRESSING DELIVERING CHALLENGES IN SCI THERAPIES USING BIOMATERIALS

The SCI research field has made significant progress towards treatments for paralysis over the last two decades with numerous candidate therapies producing exciting preclinical functional recovery data and some drugs entering early stage clinical trials. However, crossing the translational divide for many of these candidates has proven a challenge due in part because of the unsatisfactory drug delivery technology currently available. Many of these drugs cannot be administered effectively via traditional routes. Furthermore, the widely employed local administration applied in preclinical SCI studies, the intrathecal catheter and pump, is an inferior local delivery technology and possesses significant problems associated with a highly invasive procedure, secondary spinal cord compression and damage, infection, fibrotic scarring and uncertain pharmacokinetics due to catheter occlusions and long term drug instability [23,24]. Biomaterial technologies, unlike traditional administration approaches or indwelling intrathecal catheter technology, provide a versatility platform to achieve local extended delivery of appropriate concentrations of various classes of therapeutic agents to the spinal cord. For locally applied biomaterial systems, only a single surgical procedure is required and many can be injected non-invasively into or upon the spinal cord minimizing secondary cord damage and the risk of infection. Importantly, biodegradable biomaterial systems ensure that all loaded drug is delivered. Furthermore, novel biomaterials are being developed that create local microenvironments that complement the cellular and tissue reorganization promoted by the therapeutic agent rather than inducing conflicting remodeling such as created by an unfavorable foreign body response [202-204]. Furthermore, with innovative biomaterial nanoparticle technology that can penetrate the BSCB it is now feasible to achieve prolonged therapeutic drug concentrations within SCI tissue such that non-invasive IV delivery methods are a reasonable future possibility. Despite their promise there are a number of important considerations that will continue to drive the future research and innovation for biomaterial delivery technology applied to SCI.

2.5.1 LOCAL VERSUS SYSTEMIC DELIVERY USING BIOMATERIAL SYSTEMS

An inability to optimally deliver drugs at therapeutic concentrations and to the desired location in or around the spinal cord lesion can significantly dilute efficacy. Biomaterial systems offer an alternative means of achieving local delivery of drugs to the spinal cord. But what delivery approach will have the most appropriate clinical benefit to risk profile? There are two main approaches to achieving delivery to the spinal cord: (1) local application and (2) targeted systemic delivery.

Injectable materials such as hydrogels represent the best local delivery candidates. These materials can be injected either intraparenchymally or within the intrathecal space with good success[205,206]. However, it is currently unclear which application approach will be the most efficacious. The intraparenchymal approach is more invasive and potentially more prone to secondary cord damage but ideally has the best prospects for achieving optimal sustained delivery to the cells within or around the spinal cord lesion that need the therapeutic. By contrast application of the biomaterial within the intrathecal space minimizes the prospects of further cord damage. However, at this site the high rates of CSF flow across the material may speed up its degradation as well as dispersing drug away from the desired delivery location. A comparative study that determines which method achieves the safest optimal local delivery using applicable hydrogel technology will be required in the future. Achieving local administration of the therapeutic agent however is only one facet of the delivery challenge. Targeted delivery whereby the system interacts with specific cell populations such that they preferentially uptake the therapeutic agent would be ideal. To achieve this goal, one approach would be to incorporate active cell adhesion substrates within the material such that interactions with the cell populations that are the explicit target of the therapeutic being delivered are favored. These substrates are typically formed through the incorporation (either by physical or chemical manipulation) of natural ECM derived proteins or synthetic peptide ligands that contain functional amino acid sequences that integrins or other receptors on the surface of the cell will recognize. Constructing such biomimetic materials has been given considerable attention by the biomaterials research community with applications in SCI a core focus. Self-assembling peptide amphiphiles of various functional epitopes have demonstrated functional recovery as well as favorable tissue remodeling in a variety of different rodent SCI models [207]. Natural derived matrices such as salmon fibrin that contain numerous cell adhesion functional sequences have also shown to improve preclinical SCI recovery [208]. Interestingly, exploiting specific ligand-integrin interactions of cell populations in the spinal cord to improve the uptake of drugs delivered by that material has yet to be reported to our knowledge.

The second approach to delivery, which is certainly less invasive than local material administration via a surgical intervention, is systemic targeted delivery. In this approach drug delivery carriers are formulated with specific physiochemical properties and functionalized with biochemical moieties, which will allow the nanoparticles to be specifically localized to the SCI lesion site by providing some means for them to exit the systemic vasculature through preferential penetration of the BSCB. Achieving this is not trivial but the field is beginning to identify and understand the interactions of certain particles and

biomolecules have with elements of the BSCB and BBB[209]. As described in the MPSS section, glutathione has already demonstrated an ability to enhance the capacity of liposomes and PLGA nanoparticles to cross the BSCB. More recently, the therapeutic window of non-targeted nanoparticles has been characterized in a rat contusion model[210]. In this study measurable uptake of nanoparticles was only observed in the acute period up to 96 hours after injury and only particles with a size less than 200nm were detectable within the spinal cord parenchyma. Future studies focused on identifying other biochemical moieties that may enhance SCI penetration to ensure: reduced off target drug interactions; increased concentration of drug locally in the spinal cord lesion; and longer therapeutic time windows would seem a worthy research pursuit.

2.5.2 *Pre-clinical evaluation of biomaterial therapies in SCI: model considerations*

The application of the biomaterial-drug therapy is greatly influenced by the type of SCI. It is well known that the dominant mode of clinical SCI is a contusion or compressive injury resulting in a centralized non-dural penetrating necrotic lesion[27]. A preclinical rodent model of contusion injury induced using a number of different standardized devices has been in wide circulation for almost 20 years within the SCI research community[211,212]. However, despite the extensive validation and availability of this model, as seen throughout the previous section of the review, the majority of investigators studying locally applied biomaterial therapies have preferred to continue to use hemisection injury models to evaluate their respective therapies. The extensive use of this model is likely because it is relatively easy to implement and provides a convenient free space in which the material can be either injected into the open cavity or pre-gelled/fabricated and then implanted into the defect site. While application of the material to the SCI lesion is more straightforward with this model, the cellular response to injury is considerably different to that of the contusion injury. Specifically, tissue remodeling observed in the hemisection lesion such as contralateral axonal sprouting as well as fibroblast and Schwann cell infiltration is absent in the contusion lesion. There is certainly benefit in evaluating the performance of new biomaterial-drug therapies in the hemisection model and this injury type does provide a precisely controlled lesion for the detailed study of regeneration mechanisms related to specific neural pathways and for the identification of new drug candidates. However, further follow-up studies assessing the application of the material to a contusion lesion must be explored if the clinical use of these drug delivery system is to be realized. One reason such studies are not routinely preformed is due to the complications and variables associated with injection or implantation of a biomaterial into a contusion lesion. Specifically, variables such as time of biomaterial application post injury, location, volume (and consequently drug

loading) and rate of injection parameters are all capable of significantly affecting outcomes. Furthermore, the size scale of the rodent spinal cord can make it challenging to reasonably replicate the application conditions that would be intended for clinical use as well as making fabrication of appropriate sized implants difficult. While currently not a standard of surgical care clinically, there is a growing school of thought that suggests that removal of the early-formed necrotic tissue within the spinal cord parenchyma via a myelotomy procedure during decompression surgery may decrease local spinal cord pressure and enhance wound healing[213-216]. Performing a myelotomy before the introduction of any biomaterial therapy would help to reduce cord tissue pressure as well as create additional free space in which to more readily apply the biomaterial system to a contusion lesion. However, further preclinical studies are needed, particularly in larger species such as pigs or non-human primates in which the size scale of the spinal cord is more clinically representative, in order to evaluate the viability of such an approach.

2.5.3 ENHANCING THE TEMPORAL PROFILE OF DELIVERY FROM BIOMATERIAL SYSTEMS

Once optimized delivery location is achieved, long-term constant delivery of the therapeutic agent is the next desirable trait. For many treatments, the longer the active drug is applied at the lesion site, the better the outcome [217]. For many of the drugs described in this review release profiles on the order of 2-4 weeks would be most desirable. Biomaterial researchers have developed a number of approaches to enhance the release profile of various drug types. Injectable hydrogel matrices, which are a favored biomaterial technology for SCI because of their ease of local application to the spinal cord, are often extremely permeable and contain predominantly water[204,218]. This means that even the largest proteins readily diffuse out of the system resulting in complete release of drug cargo over a period of a couple of days. The two principal approaches used to achieve enhanced spatiotemporal control over drug release with these type of systems are: (a) prior encapsulation of drugs within protective vehicles such as liposomes or other nano[219,220] and micro-particles[221] and then subsequent embedding within a hydrogel matrix, or alternatively (b) attachment of drugs to bulk material substrates such as a hydrogel or scaffold through either direct covalent attachment or by facilitating binding through non-covalent affinity interactions [222]. Within this chapter we have documented several examples where composite systems involving embedded nanoparticles within hydrogel matrices have been used to enhance delivery of drugs in SCI[182,195,199]. Furthermore, drug affinity control has been explored in a SCI context to deliver neurotrophins[223], and there are exciting *in vitro* reports on other relevant SCI candidate drugs using this

method [224,225]. A final approach for improving the long term delivery of drugs from injectable materials is to increase the inherent barrier to diffusion of the molecule from the matrix itself. We recently described a hydrogel system that significantly delays release of model biomacromolecules with good tunability by utilizing biodegradable amphiphilic ethoxylated crosslinking precursors that ensure higher polymer content without any unfavorable matrix swelling[226]. Favorably, this system allows direct drug encapsulation into the hydrogel without additional processing and uses biorthogonal chemistry that ensures high preservation of complex biomolecule structure and activity. With an ability to control drug release precisely within a 5 to 35 days window exploring the use of this material as an SCI drug delivery system is a major priority for our group.

2.5.4 IMPROVING STABILITY OF THERAPIES IN BIOMATERIAL SYSTEMS

While long-term delivery of therapeutics is desired, such an achievement is rendered useless unless stable, functionally active drug can be preserved throughout the complete duration of release. Unfortunately, many SCI relevant recombinant protein drugs such as neurotrophins, ChABC, anti-NogoA antibody etc. become functionally inactive within hours or days when exposed in a carrier-free form to physiological conditions[227]. In order to improve the performance of drug formulations investigators have explored a variety of excipients that protect these molecules from sources of chemical and physical instability such as aggregation, denaturation/unfolding, oxidation, hydrolysis and disulfide exchange. As mentioned previously Bellamkonda and colleagues have shown that trehalose can effectively stabilize ChABC from thermal damage[199]. In contrast Stoichet et al. have shown preliminary *in vitro* success using trehalose and PEG to protect NT-3 and hyaluronan and trehalose to protect Anti-Nogo A during processing and release from PLGA nanoparticles embedded in HAMC respectively [196,197]. Preventing damage of biomolecule drugs during processing events from sources such as organic solvents, sonication, lyophilization, UV or thermal curing as well as the injury related events that can damage proteins (e.g. oxidative stress, local pH changes, lipid peroxidation products, enzymatic degradation) are also important considerations. Another important consideration is the long-term stability of therapeutics as they are delivered in vivo. While small molecule excipient additives may provide short-term protection for large biomacromolecules, given their size mismatch they tend to diffuse out of the matrix more quickly than the drug itself, leaving it susceptible to damage at the later stages of delivery. Such a phenomena was described within the in vitro release studies of Anti-Nogo A[197]. By using innovative chemistry techniques to incorporate excipients into the biomaterial matrix enhanced long-term stabilization of therapeutics may be possible.

2.6 Conclusions

The future is bright for the use of biomaterials to improve the clinical performance of SCI therapeutic candidates. This background chapter highlighted many promising drug candidates that have generated exciting preclinical efficacy in animal models of SCI. However, upon further study of these drugs via rigorous replication studies several barriers to achieving clinical success have been identified. Biomaterial systems provide versatile platforms for which to improve the performance of these drugs. Through greater collaboration with biomaterial scientists and the neuroscientists who are generating these pioneering drug discoveries, rigorous evaluation of the enhanced efficacy of biomaterial therapies within relevant pre-clinical contusion models will be possible and the pace toward clinical trials will be greatly accelerated.

3 Synthesis and Characterization of a Library of In-Situ Curing, Nonswelling Ethoxylated Polyol Thiol-ene Hydrogels for Tailorable Macromolecule Delivery

This work was previously published as: O'Shea, T. M., et al. (2015). Synthesis and Characterization of a Library of In-Situ Curing, Nonswelling Ethoxylated Polyol Thiol-ene Hydrogels for Tailorable Macromolecule Delivery. Advanced Materials (27): 65-72.

3.1 Introduction

There is a need for improved long term performance of therapeutics applied to numerous clinical indications such as central nervous system diseases, post-surgical analgesia and targeted chemotherapy among others[228-230]. Many of these conditions pose unique drug delivery challenges and as such the development of locally administered, and locally maintained, sustained drug therapies is of significant interest [231,232]. Locally applied bulk resorbable and non-resorbable implants are currently in clinical use for a variety of applications including the treatment of glioma, enhancement of stent performance, and improved fracture fixation [233-235]. There are many other indications that would benefit from similar local drug treatments but which the implantation of a bulk product is not feasible. Injectable hydrogels, composed of hydrophilic polymers that are covalently or physically assembled into insoluble infinite networks, represent versatile materials for local non-invasive *in vivo* drug delivery [218,236,237]. The unique biocompatibility of poly(ethylene glycol) (PEG), has seen it utilized as a dominant hydrogel material for many applications [238]. PEG hydrogels have been used to deliver small molecule drugs, proteins, polysaccharides and oligonucleotides [239-242]. These injectable systems provide spatiotemporal control of the release of therapeutics by leveraging drug diffusion, material degradation and/or drug-matrix affinity binding processes [243].

Despite their promise, many PEG hydrogels possess functional limitations that affect their prospects for clinical translation such as: (i) unfavorable toxicity and drug damage caused by the conditions/catalysts that facilitate the chemical reactions that lead to gelation [244-246], (ii) impractical or uncontrollable

gelation times [247], (iii) the tendency for PEG networks to significantly swell upon equilibration and during degradation precluding their effective use in enclosed (fixed volume) *in vivo* environments [248-250], (iv) lack of tunability of material degradation such that the material persists for periods well after the last amount of useful drug has been released exacerbating the foreign body response[251,252], and (v) restricted spatiotemporal control of drug release resulting in high percentage of total drug expelled over the initial hours of application [238,243,247]. It is important that these limitations be addressed if hydrogel materials are to be used as clinical drug delivery platforms.

3.2 Results and Discussion

Our work focuses on the synthesis of hydrogels that overcome the identified limitations and thus provide a versatile platform for the delivery of diverse drug-types. Here we synthesized a library of different tri-**t**hiol-functionalized **e**thoxylated **p**olyol **e**sters (**TEPEs**) and combined these with different molecular weight PEG diacrylates (PEGDA) to form a library of hydrogels with diverse physiochemical properties. To synthesize the TEPEs a transesterification reaction was performed between an ethoxylated polyol and excess of an ethyl ester of a thiol acid using Candida Antarctica Lipase B (CALB) immobilized on acrylic resin as a catalyst [253] **(Figure 3.1a)**. The reaction was performed at 50°C under solventless and moderate vacuum conditions to achieve high degrees of functionalization ($f_{SH} \geq 90\%$) and complete ester chemoselectivity **(Figure 3.S1-8)**. The solventless conditions for this reaction allowed for simple large-scale synthesis, while silica flash chromatography was used to effectively purify the product with limited impact on yield. To explore the structure-function effects of small chemical differences in precursor molecules on resultant network properties we modified two key parameters: (i) the core ethoxylated polyol and (ii) the terminal thiol functionalized ester. For the core ethoxylated polyol, two tri-functional structures were selected, glycerol ethoxylate (GE) and trimethylolpropane ethoxylate (TMPE). Both ethoxylated polyols possessed an equivalent number of ethylene oxide repeat units ($EO_n \approx 18$) but were derived from unique polyols **(Figure 3.1b)**. For each ethoxylated polyol, three thiol acid ethyl esters and one thiolactone were used to synthesize a total of 8 individual TEPEs that displayed hydrolytically labile tri-thiol functionalization. By reacting these eight unique thiol functionalized structures with PEGDA under physiologically buffered conditions it was possible to fabricate a hydrogel library **(Figure 3.1c)**.

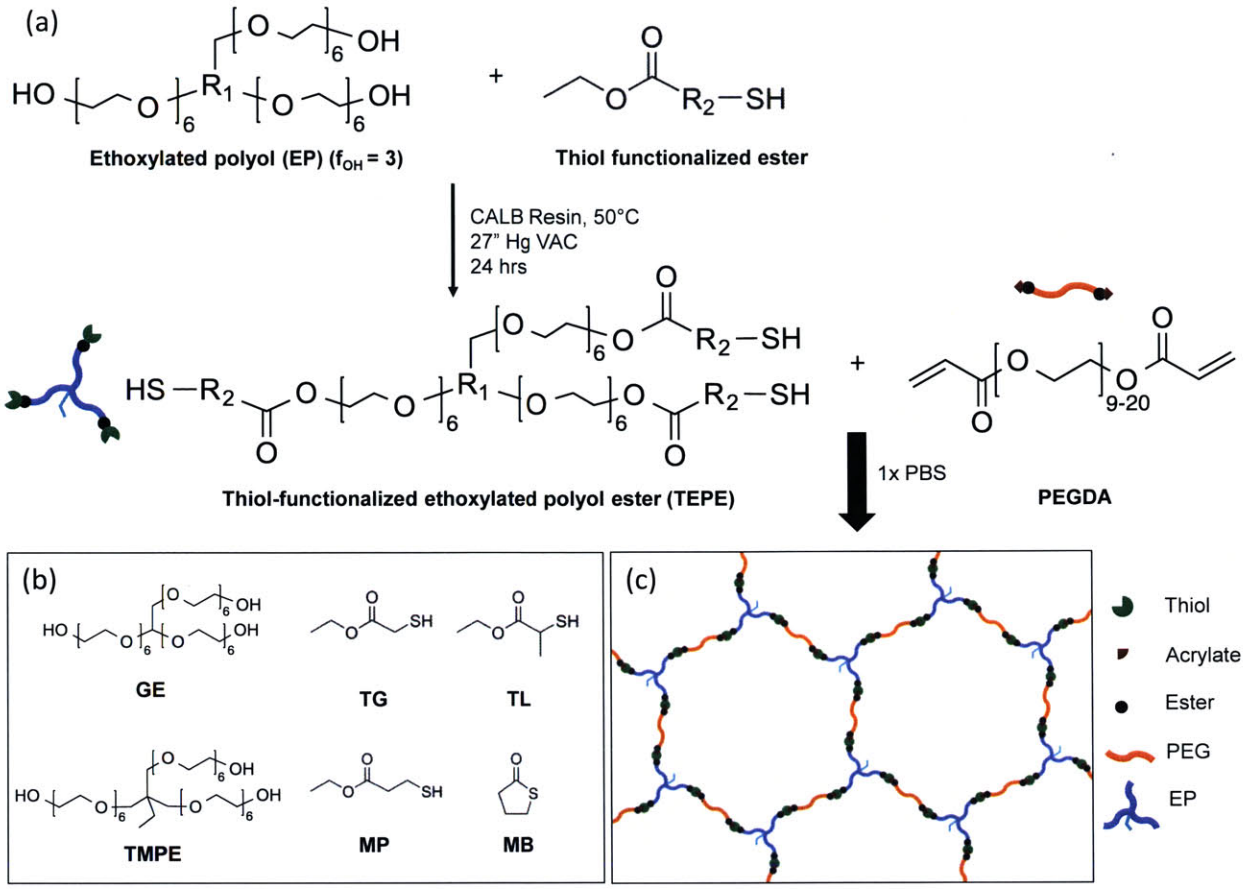

Figure 3.1 Overview of oligomer synthesis and hydrogel fabrication. **(a)** General one pot synthesis scheme for the thiol functionalized ethoxylated polyols (TEPE). **(b)** The chemical structures of the two ethoxylated polyols, three thiol acid esters and a thiolactone used to synthesize the TEPEs. **(c)** Hydrogel fabrication performed through the combination of TEPEs and PEGDA in a physiological buffer.

TEPE Solubility and thiol pKa are determinants of hydrogel formation. All but one TEPE (TMPE-tri-mercaptobutanoate) demonstrated satisfactory aqueous solubility. The thiol pKa profiles followed a trend similar to that of the individual thiol acids. Specifically, proximity of the thiol to: (i) the electron withdrawing ester carbonyl, as well as (ii) hyperconjugation induced by methyl side chains resulted in a lower pKa **(Figure 3.2)**. For the same thiol acid the pKa of the resultant TEPE was equivalent for both ethoxylated polyols. To demonstrate the importance of TEPE pKa differences on hydrogel reaction kinetics, we formed TEPE-PEGDA 575 (average $M_n \approx 575$ g/mol) hydrogels and monitored the sol to gel transition by dynamic rheology. The time point where tan (δ)=1 (i.e. G'/G'' cross over), was used to define the onset of gelation [254,255]. The Michael addition reaction mechanism is rate limited by the

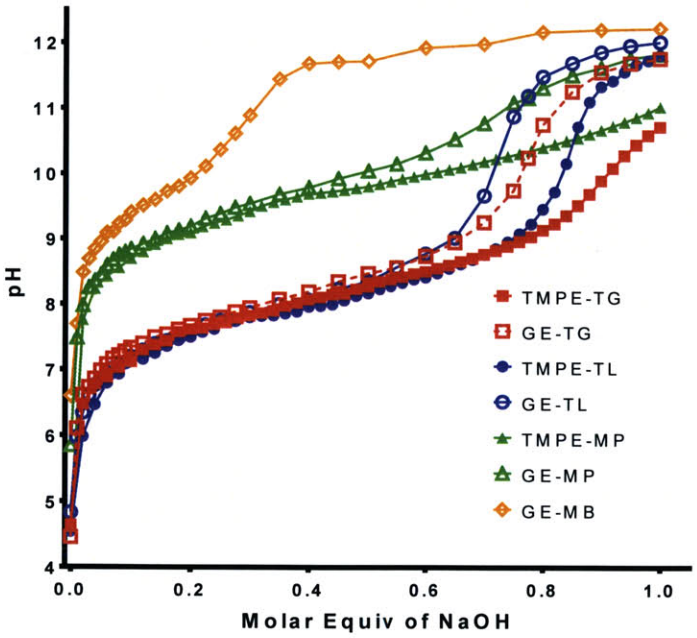

Figure 3.2 The titration curves for the various TEPES indicating that the pKa profile is dependent on the type of thiol acid but independent of the type of ethoxylated polyol.

formation of the thiolate anion and is therefore pKa dependent. It was expected that in a pH buffered environment the gelation time would be inversely related to TEPE pKa. However, gelation kinetics were also influenced by the accessibility of the thiolate nucleophile to react with the activated alkene Michael acceptor [256]. As such, thioglycolate (TG) TEPE hydrogels formed significantly faster compared to that of the thiolactate (TL) species despite the later having a lower pKa value **(Figure 3.3)**. This difference in reactivity is likely due to steric hindrance around the thiol functional group, where nucleophilic attack of the β-carbon on the acrylate is more favorable for the less constrained TG TEPEs [257]. Mercapto-proprionate (MP) and mercaptobutanoate (MB) species exhibited increased gelation times, which were indicative of their higher pKa values. Not surprisingly, the type of ethoxylated polyol had no effect on gelation kinetics. TG, TL and MP hydrogels demonstrated equivalent mechanical properties upon gelation suggesting that the overall crosslink density achieved was not affected by the rate of its formation **(Figure 3.4)**. By contrast, less densely crosslinked hydrogels were formed with GE-MB and this was attributed to a lower thiol functionalization (approximately 80-85%) as a result of the less

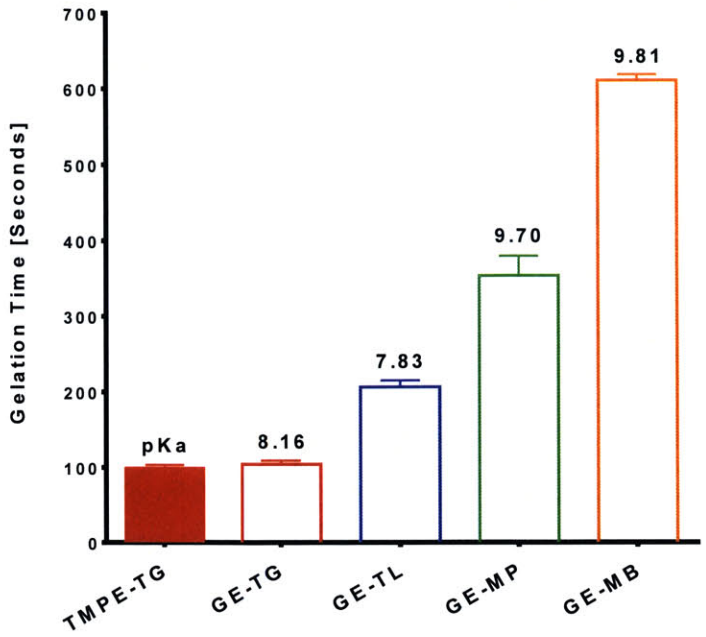

Figure 3.3 Hydrogel gelation kinetics are a function of the pKa of the thiol functionalized ethoxylated polyol. Gelation times for the different TEPEs and PEGDA 575 measured using dynamic mechanical rheology, oligomers were reacted together in a phosphate buffer (0.02M, pH=7.4) (Numbers above the bars are the estimated pKas that were derived from the titration curves in Figure 3.2)

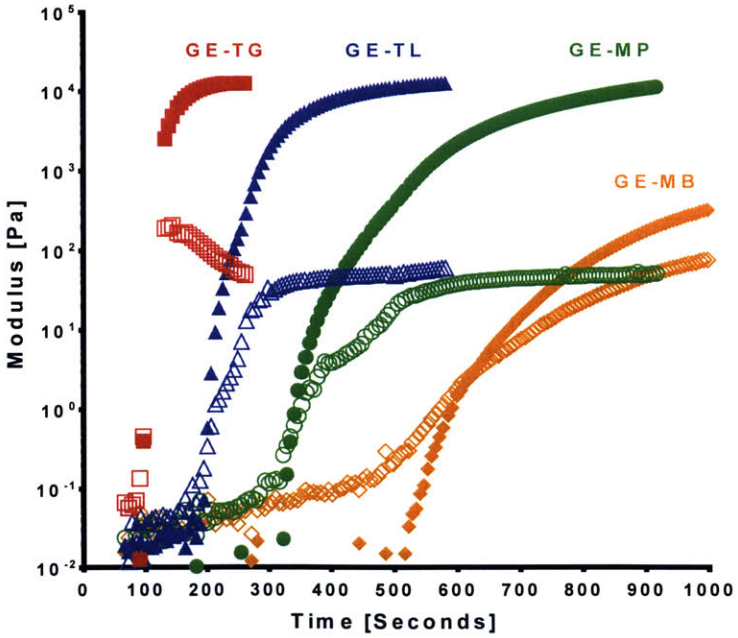

Figure 3.4 Dynamic rheology curves for hydrogels formed between PEGDA 575 and the different TEPEs demonstrating the temporal variation in time to gelation between the different TEPEs. TG, TL and MP based TEPEs formed with similar mechanical properties. G' (filled symbols) and G'' (empty symbols).

effective CALB catalyzed γ-thiobutyrolactone ring-opening reaction used in its synthesis. Overall, these data show that TEPE species selection along with minor modifications to the solvent buffer conditions (e.g. varying solution pH within the physiological range or altering buffer strength and concentration) are effective methods for tailoring gelation kinetics. These two independent mechanisms of gelation control allow for sufficiently versatile hydrogel curing times using physiological pH buffers.

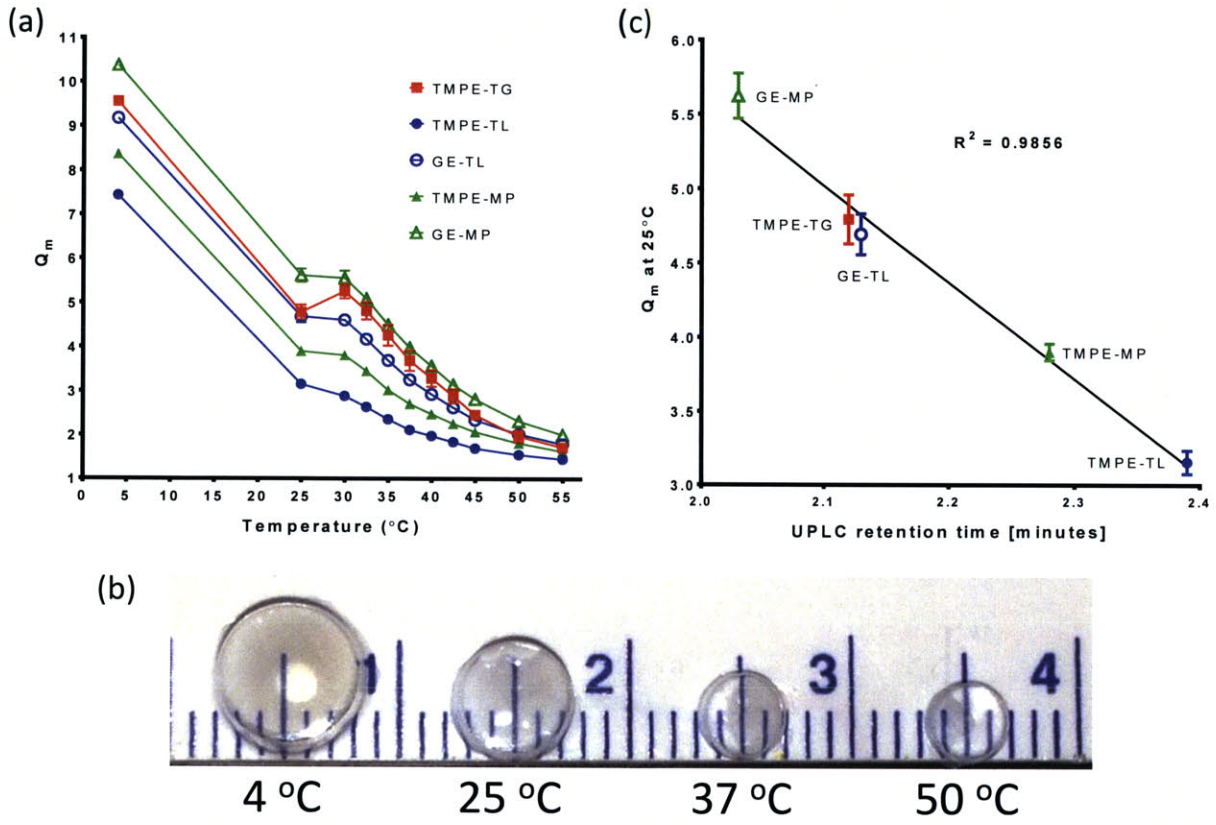

Figure 3.5 TEPE hydrogels show thermoreversible swelling/syneresis properties. **(a)** Swelling Ratio (Q_m) of TEPE hydrogels over a temperature range from 4°C to 55°C. **(b)** Image of TMPE-TL575 hydrogels equilibrated at different temperatures demonstrating temperature dependent swelling/syneresis. **(c)** Comparison of Q_m and TEPE liphophilicity at T=25°C for TEPE-PEGDA575 hydrogels. The Q_m decreases linearly with retention time as measured on a UPLC column (R2 = 0.9856).

Uncontrollable or excessive hydrogel swelling can result in compromised patient safety[249,250]. To investigate the swelling of the various TEPE-PEGDA575 hydrogels we measured the equilibrated mass of samples upon isotonic buffer incubation at discrete increasing temperature increments. All hydrogels displayed thermoreversible syneresis (expulsion of solvent and collapsing of the hydrogel mesh network), with the swelling ratio (Q_m) approaching unity as the temperature increased **(Figure 3.5 a, b)**.

The $Q_m(T)$ curve for each hydrogel was dependent on the relative lipophilic character of the individual TEPE used in its formulation. More specifically, the degree of lipophilicity for the TEPE (measured by the relative retention time on a C18 UPLC column) was characterized to be linearly proportional to the Q_m of the hydrogel across a range of temperature conditions **(Figure 3.5c)**. Both the type of ethoxylated polyol and thiol acid influenced the degree of lipophilicity observed for each TEPE, with a net lipophilic value determining the Q_m. Despite being composed of unique thiol acid and ethoxylated polyol species, the GE-TL and TMPE-TG hydrogels showed similar Q_m values and equivalent TEPE retention times on UPLC. We concluded that the degree of lipophilicity was a relevant surrogate for the lower critical solution temperature (LCST) parameter and provides a good predictor of the swelling behavior for the TEPE hydrogels[258]. The molecular weight of the PEGDA also had a significant effect on hydrogel properties **(Figure 3.6)**. As the size of the PEGDA increased from 575 g/mol to 1000 g/mol the Q_m increased significantly for all TEPEs. This phenomenon aligns with the Flory-Rehner theory of infinite networks, with the equilibrated swelling of a network dependent on the effective molecular weight of chains between crosslinks [259,260]. Although hydrogel Q_m was dependent on TEPE and PEGDA selection, the observed differences in mechanical properties showed negligible TEPE dependence **(Figure 3.S9)**.

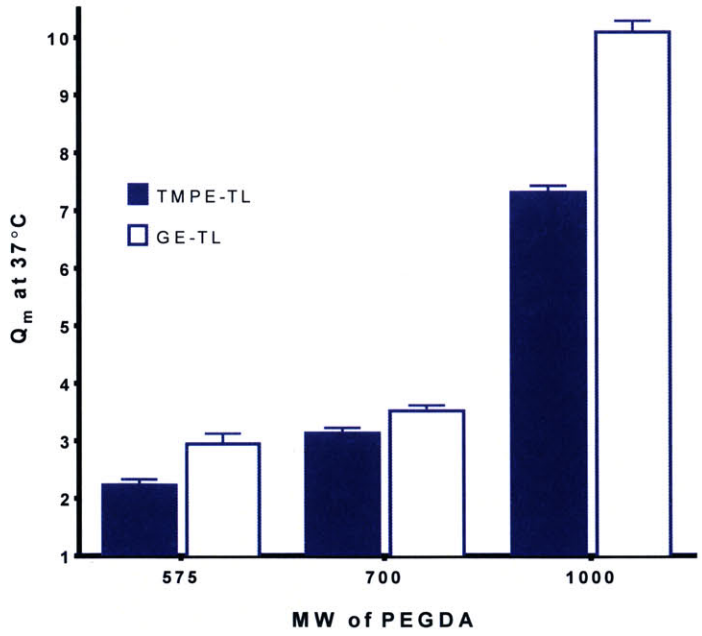

Figure 3.6 The swelling ratio for the TEPE hydrogels increases with higher molecular weight chains between crosslinks. Q_m comparisons for hydrogels formed from PEGDAs of different molecular weights and TMPE-TL and GE-TL TEPEs. The wet masses of the samples were weighed following 48 hour incubation at 37°C.

Furthermore, these TEPE hydrogels are much more compliant and less brittle than the equivalent PEGDA only hydrogels formed by the radical mediated reaction [261]. This work demonstrates that the inclusion of hydrophobic entities within specific regions of the precursor molecules, which ultimately become connectivity nodes for the PEG chains in the hydrogel matrix, can be an effective way of counteracting the entropic driving forces associated with the PEG chains that contribute to swelling [262].

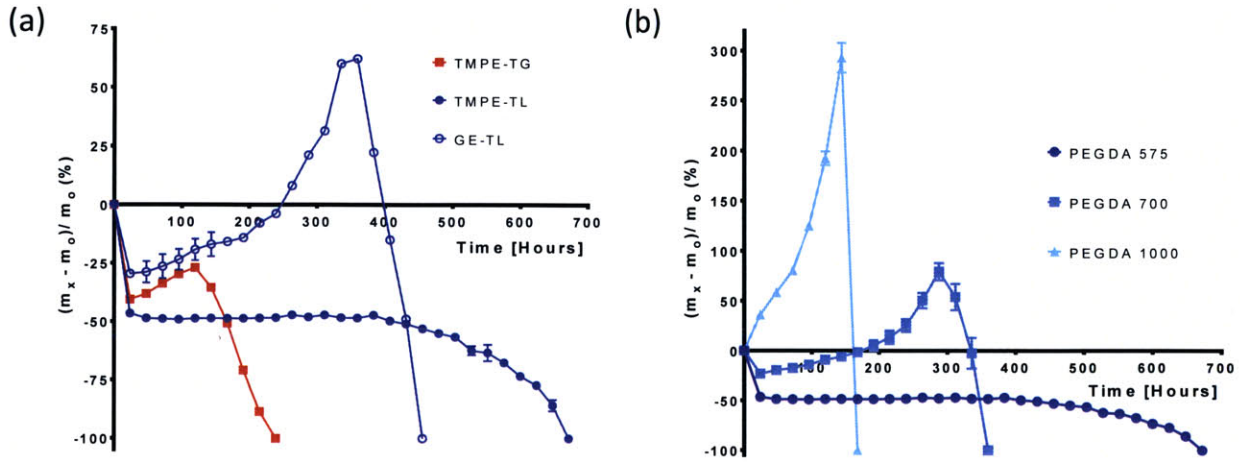

Figure 3.7 TMPE based hydrogel formulations show non swelling material degradation profiles. Percentage hydrogel wet mass changes (compared to the initial cured wet mass) over time for: **(a)** Different TEPEs formulated with PEGDA575 and **(b)** TMPE-TL formulated with different PEGDAs.

Hydrogel degradation can influence the spatiotemporal release profile of therapeutics and the overall foreign body response to the implant. Hydrogel degradation is controlled by three parameters: (1) the lipophilicity of the TEPE; (2) the crosslink density established by the PEGDA used and (3) the susceptibility of the network esters to undergo hydrolysis due to neighboring chemical constituents **(Figure 3.7a)** [263,264]. Two formulations with the same PEGDA and similar TEPE lipophilicity, TMPE-TG575 and GE-TL575, were compared to establish the effect of the ester constituent on hydrogel degradation. Hydrogels formed with the more labile TG ester displayed an enhanced rate of degradation. Hydrogels with a lower Q_m(37°C), such as TMPE-TL575, showed a more prolonged degradation timeline. Increasing the molecular weight of the PEGDA also had a significant effect on hydrogel degradation, confirming the influence of crosslink density **(Figure 3.7b)**. For hydrogel formulations using TEPEs derived from GE, degradation was associated with an increase in hydrogel sample wet weight. This is likely a result of increased swelling of the matrix as the crosslink density decreased from ester hydrolysis. The observed swelling phenomena is consistent with that reported previously for biodegradable PEG hydrogels [248]. By contrast, TMPE derived formulations showed a degradation profile with no appreciable swelling

throughout the entire life of the hydrogel. Specifically, TMPE-TL575 hydrogels maintained consistent wet masses (following the initial network syneresis) prior to the onset of terminal bulk degradation. TMPE-TG575 hydrogels demonstrated a small increase in wet mass after the initial syneresis, but the maximum wet mass observed before the onset of terminal degradation was significantly less than the original as cured value. FTIR investigations on dry TMPE hydrogels showed increased carboxylate concentrations within the network that preceded the observable wet mass changes and the onset of terminal bulk degradation **(Figure 3.8)**. For the TMPE-TL575 formulation the carboxylate IR peak at 1550–1610 cm^{-1} reached a maximum at around 432 hours (18 days) of continuous incubation. After 18 days the dry polymer mass of the TMPE-TL575 formulations began to decrease indicating the onset of terminal degradation. During, the period of terminal degradation the hydrated TMPE hydrogel formulations underwent apparent erosion. Therefore although ester hydrolysis commences after a few days of aqueous incubation it is only after reaching a critical extent of hydrolysis that the wet and dry weights of the hydrogel begin to decrease substantially.

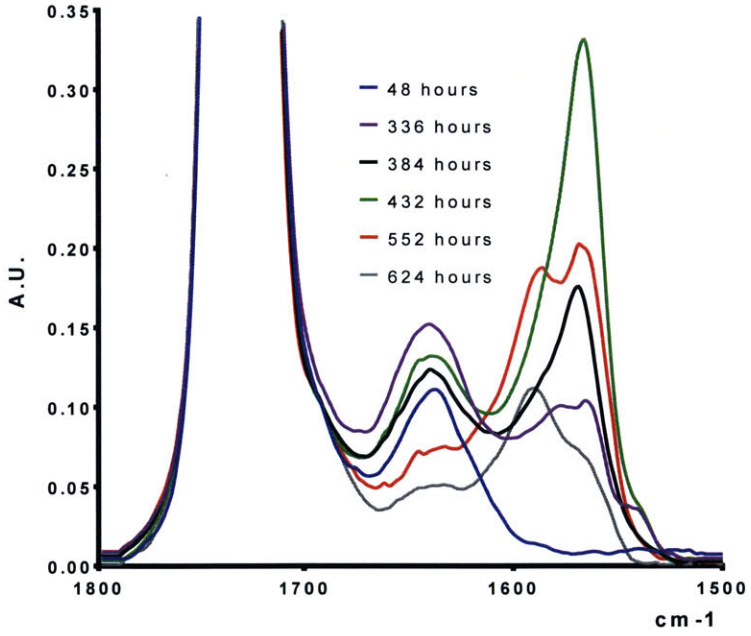

Figure 3.8 The TEPE Hydrogels degrade by hydrolysis. FTIR spectra of TMPE-TL575 hydrogels incubated for designated periods in 1x PBS showing the change in the carboxylate peak (1550–1610 cm–1) as a result of hydrogel ester hydrolysis.

It would appear that the non-swelling behavior of the TMPE hydrogels and in particular TMPE-TL, despite the apparent reduction in covalent crosslink density by hydrolysis, is the result of the preservation of physical interactions between the hydrophobic elements of the TMPE ethoxylated polyol

core and the methyl group of the TL ester. Due to this unusual property, these TMPE-PEGDA575 hydrogels may represent a new class of *in situ* curing materials suitable for local drug delivery applications in volume-constrained anatomical sites such as in the brain and spine.

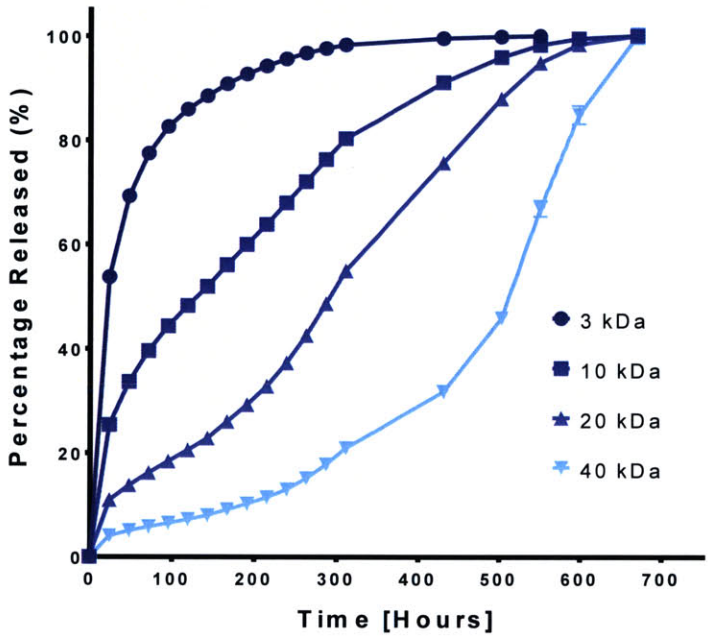

Figure 3.9 TEPE hydrogels show molecular size dependent permeability. Hydrogel permeability as measured by detection of the diffusion of FITC-Dextran from hydrogel formulations. Comparison of the cumulative release of different molecular weight FITC-Dextrans (3kDa, 10kDa, 20kDa and 40kDa) from TMPE-TL575 hydrogels.

To determine the appropriateness of the hydrogels for controlled drug delivery, an initial investigation into the molecule size permeability of the matrix was conducted. Fluorescein isothiocyanate (FITC) labeled dextrans ranging from 3kDa to 40kDa were encapsulated within different 25wt% TEPE hydrogels. For all TEPE hydrogels a molecule size dependent release effect was noted. As demonstrated in **Figure 3.9** three unique release profiles depending on the dextran molecule size were observed. For the 3kDa dextran, the hydrogels showed first order Fickian diffusion with a high initial burst. For these smaller molecules there is minimal barrier to diffusion and molecule release precedes any meaningful hydrogel degradation. With an increase in dextran molecular weight to 10 and 20kDa the release profile transitioned to practically zeroth order accompanied by a lower burst. With these intermediate sized dextrans there is a larger barrier to diffusion resulting in a slower release rate that has some hydrogel degradation dependency. Finally, for dextrans with a larger molecular weight (≥40kDa) a triphasic

release profile was observed. This type of triphasic release profile is seen with hydrophobic Poly(Lactide-co-Glycolide) (PLGA) formulations where there is initially slow diffusion of the molecules through the dense polymer substrate followed by a more rapid release due to the increasing onset of material bulk degradation and erosion [265,266]. The TEPE hydrogels appear to share release characteristics similar to these hydrophobic polyesters. Furthermore, dextran diffusivity was a function of both the TEPE and the PEGDA used **(Figures 3.10, S3.10)**.

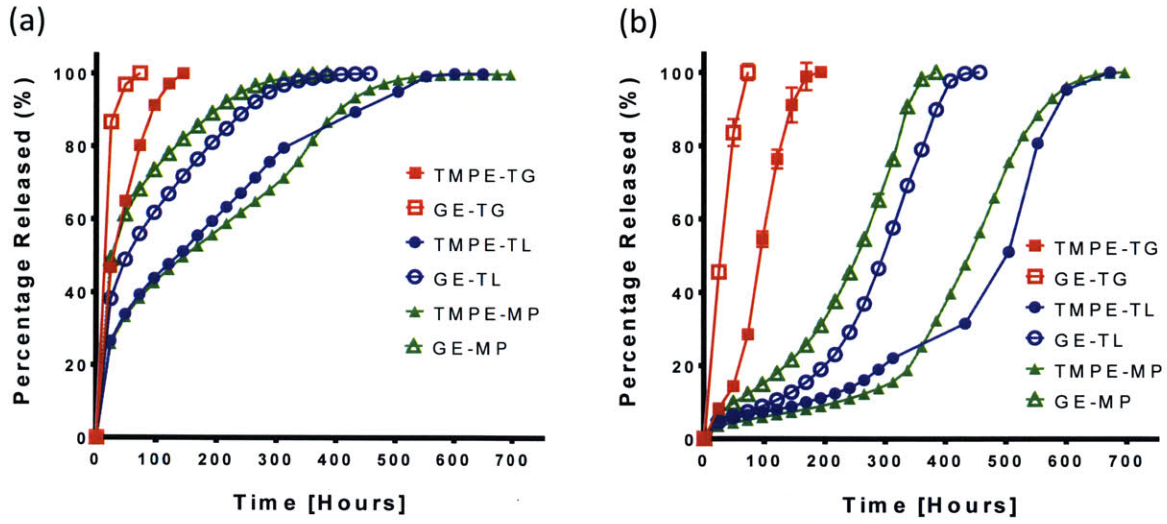

Figure 3.10 Dextran diffusivity from hydrogels was influenced by TEPE selection. Cumulative release profiles for **(a)** 10kDa and **(b)** 40KDa FITC-Dextran encapsulated within different TEPE/PEGDA 575 hydrogel formulations.

Hydrogel matrices offer the potential to be used for the controlled release of protein therapeutics. Proteins display complex tertiary or quaternary structures making their size and shape different to that of the linear dextran polysaccharides. We investigated the release of two encapsulated fluorescently labeled proteins, FITC-labeled ovalbumin (45kDa) and Alexa Fluor IgG (150kDa), from the library of hydrogels. As for the 40kDa dextran, the ovalbumin displayed characteristic triphasic release profiles from all hydrogels that was controlled by crosslink density, the lipophilicity of the TEPE and rate of degradation of the network **(Figures 3.11a, b, S3.11)**. Encapsulated IgG also showed a similar triphasic release profile, however there was a smaller initial burst and slower diffusion during the second phase compared to ovalbumin, which we attributed to IgG's larger size **(Figure 3.11c)**.

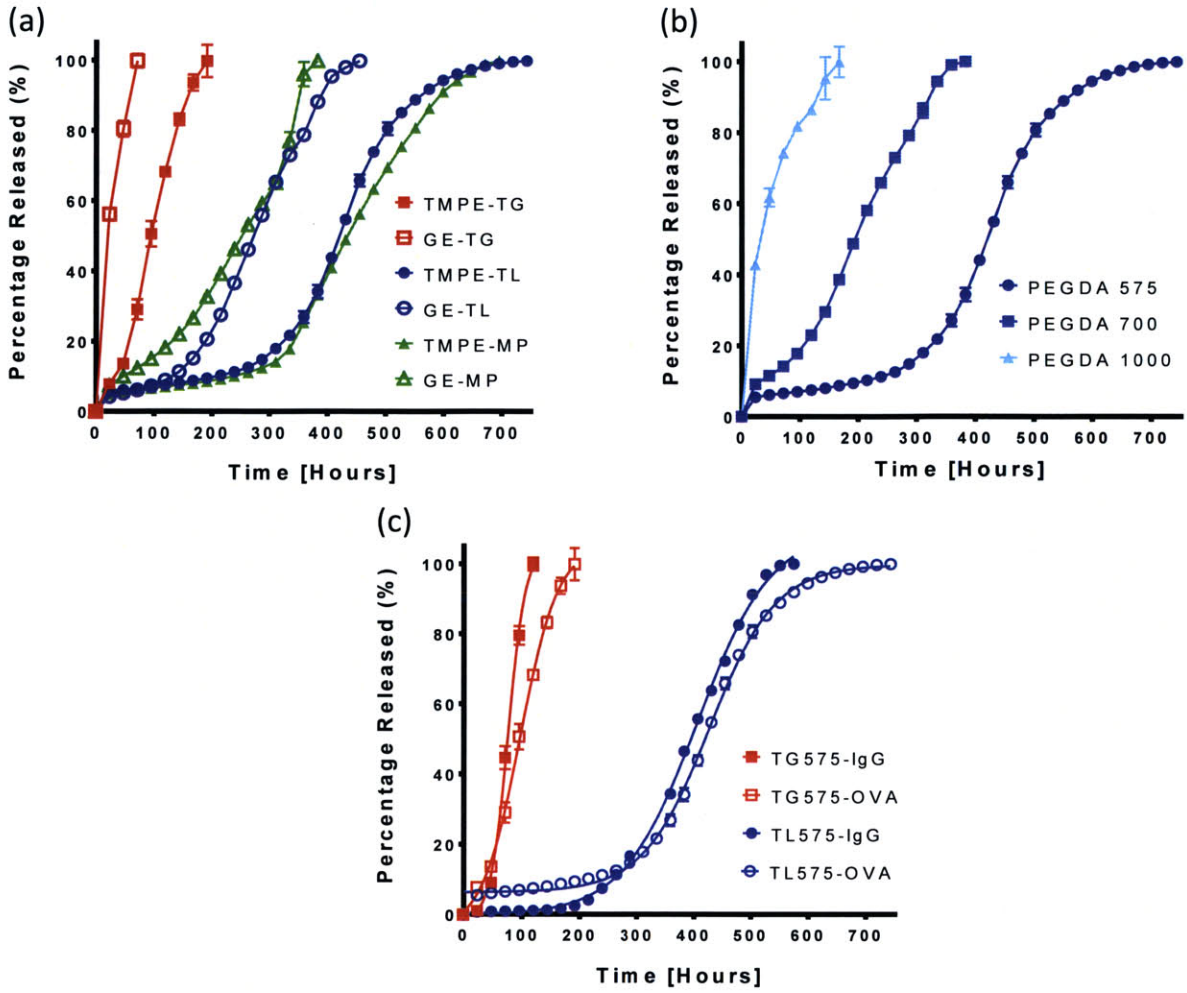

Figure 3.11 Controlled release of model proteins from TEPE hydrogels was dependent on TEPE and PEGDA selection but not the size of the protein. Cumulative release profiles for FITC labeled ovalbumin (45kDa) encapsulated within: **(a)** different TEPE/PEGDA 575 formulations and **(b)** TMPE-TL and different molecular weight PEGDAs. **(c)** Comparison of controlled release of FITC ovalbumin and Alexa Fluor 647 IgG from TMPE-TG575 and TL575 hydrogel formulations.

Furthermore, the degradation of the hydrogels encapsulating IgG appeared to occur faster than for the ovalbumin suggesting that larger sized proteins may affect the integrity of the formed network. Hybrid TMPE-TG and TMPE-TL hydrogel blend formulations were also prepared to demonstrate tunability of hydrogel degradation and protein release. By increasing the percentage composition of TMPE-TL relative to TMPE-TG, a more prolonged protein release profile and slower hydrogel degradation was observed **(Figure 3.12a, b)**. For these hybrid hydrogels the triphasic ovalbumin release profiles could be fitted to a Weibull sigmoidal distribution [265,267]. Using this model the characteristic release parameters, the T50 (time to 50% release of drug) and k (the molecule release constant), were exponentially and

linearly proportional to the relative amounts of TMPE-TG/TMPE-TL present in the hydrogel network respectively **(Figure 3.12c)**. Therefore, these hybrid hydrogels allow for tailored drug release from 5 to 35 days through careful selection of the TL/TG thiol ester proportions. This hybrid system provides for more precise control compared to that achieved by similar PLGA-PEG block copolymer formulations [239,268]. The unique drug release tunability and non-swelling degradation makes the family of TMPE TEPEs an exciting platform for injectable local drug delivery applications particularly in anatomically confined spaces.

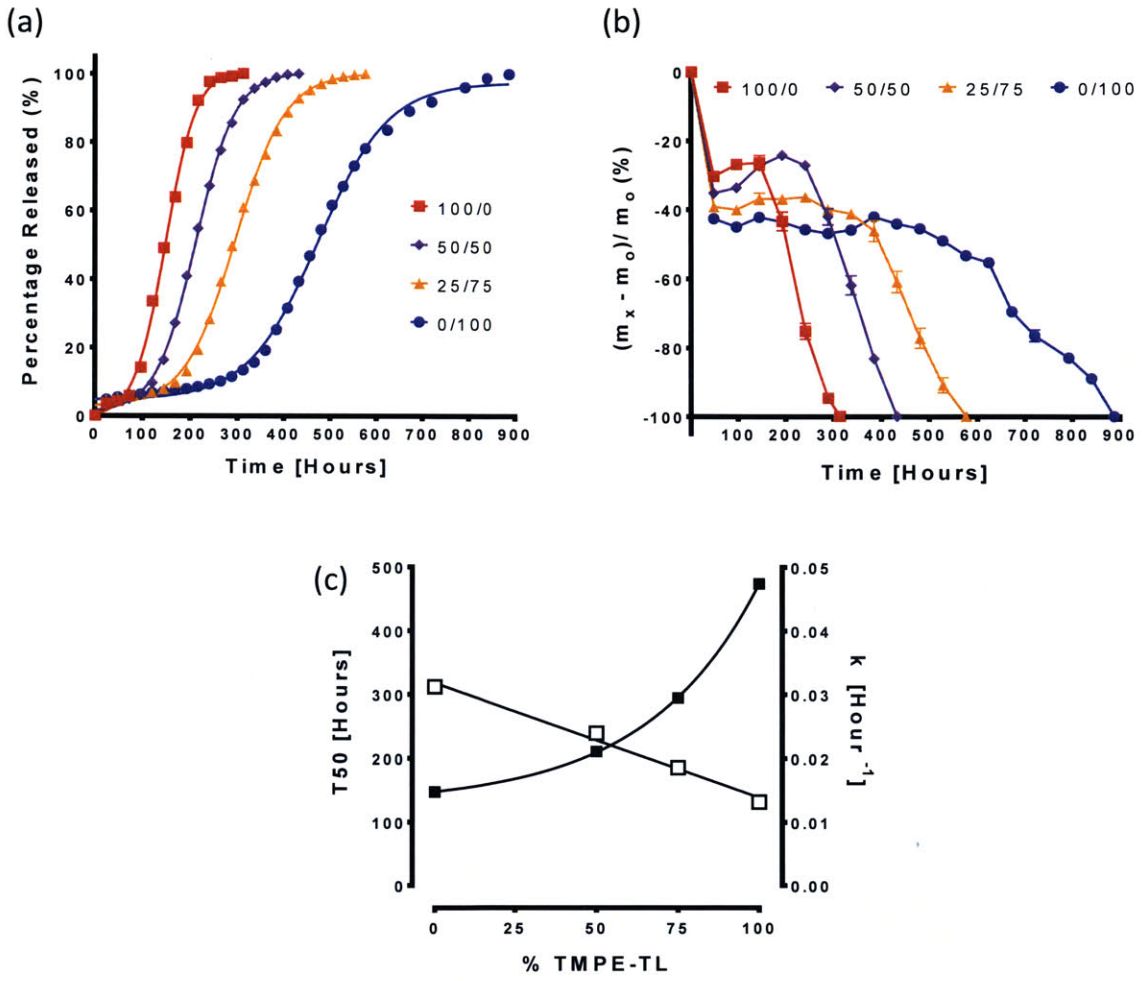

Figure 3.12 Hybrid TEPE hydrogels provide tunable protein release by blending TEPEs. **(a)** Cumulative ovalbumin release profiles for hybrid TMPE-TG/TL575 hydrogels. The first number refers to the percentage of TMPE-TG and second number the percentage of TMPE-TL. **(b)** Percentage hydrogel wet mass change (compared to the initial cured wet mass) for TMPE hybrid hydrogels. Increasing the ratio of TMPE-TL relative to TMPE-TG resulted in a delay in the onset of terminal hydrogel degradation. **(c)** Comparison of the influence of the percentage of TMPE-TL on time to 50% release, T50 (filled symbols) and release constant, k (open symbols) in TMPE hybrid hydrogels. k was linearly related to TMPE-TL percentage while T50 followed an exponential trend.

We performed a final *in vitro* immunogenicity assay to determine TEPE hydrogel biocompatibility. RAW-Blue™ macrophage cells were seeded onto TMPE-TG575, TMPE-TL575 and TMPE-MP575 hydrogels and we monitored the biomaterial-immunogenic response. All TEPE hydrogels showed a minimal immunogenic response that was comparable to the low binding cell culture plate control. Furthermore, the TEPE hydrogels showed significantly less pattern recognition receptor (PRR) activation compared to the positive control LPS-EK (p-value <0.0001) as well as a commercially available alginate hydrogel, LF 10/60 (p value < 0.0001) **(Figure 3.13a).** TEPE hydrogels were slightly less immunogenic then the highly purified sterile alginate, SLG-20, but was not statistically significant. Between the three TMPE hydrogels there was no difference in the immunogenicity suggesting that the type of thiol acid had no influence on the cell-material interaction. A cell viability assay showed that the TEPE hydrogels had minimal toxicity that was comparable to controls **(Figure 3.13b).** PEG is generally recognized as a low fouling, limited protein adsorbing and low cell binding material [269,270]. The current TEPE based hydrogels, despite being composed of low molecular weight ethoxylated polyol precursors (PEG chains approximately 300-400 Da), demonstrated equivalently limited cell binding and low immunogenicity. Based upon these *in vitro* results these low molecular weight TEPE oligomers should find utility for controlled *in vivo* biomolecule delivery in future studies.

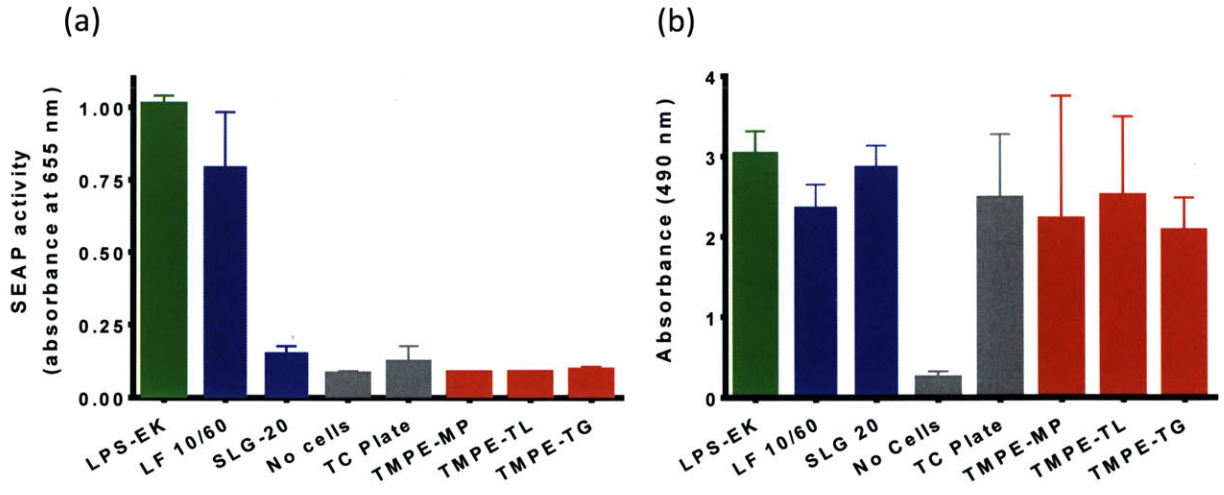

Figure 3.13 TMPE based hydrogels show excellent *in vitro* biocompatibility and low immunogenicity. **(a)** Results from QUANTI-Blue colorimetric assay (collated data: n=3 per group, two assay replications). This assay demonstrated that TMPE hydrogels induced minimal SEAP levels and consequently low NF-κB and AP-1 activation. TMPE hydrogels showed less immunogenicity then one of the commercially available alginate hydrogels, LF10/60, and the LPS-EK positive control (p-values < 0.0001). **(b)** MTS assay shows comparable live cell numbers for TMPE hydrogels, the cell culture plastic, LPS-EK and alginate controls.

In summary, we utilized a robust enzymatically catalyzed transesterfication reaction to synthesize a library of thiol functionalized ethoxylated polyol esters and used these materials to form hydrogels with diverse properties in relation to curing time, swelling, degradation and release of model polysaccharides and proteins. Specifically, we demonstrated a unique ability to temporally control both material degradation and the triphasic release of model biomolecule drugs over a range of 5 to 35 days by blending different ratios of two TEPEs in the hydrogel formulation. Favorably, these materials display degradation profiles devoid of any matrix swelling achieved through the maintenance of hydrophobic interactions within the network. These materials also demonstrated good *in vitro* biocompatibility and low immunogenicity. As a result of this investigation we have identified candidate hydrogel formulations that may find utility as *in-situ* curing injectable hydrogels for drug release applications in confined anatomical sites.

3.3 Materials and Methods

3.3.1 Materials

Ethoxylated polyols (glycerol ethoxylate and trimethylopropane ethoxylate), thiol acid ethyl esters (ethyl thiolactate, ethyl thioglycolate, and ethyl 3-mercaptopropionate), γ-Thiobutyrolactone, Lipase B acrylic resin from Candida antarctica (CALB), polyethylene diacrylates (PEGDA) (M_n = 575, 700, 1000 g/mol), activated alumina Brockman I (basic and neutral) were purchased from Sigma-Aldrich (St.Louis, MO, USA) and TCI America (Portland, OR, USA). Phosphate buffered saline, ovalbumin-FITC, dextran-FITC (3kDa, 10kDa, 20kDa, 40kDa) and IgG-Alex Fluor 647 were purchased from Life Technologies (Grand Island, NY) and Sigma-Aldrich. Filter agent Celite® 545, solvents for flash chromatography (Dichloromethane and Methanol) were purchased from Sigma Aldrich and disposable 80 gram HP Silica Gold Cartridges were purchased from Teledyne Isco. For cell culture work, RAW-Blue™ cell line, QUANTI-Blue™, Normocin, Zeocin, and LPS-EK were purchased from InvivoGen (San Diego, CA, USA). Dulbecco's Modified Eagle Medium (DMEM, high glucose), heat inactivated fetal bovine serum (HI FBS), and Penicillin-Streptomycin (5,000 U/ml) were purchased from Life Technologies. Endotoxin free water and Corning® Costar® Ultra-Low attachment 96-well plates were purchased from Sigma-Aldrich.

3.3.2 TRI-THIOL-FUNCTIONALIZED ETHOXYLATED POLYOL ESTER (TEPE) SYNTHESIS

The transesterification of ethoxylate polyols with thiol acid ethyl esters or γ-Thiobutyrolactone was performed utilizing Candida antarctica Lipase B (CALB) immobilized on acrylic resin as the catalyst under solventless conditions adapted from a previous reported protocol [253]. Ethoxylated polyol (10 mmols ~ 10 grams) starting material was added to 4A Molecular Sieves (1 gram) into a 100 mL round bottom flask, followed by a five molar excess of thiol acid ethyl ester and CALB (1 gram). The flask was placed on a magnetic stirrer at 50°C and purged with Nitrogen gas for 2 hours and then allowed to react overnight under moderate vacuum conditions at 27 inches Hg gauge vacuum or 99 mbar (≈ 90% vacuum). The reaction was purified by silica flash chromatography on a CombiFlash Rf using a disposable silica column (80 grams) with a dichloromethane/methanol (0-10%) gradient elution method. Purified fractions determined from UV absorbance at 240 nm were combined and dried on a rotary evaporator and under high vacuum before being stored under inert Nitrogen gas at 4°C. Before use the TEPE was flashed neat over a small column of activated Neutral Alumina (Brockman I).

3.3.3 LC-MS AND NMR ANALYSIS

For LC-MS analysis samples were loaded at a 1mg/ml concentration and run through a UPLC BEH C18 1.7μL, 2.1 x 50 mm column (Acquity) at a rate of 0.6 ml/min with a mobile phase of HPLC grade water and acetonitrile with 0.01% formic acid with a gradient over 3 minutes from 95:5 to 5:95 water/acetonitrile. Eluted products were characterized by UV-PDA detector and ESI QTof MS and analyzed using MassLynx software.

For NMR characterization, ^{1}H NMR spectra were recorded on a Bruker 400 MHz NMR spectrometer using the residual proton resonance of the solvent as the internal standard. Chemical shifts are reported in parts per million (ppm).

GE-TG: ^{1}H (400 MHz, $CDCl_3$, δ): 4.29 (m, 6H), 3.7-3.55 (m, 75H), 3.3 (d, *J*=8 Hz, 6H), 2.0 (t, *J*=8 Hz, 3H)

GE-TL: ^{1}H (400 MHz, $CDCl_3$, δ): 4.29 (m, 6H), 3.7-3.5 (m, 78H), 2.2 (d, 3H, *J*=8 Hz), 1.52 (d, 9H, *J*=8 Hz)

GE-MP: ^{1}H (400 MHz, $CDCl_3$, δ): 4.25 (t, *J*=8 Hz, 6H), 3.7-3.55 (m, 75H), 2.75 (t, *J*=8 Hz, 6H), 2.65 (t, *J*=8 Hz, 6H), 1.65 (t, *J*=8 Hz, 3H)

GE-MB: ^{1}H (400 MHz, $CDCl_3$, δ): 4.23 (t, *J*=4 Hz, 6H), 3.7-3.5 (m, 75H), 2.55 (q, *J*=4 Hz, 6H), 2.45 (t, *J*=8Hz, 6H), 1.9 (m, 6H), 1.35 (t, *J*=8 Hz, 3H)

TMPE-TG: ^{1}H (400 MHz, $CDCl_3$, δ): 4.25 (t, *J*=4 Hz, 6H), 3.75-3.6 (m, 72H), 3.3 (m, 6H), 2.0 (t, *J*=8 Hz, 3H), 1.4 (m, 2H), 0.8 (m, 3H)

TMPE-TL: ^{1}H (400 MHz, $CDCl_3$, δ): 4.22 (m, 6H), 3.7-3.5 (m, 75H), 2.2 (d, 3H, *J*=12 Hz), 1.52 (d, 9H, *J*=8 Hz), 1.4 (m, 2H), 0.8 (t, *J*=8 Hz, 3H)

TMPE-MP: ^{1}H (400 MHz, $CDCl_3$, δ): 4.3 (m, 6H), 3.7-3.55 (m, 72H), 2.7 (m, 6H), 2.6 (m, 6H), 1.65 (m, 3H), 1.4 (m, 2H), 0.82 (m, 3H).

3.3.4 Hydrogel Fabrication

Hydrogels were formulated by employing Thiol-Michael addition chemistry according to a similar procedure as described in detail previously [271]. Individual TEPEs and PEGDA were solubilized with 1x PBS to form unique solutions of each hydrogel constituent. To enhance the oligomer solubility the solution were placed in a 4°C environment for 10 minutes. Hydrogels were fabricated upon the addition and mixing of stoichiometric equivalent volumes of the TEPE and PEGDA solutions. In general the volume of PBS added to each hydrogel constituent solution was sufficient to obtain a 25wt% hydrogel. Prior to any hydrogel fabrication neat PEGDA liquid was flashed over activated Basic Alumina (Brockman I) to remove the (Mono Methyl Ether Hydroquinone) MEHQ inhibitor added by the manufacturer.

3.3.5 Dynamic Rheology

An ARES G2 rotational rheometer (TA Instruments, New Castle, Delaware) was used to characterize hydrogel gelation kinetics and mechanical properties. For each test hydrogel precursors were sufficiently mixed and a volume of 300 μL was applied to a temperature controlled stage at 37°C before the lowering of a 25mm parallel stainless steel plate to initiate the test. Dynamic time sweep measurements were made within the linear viscoelastic region (strain=5%, frequency=10 rad s^{-1}). The time interval between initial hydrogel mixing and commencement of rheology data collection was standardized to approximately sixty seconds and was added onto the final gelation time values.

3.3.6 Swelling and Degradation Experiments

Hydrogel cylindrical samples (≈60 μL, diam= 5mm; h= 3mm) at 25wt% total oligomer were prepared in silicone molds that had been sealed through press fitting onto a cleaned uncharged glass slide. After complete hydrogel curing, samples were removed from the mold and incubated in 1X PBS at 37°C for 48 hours to leach out the unreacted sol fraction. To determine the dry polymer mass hydrogel samples were dried in a vacuum oven at 40°C for 5 days. Evaluation of temperature dependent hydrogel swelling samples were incubated in 1.5 mL sample tubes containing 1xPBS, that were mounted in a temperature controlled digital heatblock. Samples were allowed to equilibrate at the specified temperature for a minimum of 4 hours before the new mass of hydrogel was evaluated. Q_m was evaluated by comparing the wet weight with the dry weight of the hydrogel sample. The same 60 μL hydrogel cylindrical samples were incubated in individual wells of a 48 well plate with 1mL of 1X PBS for degradation studies. To investigate the chemical modifications to the hydrogel polymer network caused by degradation samples were removed from incubation at defined time points and dried in a vacuum oven for five days before being analyzed by Bruker Alpha FTIR using the standard ATR attachment. FTIR spectra was taken from 1500 cm^{-1} to 1800 cm^{-1} at a 2cm^{-1} intervals with 80 repeat measurements. The ester peak (1730 cm^{-1}) was used to normalize the absorbance readings of the individual spectra with degradation progression assessed by comparing the evolution of the carboxylate peak (1550–1610 cm^{-1}).

3.3.7 Mechanical Testing

An 5943 single column table-top Instron mechanical testing system was used to perform compressive testing on cylindrical hydrogel samples (diameter =3mm; height = 5mm) that had been allowed to equilibrate in PBS for 48 hours prior to testing. Tests were performed at a rate of 5 mm/min with the force recorded using a 10N load cell and extension of the crosshead used in strain calculations.

3.3.8 Dextran permeability and Protein release experiments

FITC labeled dextrans of different molecular weights (3kDa, 10kDa, 20kDa, and 40kDa), FITC labeled Ovalbumin (45kDa) and Alexa Fluor 647 IgG (150 kDa) were individually encapsulated in TEPE hydrogel formulations at a concentration of 500 μg/mL. Hydrogels (n=3 or 4 per group) were incubated in 1mL of 1xPBS and replaced everyday. Duplicate 200μL aliquots of the incubation media for each sample were analyzed for fluorescent intensity (ex/em 490/525 for FITC; ex/em 650/668 for Alea Fluor 647) on an Infinite® M1000 PRO microplate reader (Tecan).

3.3.9 IN VITRO BIOCOMPATIBILITY STUDY

Hydrogels were seeded with the RAW-Blue™ cell line (InvivoGen) (murine macrophages transfected with a secreted embryonic alkaline phosphatase (SEAP) reporter gene inducible by NF-κB and AP-1 transcription factors). This cell line expresses many pattern recognition receptors (PRRs) and can be used to study in vitro the materials capacity to stimulate the innate immune system and elicit a significant foreign body response. Activation of PRRs in these cells leads to the subsequent activation of NF-κB and AP-1 transcription factors, which in turn produces SEAP. The SEAP levels were monitored using QUANTI-Blue™ colorimetric enzyme assay (InvivoGen) per the manufacturers directions. Cell viability was further determined using CellTiter 96® Aqueous One Solution Cell Proliferation Assay (Promega).

The RAW-Blue™ cells were cultured in DMEM medium (4.5g/L glucose, 2mM L-glutamine) supplemented with 10% heat inactivated fetal bovine serum, Pen-Strep (50U/ml), 100ug/ml Normocin, and 200ug/ml Zeocin. Lipopolysaccharide from *Escherichia coli* K12 (LPS-EK Ultrapure 5μg/ml) was used as a positive control for the PRR activation assay while cell culture treated plastic was used as the negative control. Alginate hydrogels were used as a comparison material and were formulated using pharmaceutical grade Protanal LF10/60 alginate (FMC BioPolymer) and Pronova SLG20 (MW 75,000–220,000 g/mol, >60% G units) (Novamatrix). Alginate hydrogels were formed by adding the alginate solution to a 2.4% barium chloride solution with mannitol with any excess barium chloride being removed through several washes of the hydrogel with HEPES and cell culture media.

3.4 Supplementary Figures

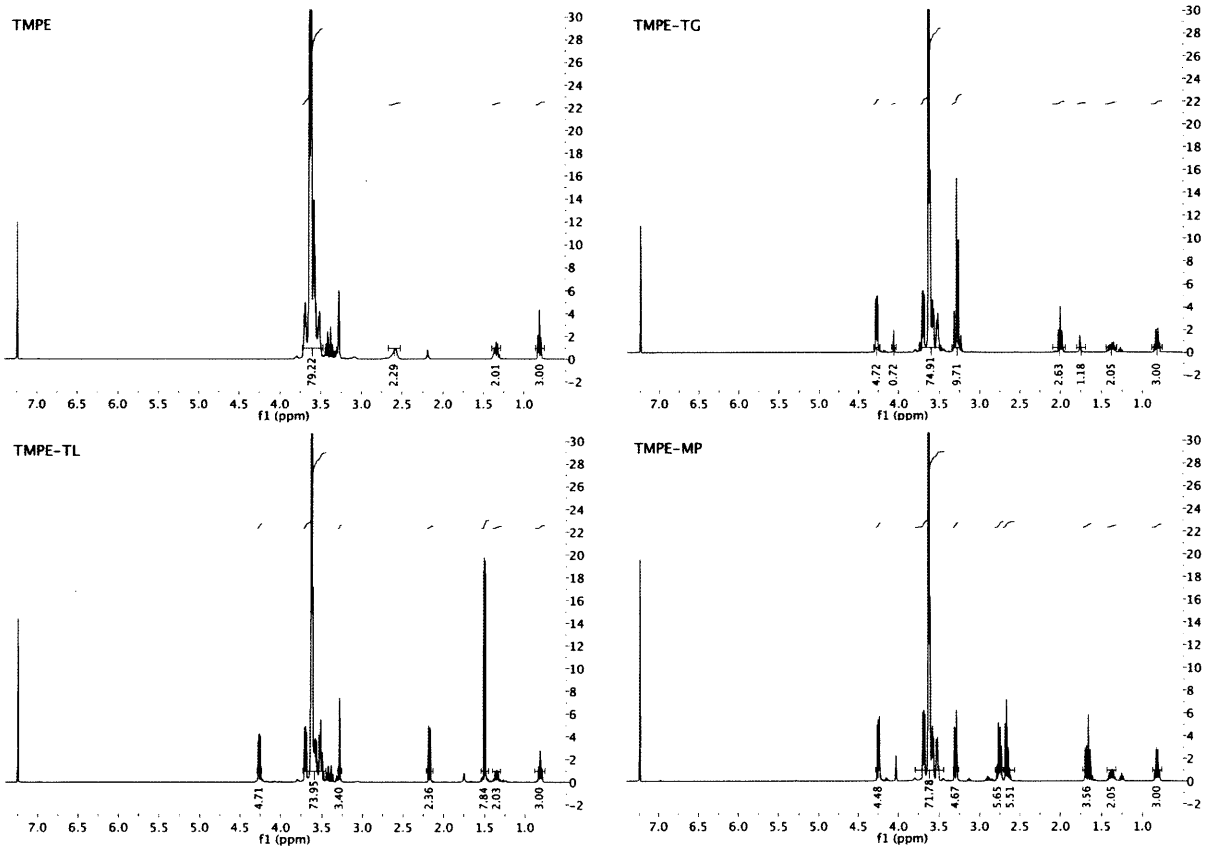

Figure S3.1 ^{1}H NMR Spectra for TMPE starting material and TMPE based TEPEs demonstrating the synthesis of highly thiol functionalized TEPEs. For detailed descriptions of proton shifts see the materials and methods section.

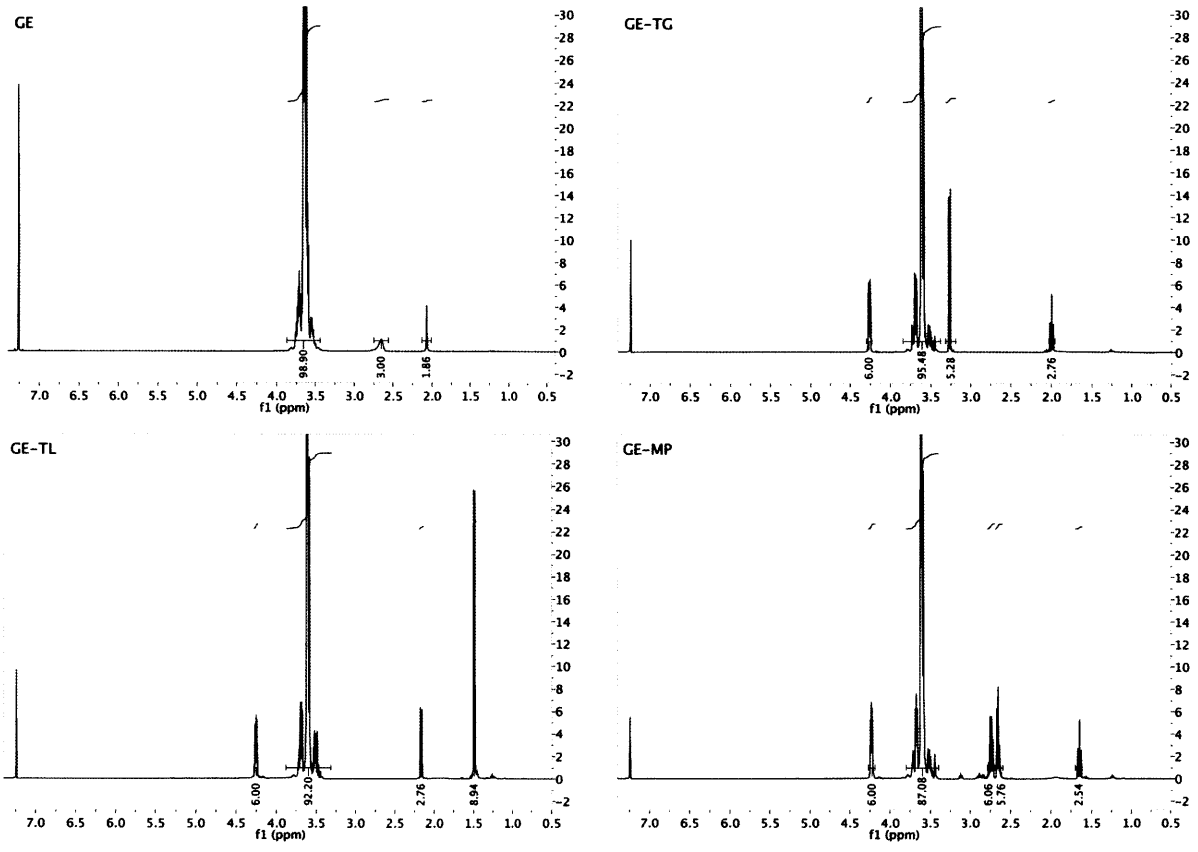

Figure S3.2 ^{1}H NMR Spectra for GE starting material and GE based TEPEs demonstrating the synthesis of highly thiol functionalized TEPEs. For detailed descriptions of proton shifts see materials and methods section.

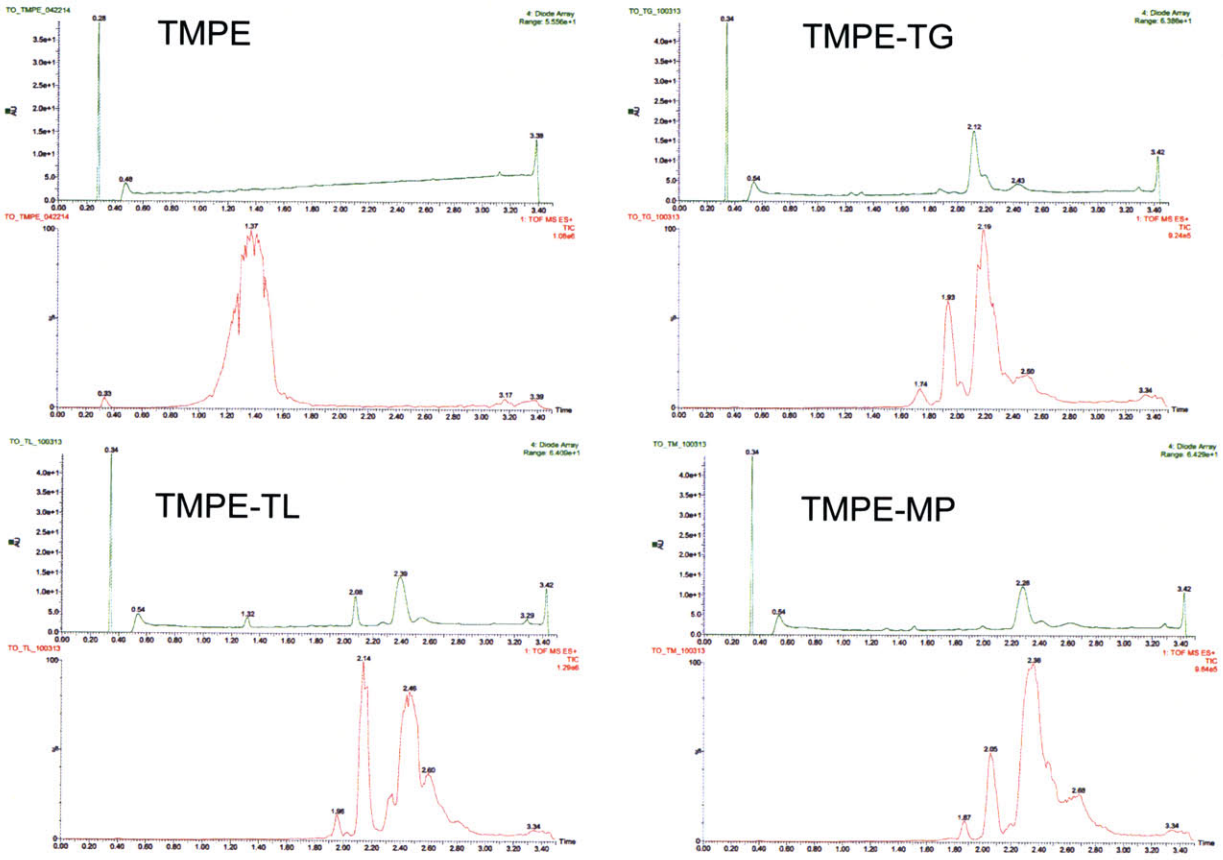

Figure S3.3 UPLC Chromatograms of TMPE starting material and purified TMPE based TEPEs. The green chromatograms represent the signal from the UV-PDA detector while the ESI QTof MS detector is shown in the red chromatograms. The starting material has no UV character but will ionize and is observable via the ESI QTof MS detector. No starting material was apparent in any of the TEPEs. The multiple peaks shown in the red chromatograms represent the three possible functionalization states. Given that the TMPE starting material is polydisperse (see MS data in Figure S3.5) it is not possible to completely separate out the bifunctional and trifunctional TEPEs. There are very small amounts of monofunctional TEPEs in the purified samples.

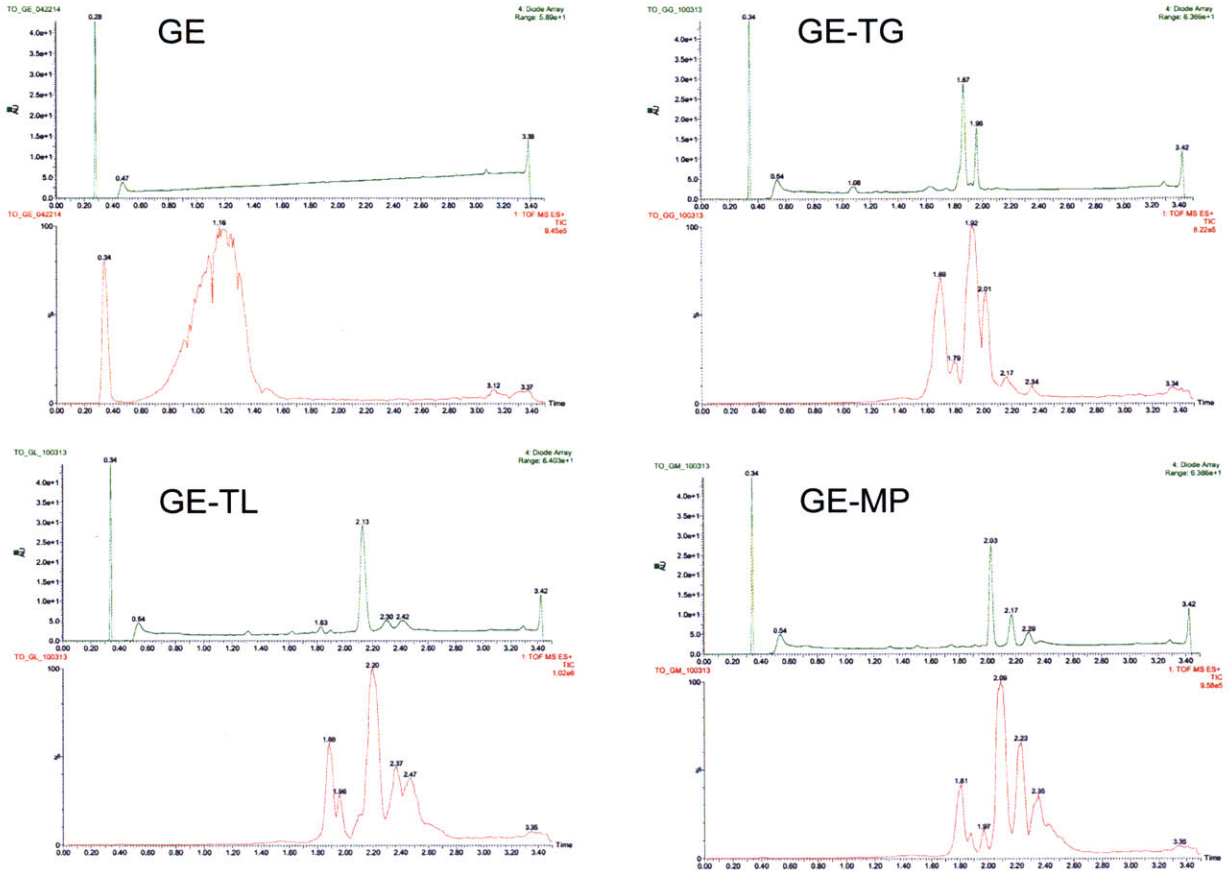

Figure S3.4 UPLC Chromatograms of GE starting material and purified GE based TEPEs. The green chromatograms represent the signal from the UV-PDA detector while the ESI QT of MS detector is shown in the red chromatograms. Again no starting material was detected in the purified GE based TEPE chromatograms.

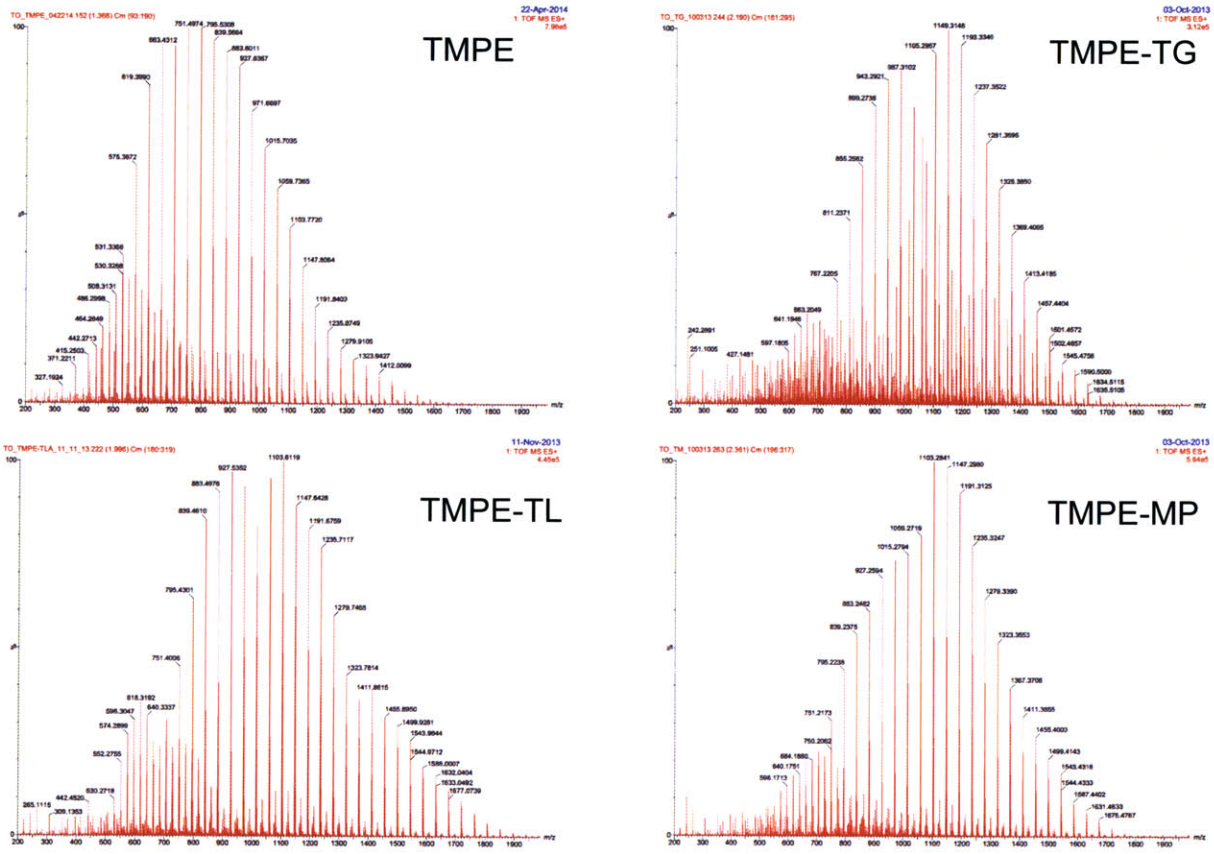

Figure S3.5 The combined mass spectrum for the TMPE starting material and purified TMPE based TEPEs. The mass spectrum was averaged over the entire region of the chromatogram that contained the TEPE (i.e. monofunctional, bifunctional and trifunctional peaks).

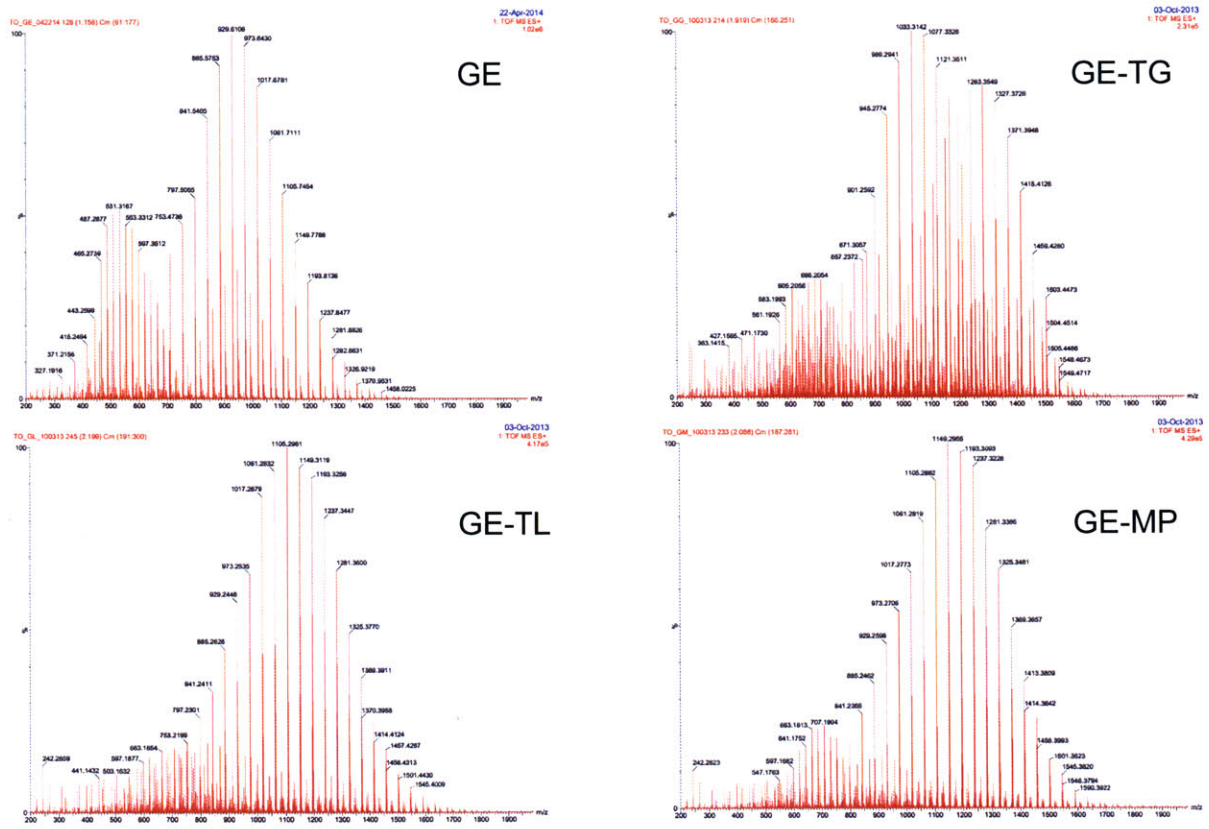

Figure S3.6 The combined mass spectrum for the GE starting material and purified GE based TEPEs. The mass spectrum was averaged over the entire region of the chromatogram that contained the TEPE (i.e. monofunctional, bifunctional and trifunctional peaks).

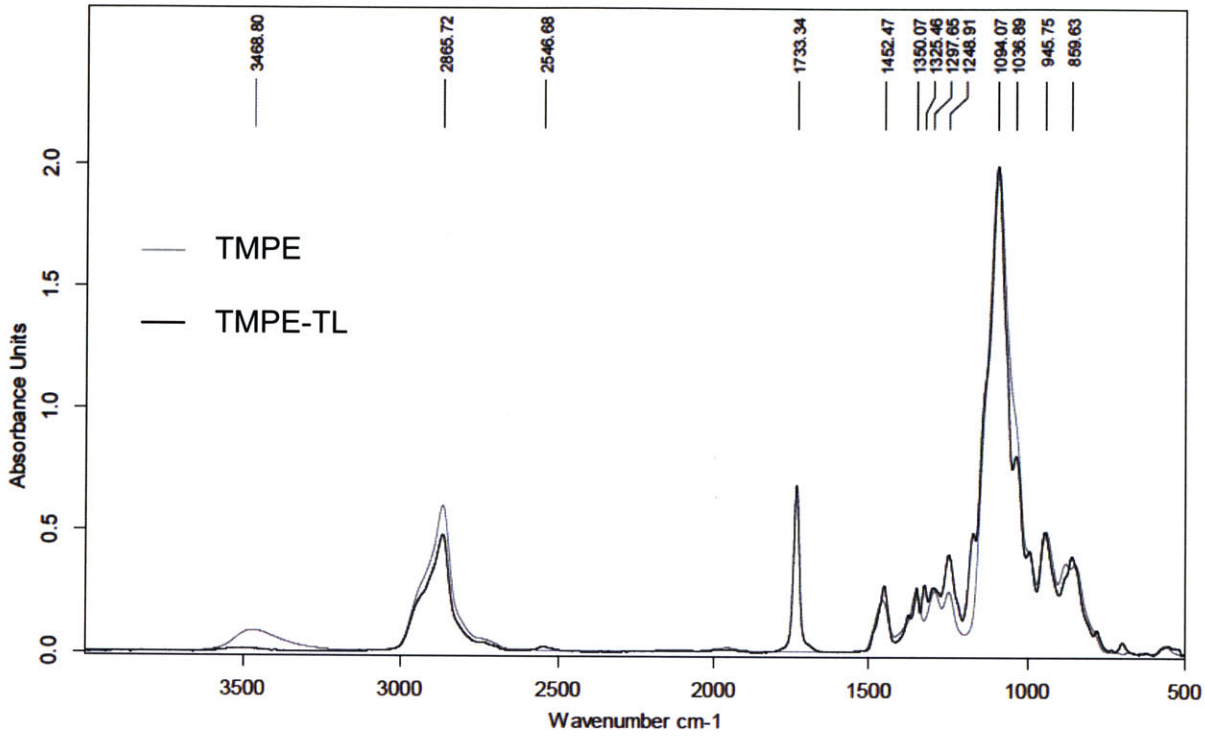

Figure S3.7 Spectra from Single reflection ATR-FTIR analysis of the TMPE starting material and one of the TMPE based TEPEs, TMPE-TL. The purified TMPE-TL sample shows characteristic features that demonstrate the achievement of high thiol functionalization: (1) ester stretch at 1733 cm^{-1} and (2) thiol stretch at 2547 cm^{-1} and (3) loss of the broad hydroxyl stretch that is present in the starting material at 3200-3600 cm^{-1}.

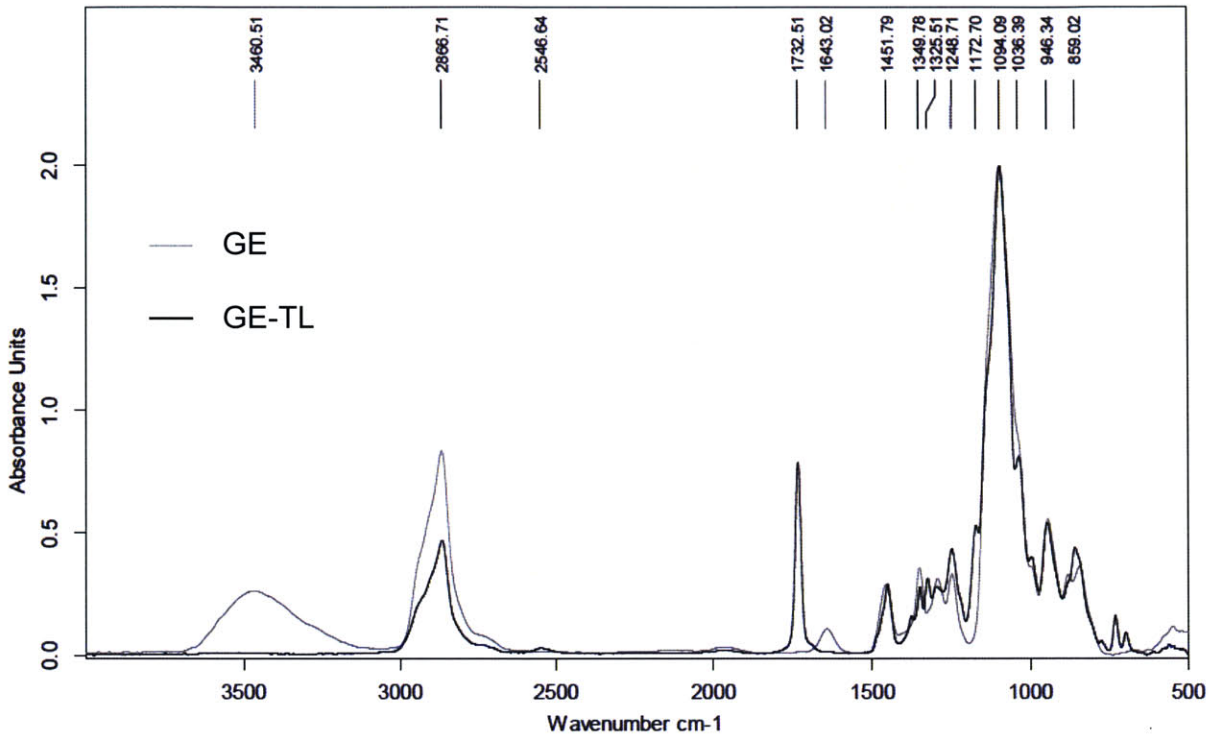

Figure S3.8 Spectra from Single reflection ATR-FTIR analysis of the GE starting material and one of the GE based TEPEs, GE-TL. Similar features to that seen in Figure S3.7 are observed that suggest a high extent of thiol functionalization.

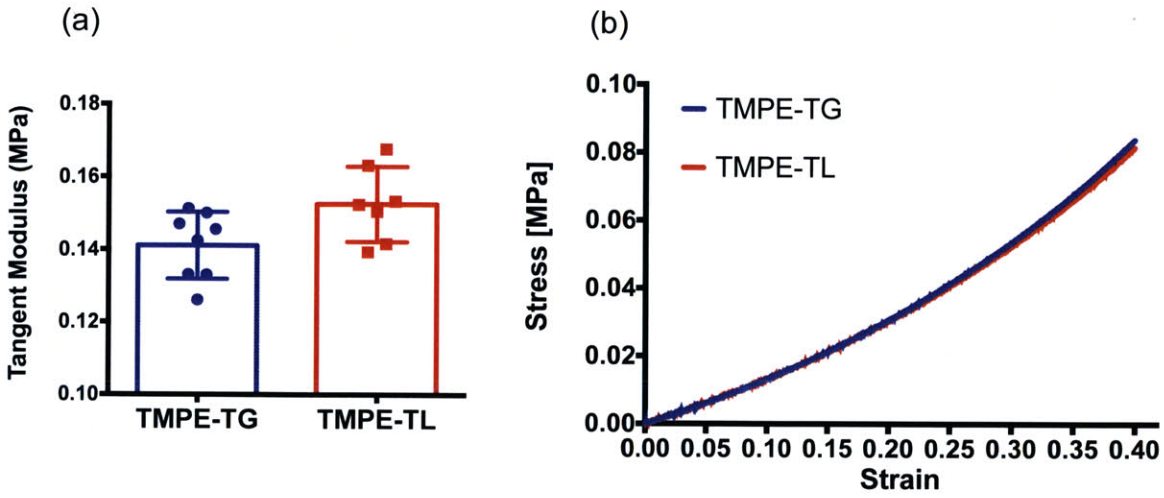

Figure S3.9 Results of compressive testing on two TEPE hydrogels that were formed by combining TMPE-TG and TMPE-TL with PEGDA 575. **(a)** Results from the calculations to assess the tangent modulus (Compressive Modulus at 10% strain) across a series of tests. **(b)** A characteristic stress strain curve demonstrating the similarity of mechanical properties for the two TEPE hydrogels. Samples were tested to approximately 45-50% strain and no samples experienced failure up to this point.

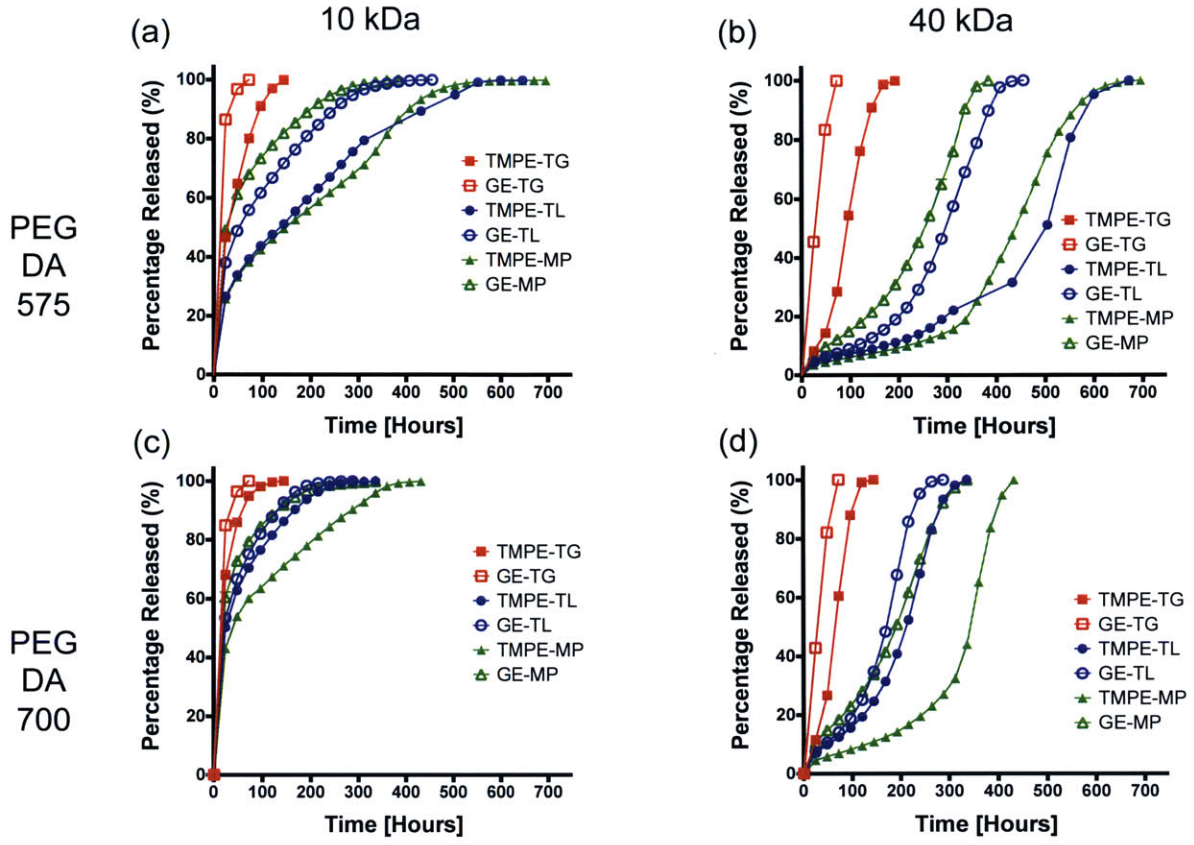

Figure S3.10 The diffusion of 10kDa and 40kDa FITC-Dextrans from hydrogel PEGDA 575 and 700 TEPE formulations. **(a)** 10kDa FITC-Dextrans released from TEPE-PEGDA 575 hydrogels; **(b)** 40kDa FITC-Dextrans released from TEPE-PEGDA 575 hydrogels; **(c)** 10kDa FITC-Dextrans released from TEPE-PEGDA 700 hydrogels; **(d)** 40kDa FITC-Dextrans released from TEPE-PEGDA 700 hydrogels.

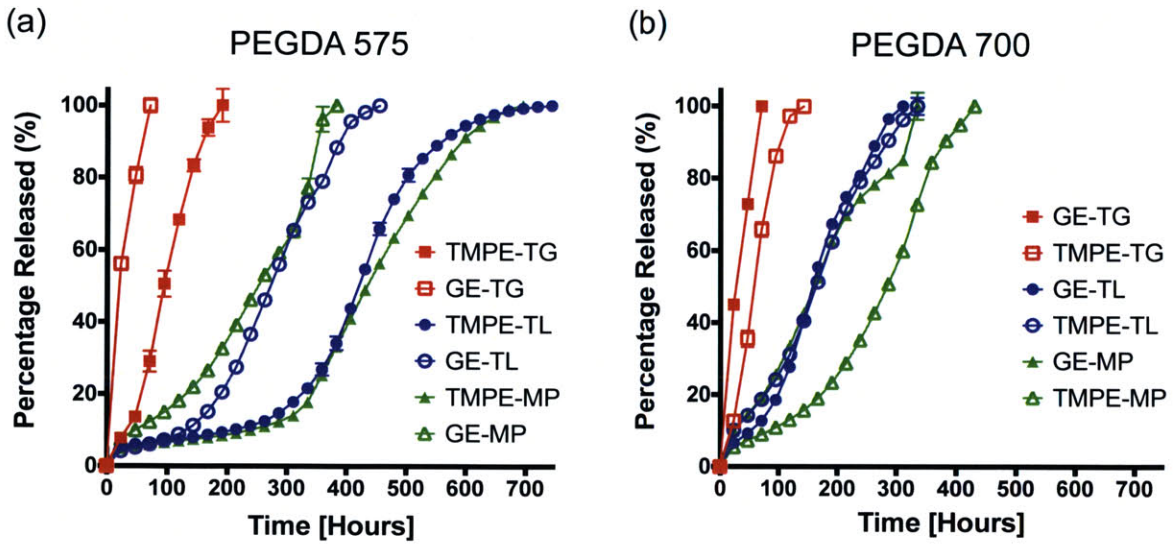

Figure S3.11 The release of FITC labeled ovalbumin from **(a)** TEPE-PEGDA 575 and **(b)** TEPE-PEGDA 700 hydrogels.

4 COVALENT INCORPORATION OF TREHALOSE WITHIN HYDROGELS FOR ENHANCED LONG-TERM FUNCTIONAL STABILITY AND CONTROLLED RELEASE OF BIOMACROMOLECULES

This work has been submitted for publication as: Timothy M. O'Shea, Matthew J. Webber, Alex A. Aimetti, and Robert Langer. Covalent incorporation of trehalose within hydrogels for enhanced long-term functional stability and controlled release of biomacromolecule. *Submitted.*

4.1 INTRODUCTION

With the advent of the biotechnology industry, numerous biopharmaceutical products in the form of peptides, proteins, antibodies, enzymes, engineered fusion proteins and conjugates have been developed for the treatment of diabetes, inflammatory and metabolic diseases as well as various cancers and neurological disorders [272-276]. The advantages of protein therapeutics compared to traditional small molecule drugs include higher potency, a reduction in toxicity and off target effects and a more predictable mechanism of action [276,277]. These favorable properties have allowed protein therapeutics to achieve higher clinical trial success rates and faster regulatory approval timelines compared to all other classes of drugs in recent times [275,278]. However, in spite of the encouraging clinical results there still remains several manufacturing, storage, formulation and administration challenges that hamper their effectiveness across a wider spectrum of indications. Owing to limitations in oral and parenteral administration, biomaterial based drug delivery systems (DDS) such as liposomal and polymeric nanoparticles, hydrophobic polymer matrices as well as locally applied injectable hydrogels have been developed to avoid undesirable repeat injections of drug-only solutions [238,279-281].

Hydrogel materials have received the most attention within the context of controlled release of biologic therapeutics, and numerous systems have been developed affording significant temporal control and localized bioavailability of these drugs [226,281]. Nonetheless, for a number of particularly fragile biomacromolecules, whose activity depends on precise structural folding and/or the specific arrangement of cofactor molecules, current hydrogel technology is inadequate. These complex biomacromolecules, which include monoclonal antibodies and therapeutic enzymes, have seen limited successful incorporation within hydrogels as they readily lose functional activity during biomaterial encapsulation and/or the controlled release period[153,282,283]. Additionally, irreversible denaturation or

aggregation of these proteins may also pose significant toxicity and undesirable immunogenic risks[277]. Understanding how existing hydrogel technologies compromise protein integrity is essential for the development of viable solutions. Hydrogels formed using covalent crosslinking chemistries have the potential to react and alter proteins. Specifically, proteins can be irreversibly modified by: (i) free radical attack in photoinitiated hydrogels [245,284]; (ii) the formation of undesirable protein-polymer conjugates in systems which employ certain amine or thiol reactive chemistries [242,285,286]; as well as (iii) disulfide interchange in free thiol containing systems. In physical gels that are formed using amphiphilic molecules, strong hydrophobic interactions needed to facilitate network formation can disrupt protein structure [287-289]. Moreover, there is currently limited understanding pertaining to long-term protein stability within hydrogel matrices where a multitude of potential biomaterial- and *in vivo*- derived forces such as material-drug electrostatic or hydrophobic interactions, thermal induced protein misfolding, hydrolytic degradation, deamidation and disulfide interchange can contribute to loss of protein activity[280,290,291].

To protect proteins from these structural perturbing sources small molecule osmolytes such as sugars, polyols and salts have been employed as stabilizing agents[196,199,292]. However, incorporating such a stabilizing mechanism within prolonged release hydrogels with high water content presents challenges. Specifically, small molecule excipients diffuse from hydrogel systems more quickly than the larger biomacromolecules requiring stabilization. Protein stabilization is therefore difficult to maintain beyond the initial formulation and delivery period. As a result of the inadequacy of small molecule excipients for enduring stabilization within biomaterial matrices, the development of strategies to preserve long-term protein bioactivity is an important area of investigation [290,293].

Here we describe a new method for the long-term stabilization of protein therapeutics within hydrogel networks through the covalent incorporation of trehalose, a well characterized non-reducing disaccharide known to be an extremely effective protein stabilizing excipient[294,295], into a synthetic polymeric hydrogel. Using diacrylate functionalized trehalose monomers we covalently incorporated the excipient into the network of a known biocompatible thiol-ene ethoxylated polyol (EP) hydrogel platform to form a biodegradable, non-swelling material[226]. The trehalose hydrogel affords prolonged stabilization of model protein therapeutics throughout a period of controlled release as well as under relevant formulation and shelf-life stressors that include heat and lyophilization. The strategy described here for trehalose incorporation within a hydrogel illustrates a robust method that could be applied to a variety of formulation, manufacturing and delivery applications of protein therapeutics.

4.2 Results and Discussion

To synthesize diacrylate functionalized trehalose (TDA) for covalent incorporation within the ethoxylated polyol hydrogel we adapted a synthetic scheme described previously by Dordick and colleagues which involves the acylation of trehalose by vinyl acrylate **(Figure 4.1)** [296]. By using Candida Antarctica Lipase B (CALB)-immobilized on acrylic resin we achieved regiospecific esterification of the trehalose at only the 6 and 6' hydroxyl sites to synthesize a diacrylate functionalized trehalose without requiring protection/deprotection steps often required in the chemical modification of carbohydrates [297] **(Figures S4.1 and 4.2)**. Next, we fabricated the trehalose hydrogels by combining the TDA monomer with specific tri-thiol-functionalized ethoxylated polyol esters oligomers (TEPEs) derived from a library used to form hydrogels via a thiol-ene Michael addition reaction [226]. Specifically, for the trehalose hydrogel system reported here, we applied trimethylolpropane ethoxylate thiolactate (TMPE-TL) as the thiol functionalized crosslinker, as well as poly(ethylene glycol) diacrylate (PEGDA575) to create materials with varied ratios of PEG to trehalose within the network (Figure 4.1). Herein we denote hydrogel formulations in terms of the percentage of diacrylated molecules attributed to the TDA (i.e. 100% trehalose hydrogel (100T) has 100% acrylate groups from TDA). Combining TMPE-TL with mixtures of PEGDA and TDA at thiol and acrylate functional group stoichiometric equivalency under physiologically buffered conditions (1X PBS, pH =7.4) resulted in an increasingly viscous solution which cured *in situ* to form a hydrogel within 2 to 3 minutes of mixing **(Figure 4.2)**.

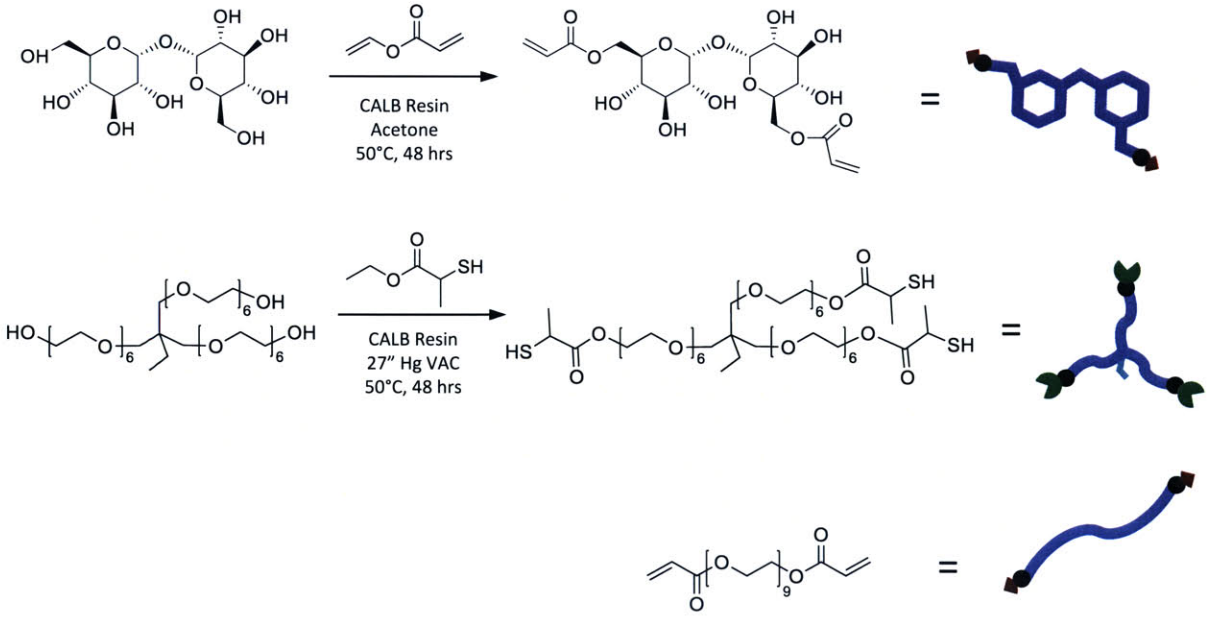

Figure 4.1 Trehalose diacrylate monomers can be synthesized without hydroxyl protecting steps using an enzymatic catalyst. Overview of trehalose diacrylate (TDA) and TMPE-TL synthesis both using CALB resin as a catalyst.

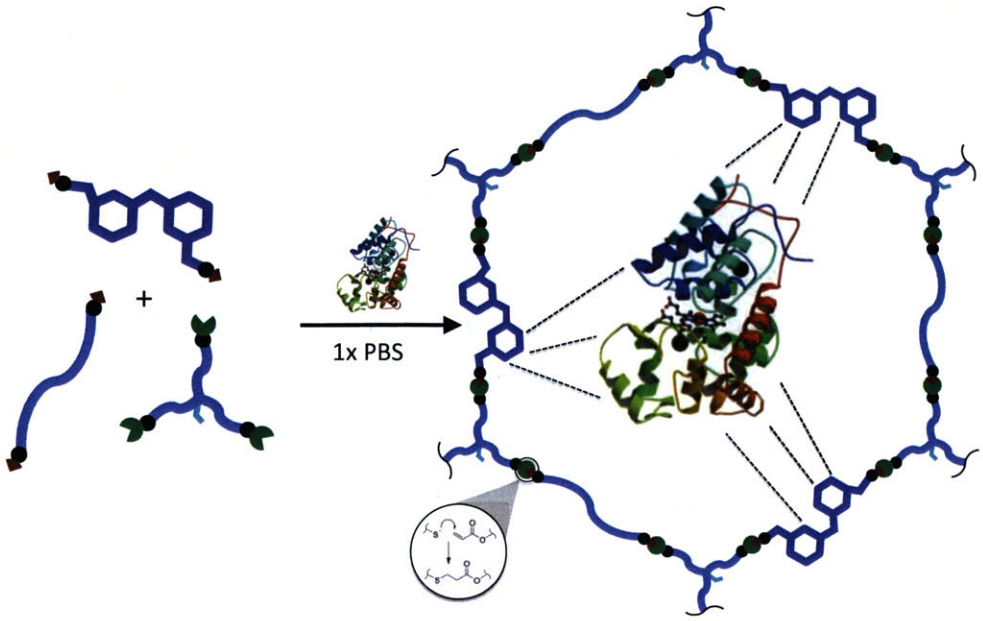

Figure 4.2 Trehalose hydrogels are formulated using thiol-acrylate Michael Addition chemistry. Combining TMPE-TL, TDA and PEGDA in PBS allows a hydrogel to form that can encapsulate and stabilize protein therapeutics.

Dynamic rheology was used to monitor the kinetics of gelation for the trehalose hydrogels. 100T hydrogels displayed a sol-gel transition and *as cured* network mechanical properties comparable to previously reported ethoxylated polyol (EP) hydrogels (**Figure 4.3**)[226]. In addition, the kinetics of gelation showed minimal deviation across the various TDA/PEGDA ratios investigated suggesting that the electrophilic character of the TDA acrylate groups were comparable to those on the PEGDA **(Figure S4.3)**. The equilibrated swelling ratio, Q_m, for the trehalose hydrogels increased with higher TDA content **(Figure S4.4)**. Furthermore, trehalose hydrogels (25 wt%) formulated at less than or equal to 75T showed syneretic behavior at 37°C (**Figure 4.4**). Much like the EP hydrogels reported previously, trehalose hydrogels that demonstrated initial syneresis upon equilibration also displayed non-swelling degradation via an ester hydrolysis mechanism[226] **(Figure S4.5)**. The rate of degradation of trehalose hydrogels was proportional to the percentage content of TDA. The faster degradation observed in hydrogels with increasing ratios of TDA was attributed to the more labile ester bonds from the TDA as well as the increased Q_m values, which corresponds to higher free water content in the equilibrated network **(Figure S4.6)**. Throughout the complete hydrogel degradation process, trehalose persisted, and was detectable, within the network **(Figure S4.7).**

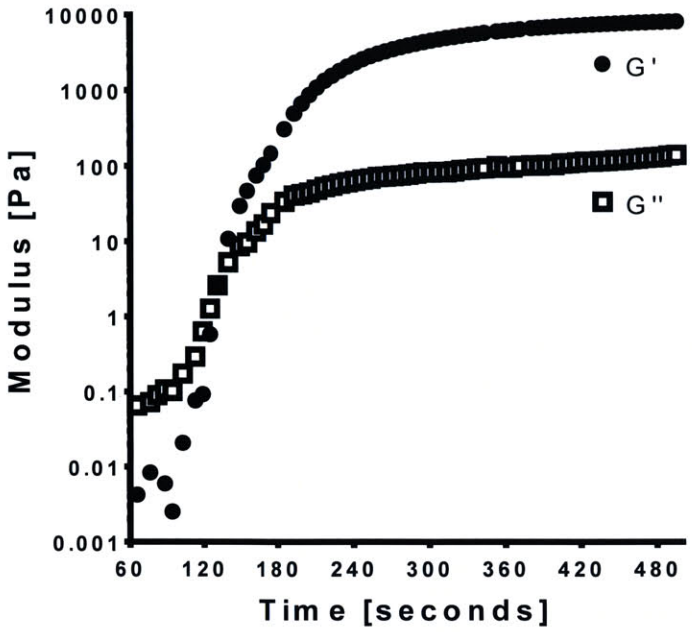

Figure 4.3 Trehalose hydrogels demonstrate sol to gel transition within 2-3 minutes after mixing of the precursors. Dynamic rheology curve for 100T hydrogel (strain=5%, frequency=10 rad s−1).

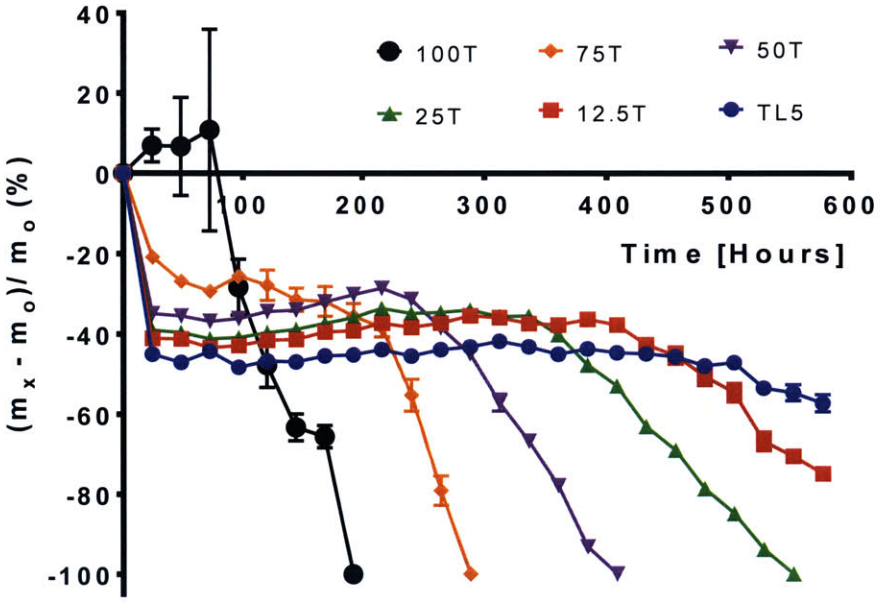

Figure 4.4 Increasing the trehalose content within hydrogels creates faster resorbing materials. Percentage hydrogel wet mass changes (compared with the initial cured wet mass) over time for hydrogels with various percentage composition of trehalose within the network (TL5 = TMPE-TL PEGDA 575).

To characterize the influence of TDA content on model protein release from hydrogels we next encapsulated FITC labeled ovalbumin (MW≈45kDa) and Alexa Fluor 647 conjugated IgG (MW≈150 kDa) within various trehalose hydrogel formulations and quantified release *in vitro* via fluorescent intensity measurements. The hydrogels displayed triphasic release profiles that were fitted to a Weibull distribution[226] (**Figure 4.5**). For ovalbumin loaded hydrogels, increasing the TDA content led to exponentially decreasing t_{50} (time to 50% release of drug) values, while k (the molecule release constant) increased linearly **(Figure S4.8).** The release kinetics were comparable for proteins of dissimilar size (ovalbumin and IgG), indicating the controlled release from the network was primarily dependent on network degradation rather than the passive diffusivity of the protein **(Figure 4.6)**. The accelerated release kinetics observed for hydrogels with increasing TDA content was reminiscent of that seen when we previously blended ratios of TMPE-TL with the faster degrading TEPE, trimethylolpropane ethoxylate thioglycolate (TMPE-TG) [226]. From this observation, we established formulation parameters allowing us to match the release kinetics for several trehalose hydrogels with a corresponding TMPE-TG/TL blend-PEGDA 575 material **(Figure 4.7)**. Specifically, 50T trehalose hydrogels had protein release and degradation profiles similar to that of a 30/70 TMPE-TG/TL 575 blend while the 25T formulation was equivalent to the 15/85 mixed hydrogel. By matching hydrogel degradation and protein release kinetics in hydrogels with and without trehalose we could now probe whether covalent trehalose incorporation would be beneficial to long term protein stability with minimal potentially confounding variables.

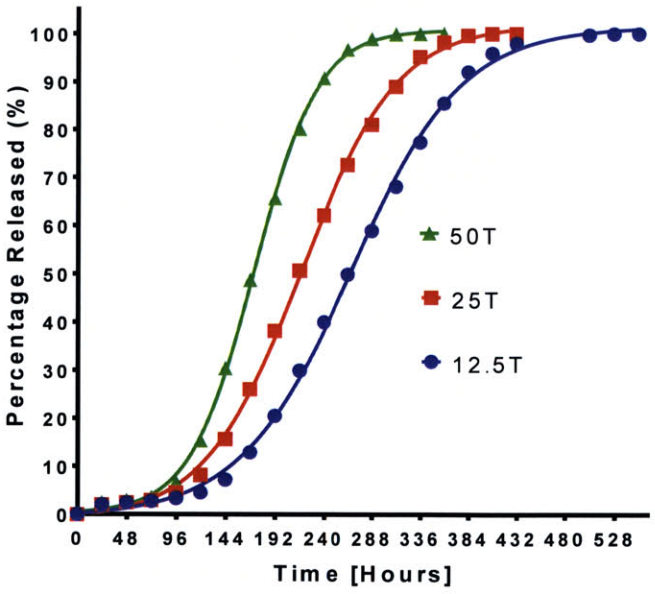

Figure 4.5 Trehalose hydrogels show triphasic release of FITC-ovalbumin. Faster release kinetics are observed with increased concentration of covalently incorporated trehalose within the hydrogel.

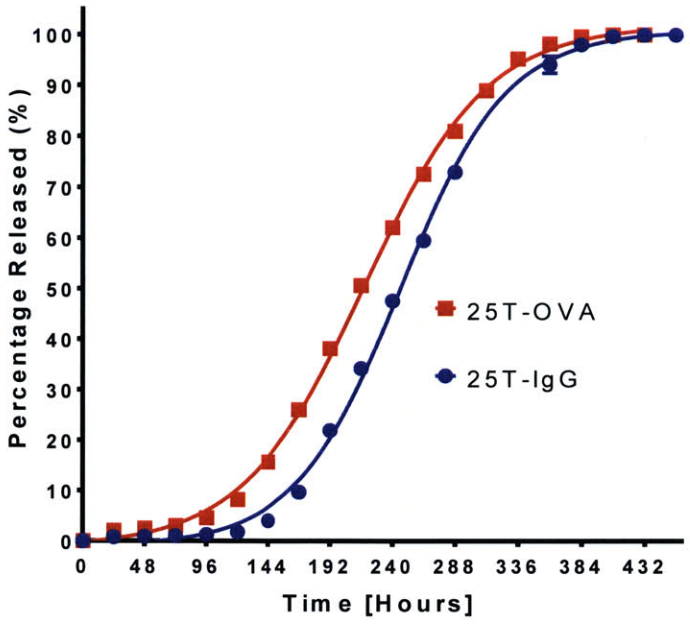

Figure 4.6 Comparative cumulative release profile for 25T hydrogels encapsulating FITC-ovalbumin and Alexa Fluor 647 IgG demonstrating that release kinetics are comparable for proteins of dissimilar size and indicating that the controlled release from the network was primarily dependent on network degradation rather than the passive diffusivity of the protein.

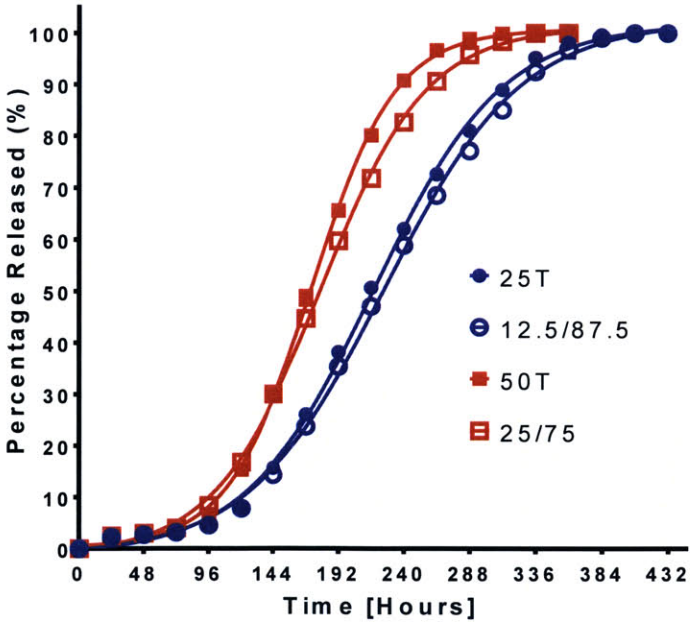

Figure 4.7 The protein release kinetics for trehalose hydrogels can be matched to a corresponding TMPE-TG/TL blend-PEGDA 575 material allowing for appropriate protein activity and stability comparisons to be undertaken.

With matched release kinetics for trehalose and EP hydrogels obtained, we next turned our attention to the effect of trehalose network incorporation on the functional activity of delivered proteins. To perform the protein activity preservation/recovery assays we used a commercially available horseradish peroxidase (HRP) isoform C as the first model protein. This 40 kDa protein is similar in size to the FITC-labelled ovalbumin used to characterize the controlled release kinetics and possesses complex structural features that make it a good model protein for analyzing the influence of various hydrogel properties on protein stability. Specifically, the protein is a metalloenzyme with an active site, a non-covalently bound heme prosthetic group, which allows the protein to catalyze the removal/conversion of hydrogen peroxide to oxidize numerous organic and inorganic molecules. The protein also contains four disulfide bonds and numerous metal binding sites that attract two divalent calcium ions to bind to the protein as enzymatic cofactors. Conformational or structural perturbations of these important elements results in loss of protein activity. For example, depletion of bound calcium ions due to structural instabilities can reduce the activity of the protein by over 50%, while heme group displacement or destruction can also substantially affect protein function[298-300]. Therefore, given the many ubiquitous features of this protein (metal/heme cofactors, the presence of numerous disulfide bonds, dominant alpha helix secondary structure) HRP represents a good first protein to evaluate the efficacy of trehalose hydrogels. Furthermore, others have documented the enhanced stabilizing effect of trehalose and trehalose polymers on HRP activity in aqueous solution upon application of heat and lyophilization stressors which enables benchmarking of the current hydrogel technology[301-304]. Prior to hydrogel encapsulation, we first characterized the solution stability of HRP at 37°C as well as against dialysis (10kDa cut off) to drive the displacement of bound cofactors **(Figure S4.9).** The thermal stability of HRP in solution was significantly concentration dependent. Specifically, 1 mg/ml solution of HRP showed no significant loss of activity over an incubation period of one week, while activity decreased significantly in solutions of 100 μg/ml (45% activity loss over first 24 hours) and 10 μg/ml (80% activity loss after just 24 hours). Furthermore, dialysis of 100 μg/ml solution accelerated this loss of activity over the subsequent days of incubation (Figure S4.9). These findings demonstrate that HRP is a highly unstable protein at physiological temperatures in dilute solutions and support its use for the long term release stability studies.

Next we evaluated the recoverability of active HRP released from trehalose and EP hydrogels *in vitro*. Using 60 μL hydrogel discs we encapsulated 2 mg/ml of HRP and incubated samples in 600 μL PBS/0.01% BSA at 37°C to simulate physiological conditions. HRP activity was assessed upon daily replacement of

incubation media using a standard HRP substrate solution, 3,3',5,5'-Tetramethylbenzidine (TMB). The percent recovery of active HRP was directly related to the trehalose content within the hydrogels **(Figure 4.8)**. When loaded with 2 mg/ml HRP, the 100T hydrogels allowed for practically total recovery of HRP over a five-day period. By comparison, 50T hydrogels showed approximately 50% recovery of HRP when loaded at the same concentration, with detection of additional active HRP limited after approximately 10 days with this material. The recovery was reduced dramatically with 25T hydrogels allowing only 7% of total active HRP to be recovered. Although suggestive of improved HRP stability, we are mindful that these studies are influenced by the degradation rate of the material, which is affected substantially by total trehalose content.

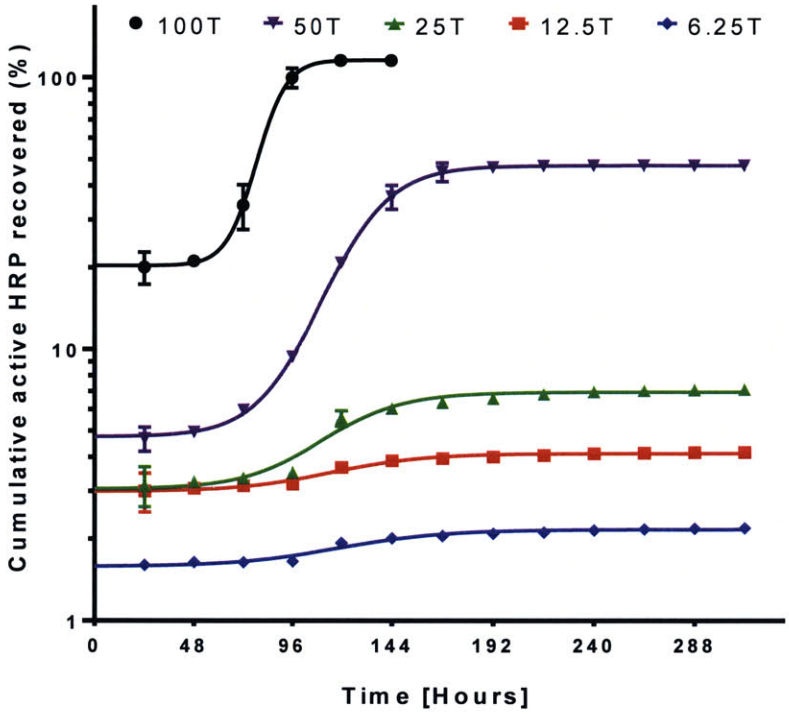

Figure 4.8 Trehalose hydrogels show greater recovery of active protein during controlled release that is trehalose concentration dependent. Cumulative HRP recovery for hydrogels with various percentage composition of trehalose. (note: the y axis is represented on a log scale for ease of visualization of the different release curves).

To control for the kinetics of network degradation we compared a 50T hydrogel with the corresponding blended EP hydrogel. Within this comparative study the 50T hydrogel demonstrated significantly superior recovery of active HRP compared to the EP hydrogel independent of HRP loading **(Figure 4.9 and Figure S4.10)**. Specifically, at 2mg/ml loading concentration recovery of active HRP was nearly 7 fold more for the 50T hydrogels (47.5%) compared to the EP material (7% HRP activity recovered). For all hydrogels the cumulative recovery showed a triphasic profile with similar kinetic parameters to the

FITC-ovalbumin release assays. However, active HRP recovery profiles demonstrated lower t_{50} values and a faster rate of third phase decay compared to the FITC-ovalbumin release curves. These differences were seen in both hydrogel groups. Protein loading also influenced recovery of active HRP, with a higher trehalose to protein ratio resulting in increased recovery **(Figure 4.10)**. Explicitly, a 4 fold reduction in protein concentration (from 2mg/ml to 500 µg/ml) resulted in a nearly 15% increase in normalized protein activity but with equivalent release kinetics. To assess the effect of possible disulfide interchange between the protein and residual thiol groups within the hydrogel we formed 50T hydrogels with varying degrees of TMPE-TL excess. The presence of free thiol groups within the hydrogel network was confirmed by Ellman's assay and can be visualized as a yellow staining of the material **(Figure 4.11)**. Unsurprisingly, increased free pendant thiols within the network significantly diminished total HRP recovery **(Figure 4.11)**. This result is consistent with other reports that have observed a loss of HRP activity in the presence of thiol reducing agents such as dithiothreitol (DTT) [305]. Taken together these results demonstrate that covalently incorporating trehalose into the hydrogel leads to improved recovery of active HRP in a manner that is dependent on trehalose concentration, network chemical composition and protein loading parameters.

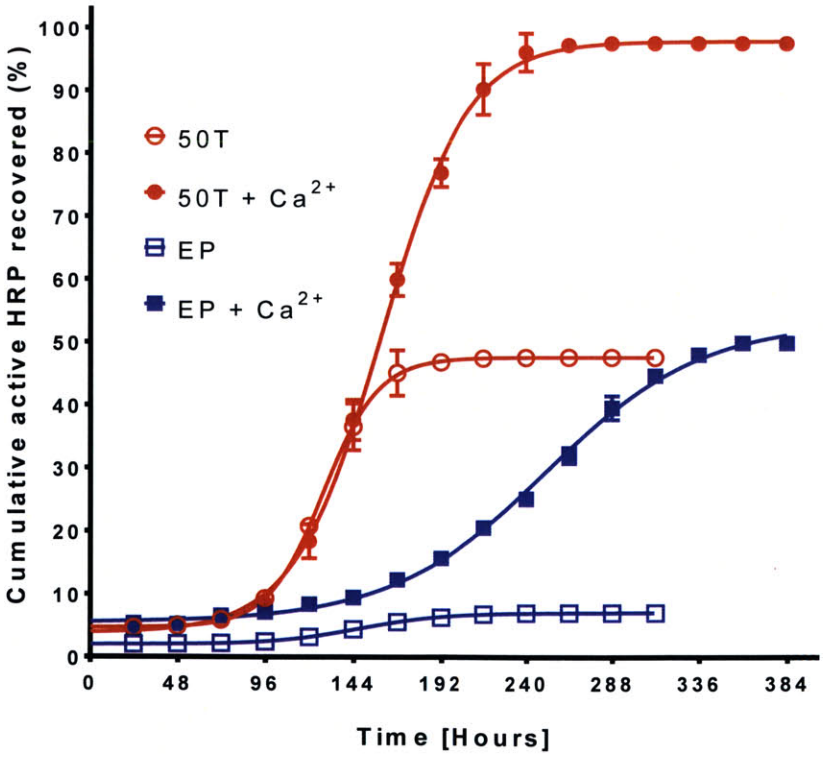

Figure 4.9 Trehalose hydrogels demonstrate enhanced HRP recovery compared to EP hydrogels with matched release kinetics. Comparison of cumulative HRP recovery for 50T and EP hydrogels released into PBS and media containing 1mM $CaCl_2$. HRP was loaded into hydrogels at 2 mg/ml.

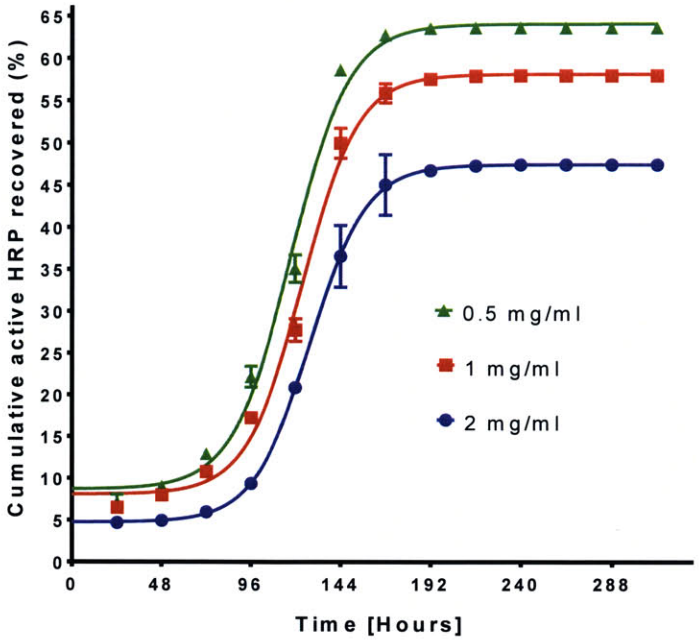

Figure 4.10 Higher trehalose to protein ratios within the hydrogel network result in great HRP recovery. Cumulative HRP recovery for various HRP loading concentrations within 50T hydrogels.

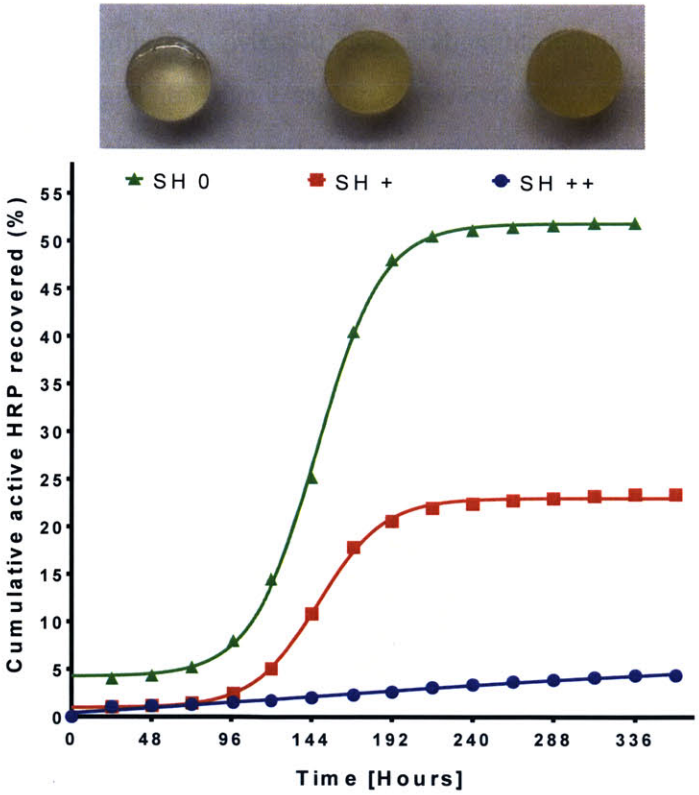

Figure 4.11 Excess free thiol groups within 50T hydrogels negatively affect cumulative HRP recovery. The image above the graph shows hydrogels stained with Ellman's reagent, with increased yellow hue within the materials demonstrating higher free thiol content.

To elucidate the mechanism by which covalent trehalose incorporation within hydrogels improves the functional HRP recovery during controlled release, we attempted to characterize protein secondary and tertiary structure within the hydrogel. Circular Dichroism (CD) demonstrated preservation of protein structural signals during gelation but upon hydrogel equilibration scattering from the material limited further analysis **(Figure S4.11)**. FTIR analysis was used to evaluate protein secondary structure on dehydrated hydrogel samples but low sensitivity and interference from hydrogen bonding of the trehalose within the network made the analysis inconclusive. Evaluation of the absorbance of the Soret band occurring around 400 nm wavelength provided some insight into the stability of the heme ring within HRP. Minimal attenuation or shifting of this visible signal attributed to the prophoryin ring was detected in either the trehalose or EP hydrogel samples over time suggesting minimal disruption of this structure **(Figure S4.12)**. To investigate whether the hydrogel caused depletion or displacement of calcium cofactors bound to HRP, a comparative study was performed whereby hydrogels were incubated in media containing calcium ions and total active HRP recovery was quantified. Interestingly, the recovery of HRP was significantly higher for EP hydrogels incubated within the calcium-containing media. Specifically, over the first 4 days of incubation the EP hydrogels showed equivalent HRP recovery to that of the trehalose hydrogel and prolonged recovery of active HRP within these hydrogels was observed up until terminal degradation at two weeks of total incubation **(Figure 4.9)**. As a result, approximately 48% of total active HRP was recovered from the EP hydrogels incubated in the calcium containing media. Despite this increased recovery, following the first four days of incubation the inclusion of calcium in the media was unable to provide the stabilization required to achieve the same levels of recovery as seen in the trehalose hydrogels (Figure 4.9). Within the calcium containing media, trehalose hydrogels demonstrated close to total recovery (97.5%) of active HRP over a two week period. The additional stabilization in the calcium media for the 50T hydrogels was detectable only after 6 days of incubation. After 6 days the active HRP recovery in PBS began to decay rapidly while in the calcium media the active recovery curve followed the same trend as total protein release. Taken together these results suggest that at early stages of incubation there is potentially reversible structural perturbations of HRP within the EP hydrogel that displaces calcium ions from the metal binding site of the protein, which is recoverable provided renewed sources of these ions are accessible to the protein. However, other structural perturbations that are either non-reversible or that are calcium ion binding site independent must also take place within the EP hydrogel to account for the near 50% unrecovered HRP noted when incubated in calcium media. The variation in total recovery for trehalose hydrogels within the two medias suggests that, at least initially, the trehalose provides a stabilizing effect on HRP that is

media independent but as the material starts to degrade, the presence of excess calcium ions act to mitigate some protein destabilization occurring within the hydrogel. It is hypothesized that an excess presence of divalent cations in the media acts to overcome chelation of HRP-bound calcium that may be readily caused otherwise by the increased concentration of carboxylate anion hydrolysis products locally within the hydrogel. This chelation theory is further supported by an observed slowing of the hydrogel degradation rate for both hydrogel groups in calcium containing media suggesting the possible formation of stabilizing ionic salt bridges involving the divalent cations and the carboxylate hydrolysis products. While beyond the scope of this paper, applying new emerging protein spectroscopy techniques could be used in the future to better understand the specific structural stabilization afforded by the trehalose hydrogels *in situ* [306,307].

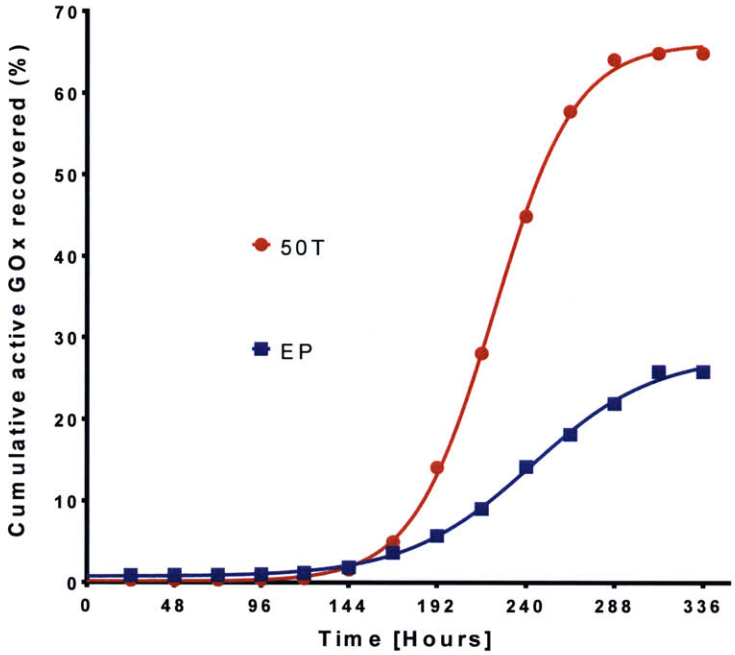

Figure 4.12 Trehalose hydrogels enhance the recovery of active GOx during long-term controlled release. Comparison of cumulative GOx recovery for 50T and EP hydrogels releasing into PBS only incubation media.

Given that as an osmolyte trehalose has demonstrated effective stabilization across a variety of different classes of proteins and enzymes we hypothesized that covalent incorporation of trehalose into hydrogels would be equivalently robust. To determine whether this was an accurate assessment we next quantified active protein recovery during controlled release for several other well characterized model enzymes. For glucose oxidase (GO), a 130 kDa dimeric enzyme with a Flavin adenine dinucleotide (FAD) redox cofactor, the trehalose hydrogel resulted in enhanced recovery compared to the EP

hydrogel over a two week period **(Figure 4.12)**. Using an Amplex red assay to quantify active GO, trehalose hydrogels showed 65% total cumulative recovery that was more than double that seen for the EP hydrogel (26%). The kinetics of release for this large protein were also triphasic, but compared to HRP all active release of GO occurred as a result of network degradation rather than diffusion. For α-chymotrypsin, a serine protease with dominant Beta sheet structure, the enzyme itself caused faster network hydrolysis and consequently more rapid protein release **(Figure S4.13)**. However, even with a rapid first order release profile a higher recovery of active protein in the trehalose hydrogel was observed. These additional protein studies demonstrate a robust stabilizing effect attributable to the covalent incorporation of trehalose into the hydrogel network.

Despite the positive release assay results these studies could not confirm whether stabilization of protein is conferred by the trehalose hydrogel itself or by trehalose containing network degradation products that diffuse into the incubation media along with the protein. To quantify stabilization of HRP within trehalose hydrogels we prepared 15 μL hydrogel discs and conducted *in vitro* activity examinations whereby we sacrificed triplicate hydrogels every two days and incubated the material in TMB substrate solution to evaluate total activity. When placed in the TMB solution, hydrogels with active HRP turn a deep blue and the converted chromophore diffuses into the incubation solution increasing the readable signal of the solution. After 5 minutes the substrate solution was quenched with acid and the gel removed from the media before the solution was read on a microplate reader. Due to high HRP loading within hydrogel samples (1mg/ml), both trehalose and EP hydrogels were at the detection limit of the assay at the time of curing. HRP activity in the 50T hydrogels remained at the detection limit for up to 6 days of incubation *in vitro* before beginning to decrease, likely resulting from protein release into the incubation media as the material begins to degrade around this time **(Figure 4.13)**. By contrast EP hydrogels with and without soluble trehalose showed significantly decreased activity from encapsulated HRP after just 48 hours with activity continuing to decay exponentially over the subsequent 12 day period (Figure 4.13). The incorporation of soluble trehalose within EP hydrogels did not enhance protein activity likely due to its rapid diffusion from the network during the initial incubation. These data complement the HRP release assay results and together demonstrate preservation of HRP activity *in vitro* that can only be attributed to the covalent incorporation of trehalose within the hydrogel network.

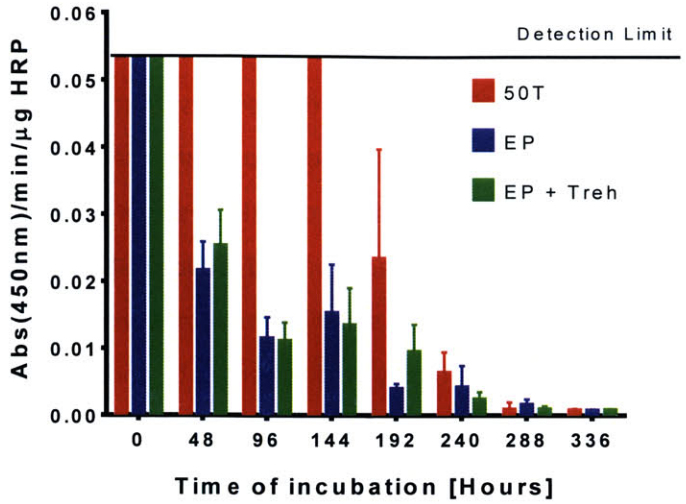

Figure 4.13 Trehalose hydrogels stabilize HRP during encapsulation within the polymer network. Comparison of HRP activity within trehalose, EP and EP plus soluble trehalose hydrogels incubated *in vitro.*

To evaluate whether covalent trehalose incorporation had similar stabilizing effects *in vivo,* we implanted hydrogels containing HRP sub-cutaneously in mice. The 15 µL hydrogel discs loaded at 2 mg/mL were retrieved at 2, 4, 8 and 10 days post-implantation and evaluated for HRP activity using the same TMB assay. In contrast to *in vitro* experimental results HRP activity was maintained at much higher levels for longer periods of time within both hydrogel groups *in vivo*. At 2 and 4 days, the HRP activity within both trehalose and EP hydrogel samples was equivalent. However, by 8 and 10 days following implantation, significantly higher activity was observed in the 50T hydrogels **(Figure 4.14)**.

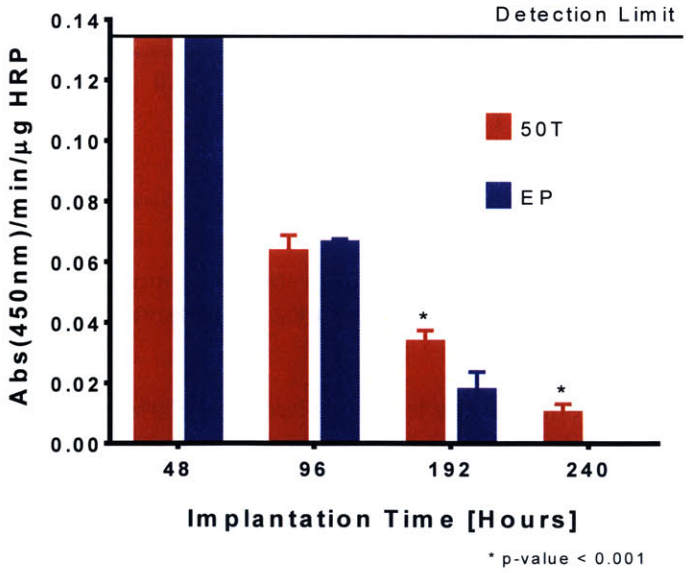

Figure 4.14 Trehalose hydrogels stabilize HRP *in vivo*. Comparison of HRP activity within hydrogels implanted *in vivo* within the subcutaneous space of mice.

Whether this differential activity is attributed entirely to an enhanced stabilizing effect of the trehalose is uncertain as the 50T hydrogels appeared to degrade slower than the EP hydrogels, in spite of this parameter having been matched *in vitro*. This finding could suggest that the trehalose hydrogel was less susceptible to sources of *in vivo* hydrolysis, such as endogenous esterases, than the EP hydrogel and warrants further investigation. The increased duration of HRP preservation *in vivo* in both hydrogel groups is likely a function of slower material degradation and reduced HRP release from the hydrogel. Slower release kinetics could be attributed to less sink-like conditions within the mouse subcutaneous space. Additionally, HRP activity preservation may be augmented by endogenous divalent cations such as Mg^{2+} and Ca^{2+} which may offset the chelating effect of the hydrogel degradation products on HRP bound calcium cofactors. Overall, these *in vivo* studies confirm predictions based on results *in vitro* as protein activity was preserved in both environments as a result of covalent incorporation of trehalose within the hydrogel network.

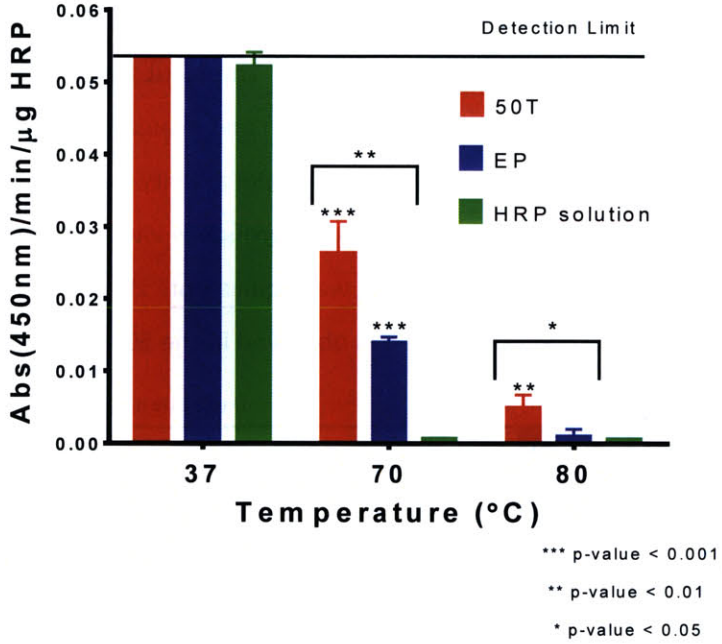

Figure 4.15 Trehalose hydrogels prevent damage and loss of encapsulated HRP activity upon one hour incubation in denaturing temperatures.

In considering the translational potential of the trehalose hydrogel platform we wanted to evaluate the stabilization of proteins upon application of various possible stressors that proteins may experience during biotherapeutic formulation, shelf-life and transportation processes. When encapsulated within 50T hydrogels HRP had enhanced activity upon the application of denaturing heat compared to the protein encapsulated within EP hydrogels or formulated in solution **(Figure 4.15)**. Though the EP

hydrogel did impart significant stabilizing effect on HRP compared to the protein solution at 70°C, this did not match the protection afforded by the 50T hydrogel. The HRP activity preservation for EP hydrogels was lost at 80°C, while the 50T material retained some stabilizing properties. When hydrogels were loaded with HRP and processed by high vacuum lyophilization for 48 hours before being rehydrated for an additional 24 hour period, the 50T hydrogel had significantly more preserved HRP activity compared to both the EP hydrogel and protein solution **(Figure 4.16)**. These data suggest additional utility of the trehalose hydrogel as a way to mitigate protein damage during manufacturing processes that are relevant to numerous biopharmaceutical applications.

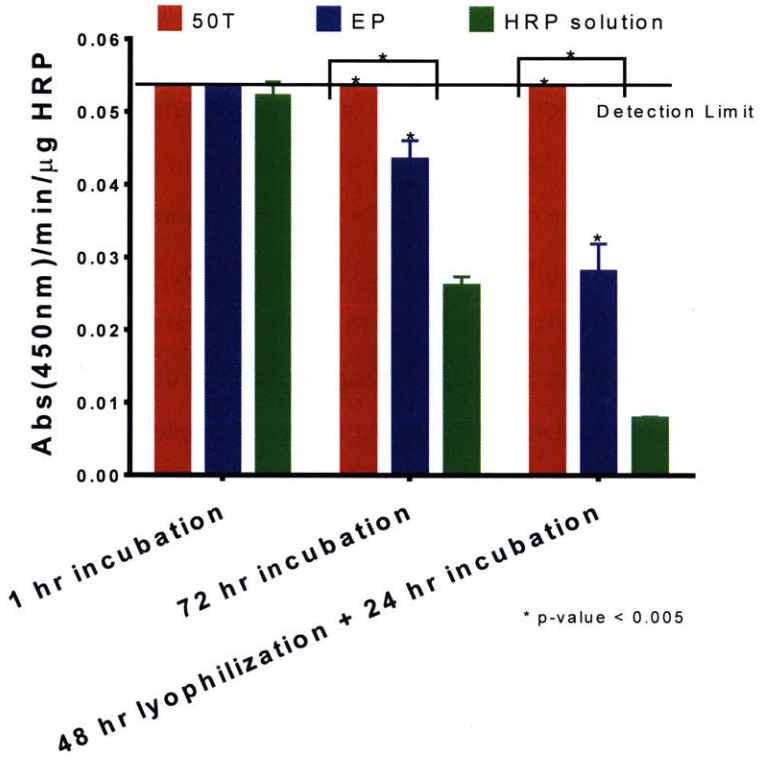

Figure 4.16 Trehalose hydrogels prevent the loss of encapsulated HRP activity upon 48 hour lyophilization and subsequent rehydration for 24 hours.

The mechanism by which trehalose as an osmolyte is able to stabilize proteins in solution during exposure to lyophilization stressors or extreme heat conditions remains poorly understood [295,308]. However, three main theories have emerged from a large body of physical chemistry literature that may explain the functionality of this excipient. These theories include protein stabilization via either: (1) mechanical entrapment of the protein within a glassy structure formed by the trehalose molecules as a result of their relatively high glass transition temperature (vitrification theory); (2) direct hydrogen bonding between the protein and trehalose which preserves protein structure in the absence of

sufficient water (water replacement theory); or (3) by rearranging and concentrating water towards the surface of the biomacromolecule also directed by hydrogen bonding (water entrapment/ preferential exclusion theory) [294]. The unique strength and spatial orientation of hydrogen bonding provided by trehalose is therefore believed to play an important role in protein stabilization. Thus, understanding how these interactions are altered when trehalose is covalently incorporated within the hydrogel is critically important to elucidating its mechanism of action in these materials. We used attenuated total reflection Fourier transform infrared (ATR-FTIR) spectroscopy to characterize the hydrogen bonding within the hydrogel (**Figure 4.17**), with a focus on the spectral signal within the OH stretch region (3000-3800 cm^{-1}) being used to evaluate the specific nature and strength of this bonding as a result of TDA inclusion. The study of hydrogen bonding using ATR-FTIR requires dehydration of the hydrogel matrix, and while direct *in situ* conditions cannot be evaluated, important information pertaining to the hydrogen bonding interactions can still be garnered by maintaining minimal network hydration. To prepare semi-dry hydrogel materials we dehydrated samples under modest house vacuum conditions for 24 hours in the absence of a desiccant. To increase the extent of hydrogel drying we made use of calcium sulfate desiccant and/or high vacuum sources to establish greater anhydrous conditions. Interestingly, under semi-dry conditions trehalose hydrogels demonstrated uniquely strong and ordered hydrogen bonding which was observed as a characteristic three principle mode distribution within the OH stretch region formed by 3 overlapping bands at 3290, 3450 and 3510 cm^{-1} **(Figure 4.17)**. The 3290 cm^{-1} *v*OH stretch indicates the existence of strong interchain hydrogen bonding interactions likely between trehalose hydroxyls (hydrogen donor) and carbonyl groups (hydrogen acceptor) that are present within the hydrogel network[309,310]. By contrast the other *v*OH stretches at 3450 cm^{-1} and 3510 cm^{-1} are likely attributable to intramolecular interactions between trehalose hydroxyls along with their interaction with ether groups on the PEG chains derived from the TMPE-TL and PEGDA[311]. The pattern of hydrogen bonding was similar for all trehalose containing hydrogels and the strength of these vibration modes was linearly dependent on TDA composition, suggesting direct involvement of the trehalose molecules in this bonding **(Figure 4.18 and Figure S4.14)**. In samples exposed to increasingly strenuous drying conditions the multimodal *v*OH signal transitioned into a higher wavenumber and a more broadly distributed hydrogen bonding pattern evident as a single mode centered at 3350 cm^{-1} **(Figure 4.19 and Figure S4.15)**. The lower wavenumber and decreased bandwidth of the *v*OH stretch with greater water content suggests that the coupled vibrations associated with these hydrogen bonding interactions are stronger in the presence of some hydration with a higher degree of homogeneity within the matrix that appears to be water assisted[311,312].

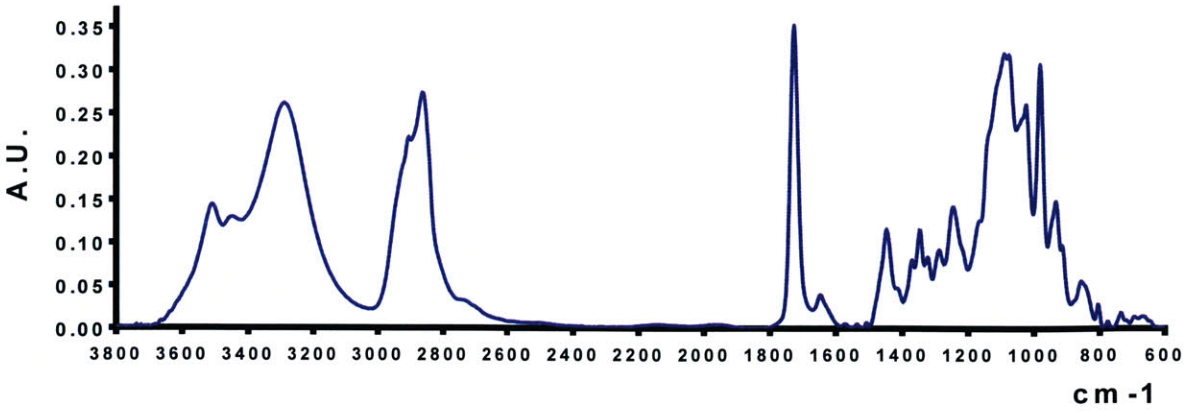

Figure 4.17 Trehalose hydrogels display unique, strong hydrogen bonding. Complete ATR-FTIR of a semi-dry 100T hydrogel.

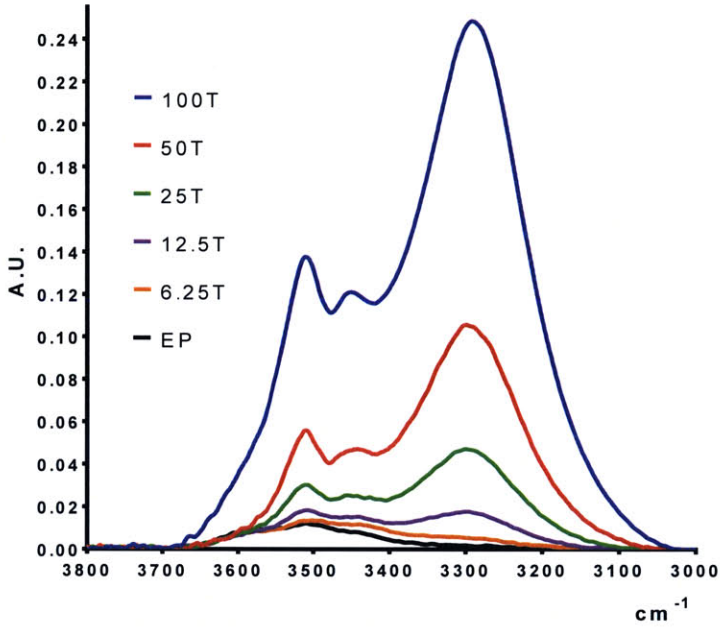

Figure 4.18 ATR-FTIR OH stretch spectra for semi dry hydrogels with various percentage composition of trehalose shows that the hydrogen bonding strength is trehalose concentration dependent (all spectra normalized at the ester peak, 1730 cm^{-1}).

Variations in the hydrogen bonding distribution as a function of hydration for the trehalose hydrogel was also reflected in mechanical property differences **(Figure S4.16)**. When fully hydrated 50T hydrogels were equilibrated at 37°C and then tested under uniaxial mechanical compression, the compressive modulus (47.42 kPa) was approximately 2.9 times more compliant than the EP hydrogel that contained no trehalose (137.6 kPa). However, upon drying to the semi-dry state the difference in mechanical properties between the two samples was remarkable, with the 50T hydrogel demonstrating stiffness and strength that was over an order of magnitude greater than the EP hydrogel while also

displaying a profile more reminiscent of a thermoplastic elastomer (TPE) than that of a classic rubber/elastomer material (Figure S4.16). However, the TPE-like character displayed by the 50T hydrogel was lost upon further drying at which point the materials mechanical properties were approximately equivalent to the dry EP hydrogel. These mechanical testing data provide evidence that water within the trehalose hydrogels acts as either a plasticizing or anti-plasticizing agent depending on the extent of hydration, in a manner similar to that described previously for other carbohydrate-polymer-polyol glassy matrices[312,313]. These data confirm that trehalose hydrogels possess unique long range ordered hydrogen bonding domains throughout the network that is maximized at a certain level of hydration where free water within the network is almost entirely removed and the residual water is compartmentalized within intramolecular hydrogen bonding. The compartmentalized water acts as an anti-plasticizing agent enhancing the molecular packing and consequently mechanical properties of the network.

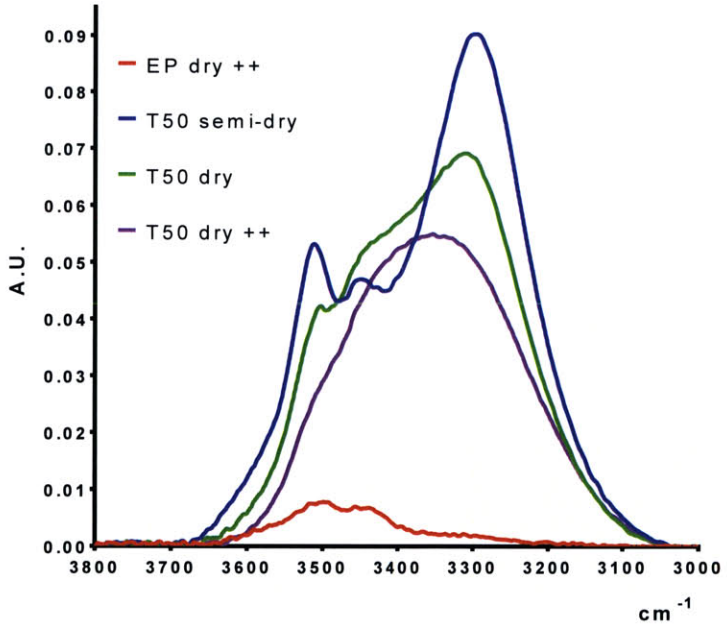

Figure 4.19 ATR-FTIR OH stretch spectra for 50T hydrogels with varied levels of hydration demonstrate that water is an active participant in network hydrogen bonding.

The inclusion of trehalose as an osmolyte dispersed within EP hydrogels did not display the same hydrogen bonding pattern as seen for covalent incorporation and instead there was a broad and much less intense spectra for the equivalent molar concentration of hydroxyl groups suggesting a heterogeneous distribution of hydrogen bonding **(Figure 4.20)**. For comparisons, hydrogels containing an alternate free polyol distribution within the network at equivalent molar concentration were

prepared through the reaction of TMPE-TL, TMPE-triacrylate and thioglycerol. This thioglycerol hydrogel containing pendant hydroxyls within the network had a broadly distributed pattern of hydrogen bonding with a single band at a higher wavenumber (3500 cm^{-1}) (Figure 5d). Disaccharide trehalose is known to have a stronger propensity for forming intermolecular hydrogen bonding as well as interacting more favorable with water molecules compared to other similar sized sugars and polyols [314,315]. Our analysis confirms that this specific polyol identity, orientation and distribution, which is preserved upon covalent trehalose incorporation within hydrogels, creates exceptionally strong hydrogen bonding within the network that cannot be matched by other hydroxyl containing entities. The strength of the multimodal hydrogen bonding in the trehalose hydrogels decreased over time and transitioned into a higher wavenumber, longer bandwidth single mode signal by 8 days *in vitro* **(Figure 4.21)**. This modulated signal coincided with an increase in the carboxylate (1550–1610 cm^{-1}) stretch **(Figure S4.5)** suggesting that network hydrolysis and the resultant carboxylate anions generated act to redistribute the hydrogen bonding seen within the network. This could have implications for the long-term stabilization of protein therapeutics as during hydrogel degradation the loss of strong hydrogen bonding may contribute to protein destabilization and/or aggregation.

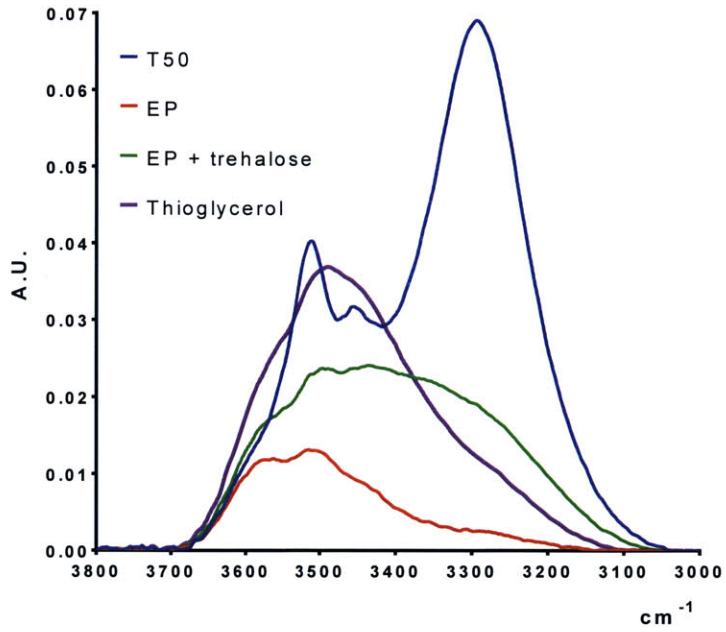

Figure 4.20 Comparative ATR-FTIR OH stretch spectra for semi-dry hydrogels containing different polyol distributions within the hydrogel network shows that covalent incorporation of trehalose affords a unique hydrogen bonding profile.

In summary, we have demonstrated that covalent incorporation of trehalose, a recognized protein excipient, into a hydrogel network resulted in enhanced long-term functional activity of a number of fragile proteins during controlled release both *in vitro* and *in vivo*. Furthermore, upon application of relevant formulation and manufacturing stressors the trehalose hydrogel provided protection of a model protein in its active state. The mechanism by which trehalose hydrogels stabilize proteins remains to be completely elucidated. However, we have identified a uniquely strong hydrogen bonding character within the trehalose hydrogel network that was hydration dependent, which could contribute to this stabilization effect in a manner that is consistent with previously described water replacement and/or entrapment theories for osmolyte trehalose. The favorable hydrogen bonding attributable to trehalose may be amplified upon covalent incorporation of the sugar into the current hydrogels as the Michael addition step growth polymerization chemistry used here is known to provide enhanced network homogeneity and cooperativity[316]. This study supports the covalent incorporation of trehalose within hydrogels for structural stabilization of encapsulated proteins during long term controlled release. Future evaluations with various classes of therapeutic proteins would ideally establish the modularity of this approach. For situations requiring more prolonged release, the development of trehalose hydrogels with slower degradation kinetics, perhaps by using non-ester based thiol crosslinkers, may be advantageous. Overall, the strategy outlined here has great potential to improve local delivery for numerous therapeutic applications and could help to overcome hurdles to clinical translation that arise from structural stability limitations of fragile protein therapeutics.

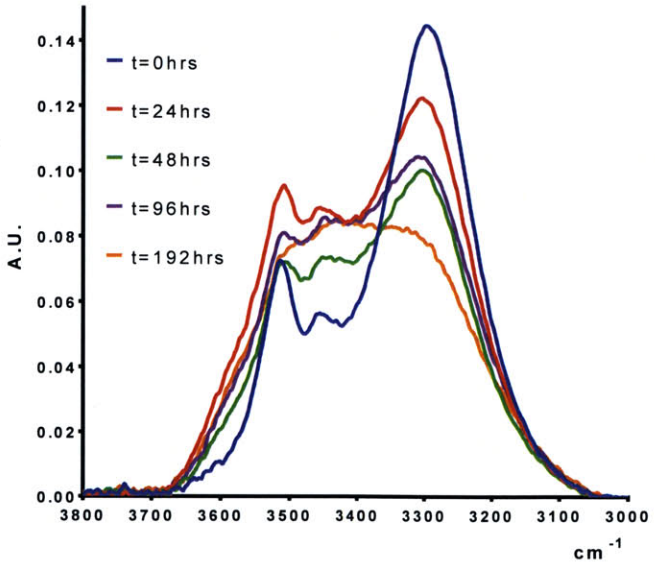

Figure 4.21 ATR-FTIR OH stretch spectra for semi-dry 50T hydrogels incubated in PBS for different periods of time shows that the strength and order of the hydrogen bonding within the network is disrupted as the material begins to degrade

4.3 Materials and Methods

4.3.1 Instrumentation and Materials

Purity and extent of functionalization of all synthesized hydrogel precursor molecules was confirmed by LC-MS and ^{1}H NMR. For **LC-MS** analysis of trehalose diacrylate, samples were loaded at a 1mg/ml concentration and run through a UPLC BEH C18, 1.7μL, 2.1 x 50 mm column at a rate of 0.6 ml/min. The mobile phase used was a 3 minute gradient of HPLC grade water and acetonitrile with 0.01% formic acid. Eluted products were characterized by UV-PDA detector and ESI QT of MS. **^{1}H NMR** spectra of trehalose diacrylate were recorded on a Bruker 400 MHz NMR spectrometer using the residual proton resonance of the deuterium oxide as the internal standard. Chemical shifts are reported in parts per million (ppm).

Dynamic Rheology was performed on mixed hydrogel solutions to monitor the sol-gel transition. Using an ARES G2 rotational rheometer (TA Instruments, New Castle, Delaware) 300 μL of hydrogel mixture was applied to a temperature-controlled stage set at 37 °C. A 25 mm parallel stainless steel plate geometry was used for all tests and dynamic time sweep measurements were made within the linear viscoelastic region at 5% strain and a frequency of 10 rad s^{-1}.

Fourier transform infrared spectroscopy (FTIR) was used to characterize the trehalose hydrogels. Using an Eco-ATR module attachment to an ALPHA FT-IR Spectrometer (Bruker) the FTIR spectra of pressed dried hydrogel discs were recorded at 2 cm^{-1} intervals with a minimum of 80 repeat measurements. The ester peak (~1730 cm^{-1}) was used to normalize the absorbance readings between hydrogel samples. The hydrogen bonding within the samples was analyzed using the OH stretch spectral region (3000-3800 cm^{-1}) while the carboxylate peak was assessed at 1550–1610 cm^{-1}. Integration of Spectra peaks was performed using the Bruker OPUS software.

Materials: Trehalose dihydrate (Sigma # T0167), vinyl acrylate (#771422), Lipase B acrylic resin from Candida antarctica (CALB) (Sigma # L4777), trimethylopropane ethoxylate (#416177), ethyl thiolactate (#W327905), ethyl thioglycolate (#E34307), polyethylene diacrylate (PEGDA) (M_n = 575 g/mol) (#

437441), activated alumina Brockman I (basic and neutral), Filter agent Celite® 545, solvents (dichloromethane, methanol, ethyl acetate, acetone, dimethyl sulfoxide), 3A and 4A molecular sieves, horseradish peroxidase (#77332, 156 U/mg), glucose oxidase from *Aspergillus Niger* (#49180, 192 U/mg), α-Chymotrypsin from bovine pancreas (#C3142), 3,3',5,5'-Tetramethylbenzidine (TMB) Liquid Substrate System for ELISA (#T0440), D-(+)-glucose anhydrous, N-Succinyl-Ala-Ala-Pro-Phe p-nitroanilide (#S7388, chymotrypsin substrate), 2N HCl solution, Tris hydrochloride (Tris-HCL), calcium chloride ($CaCl_2$) were all purchased from Sigma-Aldrich (St. Louis, MO, USA). Phosphate buffered saline pH=7.4, FITC labeled ovalbumin, IgG-Alex Fluor 647 and Amplex UltraRed reagent, were purchased from Life Technologies (Grand Island, NY, USA). Disposable 40 and 80 gram HP Silica Gold Cartridges were purchased from Teledyne Isco (Lincoln, NE, USA).

4.3.2 *Synthesis of Trehalose diacrylate*

Selective acrylation of trehalose was performed using an enzymatic catalyzed reaction similar to previously reported[296]. Briefly, trehalose diacrylate was synthesized by reacting a four-mole excess of vinyl acrylate (48 mmols, 5 ml) with trehalose dihydrate (16mmols, 4.1 grams) in the presence of CALB (1 gram) in dry acetone (500mL) at 50°C and 250 rpm for 48 hours on an orbital shaker. Trace amounts of 4-Methoxyphenol (MEHQ) were also added to prevent any radical homopolymerization of the product during the reaction. The crude product was filtered, concentrated *in vacou* and then purified via silica flash chromatography on a CombiFlash Rf system using a 40 gram disposable pre-packed Silica Gold cartridge and Ethyl Acetate and 80% methanol/water as the binary solvent mobile phases. Purified trehalose diacrylate was identified by thin layer chromatography (TLC) using Cerium-ammonium-molybdate (CAM) stain and purified fractions were collected and dried *in vacuo* using a rotary evaporator. Trace amounts of MEHQ was included in the solution of combined purified fractions just prior to solvent removal to prevent radical homopolyerization. Dried trehalose diacrylate was stored at 4°C until use. ^{1}H NMR (400MHz, D2O δ) 6.47 (dd, 2H), 6.24 (m, 2H), 6.02 (dd, 2H), 5.16 (d, 2H), 4.51 (dd, 2H), 4.40 (dd, 2H), 4.09 (m, 1H), 3.87 (t, 2H), 3.67 (dd, 2H), 3.54 (dd, 2H).

4.3.3 *Synthesis of TMPE-TL and TMPE-TG*

The synthesis of TMPE-TL and TMPE-TG was performed using a enzymatic catalyzed transesterfication reaction which is described in detail by our group elsewhere[226]. Briefly, ten grams of 4A molecular sieve

dried trimethylopropane ethoxylated (TMPE) was combined with a five molar excess of either ethyl 2-mercaptoproprionate (TL) or ethyl thioglycolate (TG) in a 100mL round bottom flask, followed by CALB (1gram). The flask was placed on a magnetic stirrer at 50°C and allowed to react overnight under moderate vacuum conditions. The reaction was purified by silica flash chromatography on a CombiFlash Rf system using a disposable pre-packed silica column (80 grams) with a dichloromethane/methanol (0-10%) gradient elution method. Purified fractions were detected by UV-VIS and then combined and dried *in vacuo* using a rotary evaporator yielding a clear viscous liquid at room temperature. Vials of TMPE-TL and TMPE-TG were stored at 4°C under nitrogen gas and were individually flashed neat over a bed of neutral alumina prior to use. The characterization of TMPE-TL and TG by LC-MS and ^{1}H NMR is described in detail by us previously[226].

4.3.4 *Hydrogel Fabrication*

Trehalose hydrogels were prepared by combining TMPE-TL, TDA and PEGDA 575 in PBS at a stoichiometric equivalency of thiol groups to acrylate groups in a manner similar to previous studies[226]. Briefly, PEGDA, a liquid at room temperature, was first flashed neat over activated basic alumina to remove the MEHQ inhibitor added by the manufacturer. Weighed masses of TDA and PEGDA were solubilized with an appropriate volume of PBS and placed on ice for 10 minutes. The volume of PBS added to the TDA/PEGDA solution was sufficient to obtain a 25wt% hydrogel. The relative amounts of TDA and PEGDA used to make the hydrogels depended upon the specific trehalose content of the hydrogel. Hydrogels were fabricated by adding the TDA/PEGDA solution to a weighed quantity of TMPE-TL. To make EP hydrogels a similar procedure was used except that a solution of PEGDA only was added to a blended quantity of TMPE-TG and TMPE-TL.

4.3.5 *In vitro protein release studies*

Model protein controlled release was investigated by encapsulating FITC-labeled Ovalbumin (45 kDa), and Alexa Fluor 647 IgG (150 kDa) into hydrogels at 1 mg/ml. Hydrogels were incubated in 1mL of PBS and replaced daily. Protein concentration was read on an Infinite® M1000 PRO microplate reader (Tecan) using appropriate fluorophore excitation and emission wavelengths (ex/em 490/525 for FITC; ex/em 650/668 for Alea Fluor 647). An eight sample serially diluted standard curve was generated for

each protein in order to convert the microplate read fluorescent intensity into a protein concentration value.

4.3.6 PROTEIN ACTIVITY ASSAYS

Horseradish peroxidase (HRP), Glucose Oxidase (GO) and α-chymotrypsin were all used as received from the vendor without any further purification. For the active protein recovery assays proteins were loaded into 60μL hydrogel discs (~5mm diameter x 3 mm height) at concentrations ranging from 500 μg/ml to 2 mg/ml and incubated in 600μL of PBS/0.01% BSA in a 48 well microplate that was shaken at 37°C and 150 rpm on an orbital shaker. Hydrogel samples were run in groups of 3 or 4 for all assays. The incubation media was replaced daily and the recovered incubation media was analyzed for protein activity.

For the **HRP activity assay**, samples were first diluted in Hanks balanced salt buffer (HBSS) (1/50 dilution) to obtain a concentration that was within the linear range of the TMB colorimetric assay. To perform the TMB colorimetric assay 50 μL of diluted recovered incubation media was added to 50 μL of TMB substrate within a 96 well microplate and was developed at 37°C for 5 minutes before adding 100 μL of 2N HCl to stop the enzymatic reaction. The colorimetric intensity of samples was read on a microplate reader at 450 nm with absorbance at 540nm used as reference. For each daily measurement an eight sample serially diluted standard series was used for HRP concentration calculations.

For the **GO activity assay** recovered aliquots were diluted at 1/20 in PBS and 50μL of the diluted solution was added to an individual well of a 96 well plate. The Amplex Red substrate solution was prepared by combining 50μL of 10mM Amplex Red Stock in DMSO, 100μL of 100 μg/mL HRP, 1.25 mL of 400 mM glucose stock and 3.6 mL of PBS. 50 μL of the Amplex Red substrate was added to the diluted aliquots to initiate the enzymatic reaction and the developing pink color was monitored at discrete time intervals on a microplate reader at wavelength of 560 nm. A 12 sample serially diluted standard series from 2.5 μg/mL was used to calculate active GO concentrations.

For the **α-chymotrypsin assay**, hydrogel incubation media was recovered and diluted as needed. The substrate solution was prepared by solubilizing the N-Succinyl-Ala-Ala-Pro-Phe p-nitroanilide substrate at a 2mM concentration in 0.2M Tri-HCl/20mM $CaCl_2$ pH=7.8 buffer. A 100 µL aliquot of the substrate was added to 100 µL of the sample aliquot and the developing yellow hue was read at 410 nm on a microplate reader continuously over a 10 minute period. An 8 sample serially diluted standard curve was generated to calculated active recovered protein.

For measurements of active HRP within hydrogels, 15 µL hydrogel discs were removed from either *in vitro* or *in vivo* conditions at defined time points, washed once in HBSS and then incubated in 50 µL of fresh HBSS before application of 50 µL TMB substrate. At defined time points the enzymatic reaction was stopped by applying 100 µL of 2N HCl and hydrogels were removed from the microplate before the colorimetric intensity was read on a microplate reader at 450 nm with absorbance at 540nm used as reference.

4.3.7 IN VIVO IMPLANTATION OF HYDROGELS

Sterile discs (~ 15 µL, 3 mm diameter, 2mm height) of 50T and 75/25 EP hydrogels containing 2 mg/ml HRP were prepared in an autoclaved silicone mold under aseptic conditions for subcutaneous implantation in 8 week old male C57BL/6J mice. To implant hydrogels, animals were anesthetized by isoflurane inhalation and a small dorsal incision was made. A pocket in the subcutaneous space was created by blunt dissection. Six animals received 5 single group hydrogels (3 animals per hydrogel group) loaded into this space, while 3 other animals received 6 mixed hydrogels. The surgical incision was closed with sutures and the animals were provided with post-surgical analgesia. At designated time points animals were euthanized by carbon dioxide asphyxia and hydrogels were retrieved and transferred to a solution of HBSS prior to performing the HRP activity assay. To determine the identity of hydrogels retrieved from animals receiving the mixed implants, ATR-FTIR analysis on the hydrogels post HRP activity assay was performed.

4.4 SUPPLEMENTARY FIGURES

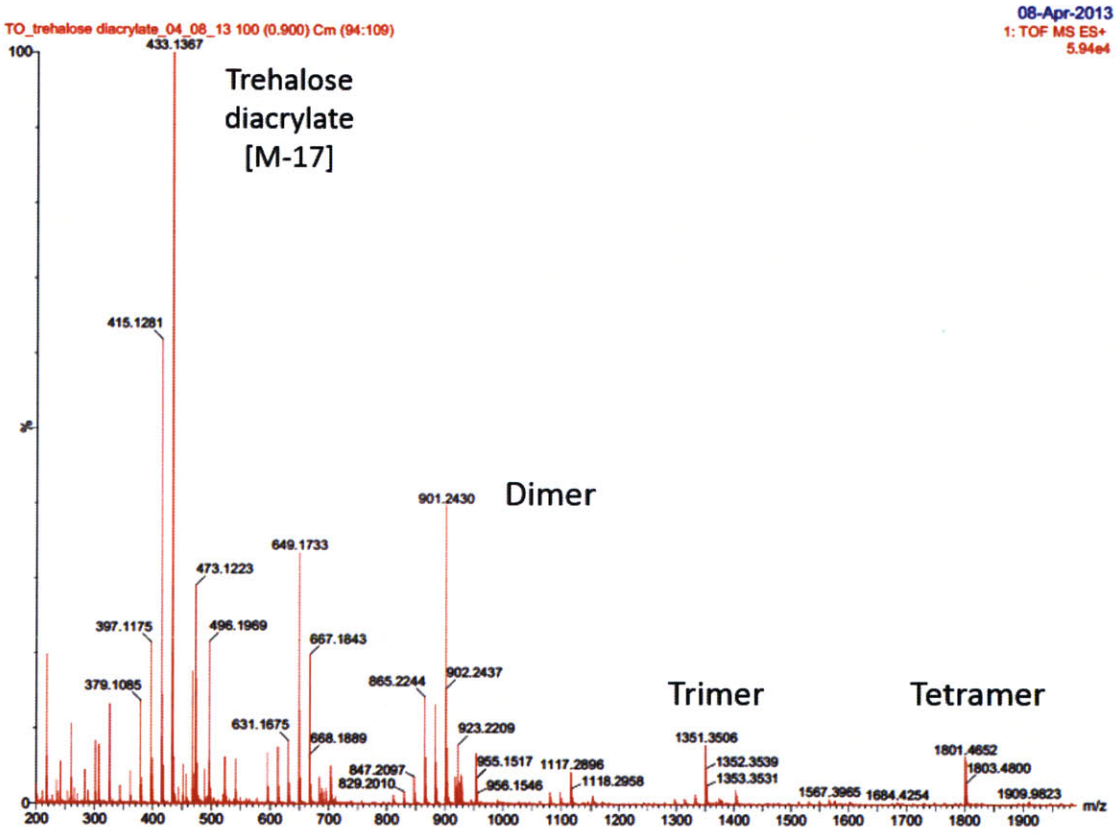

Figure S4.1 Mass Spectrum of trehalose diacrylate.

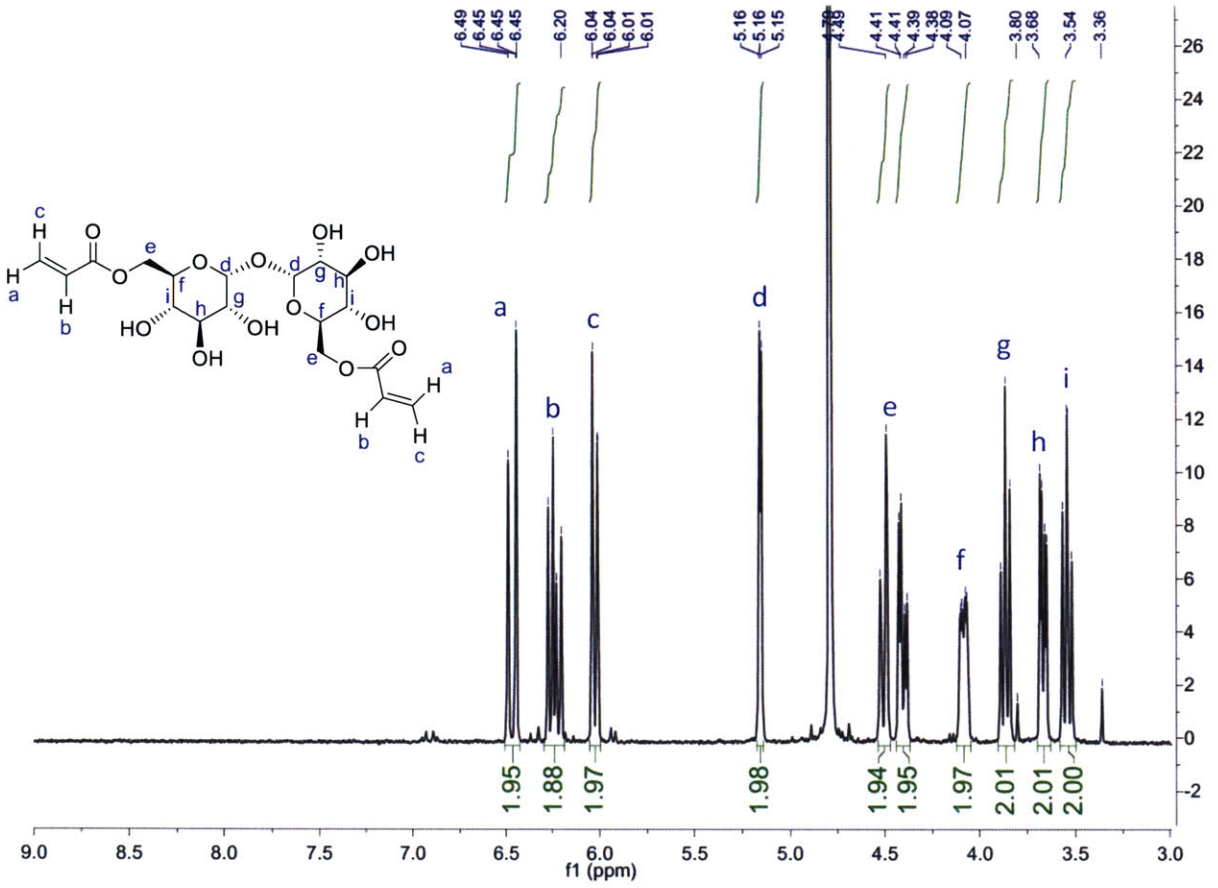

Figure S4.2 ^{1}H NMR spectra for trehalose diacrylate

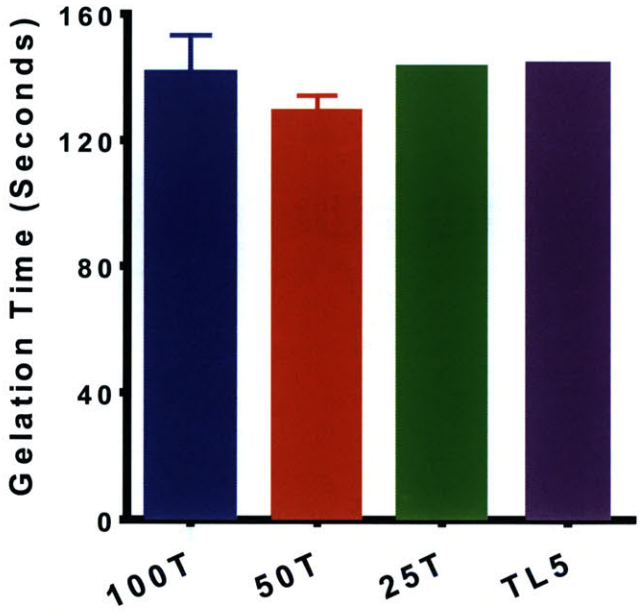

Figure S4.3 Gelation time comparisons for trehalose hydrogels with different percentage compositions of trehalose within the network as measured by dynamic rheology. Gelation time is defined as the time point where tan (δ) = 1 (i.e., G′/G″ cross over).

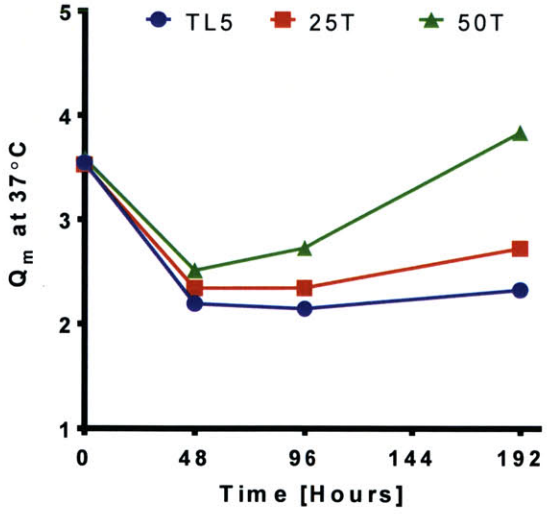

Figure S4.4 Temporal progression of the equilibrated swelling ratio, Q_m, for trehalose hydrogel formulations compared with the TMPE-TL PEGDA 575 hydrogel.

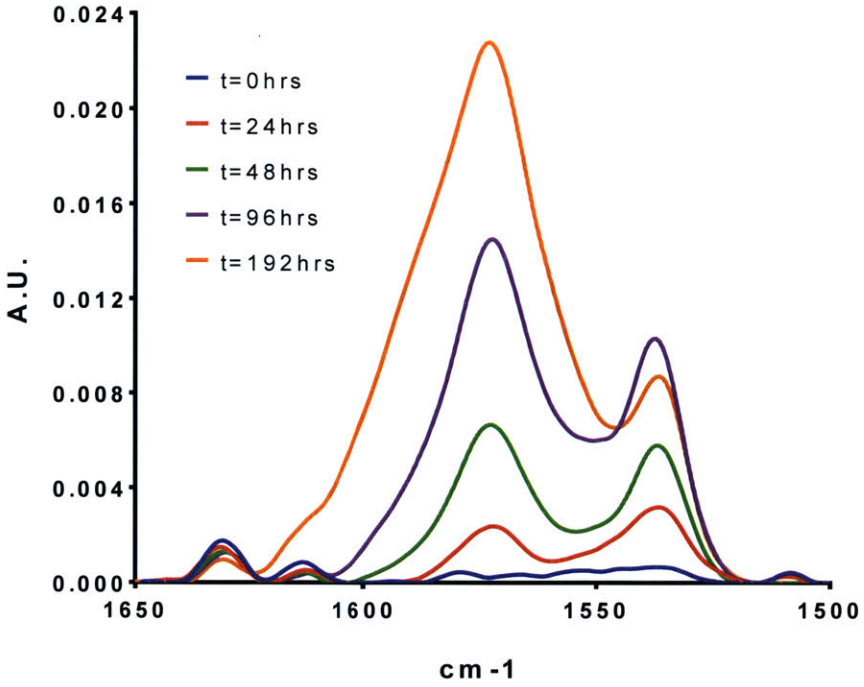

Figure S4.5 FTIR carboxylate stretch for 50T hydrogels showing the temporal increase in signal over time suggesting degradation by hydrolysis. All spectra were normalized to the ester stretch at 1730 cm^{-1}.

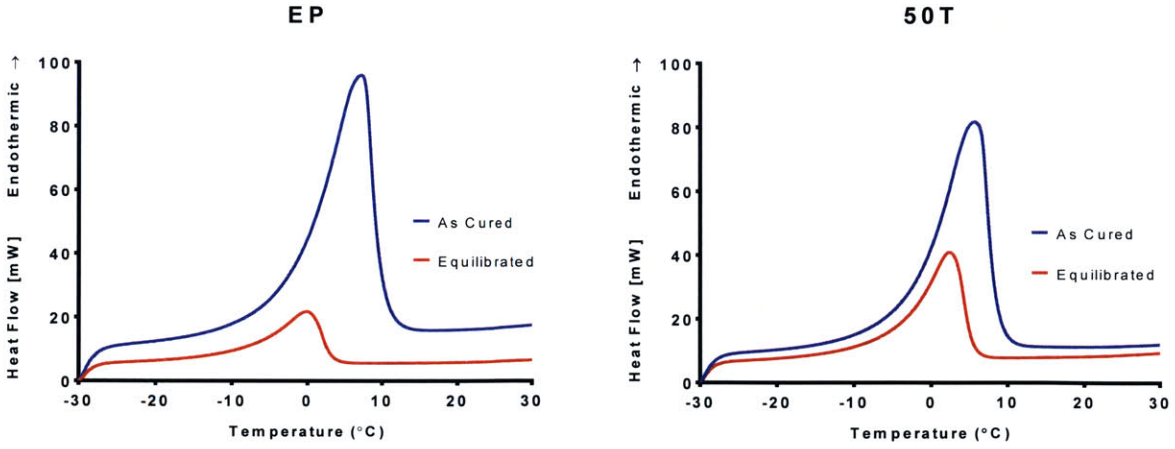

Figure S4.6 Differential scanning calorimetry (DSC) curve of EP and 50T hydrogels following initial formulation and following 24 hours incubation in PBS at 37°C. At equilibration 50T hydrogels had a higher content of free water within the network compared to EP hydrogels.

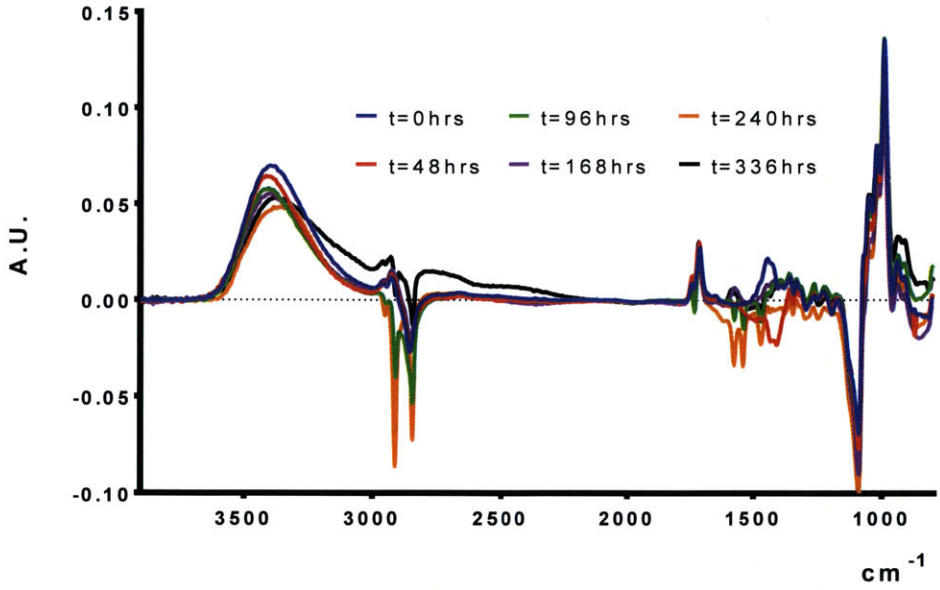

Figure S4.7 FTIR spectra of dry 50T hydrogels following subtraction of the EP hydrogel spectra after normalization at the ester stretch. The temporally maintained peaks at 3400 and 990 cm^{-1} confirm trehalose is present in the hydrogel throughout the complete life of the material.

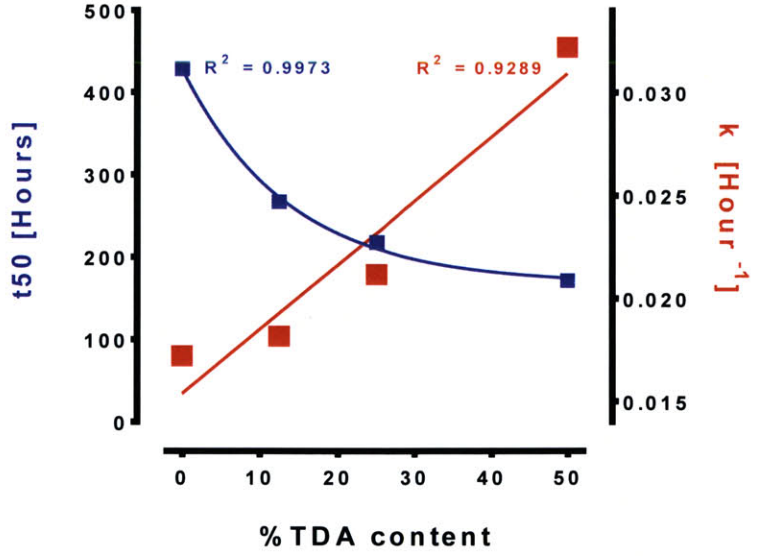

Figure S4.8 Comparison of kinetic release parameters for trehalose hydrogels with varied trehalose content. t50 (time to 50% release of drug) values decreased exponentially with increasing TDA content, while k (the molecule release constant) increased linearly with increasing TDA content.

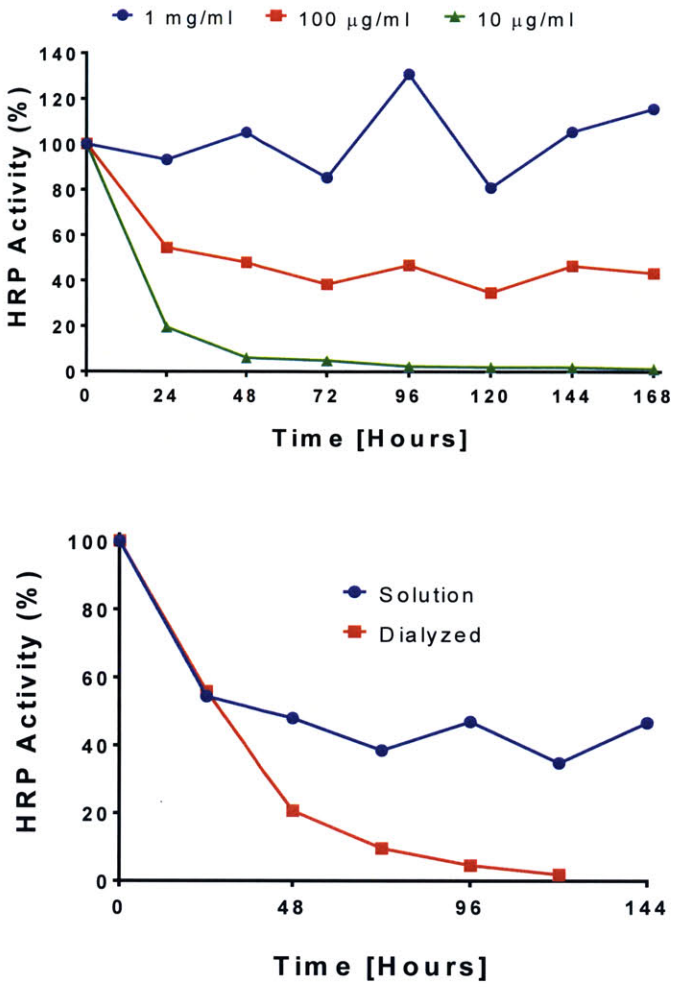

Figure S4.9 HRP stability in solution incubated at 37°C demonstrating a concentration dependent instability.

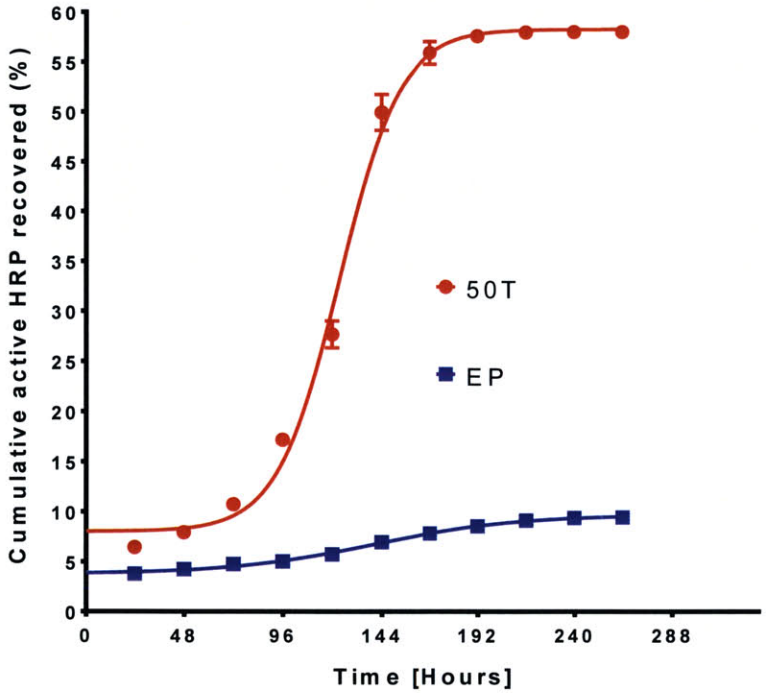

Figure S4.10 Comparison of cumulative active HRP recovery for 50T and EP hydrogel loaded at 1 mg/ml.

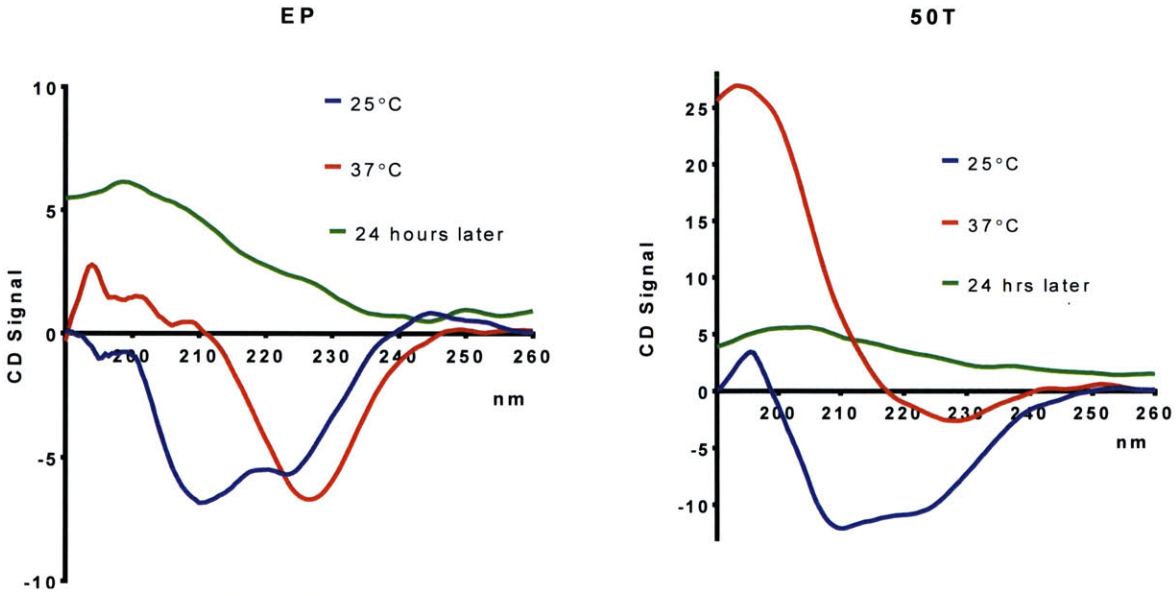

Figure S4.11 Circular Dichroisim spectra of EP and 50T hydrogels encapsulating bovine serum albumin (BSA) at 5 mg/ml. The spectra is obtained by subtracted the raw signal of the hydrogel alone from the signal of the hydrogel containing protein. When hydrogels were formed at room temperature the spectra showed preserved alpha helix secondary structure. However, upon equilibration the signal was scattered in both hydrogels.

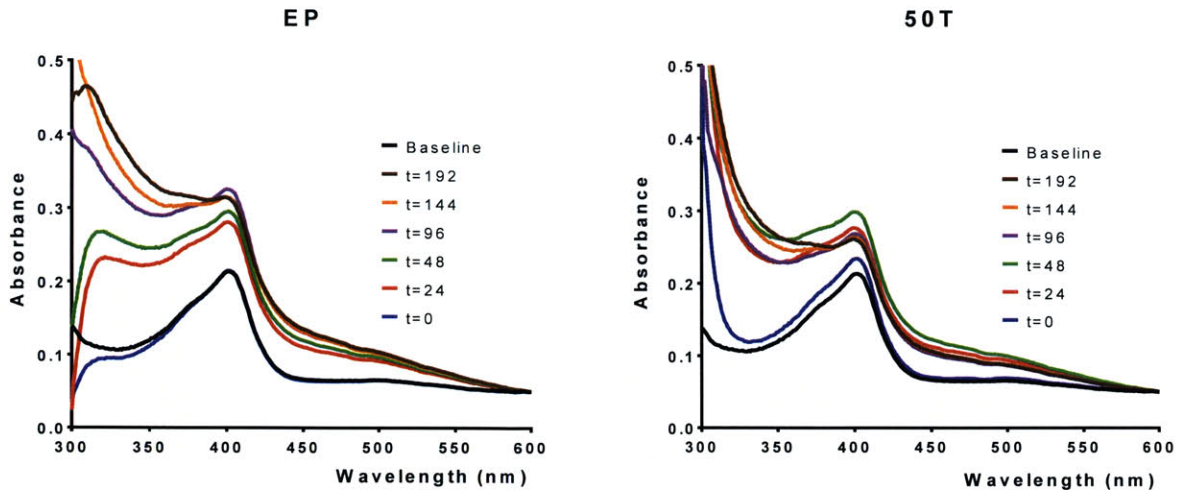

Figure S4.12 UV-VIS absorbance spectra focused on the Soret band of HRP encapsulated within EP and 50T hydrogels.

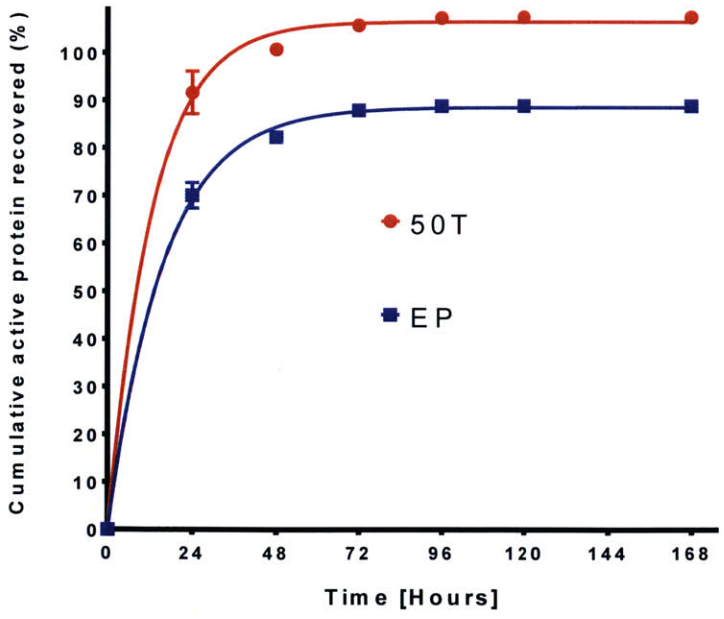

Figure S4.13 Cumulative protein recovery profiles for hydrogels encapsulating chymotrypsin at 2 mg/ml.

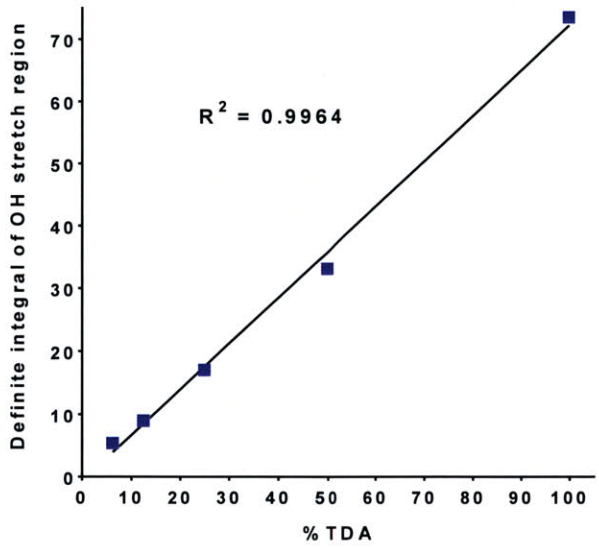

Figure S4.14 Definite integrals of the OH stretch FTIR signal (3000 to 3800 cm^{-1}) for various trehalose content hydrogels. The integrated peak area in this spectral region is linearly proportional to the amount of trehalose diacrylate in the network.

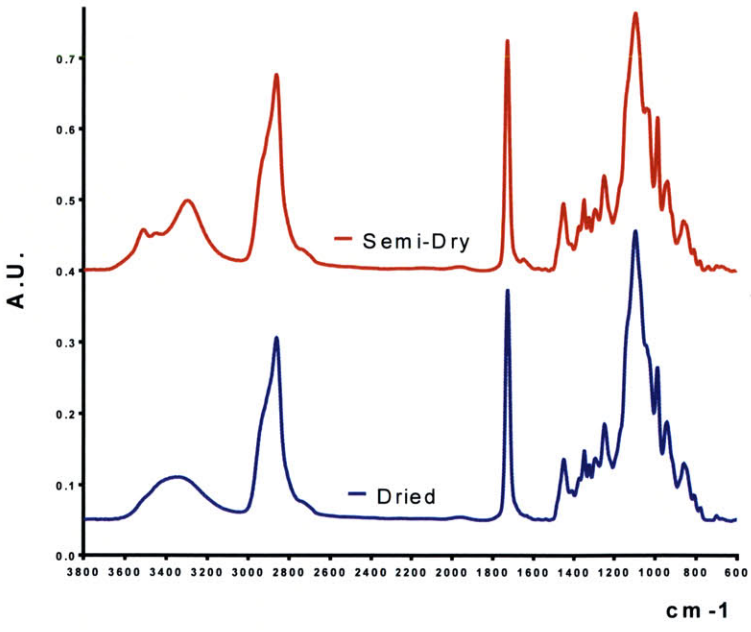

Figure S4.15 Complete ATR-FTIR spectra of 50T hydrogels after 24 hours of low vacuum and 48 hours of high vacuum with desiccant.

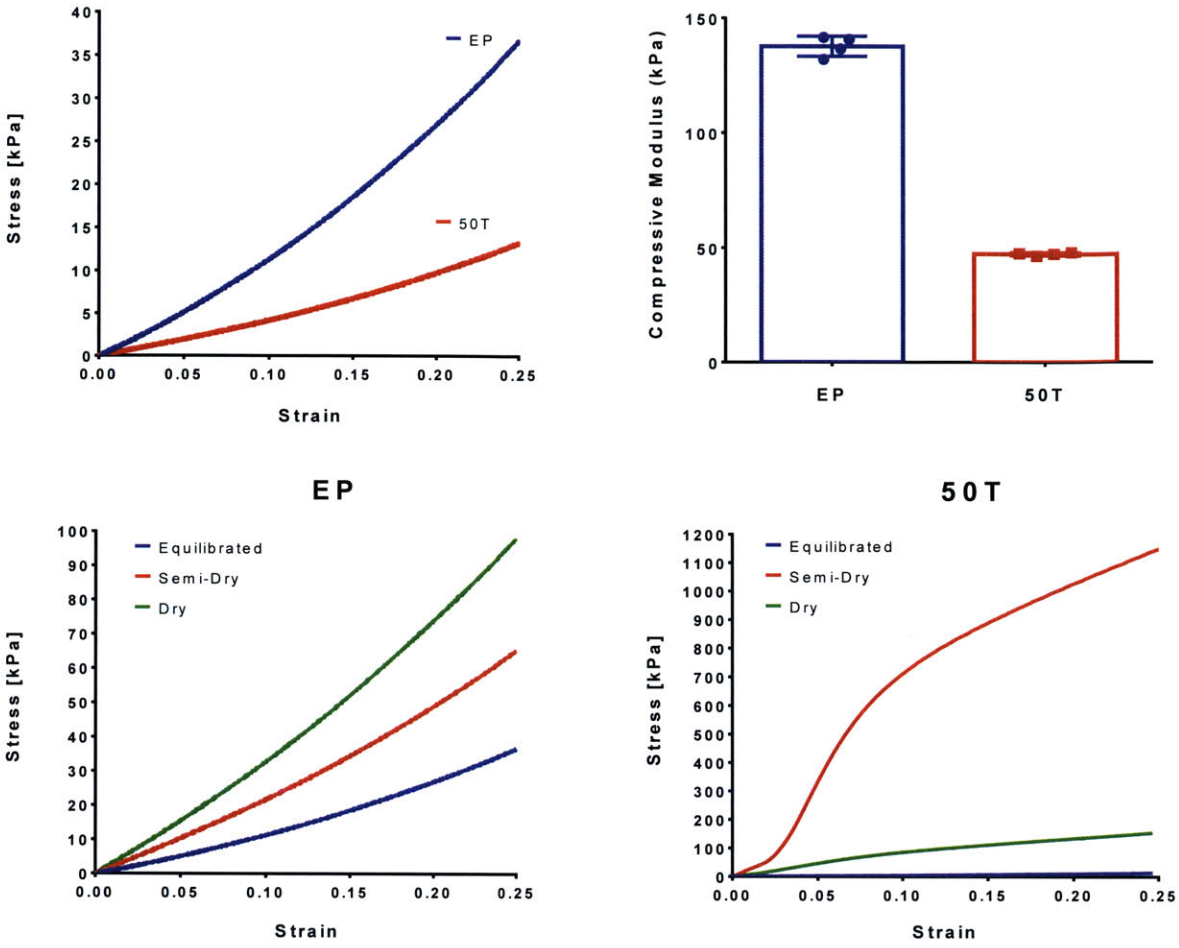

Figure S4.16 Compressive testing of EP and 50T hydrogels.

5 EVALUATING THE METHOD OF SURGICAL ADMINISTRATION OF AN INJECTABLE HYDROGEL FOR DRUG DELIVERY TO SPINAL CORD CONTUSION INJURIES

5.1 INTRODUCTION

A traumatic spinal cord injury (SCI) causes irreversible damage to this fragile but vitally important central nervous system (CNS) organ and unfortunately almost always results in a life of permanent paralysis for affected individuals. Anatomically, the spinal cord is essentially a thin tube, composed of bands of nerve fibers intertwined within a milieu of neurons and glial support cells, which runs the length of the vertebral column as a continuation of the CNS, starting at the medulla in the brain stem and continuing down to the cauda equina located in the lumbar spine. The spinal cord is positioned within a free space that is present within individual vertebra, the spinal canal, and is encased concentrically by a closely apposing bony structure called the vertebra formina. In a typical traumatic event that results in a spinal cord injury, it is damage and displacement of the bony structures that make up the vertebra that ultimately applies the injuring mechanical stimulus to the spinal cord. The application of this bony segment to the spinal cord increases the pressure locally on the spinal cord tissue causing damage to parenchymal tissue and associated blood vessels initiating a cascade of secondary injury mechanisms. Depending on the nature of this stimulus the injury can manifest as a laceration, compression, distortion, or contusion lesion. The most common injury type seen in clinical SCI is a non-penetrating compression/contusion lesion, which is estimated to account for approximately 69% of cases[27]. Given that the contusion injury, which is an injury that causes minimal to no disruption of the dura meningeal layer, is the most common injury seen in the clinic, developing treatment strategies that are specifically relevant to this mode of injury is a critically important research endeavor.

Since the spinal cord is an extension of the brain, a highly selective barrier similar to the blood brain barrier (BBB), the Blood Spinal Cord Barrier (BSCB), acts to create an isolated cell microenvironment that favorably prevents the invasion of foreign pathogens and neurotoxins[317]. However, the BSCB is also a formidable barrier for many therapeutic molecules and thus prevents adequate spinal cord parenchyma bioavailability of drug treatments that are administered by parenteral methods. Recently, it was shown that the extravasation window of drugs and nanocarrier treatments from the systemic circulation into the spinal cord parenchyma after a contusive spinal cord injury is no more than approximately 96 hours[210]. After this four day period post injury a repaired barrier function is established in the

compromised vasculature and there is minimal additional drug accumulation into the spinal cord parenchyma. For regenerative or tissue remodeling therapies an extension of this therapeutic window is required. Furthermore, in contusion injuries, since the dura mater is mostly intact, epidural application of drugs is also not a viable approach for achieving sufficient local concentrations of drug to the spinal cord parenchyma. Previously, Bellamkonda and colleagues demonstrated, through the use of a topically applied drug delivery system, that drug penetration into the contused spinal cord parenchyma could only be achieved when the dura mater had been completely compromised during surgery[162]. Therefore it is clear that these two tissue barriers provide a formidable obstacle for drug delivery that requires alternative drug delivery strategies.

To overcome these spinal cord tissue barriers and address the drug delivery inadequacies in SCI, researchers have focused on the development of locally applied treatments that can be administered at the time of decompression surgery, a procedure that typically takes place within the first hours to days after the primary trauma to the spinal cord. Direct application of the drug treatment to spinal cord parenchyma bypasses the barriers created by the BSCB and dura mater thereby ensuring that adequate local drug concentrations are established. As a way to ensure that these treatments are sustained with sufficient local concentration over an extended temporal window, chemists and material scientists have developed innovative injectable biomaterials, mostly in the form of hydrated hydrogels, to control the release of drugs. These single application bioresorbable biomaterials overcome the problems associated with indwelling catheters, the alternative technology used for prolonged drug delivery to the CNS, which often suffer from complications pertaining to CNS infection, immunogenicity and antagonistic gliosis/fibrosis[23,24].

While injectable hydrogels have been explored previously in rodent spinal cord injury, the hemisection model, whereby an opening is made in the dura and a segment of spinal cord is resected, has been almost exclusively used[204]. The hemisection model has been effectively used by neuroscientists for many decades to study mechanisms of CNS injury and repair as it creates a well-defined injury to specific neural pathways in the spinal cord. The hemisection model, while not clinically relevant, has the advantage of creating a free space for the hydrogel to occupy, with the material either injected into the open cavity[189] or pre-gelled and implanted into the defect site[193]. While administration of the hydrogel is more straightforward with this model, the cellular response to injury in the hemisection is very different to that seen in the more clinically applicable contusion injury. Specifically, tissue remodeling

observed in the hemisection lesion such as contralateral axonal sprouting as well as dominant fibromeningeal cell (fibroblast and Schwann cells) infiltration is absent in the contusion lesion. In terms of biomaterial application, other differences between the two injury types include: (a) the amount of biomaterial that can be applied and hence the amount of drug that can be administered; (b) the location of the biomaterial relative to the flowing paths of cerebral spinal fluid (CSF) such as the central canal and intrathecal space which will have implications for the spatial distribution of drug that is released from the implant; and (c) the absolute intraspinal pressure (ISP) or spinal cord perfusion pressure (SCPP) upon biomaterial administration which will increase in a contusion lesion but which is negligibly affected in the hemisection.

Hydrogel treatments must be investigated in contusion lesion models if clinical translation of these technologies is to be realized. However, injection of hydrogel materials to a contusion lesion is not without its complications. A number of parameters such as time of application post injury, location of injection, volume of material and rate of injection are likely to influence outcomes and therefore understanding their relative contribution is critical. Some work has begun to emerge describing viable approaches for the application of a biomaterial to a contusion lesion. Within these studies two dominant injection approaches have been used, namely: (1) intraparenchymal (direct injection into the spinal cord lesion) [205,318] and (2) intrathecal (injection within the space between cord tissue and the dura)[185,206]. The benefit of the intraparenchymal route is that it ensures good localization of drug within the spinal cord lesion but there are limitations associated with the volume of material that can be applied and there is also the potential to cause additional spinal cord damage during injection. By comparison, the intrathecal application ensures that no additional injury to the spinal cord is caused by the injection and the safe volumes that can be administered are almost an order of magnitude larger than with the intraparenchymal approach. However, it is uncertain how effective drug penetration is into the lesion using the intrathecal injection or how localized drugs are delivered with this method. A comparative study assessing the viability of each injection approach for a particular hydrogel formulation represents an important preliminary study before evaluation of specific treatments can take place. Therefore, to further the understanding of hydrogel administration to contusion lesions, we chose to undertake such a comparative study looking at the delivery outcomes for a surrogate drug encapsulated within the ethoxylated polyol hydrogel platform described in chapter 3, using the two aforementioned injection approaches. Outcomes from this study allow us to identify the most effective method of administration of the EP hydrogel to a contusive spinal cord injury such that temporally

sustained drug concentrations within sufficiently distributed spinal cord parenchyma tissue can be achieved. Furthermore, we wanted to understand how the temporal release profile and resident time of the hydrogel material affected outcomes. To probe this we leveraged our ability to formulate structurally similar hydrogels that degrade and release biomacromolecules over different periods of time. Specifically, we chose to explore hydrogels made from TMPE-TG PEGDA 575 (fast degrading) and TMPE-TL PEGDA 575 (slow degrading) in order to provide valuable information pertaining to the effect of drug release rate on overall drug penetration into spinal cord parenchyma. Using materials with different rates of degradation allowed us to evaluate the extent of the foreign body response in the spinal cord created by similar materials with different resident times. The data generated from the current work provides vital information necessary for future exploration of specific drug candidates released from the EP hydrogel for SCI or other CNS related applications.

5.2 Results and Discussion

To investigate the comparative drug delivery outcomes associated with the two unique administration approaches of hydrogel to a spinal cord contusion a surrogate drug was required that could be detected with high fidelity upon histological analysis. Furthermore, it was necessary that such a surrogate drug could be easily incorporated within the two hydrogel formulations, did not affect the chemical or structural properties of the hydrogels and most importantly would display prolonged release properties representative of the various therapeutic proteins of interest. An anionic FITC-Dextran (40kDa) with fixable lysine residues was selected as the surrogate drug for this study. This molecule has been used previously by others as a neuronal tracer, a marker of cell macromolecule loading as well as to study phagocytosis and other cell internalization processes. Importantly, the surrogate drug exhibits minimal immunogenicity, good aqueous solubility and excellent stability *in vivo*. Therefore, the molecule represents a good candidate drug both in terms of its controlled release profile from the hydrogels as well as its ability to be readily evaluated within spinal cord parenchyma by fluorescent microscopy. A 40 kDa molecular weight dextran was used in these studies to ensure that a characteristic triphasic release profile was achieved in a manner similar to studies described in chapter 3 and that would be representative of the release kinetics for candidate biomacromolecule therapeutics for SCI. Additionally, to allow visualization of the hydrogel network during histological analysis a bifunctional maleimide conjugated Alexa Fluor 647 fluorescent dye was combined with the hydrogel precursors prior

to the initiation of gelation. The maleimide functional group contains an electron deficient alkene allowing it to react via Michael addition with the thiolate nucleophile on the TEPEs so that the Alexa Fluor dye could be covalently incorporated into the network of the hydrogel. By crosslinking the dye into the network visualization of the hydrogel for the entirety of its life was now possible.

Before initiating the *in vivo* study we tested under *in vitro* sink conditions the release profile of this FITC-dextran to determine whether the triphasic release results from chapter 3 were replicated with this modified drug. The FITC-dextran was loaded into hydrogels at a concentration of 500μg/ml. Furthermore, for the *in vitro* modeling studies we also simulated the *in vivo* conditions of the spinal cord by injecting mixed hydrogel precursors into a 1% agarose mold (**Figure 5.1**). The high water content agarose molds had the potential to promote EP hydrogel solution dilution and dissipation before the onset of gelation that may alter the volume or structural properties of the resultant network. Similar conditions are present within the spinal cord contusion lesion, therefore, understanding whether hydrated conditions would alter hydrogel performance was considered an important preliminary investigation. Favorably, the *in vitro* release profiles for the two different EP hydrogel formulations were minimally affected by the wet field fabrication conditions and showed equivalent drug release kinetics to that of the dry field prepared formulations.

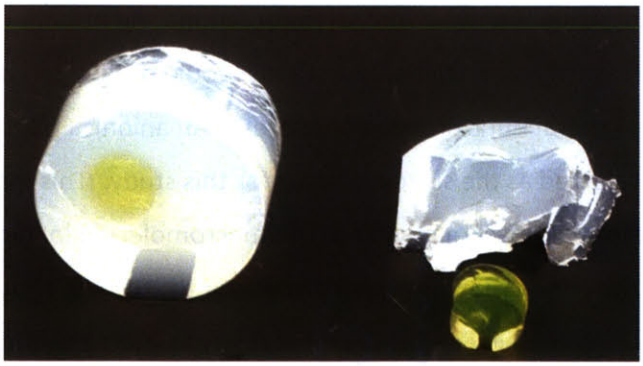

Figure 5.1 Image of TMPE-TL hydrogel with encapsulated FITC dextran injected into a 1% agarose mold. The formation of the hydrogels was minimally affected by the agarose wet field conditions.

The release profiles showed minimal burst release and limited initial diffusion mediated release from the network (**Figure 5.2**). The majority of the drug release from both EP hydrogels was attributed to network hydrolysis. Specifically, for the TMPE-TG575 hydrogel the t_{50} (time to 50% release) occurred at approximately 5 days with complete hydrogel degradation by 8 days.

By contrast the TMPE-TL hydrogel persisted *in vitro* for approximately 30 days, with the bulk of the release (nearly 80%) occurring over the last 200 hours of the materials life as part of the terminal degradation phase. A reduction in the amount of drug diffusion in favor of degradation driven release in both hydrogel formulations compared to that seen for the unmodified 40kDa FITC-dextran used previously was attributed to the additional charged entities (from the lysine and anionic components) that act to establish and maintain some drug binding interactions with the material. Both hydrogels demonstrated non swelling degradation equivalent to that reported earlier in chapter 3 **(Figure 5.3)**.

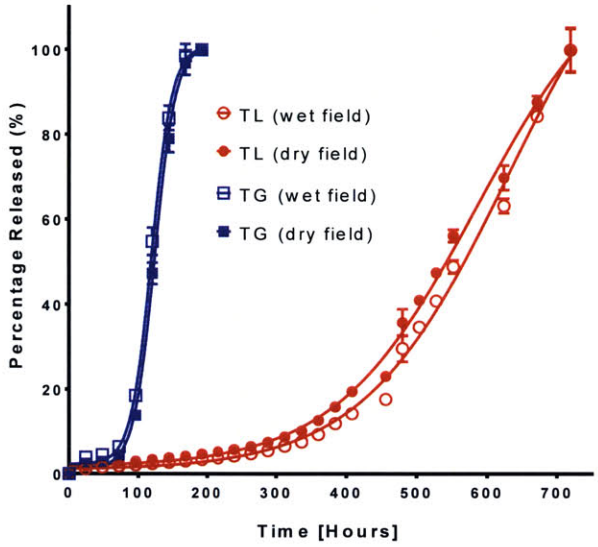

Figure 5.2 *In vitro* cumulative release profiles for anionic FITC Dextran (40 kDa) encapsulated within TEPE hydrogels demonstrating equivalent release kinetics upon curing in wet and dry fields.

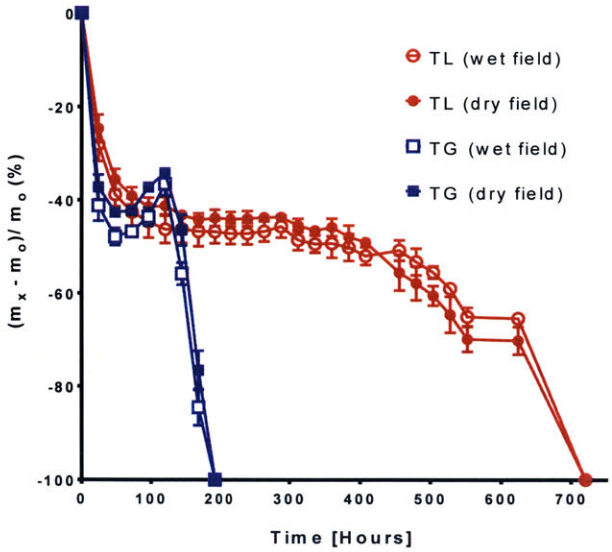

Figure 5.3 Hydrogels demonstrated non-swelling degradation when formulated in wet and dry fields. Percentage mass loss over time for the different TEPE hydrogels.

Next, we performed a 26 animal contusion study to investigate the effect of hydrogel retention time and injection protocol on drug delivery outcomes. Sprague-Dawley rats were used as the model animal for these experiments. In this study there were 13 investigation groups with 2 animals allocated to each group as follows:

Group Number	Surgical administration method	Injection media	Time of Euthanasia post injection
1	Intrathecal	Dextran Solution	One Week
2			Two Weeks
3		TMPE-TG hydrogel	One Week
4			Two Weeks
5		TMPE-TL hydrogel	One Week
6			Two Weeks
7	Intraparenchymal	Dextran Solution	One Week
8			Two Weeks
9		TMPE-TG hydrogel	One Week
10			Two Weeks
11		TMPE-TL hydrogel	One Week
12			Two Weeks
13	No injection		Two weeks

Table 5.1 Experimental groups for contusion study

Anesthetized rats underwent a laminectomy procedure at T9-10 vertebra and an Infinite Horizon impactor was used to apply a 200 kDyne (moderate to severe) contusion injury onto the exposed dorsal surface of the spinal cord at the T9 vertebral level. Consistent contusion injury parameters were observed across all animals and within treatment groups **(Figure 5.4)**.

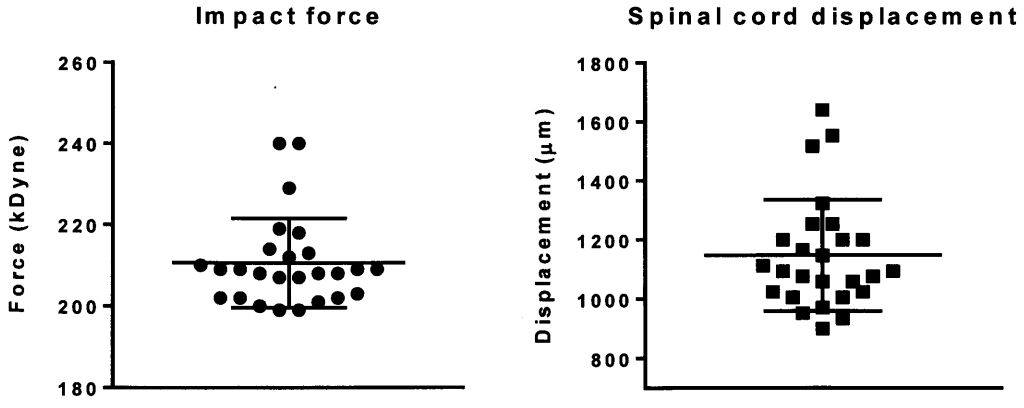

Figure 5.4 The Infinite Horizon device demonstrated reproducible contusion force and displacement values. Summary statistics for the force and displacement data for the contusion study.

The animals were given appropriate post-surgical analgesia and allowed to recover for 24 hours before administration of the various hydrogel treatments. At 24 hours post injury, the surgical incision on the dorsal surface of each animal was re-exposed under anesthesia and hydrogels were administered using either an intrathecal or intraparenchymal injection protocol. For the intrathecal procedure a 30G insulin syringe with a slightly curved needle was used **(Figure 5.5)**. Using this modified syringe a small puncture of the dura mater was made approaching from the caudal end of the spinal cord and a volume of approximately 20 μL of hydrogel was deposited into the intrathecal space. No rate control device or stereotactic frame was used to administer the hydrogel to the intrathecal space. Initial application of the hydrogel was made just rostral to the injury epicenter with continued application of the material made during retraction of the syringe over, and caudal to, the lesion. For all animals a localized, visibly green, deposit could be seen on the surface of the spinal cord that extended the width of the dorsal surface of the spinal cord as well as rostral and caudal to the lesion. However, it was challenging to ensure consistent coverage of material across all animals. In some instances, a small quantity of the hydrogel solution was displaced through the dura puncture due to the vigorous pulsatile CSF flow but this volume loss was not deemed to be significant relative to the amount administered.

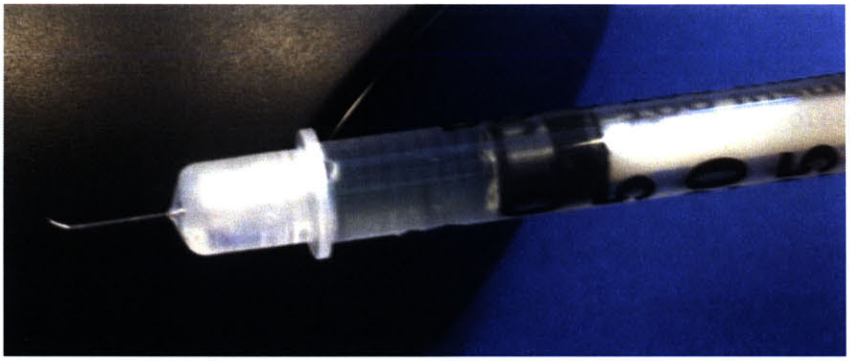

Figure 5.5 Image of the needle modification that was made to the insulin syringe for the intrathecal injections.

By comparison, the intraparenchymal injection was made directly into the epicenter of the lesion at a depth of 1.5mm from the dorsal surface of the spinal cord using a 33G needle attached to a 10 μL Hamilton syringe that was mounted to a stereotaxic frame. Using an automated microdrive pump a volume of 3 μL was injected at a rate of 1μL/min. At the completion of the injection the needle was left indwelling for one minute to ensure localized deposit of the hydrogel before slowly removing the needle. In all animals receiving intraparenchymal injections no flow back of mixed hydrogel solution was observed. To perform suitable comparisons, drug only solutions were also injected using the same two methods and two animals received no injection at all.

At one week and two weeks post injection of hydrogel (8 days and 15 days post injury) two animals from each experimental group were euthanized by IP barbiturate injection before undergoing a transcardial perfusion with 1xPBS followed by a 4% paraformaldehyde solution. No adverse gross pathology observations, outside of the spinal cord contusion, were made on necropsy for all animals. Upon spinal cord retrieval, at the one week time point, only animals receiving the TMPE-TL575 hydrogel via intraparenchymal injection showed any gross evidence of hydrogel at the lesion site. Specifically, these animals displayed a green glow that could be visually identified below the surface of the spinal cord and that seemed to be isolated locally to the confines of contusive lesion. All other spinal cords retrieved from animals from the other groups at one week looked identical with no hydrogel evident on gross inspection. The spinal cord bruising zone that is characteristic of the contusion lesion did not appear to be elongated in the hydrogel treatment groups versus the group of animals receiving solution alone. At the two week necropsy the TMPE-TL575 group no longer displayed visual evidence of the hydrogel at the lesion and appeared to be comparable to all other groups. Spinal cord atrophy at the epicenter of the lesion, which is characteristic of this injury type, was seen for all animals at two weeks with no remarkable differences between groups. The entire spinal cord from the cauda equine up to the brain stem was retrieved for all animals and post fixed in 4% PFA for an additional 24 hours before being transferred to buffer solution. No visual evidence of dye or hydrogel was identified upon gross examination in these rostral or caudal spinal cord segments at necropsy.

For histological evaluation spinal cords were cryoprotected in sucrose for several days before being embedded in OCT and cut at a thickness of 20 μm on a cryostat. We sectioned the spinal cord along the sagittal plane to evaluate the distribution of the contusion lesion and the neighboring viable tissue. To evaluate hydrogel biocompatibility and the general foreign body response to the material, spinal cord sections from one week injections were stained for hematoxylin and eosin (H&E) reagents using standardized histological techniques. Hydrogel visualization within the various H&E stained sections was consistent with the observations made at necropsy. Specifically, only in the samples receiving the intraparenchymal injection of the TMPE-TL575 hydrogel could any remnants of the hydrogel be identified **(Figure 5.6).** In all other cases no evidence of the hydrogel was found nor was there any lasting artefacts evident within cells to suggest that it had been there at all (Figure 5.6). Specifically, in the TMPE-TG intraparenchymal injection sections the lesion size and cell constituents were consistent with the drug only injection.

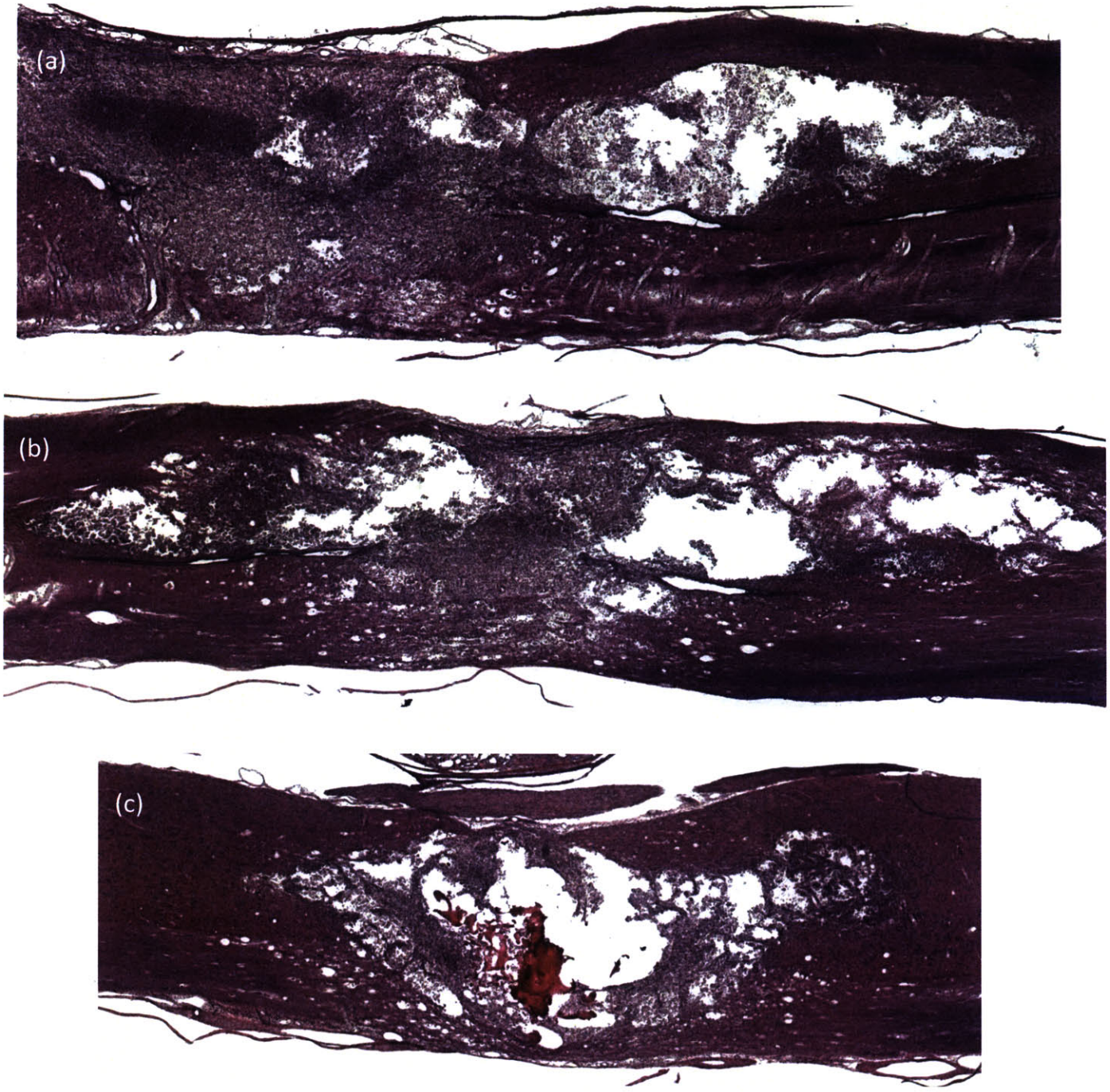

Figure 5.6 Hydrogels can be safely administered to a spinal cord injury by intraparenchymal injection. H&E stained sagittal sections of contusion injured spinal cord at one week after intraparenchymal injection of: (a) FITC-dextran only solution; (b) TMPE-TG hydrogel; (c) TMPE-TL hydrogel.

For all groups, the distribution of cells and their morphology within the lesion were consistent with the natural progression of a spinal cord injury over the first week of injury[41]. Specifically, at one week the lesion core showed evidence of resolving hemorrhage and a dominant population of foamy macrophages. Significant macrophage infiltration from the circulating vasculature as well as microglial migration from within the spinal cord parenchyma to the lesion has been shown to begin around 3 days post injury and by the one week time point the presence of these cells in the contusion lesion reaches its acute peak[41]. Qualitatively, there was no difference between groups in terms of the extent of this innate immune response. There were observable differences in the size of the lesion at the epicenter between animals but this was attributed to the inherent variability of the contusion model rather than as an effect of the injection itself. The viable tissue surrounding the contusion lesion showed mild swelling and vacuolization within the white matter that is consistent with Wallerian degeneration of the various axonal tracts.

For the intraparenchymal injection of TMPE-TL the observed hydrogel could be seen on cryosection cutting to be a hydrated volume that occupied the margins of the lesion **(Figure 5.7).**

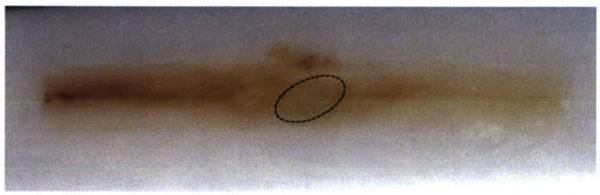

Figure 5.7 Image of spinal cord cross-section embedded within OCT showing the hydrated TMPE-TL 575 hydrogel injected intraparenchymally.

However upon further histological processing the hydrogel underwent dehydration and as a consequence retracted from the margins of the lesion to form a shrunken dark red stained rubber mass **(Figure 5.8).** Examination of the hydrogels within H&E stained sections showed no evidence of cellular infiltration within the main volume of the hydrogel. However, at the margins of the material a porous filamentous network of hydrogel was evident that seemed to be interpenetrated by beds of macrophages that naturally occupy the lesion **(Figure 5.9)**. Evaluation of the cell populations interacting at the material boundaries showed no obvious multinucleated giant cells that typically form in response to frustrated phagocytosis of the material nor was there any evidence of any amplified fibrosis or reactive gliosis compared to the control. The absence of these features suggest that the material is well tolerated and elicits a mild foreign body response. These histological analyses also confirm that there

was appropriate localization of the hydrogel to the contusion lesion using intraparenchymal injection and that no significant dilution or volume expansion of the hydrogel leading to additional spinal cord damage occurred. It is likely that the TMPE-TG was also localized at the lesion but had resorbed before the one week retrieval. Furthermore, there is no evidence that the injection of the material caused additional spinal cord injury as a result of increased intraspinal pressure or from the injection procedure itself.

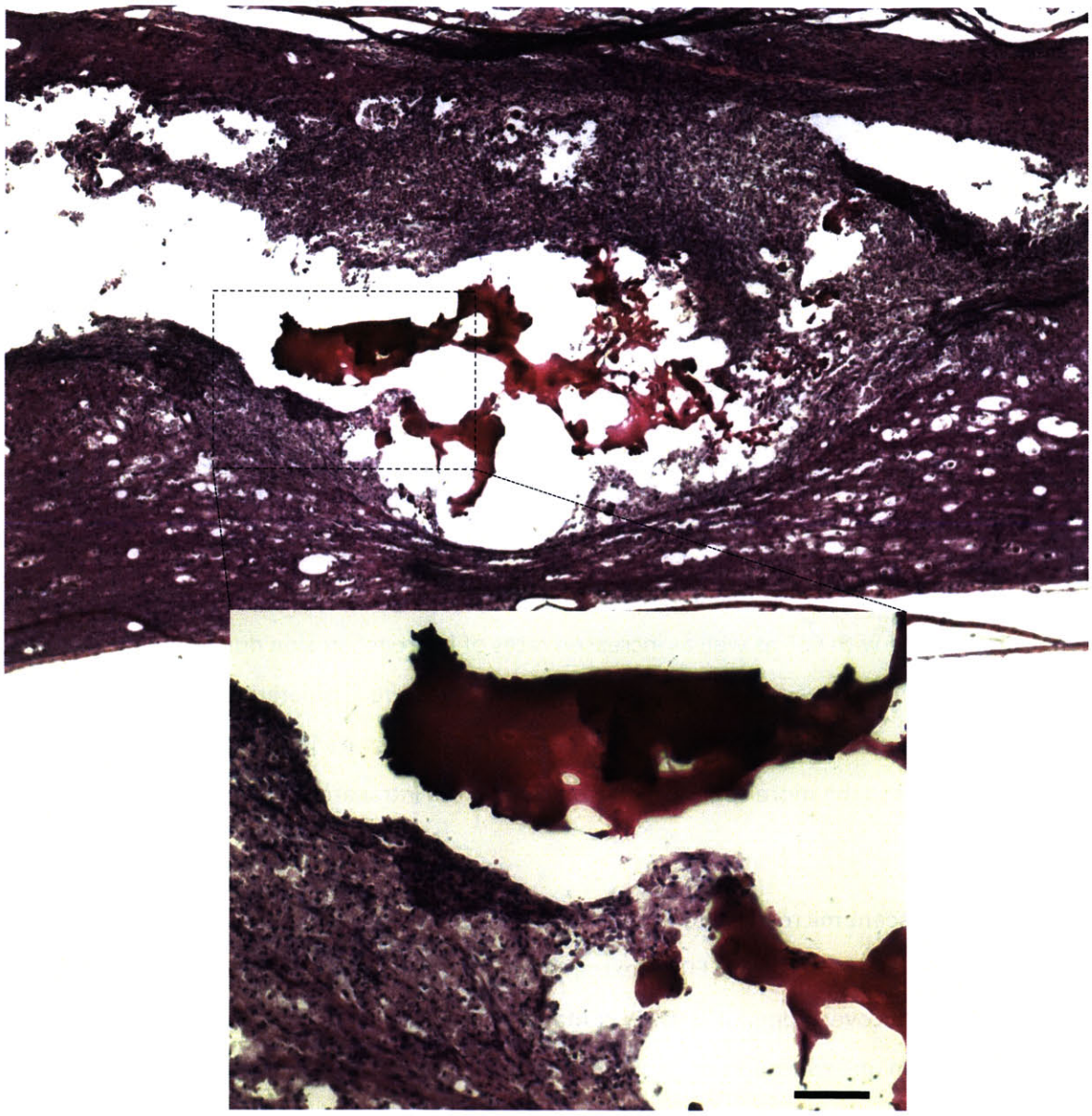

Figure 5.8 TEPE hydrogels show good biocompatibility and a minimal foreign body response in a SCI contusion lesion. Higher magnification image of a H&E stained sagittal section of spinal cord receiving an intraparenchymal injection of TMPE-TL hydrogel, the inset is 20X image of the hydrogel and cellular interface (scale bar length is 100 μm).

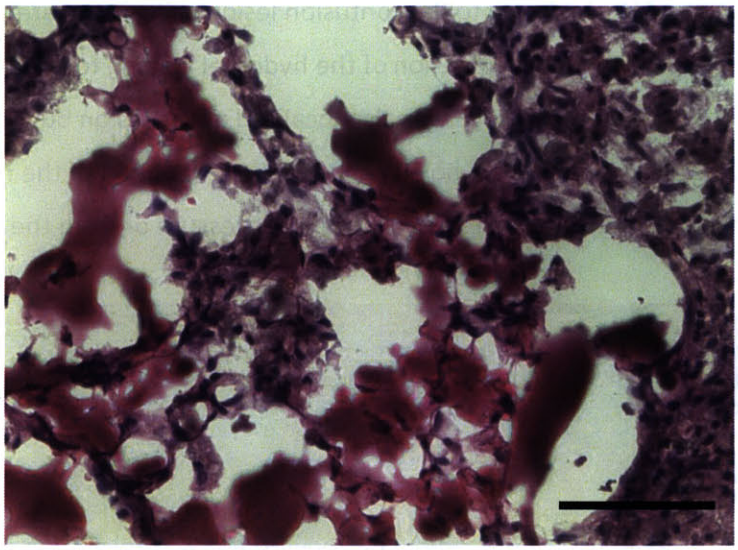

Figure 5.9 Image of the H&E stained section of spinal cord showing interpenetration of cells at the periphery of the injected TMPE-TL hydrogel. (Scale bar is 100 μm).

For the intrathecal hydrogel injections no hydrogel was detected in H&E stained sections with similar cell and tissue morphologies observed in these samples as compared to controls. Given that neither material could be located on histology it is not possible to conclude whether the hydrogel stayed localized to the lesion after injection or as material degradation took place. The more rapid material degradation observed in the intrathecal space is likely caused by a combination of hydrogel dilution due to unmitigated mixing with CSF as well as increased rates of hydrogel erosion due to the fast pulsatile nature of the CSF flow in the subarachnoid space. Furthermore, the comparatively higher surface area to volume ratio for the hydrogel "sheet" formed in the intrathecal space is likely to result in faster resorption compared to the more spherical deposit seen in the intraparenchymal injection.

Next we used fluorescent microscopy to evaluate the localized distribution within the spinal cord lesion and surrounding tissue of the anionic FITC-dextran tracer macromolecule delivered from the hydrogel. Sagittal sections were coverslipped with DAPI containing mounting media and images were taken at 4X and 10X resolution on an inverted fluorescent microscope before being stitched together using an image editing software. As a control a spinal cord that did not receive a dextran injection (either via solution or hydrogel) was imaged to determine background fluorescence at the FITC excitation/emission wavelengths **(Figure 5.10).** Minimal fluorescent signal was observed in these control spinal cords

suggestion that any signal on this channel in the dextran injected spinal cords could be attributed to the presence of this FITC labelled polysaccharide within the tissues.

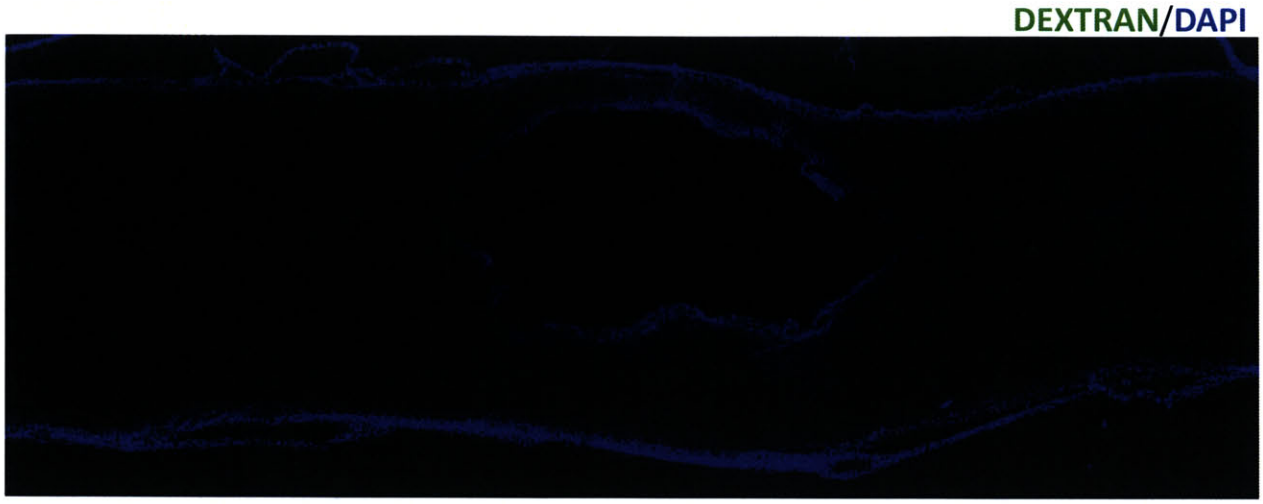

Figure 5.10 Sagittal section of spinal cord control that did not receive a Dextran injection demonstrating the limited background fluorescence observed on the FITC ex/em wavelength channel on the microscope.

Across all intraparenchymally injected spinal cord sections there was significant FITC dextran apparent within the spinal cord lesion as well as in the parenchymal tissue rostral and caudal to it. In both hydrogel groups and the solution alone the FITC dextran was seen locally in both one week and two week samples **(Figure 5.11).** In the one week spinal cords diffuse staining was apparent predominately in the neuropil with higher signal observed concentrically toward the central canal. This diffuse staining was more apparent in hydrogel administered spinal cords compared to the solution alone, with the TMPE-TL 575 hydrogel showing the largest coverage and highest intensity. In addition to this diffuse drug distribution in the neuropil, there were focal deposits scattered throughout the sagittal section in both white matter and grey matter regions. This punctated labeling pattern became increasingly apparent in the two week samples **(Figure 5.12).** Within the epicenter of the spinal cord lesion, FITC dextran was clearly detected within the localized foamy macrophages that predominate the cavity.

In sections taken from spinal cords receiving intraparenchymal injection of TMPE-TL 575 hydrogel, the residual material was clearly visualized on the Cy5/Alexa Fluor 647 filter of the fluorescent microscope indicating preserved Alexa Fluor 647 covalent incorporation within the material. In these sections, hydrogel was apparent at both the one week and two week time points and was localized exclusively to the lesion **(Figure 5.13)**. On some sections traces of residual material could be seen at the apparent injection site.

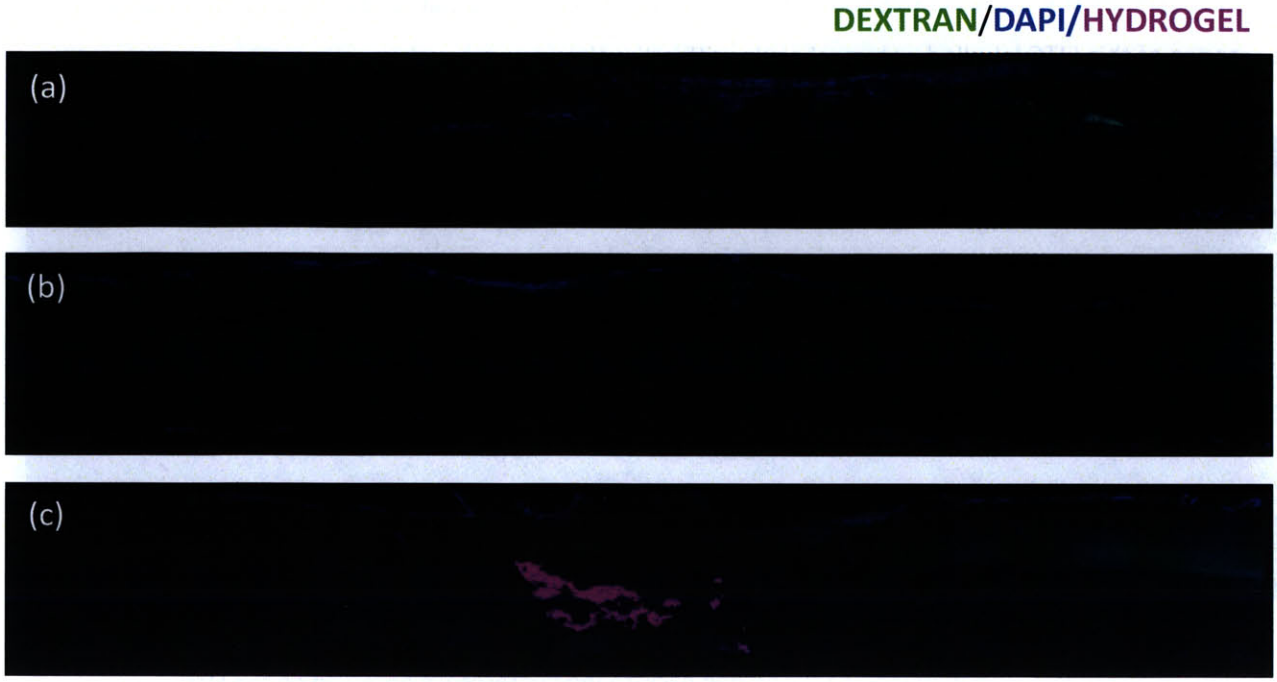

Figure 5.11 Fluorescent microscopy images of sagittal sections of contusion injured spinal cord at one week after intraparenchymal injection: (a) dextran only solution; (b) TMPE-TG hydrogel; (c) TMPE-TL hydrogel.

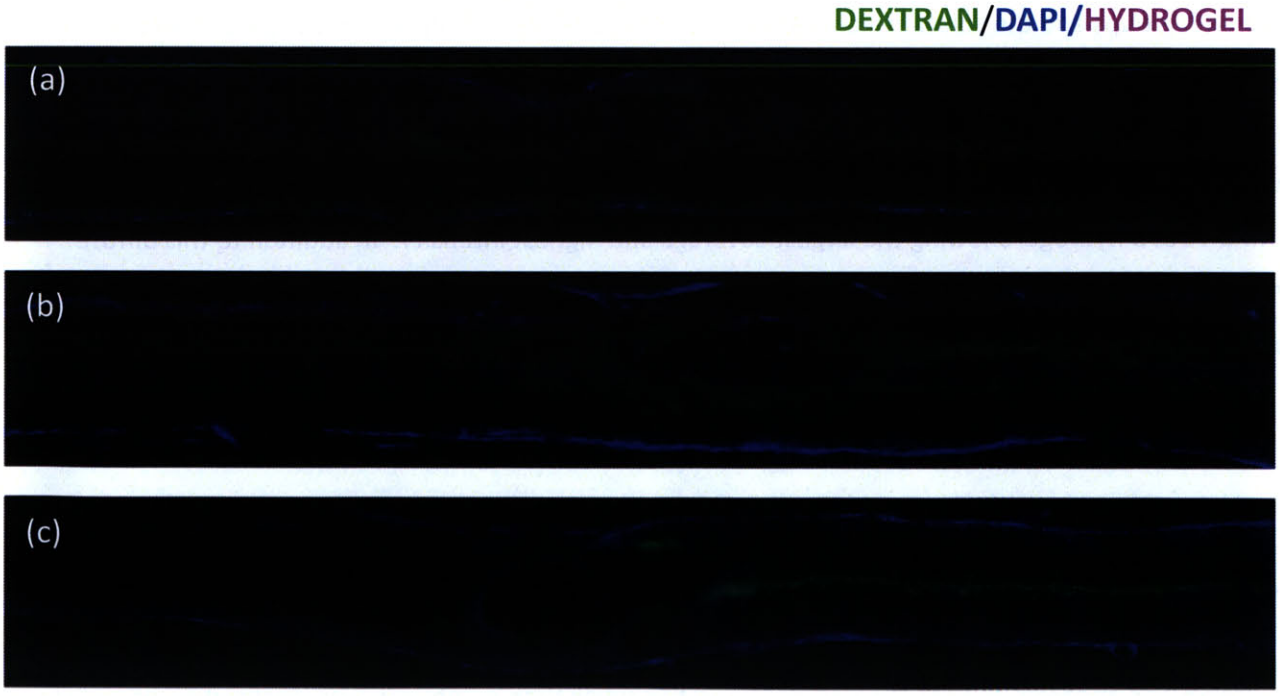

Figure 5.12 Fluorescent microscopy images at two week after intraparenchymal injection: (a) dextran only solution; (b) TMPE-TG hydrogel; (c) TMPE-TL hydrogel.

While a large focal deposit of hydrogel was observed in one week sections, within the two week histology only very small fragments of hydrogel were detected. Furthermore, in the hydrogels located within one week lesions, FITC dextran was clearly detected within the material, suggesting residual drug was still encapsulated at this time. However at the two week time point detectable FITC signal was absent in the small hydrogel fragments located within the contusion lesion **(Figure 5.13)**.

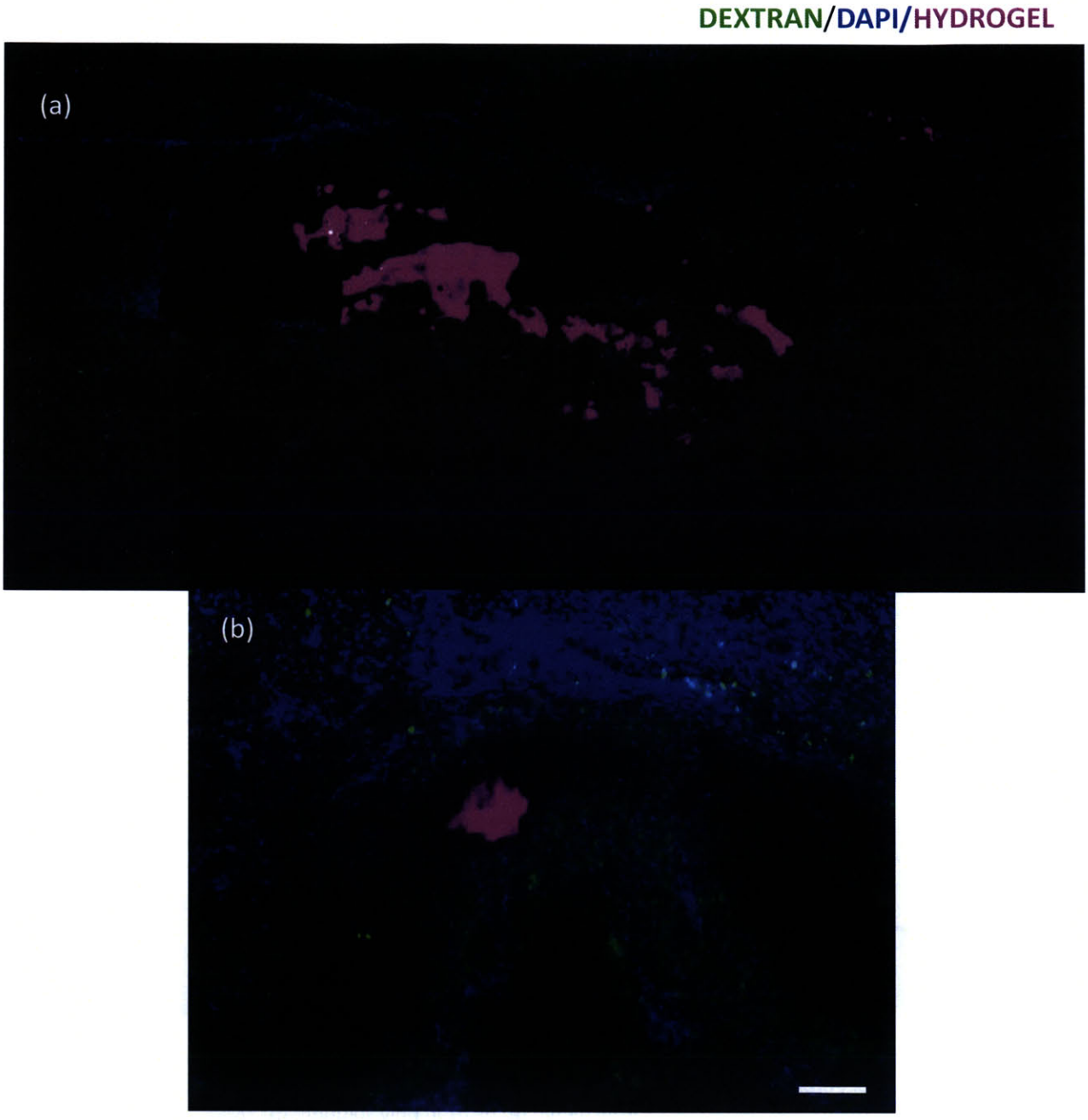

Figure 5.13 TMPE-TL hydrogel was detect within spinal cord lesions up to two weeks after injection. Microcope images of TMPE-TL 575 injected hdyrogels at (a) one week and (b) two weeks. (Scale bar is 100 μm).

For the intrathecal injected groups practically no FITC-dextran could be detected on the sagittal sections across all treatments **(Figure 5.14)**. These results were somewhat surprising as we injected close to seven times as much volume of the hydrogel and dextran solution into the intrathecal space compared to the intraparenchymal procedure. However, others have also reported limited penetration of similar sized biomacromolecule drugs using this hydrogel injection approach[319]. It is also possible that there was some initial penetration of drug into the spinal cord but that this had been cleared almost entirely by the one week time point. The limited parenchymal tissue penetration of the dextran macromolecules via the intrathecal injection suggests that SCI biomacromolecule drugs of similar size may not be sufficiently delivered using this injection approach. Furthermore, these data support the claims that there is limited spinal cord parenchyma penetration of biomacromolecule drugs using other intrathecal delivery systems, such as indwelling intrathecal catheters, which may explain the significantly variable results seen for drugs that have used such a delivery system.

Figure 5.14 Fluorescent microscopy images of sagittal sections of contusion injured spinal cord at one week after intrathecal injection showing no dextran penetration into the spinal cord parenchyma: (a) dextran only solution; (b) TMPE-TG hydrogel; (c) TMPE-TL hydrogel.

For the sections of spinal cord that received the intraparenchymal injection the punctated labeling pattern appeared to be localized within a combination of cellular and acellular compartments. For the most part, cellular uptake was restricted and mostly confined to phagocytic cells. This limited cellular uptake is likely due to the large molecular size and negative charge of the dextran which is known to restrict internalization within most cells. The dominant location of the deposits appeared to be within acellular locations suggesting that the drug had accumulated in the extracellular space (ECS) within the spinal cord parenchyma. The CNS ECS has been estimated to occupy approximately 20% of the total volume of the parenchyma and exists as narrow channels that are approximately 40-60 nm in width[320,321]. These FITC dextran deposits do not seem to have a particular pattern to them and the movement of drug is likely a dynamic process that we capture only at a single point in time with our histological analysis. It is unclear why the focal deposits occur in this manner but increased localized resistance to flow within the ECS is likely responsible[322]. Furthermore, we observed larger localized deposits at or surrounding the blood vessels radiating close to the central canal both rostral and caudal of the lesion. These larger deposits of drug are likely within perivascular spaces (PVS), which are micron sized channels surrounding CNS blood vessels **(Figure 5.15)**. These PVS are continuous with the subarachnoid space and emerging information suggests that they act as reservoirs for the drainage of CSF and interstitial fluid (ISF) from the brain and spinal cord parenchyma[323]. Recently, others have identified that these sites accumulate tracing molecules, including FITC dextran, via apparent convective bulk flow drainage from the ECS and CSF[323-325]. This convection transport is a flow process driven by tissue pressure gradients and the PVS represents a favorable sink location due to the relatively low resistance to flow it maintains. The focal dextran containing deposits within the apparent PVS also showed significant uptake of the Alexa Fluor 647 dye suggesting that the soluble hydrogel degradation products were being deposited into these spaces in a similar fashion. These histological observations support a proposed mechanism of drug distribution that involves the localized release of drug into the neuropil from the hydrogel; followed by slow diffusion transport of the drug throughout the ECS of the spinal cord parenchyma as well as into the CSF via the central canal, the subarachnoid space and mixing of ISF with CSF; before finally draining into the PVS. It is unclear what happens to the FITC-dextran once it is localized to the PVS. Possible scenarios include: drug removal from the spinal cord via further vascular drainage; drug persistence extracellularly within the PVS; and/or drug consumption by resident pericytes[326], which are a phagocytic component of the neurovasculature unit. Recent studies suggest that once drug enters the PVS that it may have the potential to re-diffuse back into the ECS via diffusion along concentration gradients[322]. This raises an exciting prospect for drug delivery from the hydrogel as

it suggests that if drug PVS drainage can be supported locally at the lesion via slow release from the hydrogel that persistent drug concentrations at the lesion could be maintained long after the hydrogel has completely degraded and resorbed. However, the advantages of such a scenario would be completely dependent on the relative stability of the drug being released. In this study, the excellent chemical stability of the FITC dextran result in longer observable resident times for this model drug within the spinal cord compared to what would likely be seen for other more fragile protein based drugs. In this current study, using the hydrogel as a means of controlling the release of drug results in a higher concentration of PVS drainage locally at the lesion site. While not conclusive, this result suggests that more persistent lesion centric concentrations of drug are promoted by the locally injected hydrogel and warrant further investigation in a larger cohort. Furthermore, since intraparenchymally injected hydrogels see released drug readily drained into the PVS there may be a future opportunity for targeted therapy to this location in order to modulate the activities of the cells within this space such as astrocytes or pericytes. Since these cells play important roles in maintaining the BSCB, disrupting or modulating their activities locally at the SCI lesion may be an effective strategy for enhancing the penetration of systemically delivered agents into the spinal cord.

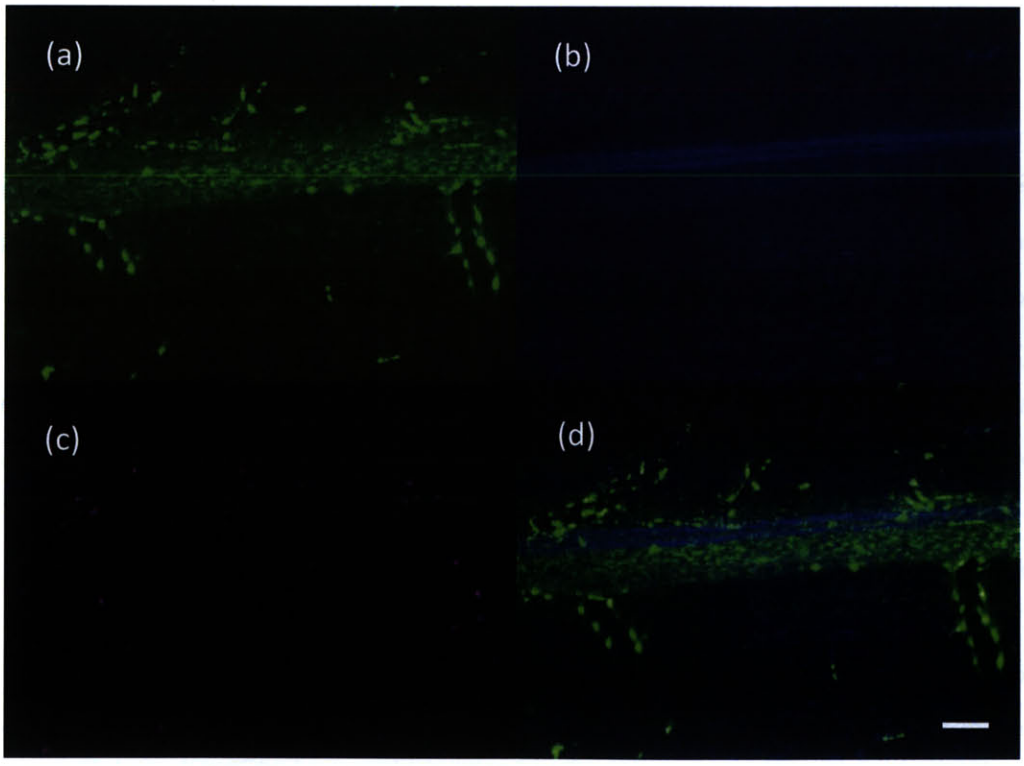

Figure 5.15 Fluorescent microscopy images of a spinal cord receiving a TMPE-TL hydrogel intraparenchymal injection focusing on the focal FITC dextran deposits within the perivascular space (PVS) (a) FITC channel, (b) DAPI channel; (c) Alexa Fluor 647 channel (d) combination of the three channels. (Scale bar is 100 μm).

To determine the overall spinal cord distribution of FITC-dextran and hence the extent of localization of drug using the hydrogel we sectioned transverse spinal cord segments from regions immediately rostral and caudal to the boundary of the tissue that we used to process sagittal lesion epicenter sections. In addition we sectioned spinal cord further rostral within the lower region of the cervical cord. These sections were counterstained with a GFAP antibody, a marker predominately expressed by astrocytes. We observed no meaningful FITC dextran signal co-staining with GFAP. These sections provide another spatial plane for observing the punctated FITC Dextran ECS deposits and shows that they are uniformly arranged throughout the spinal cord cross section and seem to flow along the ECS between axonal tracts as well as within the various regions within the neuropil of the spinal cord. The deposits were seen both rostral and caudal of the lesion in the dextran solution samples at one week but by two weeks there was only significant signal caudally **(Figure 5.16)**. By contrast the TMPE-TL 575 hydrogel sample showed limited signal at the rostral margin at one week but by two weeks signal was observed at both margins **(Figure 5.17)**. This suggests that at the initial time points dextran diffusion from the solution injection was much more extensive than the hydrogel. However, at later time points the hydrogel demonstrated enhanced diffusion of drug along the rostral-caudal axis. This result is likely because there was a greater concentration of FITC-dextran present within, and surrounding, the spinal cord lesion at the 2 week time point in animals receiving TMPE-TL hydrogel. This may indicate that the majority of the dextran being released form the hydrogel was taking place between the one and two week period. There was no dextran signal detected in the lower cervical spinal cord for any of the intraparenchymal injections suggesting that good localization to the thoracic and lumbar cord was maintained **(Figure 5.18)**. This supports the idea that extent of diffusion of drug within the spinal cord parenchyma is actually quite restricted and that convection drainage into the PVS occurs locally.

To determine whether there was any significant uptake of FITC-Dextran by any of specific classes of cells located within the spinal cord parenchyma we undertook immunohistochemical staining for ED-1 (macrophages/microglia), GFAP (astrocytes), NeuN (neurons) and NF-200 (neurofilament). As expected FITC dextran was observed within ED-1 positive macrophages surrounding the lesion **(Figure 5.19).** A phagocytic process is likely responsible for this FITC dextran uptake. However, while it is clear that there is diffuse FITC dextran signal throughout the grey matter, we did not observe any co staining of the focal punctated deposits within any of the other cell types that express the remaining antibody markers. Others have observed that these high molecular weight dextran tracers show minimal uptake into these CNS cells and investigators have instead opted to use smaller molecular weight dextrans for neuronal tracing activities. Therefore, the limited cell uptake observed here is not really that surprising.

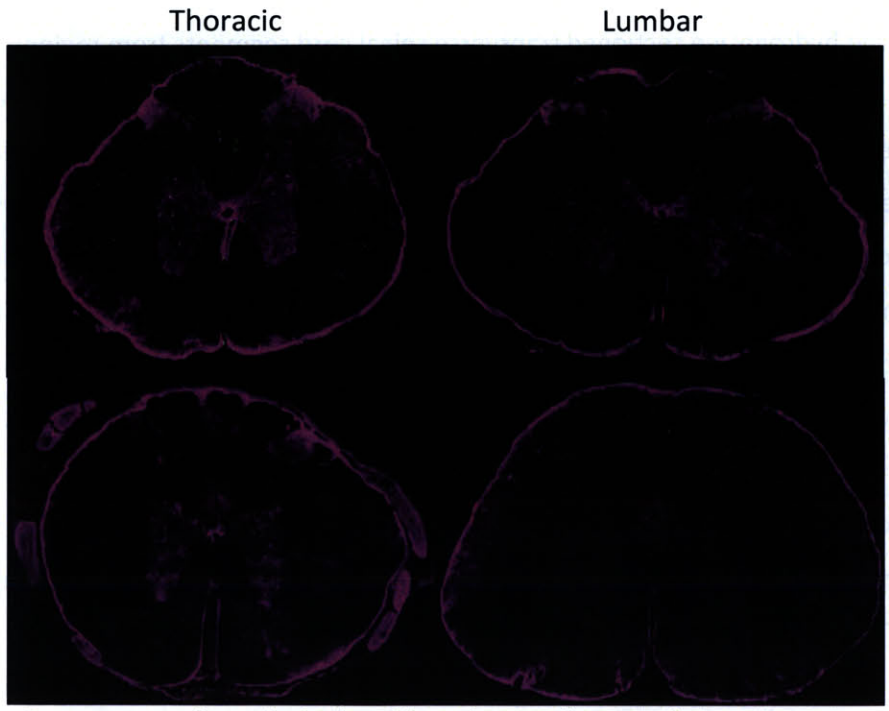

Figure 5.16 Transverse sections of spinal cord from the FITC dextran solution injection group taken from segments rostral and caudal of the lesion segment.

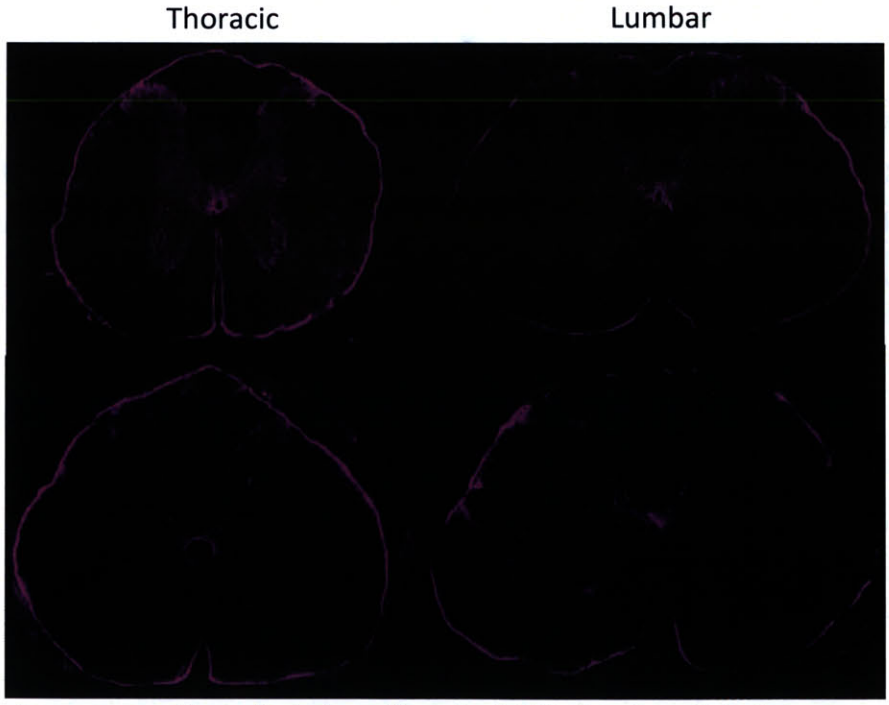

Figure 5.17 Transverse sections of spinal cord from the TMPE-TL hydrogel injection group taken from segments rostral and caudal of the lesion segment.

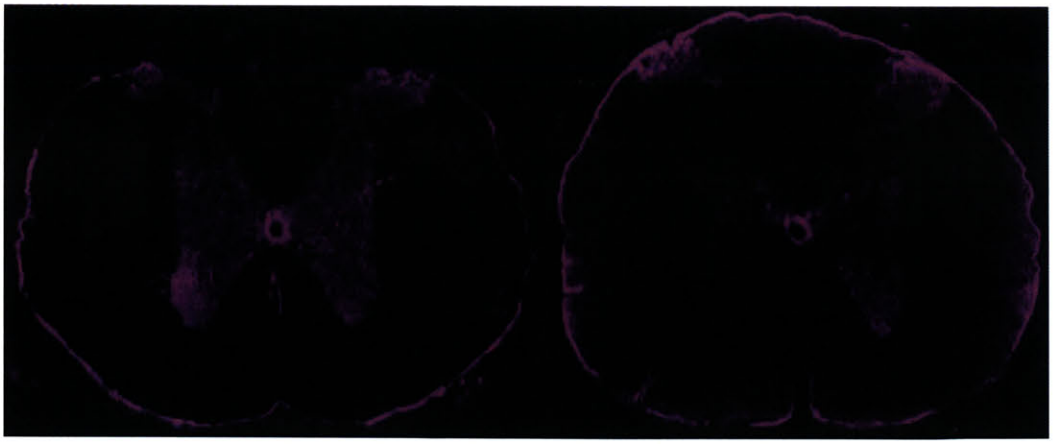

Figure 5.18 Transverse sections of a lower cervical spinal cord segment showing no detectable FITC-dextran signal in the cervical spinal cord for the TMPE-TL hydrogel intraparenchymal injection group at one and two weeks.

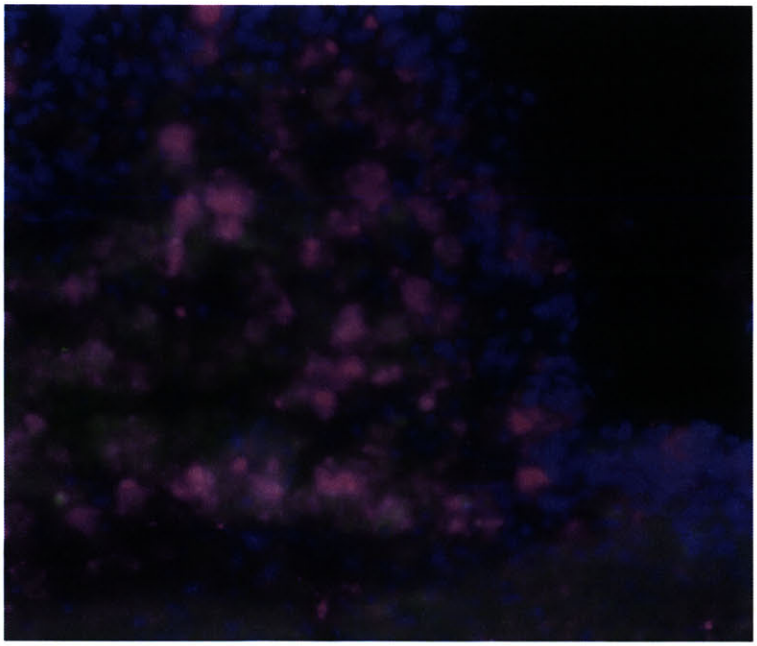

Figure 5.19 ED1+ macrophages phagocytose FITC dextran within the contusion lesion

This study served as a multi-arm pilot experiment to determine the most appropriate method for administering the EP hydrogel to a contusion lesion. The results from this experiment clearly show that the intraparenchymal injection is the only viable hydrogel administration method for achieving any significant drug delivery to the spinal cord parenchyma. The hydrogels appear to be well tolerated and elucidate a minimal foreign body response within the lesion following intraparenchymal injection. We

demonstrated the ability to formulate hydrogels that persisted within the spinal cord for a period of up to two weeks. Furthermore, significant drug concentrations were still readily identifiable within one of the formulations of this material at one week suggesting that desirable controlled release was achieved. Given the low animal size per group within this study because of the many variables tested, it was not possible to quantify with any confidence the enhanced localization of FITC-dextran within the spinal cord parenchyma as a result of the controlled release of drug from the hydrogel. Given that the FITC dextran is very stable and is not readily degraded it is difficult to interpret the effect of the controlled release using this drug as the resident time of the drug within the PVS, or perhaps within the surrounding pericytes, seems to be much longer than the studies duration. Furthermore, it is unknown whether once the dextran reaches the PVS whether any clearance of the drug does occur. If the drug does reside in the PVS or local pericytes for extended periods it may mask some of the controlled release achieved by the hydrogels. Future studies will involve a larger cohort study to compare the localized controlled release outcomes supported by the intraparenchymal injection of hydrogel versus a solution of drug with good statistical power. In such a future study, a biomacromolecule that possesses a known mechanism of action or marker that can be readily interpreted on histology but that also has a short spinal cord parenchyma half-life such that we can readily observe any effect of controlled release would be a more appropriate drug candidate. Taking guidance from other studies, biomacromolecules such as fluorescently labeled monoclonal antibodies[325], growth factors[327] or Chondroitinase ABC[200] may be viable model drug candidates that meet this criteria. Overall, we have demonstrated in this study that the EP hydrogel is a CNS biocompatible material with significant promise for the localized delivery of biomacromolecule drugs when administered via intraparenchymal injection.

5.3 Materials and Methods

5.3.1 *Hydrogel preparation*

Two unique ethoxylated based hydrogel formulations were used in the *in vitro* and *in vivo* studies described in this chapter. A detailed description of hydrogel precursor synthesis and formulation can be found within the contents of Chapter 3. Briefly, the hydrogels were fabricated using thiol-acrylate Michael addition chemistry involving the reaction of a tri-functional ethoxylated polyol tri thiol ester (TEPEs) with PEGDA in an aqueous buffered solution. For this study the TEPEs used were trimethylolpropane ethoxylate thioglycolate and thiolactate (TMPE-TG and TMPE-TL). In the preparation of these hydrogels a fluorescent dye functionalized with chemical groups capable of covalently incorporating it into the hydrogel, Alexa Fluor® 647 C2 Maleimide, (Life Technologies), was combined with the PEGDA precursor solution at 1% activated alkene concentration. A 40 kDa FITC labeled Dextran (Anionic and fixable-lysine containing) (Life Technologies) was used as the model drug for this study and loaded into the hydrogel at a concentration of 500 μg/mL. Both hydrogel oligomer precursors were solubilized in artificial Cerebral Spinal Fluid (aCSF), pH =7.2 (Harvard Apparatus). Sterile formulations of the individual hydrogel precursor solutions were prepared under aseptic conditions inside a laminar flow hood by sterile filtration of the solubilized oligomers through 0.8/02 and 0.1 μm syringe filter membranes. Appropriate volumes of each hydrogel precursor solution to ensure stoichiometric equivalency of thiol and activated alkene functional groups were aliquoted into autoclaved crimped sealed 2ml vials and stored on ice until use. To initiate the gelation reaction at the time of surgery the two solutions were mixed by transferring the contents of the PEGDA/Alexa Fluor 647 maleimide/FITC dextran solution into the appropriate TEPE solution.

5.3.2 In vitro FITC dextran release and hydrogel mass loss experiments

Prior to hydrogel fabrication 1% agarose molds were prepared by embedding a silicone rubber disc into a viscous 1% solution of heated agarose which was allowed to solidify at room temperature for 30 minutes. After the agarose had gelled, the rubber mold was carefully removed and an imprinted cavity was created. The hydrogels solutions were injected into this cavity to simulate the in vivo wet field conditions. A separate group of hydrogels were also prepared in dry silicone molds to allow for appropriate comparisons. To prepare the TEPE hydrogels a solution of FITC labeled dextran (40kDa) was added to a PEGDA solution which, after thorough mixing, was then subsequently added to a solution of

the TEPE precursor to initiate gelation. An appropriate volume of a 10 mg/ml stock of FITC Dextran was added to the hydrogel precursor solution so as to achieve a final concentration of 500 μg/mL within the formed hydrogel. Hydrogels (n=4 per group) were removed from molds 10 minutes after precursor mixing and then incubated in 1mL of 1xPBS which was replaced daily. Duplicate 200μL aliquots of the incubation media for each sample were analyzed for fluorescent intensity (ex/em 490/525 for FITC; on an Infinite® M1000 PRO microplate reader (Tecan) and the relative release quantity was derived from a standard curve. During daily incubation media replacement the hydrogels were weighed to determine the track the temporal mass loss.

5.3.3 Animal surgery and hydrogel administration

All animal use in this study followed protocols that were approved by the Institutional Animal Care and Use Committee (IACUC) of In Vivo Therapeutics, Cambridge, MA. Female Sprague-Dawley rats were obtained from Charles River Laboratories and maintained according to the NIH Guide for the Care and Use of Laboratory Animals. For the spinal cord contusions study rats were anesthetized using isoflurane and a laminectomy performed, with the assistance of a dissecting microscope, at the 9th thoracic (T9) spinal vertebrae. Following removal of the T9 lamina the rat was stabilized to the platform of an Infinite Horizon Impactor by forcep stabilization of the spine and a 200 kdyne contusion injury is applied onto the dural surface of the exposed spinal cord. Following removal of the animal from the impactor the muscle and skin layers of the surgical site were sutured and the rats were given sub-cutaneous saline and allowed to recover. The incision site was reopened 24 hours post contusion and the hydrogel or FITC dextran solution was injected into the injury site by either: (a) intraparenchymal injection using a 10 μl Hamilton syringe with a 33G needle that is directed using an automated microdrive pump mounted to a stereotaxic frame, or (b) intrathecal administration used a 500 μL 30G insulin syringe. For intraparenchymal injection 5 μL of hydrogel was administered, while in the intrathecal injection 20 μL was applied to the pial surface. Postoperative care involving bladder expression and nutrition/hydration monitoring were provided multiple times daily throughout the study.

5.3.4 Animal perfusion and histological evaluation

At 1 week and 2 week time points 2 animals from each group of animals (13 animals total per week) were perfused with heparinized saline and 4% paraformaldehyde (PFA) and the spinal cord from the mid

cervical region through to the cauda equine was excised for histological analysis. The spinal cord was post fixed in 4% PFA for 24 hours and then stored in 1X PBS containing 0.05% sodium azide at 4°C before further analysis. A 2 centimeter segment of thoracic spinal cord centered on the spinal cord contusion lesion was cryoprotected in 10% and 30% sucrose for several days respectively and then mounted in OCT in preparation for Sagittal cryosectioning on a Cryostat (Leica). Serial 20 μm sections of spinal cord were collected on Superfrost Plus slides and stored at 4°C before staining. Segments of spinal cord rostral and caudal of the lesion segment underwent the same preparative procedure but were section along the transverse plane. Sections were stained with Hematoxylin and eosin reagents using standard procedures and imaged on a bright field microscope. For FITC-Dextran imaging, spinal cord sections were mounted in DAPI containing ProLong® Diamond Antifade Mountant (Life technology) and then imaged on an Inverted fluorescent microscope (EVOS) using FITC and DAPI light cubes. Individual images were taken at various magnifications and larger fields of view were resolved by stitching together multiple images using Image Composite Editor software (Microsoft).

For immunohistochemical analysis, tissue sections were blocked in 10% goat serum, 0.5% Triton X-100 in PBS for 2 hours before an overnight incubation with a 1% goat serum 0.05% Triton x-100 in PBS solution containing a designated monoclonal antibody. After primary antibody incubation tissue sections were washed once and then incubated in an appropriate fluorescently labeled secondary antibody for 2 hours. Sections were then washed several time in PBS and coverslipped with mounting media.

The antibodies and dilutions used in this study are as follows:

Antibody Name	Vendor	Species	Dilution
GFAP	DAKO	rabbit	1:1000
NeuN	Millipore	Mouse	1:400
NF-200	Sigma	Mouse	1:200
CD 68 (ED1)	Milllipore	Mouse	1:100

Table 5.2 List of antibodies and dilutions used in this chapter.

6 APPLICATION OF INJECTABLE ETHOXYLATED POLYOL HYDROGELS FOR OTHER NERVOUS SYSTEM DISEASE APPLICATIONS

6.1 INTRODUCTION

The ethoxylated polyol hydrogel platform, characterized in great detail within Chapter 3 of this thesis, demonstrates favorable biocompatibility and versatile drug delivery properties. As such, the potential applications of the technology go well beyond the spinal cord injury drug delivery space, which is the central premise of this thesis. As such a number of collaborative studies were conducted during the thesis research period that made use of the hydrogel technology in other nervous system diseases and applications. Many of these projects have been published or are in preparation for submission. These projects are summarized briefly within this chapter and work related to the use of the hydrogel is given particular attention. The goal of this chapter is to provide the reader with a sense of additional scope for application of this hydrogel technology.

6.2 SUSTAINED LOCAL RELEASE OF SMALL MOLECULE GLUCOCORTICOID ETHOXYLATED POLYOL HYDROGELS FOR USE IN THE TREATMENT OF COMPRESSIVE RADICULAR PAIN AND PERIDURAL FIBROSIS.

This section includes a summary of the work described within the following submitted publication: Slotkin JR, Ness JK, Snyder KM, Skiles AA, Woodard EJ, **O'Shea TM**, Layer RT, Aimetti AA, Toms SA, Langer R, Tapinos N. Sustained local release of methylprednisolone from a thiol-acrylate poly(ethylene glycol) hydrogel for treating chronic compressive radicular pain (Submitted and under revision at *Spine*).

Compressive radiculopathy (CR) of the lumbar spine causes chronic pain as a result of compressive injury of the spinal roots or peripheral nerves and is the most common cause of disability in Americans under the age of 45 years old leading to significant socio-economic impacts. Furthermore, in the weeks following routine open neurosurgical procedures such as laminectomy, spinal fusion, and microdiscetomy, the formation of significant adhesive scarring and fibrosis, referred to clinically as peridural fibrosis, also promotes permanent intractable chronic pain symptoms for patients. For both

conditions neurosurgeons currently use glucocorticoid drugs to treat pain symptoms administered via epidural injection. While these drugs effectively target the biological elements responsible for the inflammation and pain symptoms observed in patients, they provide only short-term relief due to rapid drug clearance and limited targeting. The need for high dose and recurrent administration of these drugs in order to combat their short half-life and limited specificity can result in serious side effects for patients. Since there are currently no effective treatments that can ensure sustained pain relief in chronic CR or peridural fibrosis conditions there is a significant opportunity for the use of locally applied, controlled drug release systems in these disorders.

Injectable hydrogels are three-dimensional polymer networks that have the capacity to promote sustained long term local delivery of drugs and biomolecules. Poly(ethylene glycol) (PEG) is a biocompatible hydrophilic polymer that has been explored extensively in biomedical application due to its characteristic ability to resist protein adhesion (owing to the polymer's propensity to accept but not donate protons) and evoke a limited foreign body response. Using PEG as the base material we have developed a non-swelling ethoxylated polyol hydrogel platform that can cure *in situ* without requiring toxic adjuncts to initiate the covalent chemical reaction that promotes its formation.

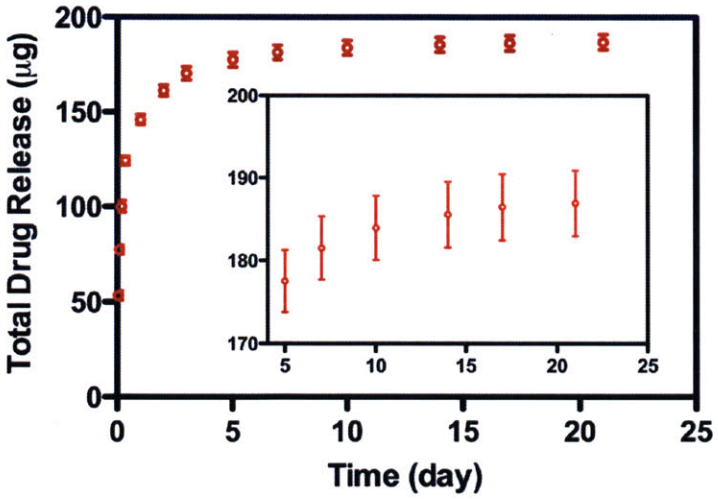

Figure 6.1 MPSS can be controllably released from hydrogels over a 21 day period under sink conditions. In vitro MPSS drug release profile from the EP hydrogel system under sink conditions as measured on HPLC.

In a collaboration with Nikos Tapinos at Geisinger Health System, Lewisburg, PA we developed an ethoxylated polyol formulation that controllably released methylprednisolone sodium succinate, the water soluble prodrug of methylprednisolone. The kinetics of drug release from the highly crosslinked

EP hydrogels were studied *in vitro* under simulated physiological conditions. MPSS demonstrated prolonged release of MPSS up to 21 days *in vitro* **(Figure 6.1).** Due to the small molecular size and hydrophilic nature of MPSS, a significant burst effect was observed in the first 24 hours (≈75%). The remaining steroid (25%, 50 μg) was released over the next 3 weeks resulting in ≈100% therapeutic recovery (200 μg total). It is important to note that these *in vitro* experiments were performed under simulated near-sink conditions in order to demonstrate non-steady state Fickian diffusion as a critical transport mechanism. However, the sink conditions modeled *in vitro* do not necessarily recreate the local tissue micro-environment *in vivo* and it is feasible that local therapeutic accumulation may occur once released from the material that would contribute to enhance mass transport resistance and limited further drug diffusion. This would result in a decreased rate of release (following the initial burst of drug facilitated by hydrogel syneresis) and hence provide the basis for delivery that is sustained for a longer time period than estimated *in vitro*. The *in vivo* data observed for this work supports this deviation from Fickian diffusion conditions within the localized peripheral nerve environment.

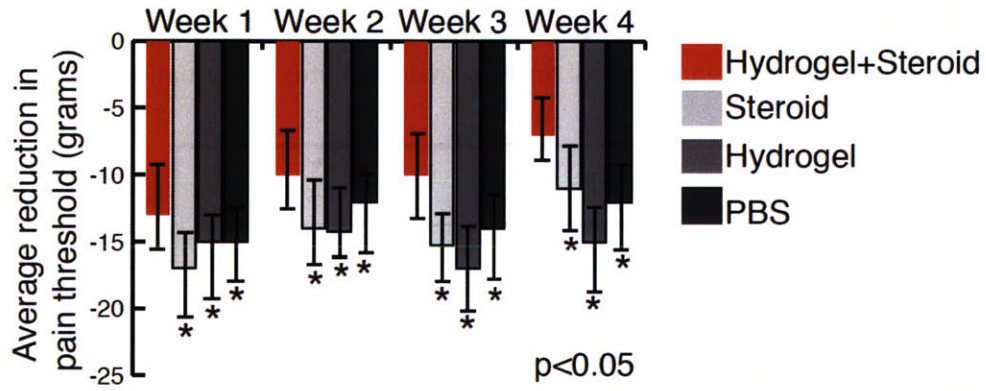

Figure 6.2 EP hydrogels encapsulating MPSS show an enhanced reduction in hyperalgesia in a chronic setting following sciatic nerve ligation compared to the drug solution injection.

An animal model of chronic CR pain involving a chronic complete ligation of the sciatic nerve was used to compare the effectiveness of the hydrogel encapsulating MPSS to a single methylprednisolone solution injection, which simulates the current standard of care. Using the hydrogel to deliver MPSS resulted in a significant reduction of hyperalgesia and improvement in the gait pattern of animals with chronic lesions as compared to animals treated with steroid alone **(Figure 6.2).** In addition, animals treated with MPSS loaded hydrogels showed a marked reduction in the number of infiltrating macrophages at the sciatic nerve **(Figure 6.3)** and significantly reduced expression of the neuro-inflammatory chemokine monocyte chemoattractant protein-1 as compared to animals treated with

steroid alone **(Figure 6.4)**. This work demonstrates the ability to encapsulate and deliver water soluble small molecule drugs within the EP hydrogels and that these materials are well tolerated upon administration to a chronically damaged peripheral nerve. Future work as part of this project will involve investigating formulation techniques to enhance the encapsulation of MPSS within the hydrogel to ensure a more sustain release profile as well as the development of slower degrading hydrogels in order to ensure a longer duration of action.

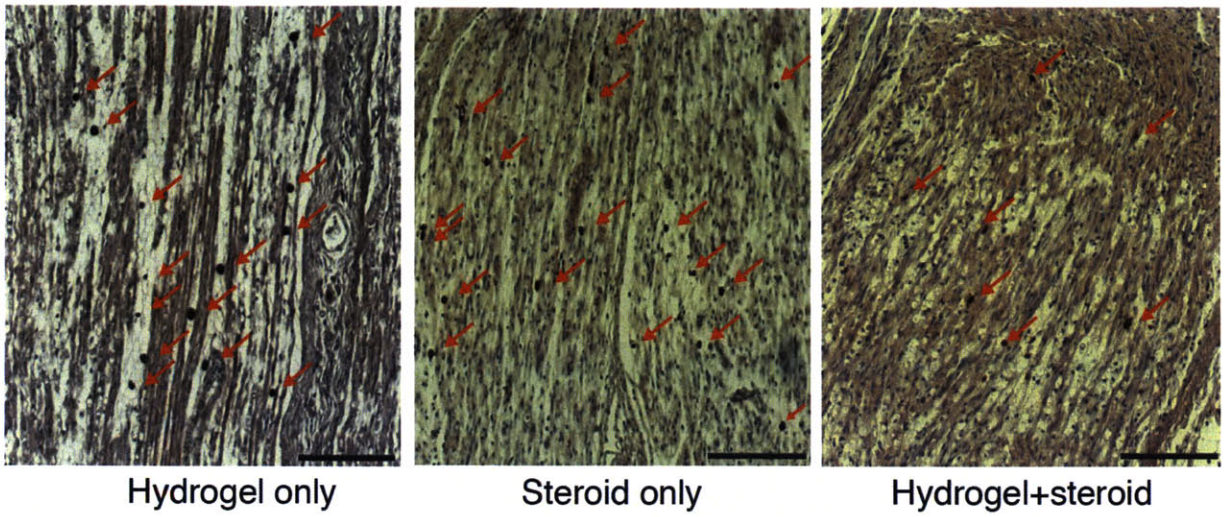

Figure 6.3 CD68 immunohistochemistry analysis on sciatic nerves. CD68 positive cells marked with red arrows infiltrate the sciatic nerve one week after sciatic nerve injury.

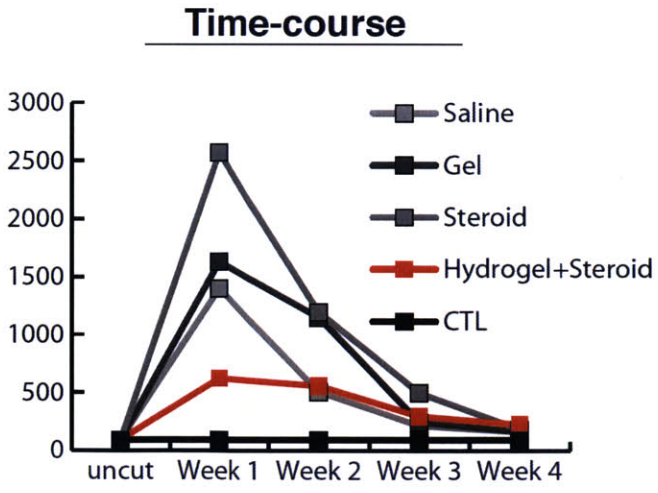

Figure 6.4 Quantification of MCP-1 expression using lysates of sciatic nerves show reduced expression of MCP-1 with hydrogel MPSS treatment.

6.3 APPLICATION OF HYDROGEL FOR USE IN AN IN VITRO MODEL OF VITREOUS REPLACEMENT

This section is a summary of the work described within the following publication: Barth, H., Crafoord S., **O'Shea, T.M.**, Pritchard, C.D Langer R, Ghosh FK. 2014. A new model for in vitro testing of novel vitreous substitute candidates. Graefe's Archive for Clinical and Experimental Ophthalmology. 252(10). 1581-1592.

In this study the EP hydrogels were evaluated in a retinal explant culture model as part of a comparative study whose aim was to identify appropriate hydrogel candidates that could be used as vitreous replacements within future *in vivo* investigations. Following a viteroretinal surgery, a procedure used to manage several eye disorders, such as retinal detachment and diabetic retinopathy, the vitreous humor, a translucent gel that occupies the eye volume between lens and the retina is inadvertently removed. Currently, inferior tamponading agents are used to minimize loss of the vitreous but their unsatisfactory performance warrants the development of better solutions. Hydrogels, cross-linked hydrated networks possess properties similar to the native vitreous and are therefore obvious candidates for their replacement. The current study aimed to develop an *in vitro* model that could be used to rapidly compare the performance of vitreous replacement candidate materials. To validate the model and determine appropriate vitreous replacement candidates the EP hydrogel was evaluated alongside a polyalkylimide hydrogel (Bio-Alcamid®) and a cross-linked sodium hyaluronic acid hydrogel (Healaflow®). Explants cultured with the EP hydrogel displayed disruption of retinal layers with moderate pyknosis of all neurons and displayed moderate labeling of apoptotic cells that was similar to the control retinas. The EP hydrogel performed better than the polyalkylimide hydrogel but not as good as the hyaluronic acid material in this assay. Furthermore, given the high polymer weight fraction and the relatively fast degradation of the EP hydrogel upon in vivo injection (approximately 2 weeks) compared to the desired performance of several months the EP hydrogel was considered to be a less appropriate candidate for vitreous replacement than the hyaluronic acid based material. However, the retinal culture results do demonstrate that the EP hydrogel is well tolerated and elicits a minimal foreign body response similar to that seen in other biological applications of the material.

6.4 Application of Ethoxylated Polyol Hydrogel to Delivery LCN-2 in Glioblastoma Model

This section describes work from a collaboration between the Langer lab led by Timothy O'Shea and the lab of Nikos Tapinos at Geisinger Health System, Lewisburg, PA. A manuscript describing this work was in preparation at the time of this thesis submission.

Gliomas are the most common primary intracranial tumors and despite modern diagnostics and chemotherapy treatments the median survival time does not exceed 15 months after diagnosis. This poor prognosis is due to the fact that after surgical removal, tumors recur predominantly within 2-3 cm of the resection cavity. The motile and infiltrating nature of glioma cells makes treatment particularly challenging. Specifically, an inability to target migrating glioma cells that diffuse within the brain parenchyma with current available treatments means that these cells will eventually form a recurrent tumor with terminal prognosis for the patient. A method to ensure the scavenging and destruction of these residual tumor cells following surgical removal could result in improved patient outcomes and represents a unique opportunity for use of a controlled release injectable hydrogel system.

In this work we studied the use of an EP hydrogel, the specific formulation being the TMPE-TL 575 variant, as a drug releasing biodegradable hydrogel that could be applied locally after tumor resection to deliver a chemoattractant of the cancer cell migratory stream. Lipocalin-2 (LCN-2), a 23 kDa protein, is secreted by the tumor cells and activates tumor cell migration and is therefore a good chemoattractant molecule for these first investigations. Our hypothesis for this study was that encapsulation of LCN-2 within EP hydrogels would promote controlled release of LCN-2 into the brain parenchyma to create spatial gradients of the chemoattractant that could be used to lure back the migrating tumor cells towards the implant. In order to achieve effective modulation of cancer cell migration locally following tumor resection the establishment of these spatial gradients of LCN-2 within the local microenvironment would need to persist for a period of time that is sufficient to force the movement of the entire residual tumor cell population towards the desired target. Since the required release duration is approximately one to two weeks we believed the TMPE-TL 575 hydrogel would be the ideal candidate material for this study.

To validate the controlled release properties of the EP hydrogel for LCN-2 we performed an *in vitro* release assay. After a small initial burst release the TMPE-TL 575 hydrogel demonstrated zeroth order release of LCN-2 over a 35 day period **(Figure 6.5)**. The rate of LCN-2 release under these *in vitro* conditions was approximately 15 ng/day over that period. To study the effect of controlled release of LCN-2 on glioma cell migration we used a mouse brain organotypic slice culture *in vitro* assay. Glioma cells were injected into one hemisphere of the brain slice, while hydrogels with and without LCN-2 were implanted into the contralateral hemisphere. Preliminary evidence suggests that the LCN-2 hydrogel acts like a sink for glioma cell migration with the entire population of cells induced to migrate towards and surround the implant after 14 days **(Figure 6.6).** By contrast, hydrogels without the encapsulated chemoattractant showed randomly distributed cells that demonstrated no obvious directionality towards the implant at the same time period of evaluation. These results suggest that the hydrogel is an excellent system for attracting glioma cells to a localized site within the brain. Future work will focus on the development of dual release system capable of also simultaneously releasing temozolomide, an approved and clinically used chemotherapy agent, which would act to destroy these attracted cells.

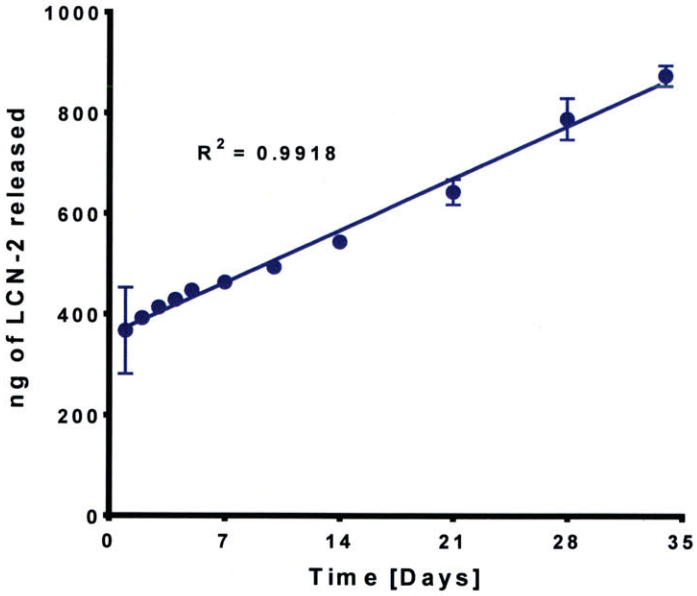

Figure 6.5 *In vitro* release kinetics for LCN-2 encapsulated within a TMPE-TL 575 hydrogel formulation demonstrate zeroth order release kinetics.

Figure 6.6 Preliminary results from the *in vitro* mouse brain organotypic slice assay showing migration of glioblastoma cells towards the LCN-2 sink created by the proteins encapsulation within the hydrogel

6.5 Application of Ethoxylated Polyol Hydrogel to Deliver Long Non Coding RNAs for the Study of Peripheral Nerve Demyelination

This section describes work from a collaboration between the Langer lab led by Timothy O'Shea and the lab of Nikos Tapinos at Geisinger Health System, Lewisburg, PA. A manuscript describing this work was in preparation at the time of this thesis submission.

Early growth response protein 2 (Egr2), is a zinc finger transcription factor found in Schwann cells whose dysfunction has been linked to a number of neuropathologies such as Charcot-Marie-Tooth disease, Dejerine–Sottas disease and congenital hypomyelinating neuropathy[328,329]. During embryonic development of the Peripheral Nervous System the Egr2 messenger RNA (mRNA) and Antisense RNA (AS-RNA) show inverse correlation of expression. In the adult sciatic nerve Egr2 mRNA is highly expressed and regulates the myelination process[330,331]. In addition, a baseline expression of Egr2 AS-RNA is always present, however during sciatic nerve injury this expression is augmented and associated with a reduction in the Egr2 mRNA expression **(Figure 6.7)**. We hypothesize that the role of Egr2 AS-RNA is to provide transcriptional buffering of the Egr2 mRNA expression and thereby acting to regulate its expression[332]. Furthermore, we postulate that under physiological conditions the baseline AS-RNA

could prevent spurious signals from deregulating Egr2 expression, while during nerve injury response the AS-RNA expression is elevated to inhibit Egr2 mRNA during the initiation of demyelination.

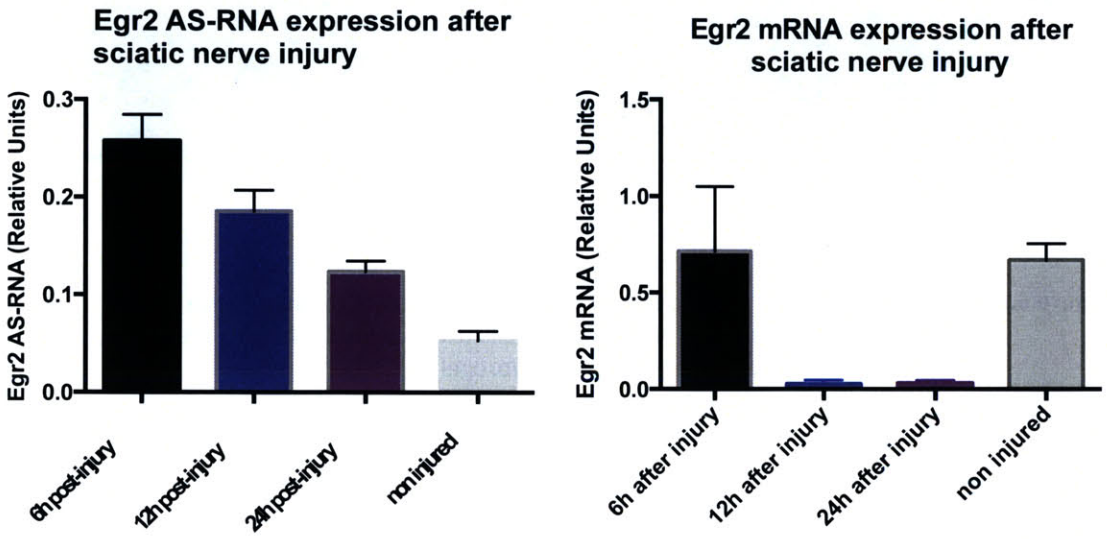

Figure 6.7 Egr2 As-RNA expression is elevated following sciatic nerve injury, which acts to inhibit Egr2 mRNA expression via a proposed transcriptional buffering mechanism.

To shed light on the role of the Egr2 AS-RNA in demyelination, we designed a number of GapMer oligonucleotides directed against the Egr2 AS-RNA so as to promote its selective inhibition. After trying to inject the GapMers via intraperitoneal means with little success, strategies that could ensure local delivery of the oligonucleotide were pursued. In order to deliver the GapMers to the sciatic nerves we encapsulated these oligonucleotides within the EP hydrogel so that they could be conveniently placed directly onto the nerve and furthermore ensure persistent localization of the GapMer. Using this approach we accomplished sustained release of GapMers locally at the sciatic nerve so to ensure prolonged inhibition of the AS-RNA. The advantage of the local and sustained application is the increased bioavailability at the sciatic nerve and the prolonged biologic effect. Preliminary evidence shows that the application of various GapMers *in vivo* against different sequence motifs of the AS-RNA using the hydrogel results in significant down regulation of the Egr2 AS-RNA **(Figure 6.8).** Work is

ongoing to characterize the effect of this AS-RNA inhibition on myelin structure using electron microscopy.

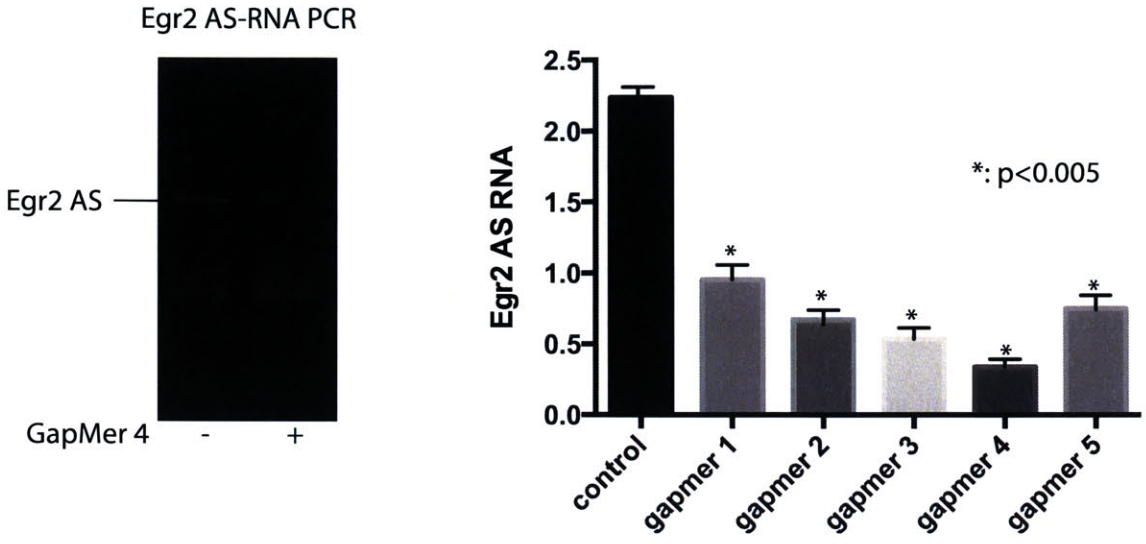

Figure 6.8 The *in vivo* delivery of various GapMers against different sequence motifs of the AS-RNA using the hydrogel results in significant down regulation of the Egr2 AS-RNA.

7 SUMMARY, CONCLUSIONS AND FUTURE WORK

7.1 SUMMARY OF FINDINGS

By striking down people suddenly in the prime of their lives and forcing them to deal with lifelong chronic medical issues that affect multiple organ systems, SCI represents one of the most debilitating and costly human injuries. Currently, promising drugs for SCI are struggling to be translated for human clinical use because of inferior drug delivery technology. Given this current inadequacy, the primary objective of this thesis was to develop and test novel biomaterial technologies that may be used to improve the local delivery of biomacromolecule drug candidates in SCI.

To achieve this important goal we first applied novel polymer chemistry techniques to develop an injectable hydrogel platform derived from biocompatible synthetic polymers. Specifically, we synthesized a library of tri-thiol functionalized ethoxylated polyol esters (TEPEs) through the use of a robust enzymatic catalyzed reaction that we performed under mild, solventless conditions. This synthetic scheme allowed us to produce economical, large gram scale batches of highly functionalized TEPEs that would be readily amendable to industrial scale production. Combining the library of TEPEs with a variety of commercially available poly(ethene glycol) diacrylates (PEGDA) allowed us to form materials with diverse physiochemical properties using a thiol-acrylate Michael addition reaction. Under physiologically buffered conditions and in the absence of toxic catalysts, hydrogels were formed with rapid but tunable gelation kinetics that displayed thermoreversible swelling and syneresis that was dependent on the relative lipophilic character of the individual TEPE. Through rigorous material properties characterization we identified candidate hydrogels that displayed non-swelling degradation by hydrolysis and that demonstrated controlled release profiles that were dependent on drug molecule size and the rate of hydrogel degradation. In particular, several hydrogel formulations showed a favorable triphasic release profile for model proteins and polysaccharides that could be tuned with high precision over a range of 5 to 35 days by blending different TEPEs. Furthermore, all TEPE based hydrogels displayed minimal macrophage immunogenicity *in vitro* and excellent biocompatibility. Given these favorable properties these EP hydrogels represent a versatile platform for local drug delivery to volume-constrained anatomical sites.

The EP Hydrogels have demonstrated the ability to temporally control the release of biomacromolecules with broad potential therapeutic applications. However, many biomacromolecules are complex and

fragile and, therefore, strategies must still be developed to improve their long-term functional stability within these materials. Within this thesis we next fabricated hydrogels with covalently incorporated trehalose, a non-reducing disaccharide, by reacting trehalose diacrylate monomers with tri-thiol-functionalized ethoxylated polyol esters (TEPEs) and PEG diacrylate (PEGDA) via a thiol-ene Michael addition mechanism. The trehalose hydrogels display fast and controllable gelation kinetics under physiological conditions as well as non-swelling degradation via a mechanism of hydrolysis. Importantly, the covalent incorporation of trehalose within hydrogels afforded prolonged stabilization and controlled release of model enzymes *in vitro* and *in vivo*. Strong and ordered hydrogen bonding interactions as a result of a homogenous and cooperative trehalose network is presented as a proposed mechanism responsible for the enhanced long-term stabilization of proteins observed. Furthermore, trehalose hydrogels maintained protein stability under relevant stressors experienced in the manufacture and storage of biotherapeutics including heat and lyophilization. The described method of covalently incorporating trehalose into hydrogels provides a tunable platform for controlled release of clinically relevant therapeutic biomacromolecules with enhanced functional stability.

To overcome the barriers posed by the blood spinal cord barrier and the meninges, locally applied injectable hydrogels are of significant interest for controlled release of drugs to the spinal cord following injury. Although the dominant mode of injury to the spinal cord in the human population is a non-penetrating contusive injury, the application of injectable hydrogels to this type of injury is rarely explored through the SCI literature. Furthermore, in the small number of studies that do use hydrogels in contusive SCI there is no consensus as to the best method of administration to ensure safe and efficacious delivery of drugs locally. To address this underappreciated area we conducted a comparative study examining the effect of hydrogel injection location on drug delivery outcomes to a rat spinal cord injury. We demonstrated via the delivery of a histologically detectable surrogate drug that intraparenchymal injection but not intrathecal application of hydrogel resulted in localized spinal cord parenchymal delivery. Furthermore, we demonstrated that EP hydrogel formulations may ensure enhanced resident time of drug within the spinal cord extracellular space over a two week period and delay complete drainage of the drug into the perivascular space via convection transport processes. We also showed that hydrogel intraparenchymal injections are safe and do not cause any additional damage to the spinal cord.

Overall, this work validates novel strategies for the development of hydrogels that can be used to achieve improved localization, temporal delivery and long term functional stability of promising

biomacromolecule drug candidates in SCI. In addition we demonstrated a safe and effective method for locally administering this material to a clinically relevant injury mode.

7.2 CONTRIBUTIONS TO HYDROGEL AND DRUG DELIVERY RESEARCH FIELDS

This work made valuable contributions to the fields of synthetic polymer chemistry, soft matter and material science in a number of important ways. Firstly, the developed synthesis scheme for the TEPEs provides a novel, one pot, robust synthesis technique for making multifunctional PEG thiols. Such polymers are used extensively throughout the drug delivery and tissue engineering communities and this particular synthetic method will allow many in the field to easily produce large scale quantities of these materials at much lower cost compared to the items they currently purchase from commercial vendors.

The EP hydrogel fabrication and characterization work in chapter 3 provided valuable material properties information on a number of candidate hydrogel formulations that may find utility across a number of applications in drug delivery and medicine. This fact is clearly demonstrated in chapter 6 where we outlined the many active collaborations that are using this material to evaluate interesting biological questions and provide innovative drug delivery solutions. Furthermore, the ability to tune drug release with ultrafine control using hydrogels made from blends of thioglycolate and thiolactate TEPEs provides for an injectable material with drug delivery properties reminiscent of Poly(Lactide-co-Glycolide) copolymers (PLGA), whereby the relative ratio of TG/TL dictates drug release duration. Since PLGA is a widely adopted hydrophobic polymer used in drug delivery but is problematic for the delivery of proteins and other biomacromolecules, this hydrogel platform could fill an important void.

Finally, the novel trehalose hydrogel formulations described in chapter 4 make a valuable contribution to the fields of biomacromolecule biochemistry and drug delivery and offer important solutions that will be of significant interest to members of the biomaterials, polymer, biochemistry, soft matter and physical chemistry research communities. In addition, this work offers a viable solution to significant issues facing production of biotherapeutics and as such various affiliates of the biotechnology industry will also be attracted to this work. Finally, given that the trehalose hydrogels provide a tunable platform for the controlled release of clinically relevant therapeutic biomacromolecules with enhanced functional stability there are numerous potential medical applications of this technology. There are currently limited options for delivering particularly fragile biomacromolecules for scientific and clinical

applications. With the emergence of more complex enzymatic systems such as CRISPR/CAS9 and zinc finger nucleases, better biomaterial systems are needed. The trehalose hydrogel may provide a new tool for the improved delivery of these complex and fragile biomacromolecules. Our group and our active collaborators are currently pursuing applications of this technology to better deliver other fragile biological therapeutics in the fields of neuroscience, cardiology and diabetes, which also attests to the impact of this platform.

7.3 CONTRIBUTIONS TO SPINAL CORD INJURY RESEARCH FIELD

Currently there are limited tools available to the SCI research community to locally deliver, with good control and certainty, the many promising drug candidates that have been identified through their rigorous mechanistic biological investigations. While biomaterial researchers have attempted to fill this void with innovatively engineered hydrogels, there is currently limited information available validating their performance or even how best to administer them to spinal cord contusion injuries, the dominant injury mode seen clinically. Within this thesis we explored hydrogel surgical administration to a spinal cord contusion model to validate an appropriate injection procedure for safety and efficacy. The outcomes from this research demonstrate conclusively that these *in situ* curing materials achieve superior drug delivery outcomes upon intraparenchymal injection rather than intrathecal application on the pial surface. Therefore, this work provides SCI researchers with a well validated tool that they can modify easily to fit with their molecule of interest.

7.4 RECOMMENDATIONS FOR FUTURE WORK

This thesis provides a comprehensive characterization of a novel hydrogel system while also providing preliminary evidence for the use of the material in spinal cord contusion injuries. Obvious future work motivated by the outcomes of this thesis research can be categorized into three main areas: (1) Further hydrogel development and fabrication refinement so as to enhance the performance of the material or make them suitable for other applications not addressed in depth within this thesis; (2) Use of the existing hydrogel technology within additional SCI studies; (3) Use of the existing material in other non-SCI applications that require local controlled drug release. A variety of concepts and examples relevant to these three areas will be highlighted within this section.

The current thesis work focused on improving the delivery of biomacromolecule drugs because they offer many advantages over small molecule therapies such as enhanced specificity, higher potency, a reduction in toxicity and off target effects and a more predictable mechanism of action. Furthermore there are a number of delivery limitations that affect the performance of this class of drugs. A significant limitation for these drugs is that they cannot be made orally bioavailable as they denature and hydrolyze readily in the gastrointestinal tract. Furthermore, their short half-lives and large bulky size means that targeted tissue penetration and localization is limited upon parenteral administration. However, there are also a number of small molecule drugs whose clinical performance may be improved using a locally applied drug delivery systems. Many small molecule drugs have similar stability and tissue targeting issues to that seen for biomacromolecules. Furthermore, many small molecule drugs cause undesirable systemic toxicity when administered by oral or parenteral methods. Therefore, developing locally applied controlled release small molecule drug therapies is of significant interest. However, hydrogels are generally not suitable for small molecule drug delivery either because of a release profile that is too fast or due to an insufficient drug encapsulation capacity owing to their hydrophilic nature.

Although the current EP hydrogels possess some lipophilic chemistry that imparts them with non-swelling degradation properties, they still have a limited capacity to encapsulate many hydrophobic small molecule drugs or ensure that meaningful release of these drugs is prolonged for longer than a week. To address these inadequacies associated with the current system, the development of hydrogels with a higher concentration of hydrophobic domains within the network would be advantageous. Three possible ways this could be achieved that would not alter the existing favorable properties of the current system include:

1. Develop acrylated monomers derived from various poloxamer polymers that could be substituted for PEGDA in the current system. The increased hydrophobicity within the resultant hydrogel network from the propylene oxide containing chains would enhance the solubilization of hydrophobic small molecule drugs.
2. Using Pentaerythritol ethoxylate as a substitute for either glycerol ethoxylate or trimethylolpropane ethoxylate in the enzymatic thiol ester transesterification reaction to create a tetra-functional thiol oligomer. The excess thiol that is not required for gelation could be used to attach various pendant fatty acids to the ethoxylated polyol using the thiol acrylate Michael addition reaction or thiol-ene photo-initiated radical reaction. The addition of a pendant fatty

acid to the TEPE would impart a surfactant like property to the hydrogel precursor that could be used to enhance the solubility of hydrophobic drugs prior to initiation of gelation. These surfactant like hydrogel precursors will likely promote the formation of concentrated hydrophobic domains within the hydrogel network that would delay the release of these drugs in aqueous conditions.

3. Explore the use of commercially available trimethylolpropane ethoxylate triacrylate or other similar activated alkene precursors to enhance the lipophilicity of the resultant hydrogel network.

Another hydrogel development activity could be to synthesize non-ester based thiol crosslinkers derived from the ethoxylated polyols. Such a hydrogel precursor would reduce the density of labile esters within the hydrogel and extend the life of the material by slowing hydrolysis. Alternatively, the development of an amide based crosslinker with thiol functionality perhaps via the amidation of a multi-arm amine or carboxylic acid functionalized PEG with cysteine or cysteamine could also be explored to reduce the rate of hydrogel degradation.

There is substantial interest in developing micro- and nano-gel formulations for a variety of systemic and local drug delivery applications[333]. Given the dominant PEG content within the current EP hydrogel formulations they would seem to be ideal candidates for the development of a non-fouling particle system. Furthermore, given that we can covalently incorporate trehalose within the network to stabilize proteins the current system offers exciting possibilities for the improved systemic delivery of monoclonal antibodies or other biotherapeutics. To create particle formulations from this hydrogel system two fabrication techniques would seem most viable. The first involves the preparation of particles through inverse emulsion whereby the aqueous polymer phase is dispersed within a hydrophobic phase such as a low toxicity vegetable oil. An exciting alternative formulation strategy could involve using a thermoprecipitation method. Specifically, given that the lower critical solution temperature (LCST) of the hydrogel precursors are around or slightly higher than physiological temperature, dilute mixed solutions of hydrogel that do not form macroscopic hydrogels could be injected into a higher temperature sink resulting in higher concentration gel precipitates to form during dispersion. Similar methods using unfavorable solvents to facilitate polymer precipitation and gelation have been used to good effect previously to form micro and nanogels[334,335]. However, by using the EP precursors from the current hydrogel system, favorable aqueous conditions and mildly elevated

temperatures (≈40°C) could be used. This strategy would allow for the formation of microparticles under conditions compatible with many biological processes and as such many fragile biotherapeutics or even mammalian cells could be readily encapsulated. Although these gel particles could be used by themselves for drug delivery applications, another exciting alternate strategy would be to encapsulate these new entities within shear thinning hydrogel formulations to create a composite system. Encapsulating the particles within shear thinning hydrogels would be beneficial for a number of applications including spinal cord injury. Specifically, a composite formulation would allow for slower injection of hydrogel, because no gelation time constraints would exist, which would ensure larger volumes could be administered safely as well as minimizing dispersion and any additional tissue damage as a result of augmented intraspinal pressures. Since most shear thinning hydrogels offer limited control of biomacromolecule release, the embedded gel particles would impart this property to the composite system and may also enhance the stabilization of these therapeutics. There are emerging examples of where polymer–nanoparticle hydrogel systems have been used effectively[336]. Therefore, the use of the current EP hydrogel system to create viable gel particles would seem to be a worthy area of future investigation.

Exploring application of the EP hydrogel platform described within this thesis to improve the delivery of specific promising SCI candidate drugs is also an important area for future investigation. As highlighted in Chapter 2 of this thesis, there are a number of drug candidates, which demonstrate a favorable and known mechanism of action that may be lead to better outcomes in SCI but which face considerable delivery obstacles. The EP hydrogel platform could be readily applied to improve the delivery of several of these drugs such as Chondroitinase ABC, Anti-Nogo antibody, BA-210 (Cethrin), erythropoietin as well as the many neurotrophins and growth factors that were identified previously. However, additional work validating the intraparenchymal injection approach for the hydrogel as well as considering the other important parameters such as volume, rate and time of injection in a larger cohort of animals would be an important preliminary step prior to investigating specific therapies. It is likely that new biomacromolecule therapies will continue to emerge for SCI which will face similar delivery challenges to the current pool of promising drugs. The EP hydrogel platform will equip SCI researchers not only with a tool to better deliver previously identified drugs but it may also find utility in the discovery of new candidates. Efforts to establish a network of collaborators working in the SCI drug discovery field such that this novel hydrogel platform can be disseminated more widely should be prioritized.

Finally, there are many other medical disorders and diseases that would benefit from the current hydrogel technology. In addition, there are several emerging basic biological research fields that may be able to use the platform described in this thesis to improve the performance of their assays. Some possible future studies in the biomedical research space outside of SCI that may be amendable to EP hydrogel use include:

- Application of the hydrogel to delivery drugs to other volume constrained anatomical locations such as the inner ear, brain or heart.
- Application of the hydrogel to prevent surgical adhesions, such as seen following abdominal surgery.
- Subcutaneous application of the hydrogel to improve long term systemic delivery of biomacromolecule drugs through stabilization of secondary and tertiary structure.
- *In vitro* assays that use the hydrogel to create spatial gradients of possible chemoattractant biomacromolecules to identify entities that may direct cell activities such as differentiation, proliferation and migration.
- Application of the trehalose hydrogel in biochemistry assays to study protein folding or as a new way to stabilize proteins during crystallization procedures.

There are bound to be many more potential opportunities for which the EP hydrogel may find application. By developing a versatile and economical hydrogel platform and rigorously characterizing its properties the outcomes of this thesis research ensure that future researchers can use this technology to make positive contributions to the most challenging problems facing modern medicine.

REFERENCES

1 Steward, O., Popovich, P. G., Dietrich, W. D. & Kleitman, N. Replication and reproducibility in spinal cord injury research. *Experimental Neurology* **233**, 597-605, (2012).

2 Wyndaele, M. & Wyndaele, J. J. Incidence, prevalence and epidemiology of spinal cord injury: what learns a worldwide literature survey? *Spinal Cord* **44**, 523-529, (2006).

3 DeVivo, M. J. Epidemiology of traumatic spinal cord injury: trends and future implications. *Spinal Cord* **50**, 365-372, (2012).

4 Bickenbach, J. International perspectives on spinal cord injury (World Health Organization, Geneva, Switzerland, (2013).

5 Hagen, E. M., Lie, S. A., Rekand, T., Gilhus, N. E. & Gronning, M. Mortality after traumatic spinal cord injury: 50 years of follow-up. *Journal of Neurology, Neurosurgery & Psychiatry* **81**, 368-373, (2009).

6 Ditunno, J. F. & Formal, C. S. Chronic Spinal Cord Injury. *N Engl J Med* **330**, 550-556, (1994).

7 McDonald, J. W. & Sadowsky, C. Spinal-cord injury. *The Lancet* **359**, 417-425, (2002).

8 Furlan, J. & Fehlings, M. Cardiovascular complications after acute spinal cord injury: pathophysiology, diagnosis, and management. *Neurosurgical FOCUS* **25**, E13, (2008).

9 Goldstein, B. Musculoskeletal conditions after spinal cord injury. *Physical medicine and rehabilitation clinics of North America* **11**, 91-108, viii-ix, (2000).

10 Schilero, G. J., Spungen, A. M., Bauman, W. A., Radulovic, M. & Lesser, M. Pulmonary function and spinal cord injury. *Respiratory Physiology & Neurobiology* **166**, 129-141, (2009).

11 Fehlings, M. G. & Vaccaro, A. R. *Essentials of Spinal Cord Injury: Basic Research to Clinical Practice*. (Thieme, 2012).

12 Berkowitz, M., O'Leary, P., Kruse, D. & Harvey, C. *Spinal Cord Injury: An Analysis of Medical and Social Costs*. (Demos Medical Publishing Inc, 1998).

13 Kwon, B. K. *et al.* A Systematic Review of Directly Applied Biologic Therapies for Acute Spinal Cord Injury. *Journal of Neurotrauma*, **28** (8):1589-610, (2011).

14 Tetzlaff, W. *et al.* A systematic review of cellular transplantation therapies for spinal cord injury. *Journal of Neurotrauma* **28**, 1611-1682 (2011).

15 Kwon, B. K. *et al.* A systematic review of non-invasive pharmacologic neuroprotective treatments for acute spinal cord injury. *Journal of Neurotrauma* **28**, 1545-1588 (2011).

16 Hawryluk, G. W. J., Rowland, J., Kwon, B. K. & Fehlings, M. G. Protection and repair of the injured spinal cord: a review of completed, ongoing, and planned clinical trials for acute spinal cord injury: A review. *Neurosurgical FOCUS* **25**, E14 (2008).

17 Gensel, J. C., Donnelly, D. J. & Popovich, P. G. Spinal cord injury therapies in humans: an overview of current clinical trials and their potential effects on intrinsic CNS macrophages. *Expert Opinion on Therapeutic Targets* **15**, 505-518 (2011).

18 Casha, S. *et al.* Results of a phase II placebo-controlled randomized trial of minocycline in acute spinal cord injury. *Brain* **135**, 1224-1236 (2012).

19 Hurlbert, R. J. *et al.* Pharmacological Therapy for Acute Spinal Cord Injury. In Guidelines for the management of acute cervical spine and spinal cord injuries. *Neurosurgery* **72**, 93-105 (2013).

20 Erschbamer, M., Pernold, K. & Olson, L. Inhibiting Epidermal Growth Factor Receptor Improves Structural, Locomotor, Sensory, and Bladder Recovery from Experimental Spinal Cord Injury. *The Journal of Neuroscience* **27**, 6428-6435, (2007).

21 Hellal, F. *et al.* Microtubule Stabilization Reduces Scarring and Causes Axon Regeneration After Spinal Cord Injury. *Science* **331**, 928-931, (2011).

22 Bradbury, E. J. *et al.* Chondroitinase ABC promotes functional recovery after spinal cord injury. *Nature* **416**, 636-640, (2002).

23 Zhang, S.-x., Huang, F., Gates, M., White, J. & Holmberg, E. G. Extensive scarring induced by chronic intrathecal tubing augmented cord tissue damage and worsened functional recovery after rat spinal cord injury. *Journal of Neuroscience Methods* **191**, 201-207, (2010).

24 Jones, L. L. & Tuszynski, M. H. Chronic intrathecal infusions after spinal cord injury cause scarring and compression. *Microscopy Research and Technique* **54**, 317-324, (2001).

25 Erschbamer, M., Pernold, K. & Olson, L. Comments on the re-assessment study by Sharp et al. of Erschbamer et al. *Experimental Neurology* **233**, 660-661, (2012).

26 Sharp, K., Yee, K. M. & Steward, O. A re-assessment of the effects of treatment with an epidermal growth factor receptor (EGFR) inhibitor on recovery of bladder and locomotor function following thoracic spinal cord injury in rats. *Experimental Neurology* **233**, 649-659, (2012).

27 Norenberg, M. D., Smith, J. & Marcillo, A. The Pathology of Human Spinal Cord Injury: Defining the Problems. *Journal of Neurotrauma* **21**, 429-440, (2004).

28 Hulsebosch, C. E. Recent Advances in Pathophysiology and Treatment of Spinal Cord Injury. *Adances in Physiology Eduation* **26**, 238-255, (2002).

29 Donnelly, D. J. & Popovich, P. G. Inflammation and its role in neuroprotection, axonal regeneration and functional recovery after spinal cord injury. *Experimental Neurology* **209**, 378-388, (2008).

30 Rowland, J. W., Hawryluk, G. W. J., Kwon, B. & Fehlings, M. G. Current status of acute spinal cord injury pathophysiology and emerging therapies: promise on the horizon. *Neurosurgical FOCUS* **25**, E2, (2008).

31 Popovich, P. G. & Longbrake, E. E. Can the immune system be harnessed to repair the CNS? *Nat Rev Neurosci* **9**, 481-493, (2008).

32 Dennis, W. C. Excitotoxic cell death. *Journal of Neurobiology* **23**, 1261-1276 (1992).

33 Kielian, T., Kigerl, K. & Popovich, P. in *Toll-like Receptors: Roles in Infection and Neuropathology Current Topics in Microbiology and Immunology* 121-136 (Springer Berlin Heidelberg, 2009).

34 Luo, J., Uchida, K. & Shi, R. Accumulation of Acrolein-Protein Adducts after Traumatic Spinal Cord Injury. *Neurochemical Research* **30**, 291-295, (2005).

35 Carrico, K. M., Vaishnav, R. & Hall, E. D. Temporal and Spatial Dynamics of Peroxynitrite-Induced Oxidative Damage after Spinal Cord Contusion Injury. *Journal of Neurotrauma* **26**, 1369-1378, (2009).

36 Hall, E. Antioxidant Therapies for Acute Spinal Cord Injury. *Neurotherapeutics* **8**, 152-167, (2011).

37 Jia, Z. *et al.* Oxidative stress in spinal cord injury and antioxidant-based intervention. *Spinal Cord* **50**, 264-274, (2012).

38 Yiu, G. & He, Z. Glial inhibition of CNS axon regeneration. *Nat Rev Neurosci* **7**, 617-627, (2006).

39 Gaudet, A. D. & Popovich, P. G. Extracellular matrix regulation of inflammation in the healthy and injured spinal cord. *Experimental Neurology* **258**, 24-34, (2014).

40 Totoiu, M. O. & Keirstead, H. S. Spinal cord injury is accompanied by chronic progressive demyelination. *The Journal of Comparative Neurology* **486**, (2005).

41 Beck, K. D. *et al.* Quantitative analysis of cellular inflammation after traumatic spinal cord injury: evidence for a multiphasic inflammatory response in the acute to chronic environment. *Brain* **133** 433-447, (2010).

42 Sofroniew, M. V. Astrogliosis. *Cold Spring Harbor Perspectives in Biology*, (2014).

43 Faulkner, J. R. *et al.* Reactive Astrocytes Protect Tissue and Preserve Function after Spinal Cord Injury. *The Journal of Neuroscience* **24**, 2143-2155, (2004).

44 Silver, J. & Miller, J. H. Regeneration beyond the glial scar. *Nat Rev Neurosci* **5**, 146-156, (2004).

45 Bartus, K., James, N. D., Bosch, K. D. & Bradbury, E. J. Chondroitin sulphate proteoglycans: Key modulators of spinal cord and brain plasticity. *Experimental Neurology* **235**, 5-17, (2012).

46 Bracken, M. B. *et al.* A randomized, controlled trial of methylprednisolone or naloxone in the treatment of acute spinal-cord injury. Results of the Second National Acute Spinal Cord Injury Study. *N Engl J Med* **322**, 1405-1411, (1990).

47 Singh, P. L., Agarwal, N., Barrese, J. C. & Heary, R. F. Current therapeutic strategies for inflammation following traumatic spinal cord injury. *Neural Regeneration Research* **7**, 1812-1821, (2012).

48 Widenfalk, J. *et al.* Vascular endothelial growth factor improves functional outcome and decreases secondary degeneration in experimental spinal cord contusion injury. *Neuroscience* **120**, 951-960, (2003).

49 Sun, F. & He, Z. Neuronal intrinsic barriers for axon regeneration in the adult CNS. *Current Opinion in Neurobiology* **20**, 510-518, (2010).

50 Sahni, V. & Kessler, J. A. Stem cell therapies for spinal cord injury. *Nat Rev Neurol* **6**, 363-372, (2010).

51 Thuret, S., Moon, L. D. F. & Gage, F. H. Therapeutic interventions after spinal cord injury. *Nat Rev Neurosci* **7**, 628-643, (2006).

52 Steinmetz, M. P. *et al.* Chronic Enhancement of the Intrinsic Growth Capacity of Sensory Neurons Combined with the Degradation of Inhibitory Proteoglycans Allows Functional Regeneration of Sensory Axons through the Dorsal Root Entry Zone in the Mammalian Spinal Cord. *J. Neurosci.* **25**, 8066-8076, (2005).

53 Kadoya, K. *et al.* Combined Intrinsic and Extrinsic Neuronal Mechanisms Facilitate Bridging Axonal Regeneration One Year after Spinal Cord Injury. *Neuron* **64**, 165-172, (2009).

54 Lu, P. & Tuszynski, M. H. Growth factors and combinatorial therapies for CNS regeneration. *Experimental Neurology* **209**, 313-320, (2008).

55 Karimi-Abdolrezaee, S., Eftekharpour, E., Wang, J., Schut, D. & Fehlings, M. G. Synergistic Effects of Transplanted Adult Neural Stem/Progenitor Cells, Chondroitinase, and Growth Factors Promote Functional Repair and Plasticity of the Chronically Injured Spinal Cord. *J. Neurosci.* **30**, (2010).

56 Alilain, W. J., Horn, K. P., Hu, H., Dick, T. E. & Silver, J. Functional regeneration of respiratory pathways after spinal cord injury. *Nature* **475**, 196-200, (2011).

57 Tetzlaff, W. *et al.* A Systematic Review of Cellular Transplantation Therapies for Spinal Cord Injury. *Journal of Neurotrauma* **28**, 1611-1682, (2011).

58 Ronaghi, M., Erceg, S., Moreno-Manzano, V. & Stojkovic, M. Challenges of Stem Cell Therapy for Spinal Cord Injury: Human Embryonic Stem Cells, Endogenous Neural Stem Cells, or Induced Pluripotent Stem Cells? *Stem Cells* **28**, 93-99, (2009).

59 Sandner, B. *et al.* Neural stem cells for spinal cord repair. *Cell and Tissue Research* **349**, 349-362, (2012).

60 Guest, J., Benavides, F., Padgett, K., Mendez, E. & Tovar, D. Technical aspects of spinal cord injections for cell transplantation. Clinical and translational considerations. *Brain Research Bulletin* **84**, 267-279, (2011).

61 Bracken, M. B. *et al.* A Randomized, Controlled Trial of Methylprednisolone or Naloxone in the Treatment of Acute Spinal-Cord Injury. *New England Journal of Medicine* **322**, 1405-1411, (1990).

62 Gris, D. *et al.* Transient Blockade of the CD11d/CD18 Integrin Reduces Secondary Damage after Spinal Cord Injury, Improving Sensory, Autonomic, and Motor Function. *The Journal of Neuroscience* **24**, 4043-4051, (2004).

63 Ditor, D. S., Bao, F., Chen, Y., Gregory A. Dekaban & Weaver, L. C. A therapeutic time window for anti-CD11d monoclonal antibody treatment yielding reduced secondary tissue damage and enhanced behavioral recovery following severe spinal cord injury. *Journal of Neurosurgery: Spine* **5**, 343-352, (2006).

64 Geremia, N. M. *et al.* CD11d Antibody Treatment Improves Recovery in Spinal Cord-Injured Mice. *Journal of Neurotrauma* **29**, 539-550, (2012).

65 Hurtado, A. *et al.* Anti-CD11d monoclonal antibody treatment for rat spinal cord compression injury. *Experimental Neurology* **233**, 606-611, (2012).

66 Trivedi, A., Olivas, A. D. & Noble-Haeusslein, L. J. Inflammation and Spinal Cord Injury: Infiltrating Leukocytes as Determinants of Injury and Repair Processes. *Clinical neuroscience research* **6**, 283-292, doi:10.1016/j.cnr.2006.09.007 (2006).

67 Esposito, E. & Cuzzocrea, S. Anti-TNF therapy in the injured spinal cord. *Trends in Pharmacological Sciences* **32**, 107-115, (2011).

68 Genovese, T. *et al.* Immunomodulatory Effects of Etanercept in an Experimental Model of Spinal Cord Injury. *Journal of Pharmacology and Experimental Therapeutics* **316**, 1006-1016, (2006).

69 Kurt, G. k. *et al.* Neuroprotective effects of infliximab in experimental spinal cord injury. *Surgical Neurology* **71**, 332-336, (2009).

70 Guven, C. *et al.* Neuroprotective effects of infliximab in experimental spinal cord ischemic injury. *Journal of Clinical Neuroscience* **17**, 1563-1567, (2010).

71 Lobo, E. D., Hansen, R. J. & Balthasar, J. P. Antibody pharmacokinetics and pharmacodynamics. *Journal of Pharmaceutical Sciences* **93**, 2645-2668, (2004).

72 Schweizer, D., Serno, T. & Goepferich, A. Controlled release of therapeutic antibody formats. *European Journal of Pharmaceutics and Biopharmaceutics* **88**, 291-309, (2014).

73 Dennis, M. S. & Watts, R. J. Transferrin Antibodies Into the Brain. *Neuropsychopharmacology* **37**, 302-303, (2012).

74 Atwal, J. K. *et al.* A Therapeutic Antibody Targeting BACE1 Inhibits Amyloid-β Production in Vivo. *Science Translational Medicine* **3**, (2011).

75 Daugherty, A. L. & Mrsny, R. J. Formulation and delivery issues for monoclonal antibody therapeutics. *Advanced Drug Delivery Reviews* **58**, 686-706, (2006).

76 Stirling, D. P. *et al.* Minocycline Treatment Reduces Delayed Oligodendrocyte Death, Attenuates Axonal Dieback, and Improves Functional Outcome after Spinal Cord Injury. *The Journal of Neuroscience* **24**, 2182-2190, (2004).

77 Wells, J. E. A., Hurlbert, R. J., Fehlings, M. G. & Yong, V. W. Neuroprotection by minocycline facilitates significant recovery from spinal cord injury in mice. *Brain* **126**, 1628-1637, (2003).

78 Teng, Y. D. *et al.* Minocyclinė inhibits contusion-triggered mitochondrial cytochrome c release and mitigates functional deficits after spinal cord injury. *Proceedings of the National Academy of Sciences of the United States of America* **101**, 3071-3076, (2004).

79 Lee, S. M. *et al.* Minocycline Reduces Cell Death and Improves Functional Recovery after Traumatic Spinal Cord Injury in the Rat. *Journal of Neurotrauma* **20**, 1017-1027, (2003).

80 Gorio, A. *et al.* Recombinant human erythropoietin counteracts secondary injury and markedly enhances neurological recovery from experimental spinal cord trauma. *Proceedings of the National Academy of Sciences* **99**, 9450-9455, (2002).

81 Bradbury, E. J., King, V. R., Simmons, L. J., Priestley, J. V. & McMahon, S. B. NT-3, but not BDNF, prevents atrophy and death of axotomized spinal cord projection neurons. *European Journal of Neuroscience* **10**, 3058-3068, (1998).

82 Sharma, H. S. A Select Combination of Neurotrophins Enhances Neuroprotection and Functional Recovery following Spinal Cord Injury. *Annals of the New York Academy of Sciences* **1122**, 95-111, (2007).

83 Fagan, S. C. *et al.* Optimal delivery of minocycline to the brain: implication for human studies of acute neuroprotection. *Experimental Neurology* **186**, 248-251, (2004).

84 Pinzon, A. *et al.* A re-assessment of minocycline as a neuroprotective agent in a rat spinal cord contusion model. *Brain Research* **1243**, 146-151, (2008).

85 Lee, J. H. T. *et al.* Lack of neuroprotective effects of simvastatin and minocycline in a model of cervical spinal cord injury. *Experimental Neurology* **225**, 219-230, (2010).

86 Soliman, G. M., Choi, A. O., Maysinger, D. & Winnik, F. M. Minocycline Block Copolymer Micelles and their Anti-Inflammatory Effects on Microglia. *Macromolecular Bioscience* **10**, 278-288, (2010).

87 Jain, N., Jain, G. K., Ahmad, F. J. & Khar, R. K. Validated stability-indicating densitometric thin-layer chromatography: Application to stress degradation studies of minocycline. *Analytica Chimica Acta* **599**, 302-309, (2007).

88 Marchand, F. *et al.* Effects of Etanercept and Minocycline in a rat model of spinal cord injury. *European Journal of Pain* **13**, 673-681, (2009).

89 Casha, S. *et al.* Results of a phase II placebo-controlled randomized trial of minocycline in acute spinal cord injury. *Brain* **135**, 1224-36, (2012).

90 Kwon, B. K. *et al.* A Grading System To Evaluate Objectively the Strength of Pre-Clinical Data of Acute Neuroprotective Therapies for Clinical Translation in Spinal Cord Injury. *Journal of Neurotrauma* **28**, 1525-1543, (2010).

91 Kontogeorgakos, V. *et al.* The efficacy of erythropoietin on acute spinal cord injury. An experimental study on a rat model. *Archives of Orthopaedic and Trauma Surgery* **129**, 189-194, (2009).

92 Tsai, P. T. *et al.* A Critical Role of Erythropoietin Receptor in Neurogenesis and Post-Stroke Recovery. *The Journal of Neuroscience* **26**, 1269-1274, (2006).

93 Sargin, D., Friedrichs, H., El-Kordi, A. & Ehrenreich, H. Erythropoietin as neuroprotective and neuroregenerative treatment strategy: Comprehensive overview of 12 years of preclinical and clinical research. *Best Practice & Research Clinical Anaesthesiology* **24**, 573-594, (2010).

94 Gorio, A. *et al.* Methylprednisolone neutralizes the beneficial effects of erythropoietin in experimental spinal cord injury. *Proceedings of the National Academy of Sciences of the United States of America* **102**, 16379-16384, (2005).

95 Pinzon, A. *et al.* A re-assessment of erythropoietin as a neuroprotective agent following rat spinal cord compression or contusion injury. *Experimental Neurology* **213**, 129-136, (2008).

96 Mann, C. *et al.* Delayed treatment of spinal cord injury with erythropoietin or darbepoetin,ÄîA lack of neuroprotective efficacy in a contusion model of cord injury. *Experimental Neurology* **211**, 34-40, (2008).

97 Wang, Y., Cooke, M. J., Morshead, C. M. & Shoichet, M. S. Hydrogel delivery of erythropoietin to the brain for endogenous stem cell stimulation after stroke injury. *Biomaterials* **33**, 2681-2692, (2012).

98 Uchida, E. *et al.* Effect of active oxygen radicals on protein and carbohydrate moieties of recombinant human erythropoietin. *Free radical research* **27**, 311-323, (1997).

99 Zhang, F. *et al.* Enhanced Delivery of Erythropoietin Across the Blood-Brain Barrier for Neuroprotection against Ischemic Neuronal Injury. *Translational stroke research* **1**, 113-121, (2010).

100 Murua, A., Orive, G., Hernández, R. M. & Pedraz, J. L. Emerging technologies in the delivery of erythropoietin for therapeutics. *Medicinal Research Reviews* **31**, 284-309, (2011).

101 Zhilai, Z. *et al.* A combination of taxol infusion and human umbilical cord mesenchymal stem cells transplantation for the treatment of rat spinal cord injury. *Brain Research* **1481**, 79-89, (2012).

102 Erturk, A., Hellal, F., Enes, J. & Bradke, F. Disorganized Microtubules Underlie the Formation of Retraction Bulbs and the Failure of Axonal Regeneration. *J. Neurosci.* **27**, 9169-9180, (2007).

103 Sengottuvel, V., Leibinger, M., Pfreimer, M., Andreadaki, A. & Fischer, D. Taxol Facilitates Axon Regeneration in the Mature CNS. *The Journal of Neuroscience* **31**, 2688-2699, (2011).

104 Popovich, P. G., Tovar, C. A., Lemeshow, S., Yin, Q. & Jakeman, L. B. Independent evaluation of the anatomical and behavioral effects of Taxol in rat models of spinal cord injury. *Experimental Neurology* **261**, 97-108, (2014).

105 Schnell, L., Schneider, R., Kolbeck, R., Barde, Y. A. & Schwab, M. E. Neurotrophin-3 enhances sprouting of corticospinal tract during development and after adult spinal cord lesion. *Nature (London)* **367**, 170-173, (1994).

106 Brock, J. H. *et al.* Local and Remote Growth Factor Effects after Primate Spinal Cord Injury. *J. Neurosci.* **30**, 9728-9737, (2010).

107 Grill, R., Murai, K., Blesch, A., Gage, F. H. & Tuszynski, M. H. Cellular Delivery of Neurotrophin-3 Promotes Corticospinal Axonal Growth and Partial Functional Recovery after Spinal Cord Injury. *The Journal of Neuroscience* **17**, 5560-5572, (1997).

108 Bregman, B. S., McAtee, M., Dai, H. N. & Kuhn, P. L. Neurotrophic Factors Increase Axonal Growth after Spinal Cord Injury and Transplantation in the Adult Rat. *Experimental Neurology* **148**, 475-494, (1997).

109 Lee, T. T., Green, B. A., Dietrich, W. D. & Yezierski, R. P. Neuroprotective Effects of Basic Fibroblast Growth Factor Following Spinal Cord Contusion Injury in the Rat. *Journal of Neurotrauma* **16**, 347-356, (1999).

110 Jakeman, L. B., Wei, P., Guan, Z. & Stokes, B. T. Brain-Derived Neurotrophic Factor Stimulates Hindlimb Stepping and Sprouting of Cholinergic Fibers after Spinal Cord Injury. *Experimental Neurology* **154**, 170-184, (1998).

111 Lutton, C. *et al.* Combined VEGF and PDGF Treatment Reduces Secondary Degeneration after Spinal Cord Injury. *Journal of Neurotrauma* **20**, 957-970, (2012).

112 Chehrehasa, F., Cobcroft, M., Young, Y. W., Mackay-Sim, A. & Goss, B. An Acute Growth Factor Treatment that Preserves Function after Spinal Cord Contusion Injury. *Journal of Neurotrauma* **31**, 1807-1813, (2014).

113 Rabchevsky, A. G. *et al.* Basic Fibroblast Growth Factor (bFGF) Enhances Tissue Sparing and Functional Recovery Following Moderate Spinal Cord Injury. *Journal of Neurotrauma* **16**, 817-830, (1999).

114 Rabchevsky, A. G. *et al.* Basic Fibroblast Growth Factor (bFGF) Enhances Functional Recovery Following Severe Spinal Cord Injury to the Rat. *Experimental Neurology* **164**, 280-291, (2000).

115 Huebner, E. & Strittmatter, S. in *Cell Biology of the Axon*, 339-351 (2009).

116 Shen, Y. *et al.* PTP{sigma} Is a Receptor for Chondroitin Sulfate Proteoglycan, an Inhibitor of Neural Regeneration. *Science* **326**, 592-596, (2009).

117 Schnell, L. & Schwab, M. E. Axonal regeneration in the rat spinal cord produced by an antibody against myelin-associated neurite growth inhibitors. *Nature* **343**, 269-272, (1990).

118 Liebscher, T. *et al.* Nogo-A antibody improves regeneration and locomotion of spinal cord–injured rats. *Annals of Neurology* **58**, 706-719, (2005).

119 Li, S. & Strittmatter, S. M. Delayed Systemic Nogo-66 Receptor Antagonist Promotes Recovery from Spinal Cord Injury. *The Journal of Neuroscience* **23**, 4219-4227, (2003).

120 Dergham, P. *et al.* Rho Signaling Pathway Targeted to Promote Spinal Cord Repair. *Journal of Neuroscience* **22**, 6570-6577, (2002).

121 Lord-Fontaine, S. *et al.* Local Inhibition of Rho Signaling by Cell-Permeable Recombinant Protein BA-210 Prevents Secondary Damage and Promotes Functional Recovery following Acute Spinal Cord Injury. *Journal of Neurotrauma* **25**, 1309-1322, (2008).

122 McKerracher, L. & Higuchi, H. Targeting Rho To Stimulate Repair after Spinal Cord Injury. *Journal of Neurotrauma* **23**, 309-317, (2006).

123 Caroni, P. & Schwab, M. E. Antibody against myelin associated inhibitor of neurite growth neutralizes nonpermissive substrate properties of CNS white matter. *Neuron* **1**, 85-96, (1988).

124 Schwab, M. E. Nogo and axon regeneration. *Current Opinion in Neurobiology* **14**, 118-124, (2004).

125 Brosamle, C., Huber, A. B., Fiedler, M., Skerra, A. & Schwab, M. E. Regeneration of Lesioned Corticospinal Tract Fibers in the Adult Rat Induced by a Recombinant, Humanized IN-1 Antibody Fragment. *The Journal of Neuroscience* **20**, 8061-8068, (2000).

126 Freund, P. *et al.* Nogo-A-specific antibody treatment enhances sprouting and functional recovery after cervical lesion in adult primates. *Nat Med* **12**, 790-792, (2006).

127 Freund, P. *et al.* Anti-Nogo-A antibody treatment promotes recovery of manual dexterity after unilateral cervical lesion in adult primates – re-examination and extension of behavioral data. *European Journal of Neuroscience* **29**, 983-996, (2009).

128 Freund, P. *et al.* Anti-Nogo-A antibody treatment enhances sprouting of corticospinal axons rostral to a unilateral cervical spinal cord lesion in adult macaque monkey. *The Journal of Comparative Neurology* **502**, 644-659, (2007).

129 Kwon, B. K., Sekhon, L. H. & Fehlings, M. G. Emerging Repair, Regeneration, and Translational Research Advances for Spinal Cord Injury. *Spine* **35**, S263-S270, (2010).

130 Cully, M. Drug development: Chemical brace. *Nature* **503**, S10-S12, (2013).

131 Ramer, L. M., Ramer, M. S. & Bradbury, E. J. Restoring function after spinal cord injury: towards clinical translation of experimental strategies. *The Lancet Neurology* **13**, 1241-1256, (2014).

132 GrandPre, T., Li, S. & Strittmatter, S. M. Nogo-66 receptor antagonist peptide promotes axonal regeneration. *Nature* **417**, 547-551, (2002).

133 Cao, Y. *et al.* Nogo-66 Receptor Antagonist Peptide (NEP1-40) Administration Promotes Functional Recovery and Axonal Growth After Lateral Funiculus Injury in the Adult Rat. *Neurorehabilitation and Neural Repair* **22**, 262-278, (2008).

134 Fang, P.-c. *et al.* Combination of NEP 1-40 Treatment and Motor Training Enhances Behavioral Recovery After a Focal Cortical Infarct in Rats. *Stroke* **41**, 544-549, (2010).

135 Steward, O., Sharp, K., Yee, K. M. & Hofstadter, M. A re-assessment of the effects of a Nogo-66 receptor antagonist on regenerative growth of axons and locomotor recovery after spinal cord injury in mice. *Experimental Neurology* **209**, 446-468, (2008).

136 Santos, N. C., Figueira-Coelho, J., Martins-Silva, J. & Saldanha, C. Multidisciplinary utilization of dimethyl sulfoxide: pharmacological, cellular, and molecular aspects. *Biochemical Pharmacology* **65**, 1035-1041, (2003).

137 Li, S. *et al.* Blockade of Nogo-66, Myelin-Associated Glycoprotein, and Oligodendrocyte Myelin Glycoprotein by Soluble Nogo-66 Receptor Promotes Axonal Sprouting and Recovery after Spinal Injury. *The Journal of Neuroscience* **24**, 10511-10520, (2004).

138 Wang, X., Baughman, K. W., Basso, D. M. & Strittmatter, S. M. Delayed Nogo receptor therapy improves recovery from spinal cord contusion. *Annals of Neurology* **60**, 540-549, (2006).

139 Wang, X. *et al.* Human NgR-Fc Decoy Protein via Lumbar Intrathecal Bolus Administration Enhances Recovery from Rat Spinal Cord Contusion. *Journal of Neurotrauma* **31**, 1955-1966, (2014).

140 Dubreuil, C. I., Winton, M. J. & McKerracher, L. Rho activation patterns after spinal cord injury and the role of activated Rho in apoptosis in the central nervous system. *The Journal of Cell Biology* **162**, 233-243, (2003).

141 Fehlings, M. G. *et al.* A Phase I/IIa Clinical Trial of a Recombinant Rho Protein Antagonist in Acute Spinal Cord Injury. *Journal of Neurotrauma* **28**, 787-796, (2011).

142 McKerracher, L. & Anderson, K. D. Analysis of Recruitment and Outcomes in the Phase I/IIa Cethrin Clinical Trial for Acute Spinal Cord Injury. *Journal of Neurotrauma* **30**, 1795-1804, (2013).

143 Wong, C., Inman, E., Spaethe, R. & Helgerson, S. Fibrin-based biomaterials to deliver human growth factors. *Thrombosis and Haemostasis* **89**, 573-582, (2003).

144 Prabhakar, V. *et al.* Biochemical characterization of the chondroitinase ABC I active site. *Biochemical Journal* **390**, 395-405, (2005).

145 Garcia-Alias, G., Barkhuysen, S., Buckle, M. & Fawcett, J. W. Chondroitinase ABC treatment opens a window of opportunity for task-specific rehabilitation. *Nat Neurosci* **12**, 1145-1151, (2009).

146 Tom, V. J., Kadakia, R., Santi, L. & Houle, J. D. Administration of Chondroitinase ABC Rostral or Caudal to a Spinal Cord Injury Site Promotes Anatomical but Not Functional Plasticity. *Journal of Neurotrauma* **26**, 2323-2333, (2009).

147 Zhao, R.-R. *et al.* Combination treatment with anti-Nogo-A and chondroitinase ABC is more effective than single treatments at enhancing functional recovery after spinal cord injury. *European Journal of Neuroscience* **38**, 2946-2961, (2013).

148 Alilain, W. J., Horn, K. P., Hu, H., Dick, T. E. & Silver, J. Functional regeneration of respiratory pathways after spinal cord injury. *Nature* **475**, 196-200, (2011).

149 Wang, D., Ichiyama, R. M., Zhao, R., Andrews, M. R. & Fawcett, J. W. Chondroitinase Combined with Rehabilitation Promotes Recovery of Forelimb Function in Rats with Chronic Spinal Cord Injury. *The Journal of Neuroscience* **31**, 9332-9344, (2011).

150 Garcia-Alias, G., Barkhuysen, S., Buckle, M. & Fawcett, J. W. Chondroitinase ABC treatment opens a window of opportunity for task-specific rehabilitation. *Nat Neurosci* **12**, 1145-1151, (2009).

151 Iseda, T. *et al.* Single, High-Dose Intraspinal Injection of Chondroitinase Reduces Glycosaminoglycans in Injured Spinal Cord and Promotes Corticospinal Axonal Regrowth after Hemisection but Not Contusion. *Journal of Neurotrauma* **25**, 334-349, (2008).

152 Lin, R., Kwok, J. C. F., Crespo, D. & Fawcett, J. W. Chondroitinase ABC has a long-lasting effect on chondroitin sulphate glycosaminoglycan content in the injured rat brain. *Journal of Neurochemistry* **104**, 400-408, (2008).

153 Tester, N. J., Plaas, A. H. & Howland, D. R. Effect of body temperature on chondroitinase ABC's ability to cleave chondroitin sulfate glycosaminoglycans. *Journal of Neuroscience Research* **85**, 1110-1118, (2007).

154 Nazari-Robati, M., Khajeh, K., Aminian, M., Mollania, N. & Golestani, A. Enhancement of thermal stability of chondroitinase ABC I by site-directed mutagenesis: An insight from Ramachandran plot. *Biochimica et Biophysica Acta (BBA) - Proteins and Proteomics* **1834**, 479-486, (2013).

155 Nazari-Robati, M., Khajeh, K., Aminian, M., Fathi-Roudsari, M. & Golestani, A. Co-solvent mediated thermal stabilization of chondroitinase ABC I form Proteus vulgaris. *International Journal of Biological Macromolecules* **50**, 487-492, (2012).

156 Bartus, K. *et al.* Large-Scale Chondroitin Sulfate Proteoglycan Digestion with Chondroitinase Gene Therapy Leads to Reduced Pathology and Modulates Macrophage Phenotype following Spinal Cord Contusion Injury. *The Journal of Neuroscience* **34**, 4822-4836, (2014).

157 Coulson-Thomas, Y. M. *et al.* Adult bone marrow-derived mononuclear cells expressing chondroitinase AC transplanted into CNS injury sites promote local brain chondroitin sulphate degradation. *Journal of Neuroscience Methods* **171**, 19-29, (2008).

158 Jakobsson, J. & Lundberg, C. Lentiviral Vectors for Use in the Central Nervous System. *Mol Ther* **13**, 484-493, (2006).

159 Fry, D. W. *et al.* Specific, irreversible inactivation of the epidermal growth factor receptor and erbB2, by a new class of tyrosine kinase inhibitor. *Proceedings of the National Academy of Sciences* **95**, (1998).

160 Koprivica, V. *et al.* EGFR Activation Mediates Inhibition of Axon Regeneration by Myelin and Chondroitin Sulfate Proteoglycans. *Science* **310**, 106-110, (2005).

161 Leinster, V. H. L., Joy, M. T., Vuononvirta, R. E., Bolsover, S. R. & Anderson, P. N. ErbB1 epidermal growth factor receptor is a valid target for reducing the effects of multiple inhibitors of axonal regeneration. *Experimental Neurology* **239**, 82-90, (2013).

162 Chvatal, S. A., Kim, Y.-T., Bratt-Leal, A. M., Lee, H. & Bellamkonda, R. V. Spatial distribution and acute anti-inflammatory effects of Methylprednisolone after sustained local delivery to the contused spinal cord. *Biomaterials* **29**, 1967-1975, (2008).

163 Kim, Y.-t., Caldwell, J.-M. & Bellamkonda, R. V. Nanoparticle-mediated local delivery of methylprednisolone after spinal cord injury. *Biomaterials* **30**, 2582-2590 (2009).

164 Cerqueira, S. R. *et al.* Microglia Response and In Vivo Therapeutic Potential of Methylprednisolone-Loaded Dendrimer Nanoparticles in Spinal Cord Injury. *Small* **9**, 738-749, (2012).

165 Schmidt, J. *et al.* Drug targeting by long-circulating liposomal glucocorticosteroids increases therapeutic efficacy in a model of multiple sclerosis. *Brain* **126**, 1895-1904, (2003).

166 Gaillard, P. J. *et al.* Enhanced brain delivery of liposomal methylprednisolone improved therapeutic efficacy in a model of neuroinflammation. *Journal of Controlled Release* **164**, 364-369, (2012).

167 Lee, D.-H. *et al.* Glutathione PEGylated liposomal methylprednisolone (2B3-201) attenuates CNS inflammation and degeneration in murine myelin oligodendrocyte glycoprotein induced experimental autoimmune encephalomyelitis. *Journal of Neuroimmunology* **274**, 96-101, (2014).

168 Evans, M. *et al.* CNS-targeted glucocorticoid reduces pathology in mouse model of amyotrophic lateral sclerosis. *Acta Neuropathologica Communications* **2**, 66, (2014).

169 Kang, Y., Hwang, D., Kim, B., Go, D. & Park, K. Thermosensitive polymer-based hydrogel mixed with the anti-inflammatory agent minocycline induces axonal regeneration in hemisected spinal cord. *Macromolecular Research* **18**, 399-403, (2010).

170 Hu, W. *et al.* PEG Minocycline-Liposomes Ameliorate CNS Autoimmune Disease. *PLoS ONE* **4**, e4151, (2009).

171 Kang, C. E., Poon, P. C., Tator, C. H. & Shoichet, M. S. A New Paradigm for Local and Sustained Release of Therapeutic Molecules to the Injured Spinal Cord for Neuroprotection and Tissue Repair. *Tissue Engineering Part A* **15**, 595, (2009).

172 Gupta, D., Tator, C. H. & Shoichet, M. S. Fast-gelling injectable blend of hyaluronan and methylcellulose for intrathecal, localized delivery to the injured spinal cord. *Biomaterials* **27**, 2370-2379, (2006).

173 Chen, H. *et al.* Nanoerythropoietin Is 10-Times More Effective Than Regular Erythropoietin in Neuroprotection in a Neonatal Rat Model of Hypoxia and Ischemia. *Stroke* **43**, 884-887, (2012).

174 Zhang, Z., Mei, L. & Feng, S.-S. Paclitaxel drug delivery systems. *Expert Opinion on Drug Delivery* **10**, 325-340, (2013).

175 Li, K. W. *et al.* Polilactofate Microspheres for Paclitaxel Delivery to Central Nervous System Malignancies. *Clinical Cancer Research* **9**, 3441-3447, (2003).

176 Tyler, B. *et al.* A thermal gel depot for local delivery of paclitaxel to treat experimental brain tumors in rats. *Journal of Neurosurgery* **113**, 210-217, (2010).

177 Elstad, N. L. & Fowers, K. D. OncoGel (ReGel/paclitaxel) - Clinical applications for a novel paclitaxel delivery system. *Advanced Drug Delivery Reviews* **61**, 785-794, (2009).

178 Geldenhuys, W., Mbimba, T., Bui, T., Harrison, K. & Sutariya, V. Brain-targeted delivery of paclitaxel using glutathione-coated nanoparticles for brain cancers. *Journal of Drug Targeting* **19**, 837-845, (2011).

179 Gradishar, W. J. Albumin-bound paclitaxel: a next-generation taxane. *Expert Opinion on Pharmacotherapy* **7**, 1041-1053, (2006).

180 Khaing, Z. Z., Thomas, R. C., Geissler, S. A. & Schmidt, C. E. Advanced biomaterials for repairing the nervous system: what can hydrogels do for the brain? *Materials Today* **17**, 332-340, (2014).

181 Elliott Donaghue, I., Tam, R., Sefton, M. V. & Shoichet, M. S. Cell and biomolecule delivery for tissue repair and regeneration in the central nervous system. *Journal of Controlled Release* **190**, 219-227, (2014).

182 Kang, C. E., Baumann, M. D., Tator, C. H. & Shoichet, M. S. Localized and Sustained Delivery of Fibroblast Growth Factor-2 from a Nanoparticle-Hydrogel Composite for Treatment of Spinal Cord Injury. *Cells Tissues Organs* **197**, 55-63, (2013).

183 Kang, C. E., Tator, C. H. & Shoichet, M. S. Poly(ethylene glycol) modification enhances penetration of fibroblast growth factor 2 to injured spinal cord tissue from an intrathecal delivery system. *Journal of Controlled Release* **144**, 25-31, (2010).

184 des Rieux, A. *et al.* Vascular endothelial growth factor-loaded injectable hydrogel enhances plasticity in the injured spinal cord. *Journal of Biomedical Materials Research Part A* **102**, 2345-2355, (2014).

185 Jimenez Hamann, M. C., Tator, C. H. & Shoichet, M. S. Injectable intrathecal delivery system for localized administration of EGF and FGF-2 to the injured rat spinal cord. *Experimental Neurology* **194**, 106-119, (2005).

186 Jain, A., Kim, Y.-T., McKeon, R. J. & Bellamkonda, R. V. In situ gelling hydrogels for conformal repair of spinal cord defects, and local delivery of BDNF after spinal cord injury. *Biomaterials* **27**, 497-504, (2006).

187 Jain, A., McKeon, R. J., Brady-Kalnay, S. M. & Bellamkonda, R. V. Sustained Delivery of Activated Rho GTPases and BDNF Promotes Axon Growth in CSPG-Rich Regions Following Spinal Cord Injury. *PLoS ONE* **6**, e16135, (2011).

188 Grous, L. C. *et al.* Implications of poly(N-isopropylacrylamide)-g-poly(ethylene glycol) with codissolved brain-derived neurotrophic factor injectable scaffold on motor function recovery

rate following cervical dorsolateral funiculotomy in the rat. *Journal of Neurosurgery: Spine* **18**, 641-652, (2013).

189 Piantino, J., Burdick, J. A., Goldberg, D., Langer, R. & Benowitz, L. I. An injectable, biodegradable hydrogel for trophic factor delivery enhances axonal rewiring and improves performance after spinal cord injury. *Experimental Neurology* **201**, 359-367, (2006).

190 Taylor, S. J. & Sakiyama-Elbert, S. E. Effect of controlled delivery of neurotrophin-3 from fibrin on spinal cord injury in a long term model. *Journal of Controlled Release* **116**, 204-210, (2006).

191 Johnson, P. J., Parker, S. R. & Sakiyama-Elbert, S. E. Controlled release of neurotrophin-3 from fibrin-based tissue engineering scaffolds enhances neural fiber sprouting following subacute spinal cord injury. *Biotechnology and Bioengineering* **104**, 1207-1214, (2009).

192 Stokols, S. & Tuszynski, M. H. Freeze-dried agarose scaffolds with uniaxial channels stimulate and guide linear axonal growth following spinal cord injury. *Biomaterials* **27**, 443-451, (2006).

193 Bakshi, A. *et al.* Mechanically engineered hydrogel scaffolds for axonal growth and angiogenesis after transplantation in spinal cord injury. *Journal of Neurosurgery: Spine* **1**, 322-329, (2004).

194 Wang, Y.-C. *et al.* Sustained intraspinal delivery of neurotrophic factor encapsulated in biodegradable nanoparticles following contusive spinal cord injury. *Biomaterials* **29**, 4546-4553, (2008).

195 Elliott Donaghue, I., Tator, C. H. & Shoichet, M. S. Sustained delivery of bioactive neurotrophin-3 to the injured spinal cord. *Biomaterials Science* **3**, 65-72, (2015).

196 Stanwick, J. C., Baumann, M. D. & Shoichet, M. S. Enhanced neurotrophin-3 bioactivity and release from a nanoparticle-loaded composite hydrogel. *Journal of Controlled Release* **160**, 666-675, (2012).

197 Stanwick, J. C., Baumann, M. D. & Shoichet, M. S. In vitro sustained release of bioactive anti-NogoA, a molecule in clinical development for treatment of spinal cord injury. *International Journal of Pharmaceutics* **426**, 284-290, (2012).

198 Wei, Y.-T. *et al.* Hyaluronic acid hydrogel modified with nogo-66 receptor antibody and poly-L-lysine to promote axon regrowth after spinal cord injury. *Journal of Biomedical Materials Research Part B: Applied Biomaterials* **95B**, 110-117, (2010).

199 Lee, H., McKeon, R. J. & Bellamkonda, R. V. Sustained delivery of thermostabilized chABC enhances axonal sprouting and functional recovery after spinal cord injury. *Proceedings of the National Academy of Sciences*, doi:10.1073/pnas.0905437106, (2009).

200 Hyatt, A. J. T., Wang, D., Kwok, J. C., Fawcett, J. W. & Martin, K. R. Controlled release of chondroitinase ABC from fibrin gel reduces the level of inhibitory glycosaminoglycan chains in lesioned spinal cord. *Journal of Controlled Release* **147**, 24-29, (2010).

201 Colello, R. J. *et al.* The incorporation of growth factor and chondroitinase ABC into an electrospun scaffold to promote axon regrowth following spinal cord injury. *Journal of Tissue Engineering and Regenerative Medicine*, (2013).

202 Straley, K. S., Wong Po Foo, C. & Heilshorn, S. Biomaterial Design Strategies for the Treatment of Spinal Cord Injuries. *Journal of Neurotrauma* **27**, 1-19, (2010).

203 Perale, G. *et al.* Hydrogels in Spinal Cord Injury Repair Strategies. *ACS Chemical Neuroscience* **2**, 336-345, (2011).

204 Macaya, D. & Spector, M. Injectable hydrogel materials for spinal cord regeneration: a review. *Biomedical Materials* **7**, 012001 (2012).

205 Cigognini, D. *et al.* Evaluation of Early and Late Effects into the Acute Spinal Cord Injury of an Injectable Functionalized Self-Assembling Scaffold. *PLoS ONE* **6**, e19782, (2011).

206 Jimenez Hamann, M. C., Tsai, E. C., Tator, C. H. & Shoichet, M. S. Novel intrathecal delivery system for treatment of spinal cord injury. *Experimental Neurology* **182**, 300-309, (2003).

207 Tysseling-Mattiace, V. M. *et al.* Self-Assembling Nanofibers Inhibit Glial Scar Formation and Promote Axon Elongation after Spinal Cord Injury. *J. Neurosci.* **28**, 3814-3823, (2008).

208 Sharp, K. G. *et al.* Salmon fibrin treatment of spinal cord injury promotes functional recovery and density of serotonergic innervation. *Experimental Neurology* **235**, 345-356, (2012).

209 Wohlfart, S., Gelperina, S. & Kreuter, J. Transport of drugs across the blood-brain barrier by nanoparticles. *Journal of Controlled Release* **161**, 264-273, (2012).

210 Saxena, T. *et al.* Nanocarrier-Mediated Inhibition of Macrophage Migration Inhibitory Factor Attenuates Secondary Injury after Spinal Cord Injury. *ACS Nano* **9**, 1492-1505, (2015).

211 Kwo, S., Young, W. & Decrescito, V. Spinal Cord Sodium, Potassium, Calcium, and Water Concentration Changes in Rats After Graded Contusion Injury. *Journal of Neurotrauma* **6**, 13-24, doi:10.1089/neu.1989.6.13 (1989).

212 Wrathall, J. R., Pettegrew, R. K. & Harvey, F. Spinal cord contusion in the rat: Production of graded, reproducible, injury groups. *Experimental Neurology* **88**, 108-122, (1985).

213 Rivlin, A. S. & Tator, C. H. Effect of vasodilators and myelotomy on recovery after acute spinal cord injury in rats. *Journal of Neurosurgery* **50**, 349-352, (1979).

214 Zhu, H. *et al.* Early neurosurgical intervention of spinal cord contusion: an analysis of 30 cases. *Chin Med J (Engl)* **121**, 2473-2478, (2008).

215 Yang, D. G. *et al.* Optimal time window of myelotomy in rats with acute traumatic spinal cord injury: a preliminary study. *Spinal Cord* **51**, 673-678, (2013).

216 Hu, A. M. *et al.* Myelotomy reduces spinal cord edema and inhibits aquaporin-4 and aquaporin-9 expression in rats with spinal cord injury. *Spinal Cord* **53**, 98-102, (2015).

217 Hou, S., Nicholson, L., van Niekerk, E., Motsch, M. & Blesch, A. Dependence of Regenerated Sensory Axons on Continuous Neurotrophin-3 Delivery. *The Journal of Neuroscience* **32**, 13206-13220, (2012).

218 Slaughter, B. V., Khurshid, S. S., Omar, Z. F., Khademhosseini, A. & Peppas, N. A. Hydrogels in Regenerative Medicine. *Advanced Materials* **21**, 3307-3329, (2009).

219 Love, K. T. *et al.* Lipid-like materials for low-dose, in vivo gene silencing. *Proceedings of the National Academy of Sciences* **107**, 1864-1869, (2010).

220 Gu, F. *et al.* Precise engineering of targeted nanoparticles by using self-assembled biointegrated block copolymers. *Proceedings of the National Academy of Sciences* **105**, 2586-2591, (2008).

221 Cohen, S., Yoshioka, T., Lucarelli, M., Hwang, L. H. & Langer, R. Controlled Delivery Systems for Proteins Based on Poly(Lactic/Glycolic Acid) Microspheres. *Pharmaceutical Research* **8**, 713-720, (1991).

222 Lee, K., Silva, E. A. & Mooney, D. J. Growth factor delivery-based tissue engineering: general approaches and a review of recent developments. *Journal of the Royal Society Interface* **8**, 153-170, (2011).

223 Taylor, S. J., McDonald Iii, J. W. & Sakiyama-Elbert, S. E. Controlled release of neurotrophin-3 from fibrin gels for spinal cord injury. *Journal of Controlled Release* **98**, 281-294, (2004).

224 Pakulska, M. M., Vulic, K. & Shoichet, M. S. Affinity-based release of chondroitinase ABC from a modified methylcellulose hydrogel. *Journal of Controlled Release* **171**, 11-16, (2013).

225 Vulic, K. & Shoichet, M. S. Tunable Growth Factor Delivery from Injectable Hydrogels for Tissue Engineering. *Journal of the American Chemical Society* **134**, 882-885, (2012).

226 O'Shea, T. M., Aimetti, A. A., Kim, E., Yesilyurt, V. & Langer, R. Synthesis and Characterization of a Library of In-Situ Curing, Nonswelling Ethoxylated Polyol Thiol-ene Hydrogels for Tailorable Macromolecule Delivery. *Advanced Materials* **27**, 65-72, (2015).

227 Nazari-Robati, M., Khajeh, K., Aminian, M., Fathi-Roudsari, M. & Golestani, A. Co-solvent mediated thermal stabilization of chondroitinase ABC I form Proteus vulgaris. *International Journal of Biological Macromolecules* **50**, 487-492, (2012).

228 Cima, M. J. *et al.* Single compartment drug delivery. *Journal of Controlled Release*, **190**, 157-171, (2014).

229 Wolinsky, J. B., Colson, Y. L. & Grinstaff, M. W. Local drug delivery strategies for cancer treatment: Gels, nanoparticles, polymeric films, rods, and wafers. *Journal of Controlled Release* **159**, 14-26, (2012).

230 Wang, P. P., Frazier, J. & Brem, H. Local drug delivery to the brain. *Advanced Drug Delivery Reviews* **54**, 987-1013, (2002).

231 LaVan, D. A., McGuire, T. & Langer, R. Small-scale systems for in vivo drug delivery. *Nat Biotech* **21**, 1184-1191, (2003).

232 Weiser, J. R. & Saltzman, W. M. Controlled release for local delivery of drugs: barriers and models. *Journal of Controlled Release* **190**, 664-673, (2014).

233 Abdi, S. *et al.* Epidural Steroids in the Management of Chronic Spinal Pain: A Systematic Review. *Pain Physician* **10**, 185-212, (2007).

234 Kearney, C. J. & Mooney, D. J. Macroscale delivery systems for molecular and cellular payloads. *Nature Materials* **12**, 1004-1017, (2013).

235 Wu, P. & Grainger, D. W. Drug/device combinations for local drug therapies and infection prophylaxis. *Biomaterials* **27**, 2450-2467, (2006).

236 Hoare, T. R. & Kohane, D. S. Hydrogels in drug delivery: Progress and challenges. *Polymer* **49**, 1993-2007, (2008).

237 Ko, D. Y., Shinde, U. P., Yeon, B. & Jeong, B. Recent progress of in situ formed gels for biomedical applications. *Progress in Polymer Science* **38**, 672-701, (2013).

238 Lin, C.-C. & Anseth, K. PEG Hydrogels for the Controlled Release of Biomolecules in Regenerative Medicine. *Pharmaceutical Research* **26**, 631-643, (2009).

239 Sawhney, A. S., Pathak, C. P. & Hubbell, J. A. Bioerodible hydrogels based on photopolymerized poly(ethylene glycol)-co-poly(.alpha.-hydroxy acid) diacrylate macromers. *Macromolecules* **26**, 581-587, (1993).

240 Peppas, N. A., Keys, K. B., Torres-Lugo, M. & Lowman, A. M. Poly(ethylene glycol)-containing hydrogels in drug delivery. *Journal of Controlled Release* **62**, 81-87, (1999).

241 Aimetti, A. A., Machen, A. J. & Anseth, K. S. Poly(ethylene glycol) hydrogels formed by thiol-ene photopolymerization for enzyme-responsive protein delivery. *Biomaterials* **30**, 6048-6054, (2009).

242 van de Wetering, P., Metters, A. T., Schoenmakers, R. G. & Hubbell, J. A. Poly(ethylene glycol) hydrogels formed by conjugate addition with controllable swelling, degradation, and release of pharmaceutically active proteins. *Journal of Controlled Release* **102**, 619-627, (2005).

243 Lin, C.-C. & Metters, A. T. Hydrogels in controlled release formulations: Network design and mathematical modeling. *Advanced Drug Delivery Reviews* **58**, 1379-1408, (2006).

244 Zhao, C. *et al.* PEG Molecular Net-Cloth Grafted on Polymeric Substrates and Its Bio-Merits. *Sci. Rep.* **4**, 4982, (2014)

245 Lin, C.-C., Sawicki, S. M. & Metters, A. T. Free-Radical-Mediated Protein Inactivation and Recovery during Protein Photoencapsulation. *Biomacromolecules* **9**, 75-83, (2007).

246 Gu, F., Neufeld, R. & Amsden, B. Maintenance of vascular endothelial growth factor and potentially other therapeutic proteins bioactivity during a photo-initiated free radical cross-linking reaction forming biodegradable elastomers. *European Journal of Pharmaceutics and Biopharmaceutics* **66**, 21-27, (2007).

247 Fu, Y. & Kao, W. J. In situ forming poly(ethylene glycol)-based hydrogels via thiol-maleimide Michael-type addition. *Journal of Biomedical Materials Research Part A* **98A**, 201-211, (2011).

248 Metters, A. & Hubbell, J. Network Formation and Degradation Behavior of Hydrogels Formed by Michael-Type Addition Reactions. *Biomacromolecules* **6**, 290-301, (2004).

249 Neuman, B., Radcliff, K. & Rihn, J. Cauda Equina Syndrome After a TLIF Resulting From Postoperative Expansion of a Hydrogel Dural Sealant. *Clinical Orthopaedics and Related Research* **470**, 1640-1645, (2012).

250 Lee, S.-H., Park, C.-W., Lee, S.-G. & Kim, W.-K. Postoperative Cervical Cord Compression Induced by Hydrogel Dural Sealant (DuraSeal). *Korean J Spine* **10**, 44-46, (2013).

251 Lynn, A. D., Kyriakides, T. R. & Bryant, S. J. Characterization of the in vitro macrophage response and in vivo host response to poly(ethylene glycol)-based hydrogels. *Journal of Biomedical Materials Research Part A* **93A**, 941-953, (2010).

252 Browning, M. B., Cereceres, S. N., Luong, P. T. & Cosgriff-Hernandez, E. M. Determination of the in vivo degradation mechanism of PEGDA hydrogels. *Journal of Biomedical Materials Research Part A*, 102, 4244-4251, (2014).

253 Hedfors, C., Ostmark, E., Malmstrom, E., Hult, K. & Martinelle, M. Thiol end-functionalization of poly(epsilon-caprolactone), catalyzed by Candida antarctica lipase B. *Macromolecules* **38**, 647-649, (2005).

254 Chambon, F. & Winter, H. H. Linear Viscoelasticity at the Gel Point of a Crosslinking PDMS with Imbalanced Stoichiometry. *Journal of Rheology* **31**, 683-697, (1987).

255 Winter, H. H. Can the gel point of a cross-linking polymer be detected by the G' - G" crossover? *Polymer Engineering & Science* **27**, 1698-1702, (1987).

256 Chan, J. W., Hoyle, C. E., Lowe, A. B. & Bowman, M. Nucleophile-Initiated Thiol-Michael Reactions: Effect of Organocatalyst, Thiol, and Ene. *Macromolecules* **43**, 6381-6388, (2010).

257 Nair, D. P. *et al.* The Thiol-Michael Addition Click Reaction: A Powerful and Widely Used Tool in Materials Chemistry. *Chemistry of Materials* **26**, 724-744, (2013).

258 Chen, G. & Hoffman, A. S. Graft copolymers that exhibit temperature-induced phase transitions over a wide range of pH. *Nature* **373**, 49-52, (1995).

259 Flory, P. J. & Rehner, J. Statistical Mechanics of Cross-Linked Polymer Networks II. Swelling. *The Journal of Chemical Physics* **11**, 521-526, (1943).

260 Brazel, C. S. & Peppas, N. A. Synthesis and Characterization of Thermo- and Chemomechanically Responsive Poly(N-isopropylacrylamide-co-methacrylic acid) Hydrogels. *Macromolecules* **28**, 8016-8020, (1995).

261 Pan, J. *et al.* Fabrication of a 3D hair follicle-like hydrogel by soft lithography. *Journal of Biomedical Materials Research Part A* **101**, 3159-3169, (2013).

262 Padmavathi, N. C. & Chatterji, P. R. Structural Characteristics and Swelling Behavior of Poly(ethylene glycol) Diacrylate Hydrogels. *Macromolecules* **29**, 1976-1979, (1996).

263 Rydholm, A. E., Anseth, K. S. & Bowman, C. N. Effects of neighboring sulfides and pH on ester hydrolysis in thiol-acrylate photopolymers. *Acta Biomaterialia* **3**, 449-455, (2007).

264 Schoenmakers, R. G., van de Wetering, P., Elbert, D. L. & Hubbell, J. A. The effect of the linker on the hydrolysis rate of drug-linked ester bonds. *Journal of Controlled Release* **95**, 291-300, (2004).

265 Fredenberg, S., Wahlgren, M., Reslow, M. & Axelsson, A. The mechanisms of drug release in poly(lactic-co-glycolic acid)-based drug delivery systems: A review. *International Journal of Pharmaceutics* **415**, 34-52, (2011).

266 Fu, Y. & Kao, W. J. Drug release kinetics and transport mechanisms of non-degradable and degradable polymeric delivery systems. *Expert Opinion on Drug Delivery* **7**, 429-444, (2010).

267 Duvvuri, S., Gaurav Janoria, K. & Mitra, A. Effect of Polymer Blending on the Release of Ganciclovir from PLGA Microspheres. *Pharmaceutical Research* **23**, 215-223, (2006).

268 Jeong, B., Bae, Y. H., Lee, D. S. & Kim, S. W. Biodegradable block copolymers as injectable drug-delivery systems. *Nature* **388**, 860-862, (1997).

269 Knop, K., Hoogenboom, R., Fischer, D. & Schubert, U. S. Poly(ethylene glycol) in Drug Delivery: Pros and Cons as Well as Potential Alternatives. *Angewandte Chemie International Edition* **49**, 6288-6308, (2010).

270 Gombotz, W. R., Guanghui, W., Horbett, T. A. & Hoffman, A. S. Protein adsorption to poly(ethylene oxide) surfaces. *Journal of Biomedical Materials Research* **25**, 1547-1562, (1991).

271 Pritchard, C. D. *et al.* An injectable thiol-acrylate poly(ethylene glycol) hydrogel for sustained release of methylprednisolone sodium succinate. *Biomaterials* **32**, 587-597, (2011).

272 Kaspar, A. A. & Reichert, J. M. Future directions for peptide therapeutics development. *Drug Discovery Today* **18**, 807-817, (2013).

273 Scott, A. M., Wolchok, J. D. & Old, L. J. Antibody therapy of cancer. *Nat Rev Cancer* **12**, 278-287, (2012).

274 Kariolis, M. S., Kapur, S. & Cochran, J. R. Beyond antibodies: using biological principles to guide the development of next-generation protein therapeutics. *Current Opinion in Biotechnology* **24**, 1072-1077, (2013).

275 Carter, P. J. Introduction to current and future protein therapeutics: A protein engineering perspective. *Experimental Cell Research* **317**, 1261-1269, (2011).

276 Leader, B., Baca, Q. J. & Golan, D. E. Protein therapeutics: a summary and pharmacological classification. *Nat Rev Drug Discov* **7**, 21-39, (2008).

277 Frokjaer, S. & Otzen, D. E. Protein drug stability: a formulation challenge. *Nat Rev Drug Discov* **4**, 298-306, (2005).

278 Reichert, J. M. Trends in development and approval times for new therapeutics in the United States. *Nat Rev Drug Discov* **2**, 695-702, (2003).

279 Vermonden, T., Censi, R. & Hennink, W. E. Hydrogels for Protein Delivery. *Chemical Reviews* **112**, 2853-2888, (2012).

280 Langer, R. New methods of drug delivery. *Science* **249**, 1527-1533, (1990).

281 Censi, R., Di Martino, P., Vermonden, T. & Hennink, W. E. Hydrogels for protein delivery in tissue engineering. *Journal of Controlled Release* **161**, 680-692, (2012).

282 Ramakrishna, S., Kim, Y.-H. & Kim, H. Stability of Zinc Finger Nuclease Protein Is Enhanced by the Proteasome Inhibitor MG132. *PLoS ONE* **8**, e54282, (2013).

283 Jiskoot, W. *et al.* Protein instability and immunogenicity: Roadblocks to clinical application of injectable protein delivery systems for sustained release. *Journal of Pharmaceutical Sciences* **101**, 946-954, (2012).

284 McCall, J. D. & Anseth, K. S. Thiol–Ene Photopolymerizations Provide a Facile Method To Encapsulate Proteins and Maintain Their Bioactivity. *Biomacromolecules* **13**, 2410-2417, (2012).

285 Hammer, N., Brandl, F. P., Kirchhof, S., Messmann, V. & Goepferich, A. M. Protein Compatibility of Selected Cross-linking Reactions for Hydrogels. *Macromolecular Bioscience* **15**, 405-413, (2014).

286 Chen, S.-C. *et al.* A novel pH-sensitive hydrogel composed of N,O-carboxymethyl chitosan and alginate cross-linked by genipin for protein drug delivery. *Journal of Controlled Release* **96**, 285-300, (2004).

287 Zhu, G., Mallery, S. R. & Schwendeman, S. P. Stabilization of proteins encapsulated in injectable poly (lactide- co-glycolide). *Nat Biotech* **18**, 52-57, (2000).

288 Fu, K., Griebenow, K., Hsieh, L., Klibanov, A. M. & Robert, L. FTIR characterization of the secondary structure of proteins encapsulated within PLGA microspheres1. *Journal of Controlled Release* **58**, 357-366, (1999).

289 Koutsopoulos, S., Unsworth, L. D., Nagai, Y. & Zhang, S. Controlled release of functional proteins through designer self-assembling peptide nanofiber hydrogel scaffold. *Proceedings of the National Academy of Sciences* **106**, 4623-4628, (2009).

290 Pérez, C., Castellanos, I. J., Costantino, H. R., Al-Azzam, W. & Griebenow, K. Recent trends in stabilizing protein structure upon encapsulation and release from bioerodible polymers. *Journal of Pharmacy and Pharmacology* **54**, 301-313, (2002).

291 Jeffrey, L. C. & Langer, R. in *Formulation and Delivery of Proteins and Peptides* Vol. 567 *ACS Symposium Series* Ch. 1, 1-19 (American Chemical Society, 1994).

292 Iyer, P. V. & Ananthanarayan, L. Enzyme stability and stabilization—Aqueous and non-aqueous environment. *Process Biochemistry* **43**, 1019-1032, (2008).

293 Fu, K., Klibanov, A. M. & Langer, R. Protein stability in controlled-release systems. *Nat Biotech* **18**, 24-25, (2000).

294 Jain, N. K. & Roy, I. in *Current Protocols in Protein Science* (John Wiley & Sons, Inc., 2001).

295 Kaushik, J. K. & Bhat, R. Why Is Trehalose an Exceptional Protein Stabilizer?: AN ANALYSIS OF THE THERMAL STABILITY OF PROTEINS IN THE PRESENCE OF THE COMPATIBLE OSMOLYTE TREHALOSE. *Journal of Biological Chemistry* **278**, 26458-26465, (2003).

296 John, G., Zhu, G., Li, J. & Dordick, J. S. Enzymatically Derived Sugar-Containing Self-Assembled Organogels with Nanostructured Morphologies. *Angewandte Chemie International Edition* **45**, 4772-4775, (2006).

297 Taguchi, H., Sunayama, H., Takano, E., Kitayama, Y. & Takeuchi, T. Preparation of molecularly imprinted polymers for the recognition of proteins via the generation of peptide-fragment binding sites by semi-covalent imprinting and enzymatic digestion. *Analyst* **140**, 1448-1452, (2015).

298 Mao, L., Luo, S., Huang, Q. & Lu, J. Horseradish Peroxidase Inactivation: Heme Destruction and Influence of Polyethylene Glycol. *Sci. Rep.* **3**, (2013).

299 Veitch, N. C. Horseradish peroxidase: a modern view of a classic enzyme. *Phytochemistry* **65**, 249-259, (2004).

300 Szigeti, K., Smeller, L., Osváth, S., Majer, Z. & Fidy, J. The structure of horseradish peroxidase C characterized as a molten globule state after Ca2+ depletion. *Biochimica et Biophysica Acta (BBA) - Proteins and Proteomics* **1784**, 1965-1974, (2008).

301 Hassani, L. *et al.* Horseradish peroxidase thermostabilization: The combinatorial effects of the surface modification and the polyols. *Enzyme and Microbial Technology* **38**, 118-125, (2006).

302 Mancini, R. J., Lee, J. & Maynard, H. D. Trehalose Glycopolymers for Stabilization of Protein Conjugates to Environmental Stressors. *Journal of the American Chemical Society* **134**, 8474-8479, (2012).

303 Lee, J. *et al.* Trehalose Glycopolymers as Excipients for Protein Stabilization. *Biomacromolecules* **14**, 2561-2569, (2013).

304 Bat, E., Lee, J., Lau, U. Y. & Maynard, H. D. Trehalose glycopolymer resists allow direct writing of protein patterns by electron-beam lithography. *Nat Commun* **6**, (2015).

305 Chattopadhyay, K. & Mazumdar, S. Structural and Conformational Stability of Horseradish Peroxidase: Effect of Temperature and pH. *Biochemistry* **39**, 263-270, (2000).

306 Fu, L., Liu, J. & Yan, E. C. Y. Chiral Sum Frequency Generation Spectroscopy for Characterizing Protein Secondary Structures at Interfaces. *Journal of the American Chemical Society* **133**, 8094-8097, (2011).

307 Schuler, B. & Hofmann, H. Single-molecule spectroscopy of protein folding dynamics—expanding scope and timescales. *Current Opinion in Structural Biology* **23**, 36-47, (2013).

308 Singer, M. A. & Lindquist, S. Multiple Effects of Trehalose on Protein Folding In Vitro and In Vivo. *Molecular Cell* **1**, 639-648, (1998).

309 Imamura, K. *et al.* Temperature scanning FTIR analysis of interactions between sugar and polymer additive in amorphous sugar–polymer mixtures. *Journal of Pharmaceutical Sciences* **97**, 519-528, (2008).

310 Taylor, L. S. & Zografi, G. Sugar–polymer hydrogen bond interactions in lyophilized amorphous mixtures. *Journal of Pharmaceutical Sciences* **87**, 1615-1621, (1998).

311 Wolkers, W. F., Oliver, A. E., Tablin, F. & Crowe, J. H. A Fourier-transform infrared spectroscopy study of sugar glasses. *Carbohydrate Research* **339**, 1077-1085, (2004).

312 Roussenova, M., Murith, M., Alam, A. & Ubbink, J. Plasticization, Antiplasticization, and Molecular Packing in Amorphous Carbohydrate-Glycerol Matrices. *Biomacromolecules* **11**, 3237-3247, (2010).

313 Roussenova, M., Andrieux, J.-C., Alam, M. A. & Ubbink, J. Hydrogen bonding in maltooligomer–glycerol–water matrices: Relation to physical state and molecular free volume. *Carbohydrate Polymers* **102**, 566-575, (2014).

314 Wyatt, T. T. *et al.* Functionality and prevalence of trehalose-based oligosaccharides as novel compatible solutes in ascospores of Neosartorya fischeri (Aspergillus fischeri) and other fungi. *Environmental Microbiology* **17**, 395-411, (2015).

315 Jain, N. K. & Roy, I. Effect of trehalose on protein structure. *Protein Science : A Publication of the Protein Society* **18**, 24-36, (2009).

316 Tibbitt, M. W., Kloxin, A. M., Sawicki, L. A. & Anseth, K. S. Mechanical Properties and Degradation of Chain and Step-Polymerized Photodegradable Hydrogels. *Macromolecules* **46**, 2785-2792, (2013).

317 Bartanusz, V., Jezova, D., Alajajian, B. & Digicaylioglu, M. The blood–spinal cord barrier: Morphology and Clinical Implications. *Annals of Neurology* **70**, 194-206, (2011).

318 Zhang, S. *et al.* Tunable diblock copolypeptide hydrogel depots for local delivery of hydrophobic molecules in healthy and injured central nervous system. *Biomaterials* **35**, 1989-2000, (2014).

319 Kang, C. E., Tator, C. H. & Shoichet, M. S. Poly(ethylene glycol) modification enhances penetration of fibroblast growth factor 2 to injured spinal cord tissue from an intrathecal delivery system. *Journal of Controlled Release* **144**, 25-31, (2010).

320 Syková, E. & Nicholson, C. *Diffusion in Brain Extracellular Space*. Vol. 88 (2008).

321 Thorne, R. G. & Nicholson, C. In vivo diffusion analysis with quantum dots and dextrans predicts the width of brain extracellular space. *Proceedings of the National Academy of Sciences* **103**, 5567-5572, (2006).

322 Wolak, D. J. & Thorne, R. G. Diffusion of Macromolecules in the Brain: Implications for Drug Delivery. *Molecular Pharmaceutics* **10**, 1492-1504, (2013).

323 Iliff, J. J. *et al.* A Paravascular Pathway Facilitates CSF Flow Through the Brain Parenchyma and the Clearance of Interstitial Solutes, Including Amyloid β. *Science Translational Medicine* **4**, 147ra111, (2012).

324 Lochhead, J. J., Wolak, D. J., Pizzo, M. E. & Thorne, R. G. Rapid transport within cerebral perivascular spaces underlies widespread tracer distribution in the brain after intranasal administration. *J Cereb Blood Flow Metab* **35**, 371-381, (2015).

325 Wolak, D. J., Pizzo, M. E. & Thorne, R. G. Probing the extracellular diffusion of antibodies in brain using in vivo integrative optical imaging and ex vivo fluorescence imaging. *Journal of Controlled Release* **197**, 78-86, (2015).

326 Sarkar, S. & Schmued, L. In vivo administration of fluorescent dextrans for the specific and sensitive localization of brain vascular pericytes and their characterization in normal and neurotoxin exposed brains. *NeuroToxicology* **33**, 436-443, (2012).

327 Song, B. *et al.* Sustained local delivery of bioactive nerve growth factor in the central nervous system via tunable diblock copolypeptide hydrogel depots. *Biomaterials* **33**, 9105-9116, (2012).

328 Young, P. & Suter, U. Disease mechanisms and potential therapeutic strategies in Charcot–Marie–Tooth disease. *Brain Research Reviews* **36**, 213-221, (2001).

329 Nave, K.-A., Sereda, M. W. & Ehrenreich, H. Mechanisms of Disease: inherited demyelinating neuropathies--from basic to clinical research. *Nat Clin Pract Neuro* **3**, 453-464 (2007).

330 Jang, S.-W., LeBlanc, S. E., Roopra, A., Wrabetz, L. & Svaren, J. In vivo detection of Egr2 binding to target genes during peripheral nerve myelination. *Journal of Neurochemistry* **98**, 1678-1687, (2006).

331 LeBlanc, S. E., Jang, S.-W., Ward, R. M., Wrabetz, L. & Svaren, J. Direct Regulation of Myelin Protein Zero Expression by the Egr2 Transactivator. *Journal of Biological Chemistry* **281**, 5453-5460, (2006).

332 Pelechano, V. & Steinmetz, L. M. Gene regulation by antisense transcription. *Nat Rev Genet* **14**, 880-893, (2013).

333 Oh, J. K., Drumright, R., Siegwart, D. J. & Matyjaszewski, K. The development of microgels/nanogels for drug delivery applications. *Progress in Polymer Science* **33**, 448-477, (2008).

334 Steinhilber, D. *et al.* A Microgel Construction Kit for Bioorthogonal Encapsulation and pH-Controlled Release of Living Cells. *Angewandte Chemie International Edition* **52**, 13538-13543, (2013).

335 Giulbudagian, M. *et al.* Fabrication of thermoresponsive nanogels by thermo-nanoprecipitation and in situ encapsulation of bioactives. *Polymer Chemistry* **5**, 6909-6913, (2014).

336 Appel, E. A. *et al.* Self-assembled hydrogels utilizing polymer–nanoparticle interactions. *Nat Commun* **6**, (2015).